

**SUBSTRATE BIOAVAILABILITY AND BIODEGRADATION
OF NAPHTHALENE ANTHRACENE AND PYRENE ON
CONTAMINATED AQUEOUS-SOIL MATRIX**

BY

OWABOR, CHIEDU NGOZI

AUGUST, 2007

**SUBSTRATE BIOAVAILABILITY AND BIODEGRADATION OF
NAPHTHALENE ANTHRACENE AND PYRENE ON
CONTAMINATED AQUEOUS-SOIL MATRIX**

BY

OWABOR CHIEDU NGOZI MNSChE, COREN

B.Sc (Hons), PGD Chem. Eng, M.Eng (Benin)

**A THESIS SUBMITTED TO THE SCHOOL OF POSTGRADUATE
STUDIES IN PARTIAL FULFILLMENT OF THE
REQUIREMENTS FOR THE DEGREE OF DOCTOR OF
PHILOSOPHY (Ph.D) IN CHEMICAL ENGINEERING AT THE
UNIVERSITY OF LAGOS, NIGERIA.**

AUGUST, 2007

SCHOOL OF POSTGRADUATE STUDIES UNIVERSITY OF LAGOS

CERTIFICATION

This is to certify that the Thesis:

**"SUBSTRATE BIOAVAILABILITY AND BIODEGRADATION OF
NAPHTHALENE, ANTHRACENE AND PYRENE ON CONTAMINATED
AQUEOUS- SOIL MATRIX"**

Submitted to the
School of Postgraduate Studies
University of Lagos

For the award of the degree of
DOCTOR OF PHILOSOPHY (Ph. D)
is a record of original research carried out

By
OWABOR, CHIEDU NGOZI
in the Department of Chemical Engineering

MISS C.N. DWABOR

AUTHOR'S NAME



SIGNATURE

16/01/08

DATE

PROF. A. A. SUSU

1ST SUPERVISOR'S NAME



SIGNATURE

16/1/08

DATE

DR. S.E. OGBEIDE

2ND SUPERVISOR'S NAME



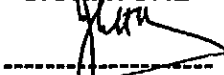
SIGNATURE

16/1/08

DATE

DR. J.U. NWALOR

3RD SUPERVISOR'S NAME



SIGNATURE

16/1/08

DATE

Prof C.T. AKU

1ST INTERNAL EXAMINER



SIGNATURE

16/1/08

DATE

DR L.O. CHUKWU

2ND INTERNAL EXAMINER



SIGNATURE

16/01/08

DATE

Prof SK Lasekun

EXTERNAL EXAMINER



SIGNATURE

16/01/08

DATE

DR. S.E. OJOLU

SPGS REPRESENTATIVE



SIGNATURE

16-01-08

DATE

DECLARATION

I do hereby declare that I am the sole author of this thesis. I do authorize the University of Lagos to lend this thesis to other institutions or individuals for the purpose of scholarly research.

Signature: _____

Date: _____

I do further authorize the University of Lagos to reproduce this thesis by photocopying or by other means in total or in part at the request of other institutions or individuals for the purpose of scholarly research.

Signature: _____

Date: _____

DEDICATION

This work is dedicated to:

- The Almighty and Covenant-keeping God whose Grace has remained sufficient for me. Glory be to Him for the gift of wisdom, knowledge, and understanding, and above all, life.
- The beloved memory of my kid brother, Ijeoma Ihemegbulem Owabor. May his gentle soul continue to rest in peace and in the bosom of our Lord Jesus Christ. Amen.

ACKNOWLEDGEMENT

I wish to express my profound gratitude and sincere appreciation to my supervisor, Prof. A.A. Susu, for his patience, guidance, dedication, commitment, encouragement, enlightenment and above all, careful and painstaking review of my manuscript. He is a mentor, a source of inspiration and indeed a Father to me. Prof, I remain most grateful and indebted to you.

My sincere gratitude also goes to my co-supervisor, Dr. S.E. Ogbeide. I thank you Sir for your assistance, guidance, editing of my manuscript, and your innumerable and invaluable pieces of advice. Sir, I highly recognize and appreciate your profound contributions which are by no means little.

Special thanks go to Prof F. Olatunji, Prof T.O.K Audu, Prof K. Echenim and Prof C.T Ako for their encouragement and support throughout the period of this research work.

Words are insufficient for me to express my deep appreciation to my family especially my parents, Ezinna and Ezinne G.S.I Owabor, my brother Nkenchor, my sisters, Mrs N. Ogbechi, Nkechi, Uche and Mrs N. Isikwu. I am wholly indebted to you all for your love, encouragement, prayers and moral support, which have been a source of great strength to

me. I am specially saying *unu e'meke*. God bless you all!

To my friends and colleagues, especially Jaiyeola Leke, Fred Ekhaise, and Jude Osarumwense, who contributed in one way or the other to the realization of this work, i say thank you so very much.

I also wish to thank the technical staff of the Equipment Maintenance Centre, University of Benin, especially the Head, Mr Imana and Mr Sunny Aigbedion, for their interest and support during the design and fabrication of the Soil Microcosm Reactor used for this research.

My thanks also go to John of Microbiology Laboratory, Chinedu of Benin-Owena River Basin Authority Laboratory, University of Benin and Pa Awosanya, of the Department of Chemistry for the fabrication of the Orsat Gas Analyzer used for this research work. Nwaekwu Kingsley Chioma, you are not left out. I am very grateful to you for your assistance with regards to the final manuscript. Thank you very much.

My warmest and sincere appreciation to my Adorable friend- Austin Moye. For your priceless love and understanding, I say thank you. Above all, I thank God Almighty who is His own interpreter and makes things plain in His time. I thank Him who made all things possible in the pursuit of my academic career.

ABSTRACT

The focus of this research work is the unraveling of the microbial dynamics of the biodegradation of a mixture of polycyclic aromatic hydrocarbons (PAHs), naphthalene, anthracene and pyrene in an aqueous-soil matrix. The soil used in these studies was characterized as highly porous with a sandy-clay ratio of 85-14%. The microbial growth study was characterized by an initial lag phase, a rapid and an exponential increase in cell biomass, a stationary phase and finally a death phase. The growth and consumption rates estimated using the Monod kinetics showed that all the microbes (bacteria and fungi isolated from the indigenous soil and used in this study exhibited a high metabolic affinity for naphthalene.

Respirometric studies conducted to measure the level of microbial activity and PAH biodegradation rates in the soil microcosm reactor indicated that a reasonable degree of PAH acclimation was achieved in the reactor, with a net cumulative oxygen uptake and carbon (iv) oxide evolution attaining their maximum limit within 60days of exposure.

Results on the batch adsorption/desorption kinetics and equilibria depicted that the desorption rate was slower than the adsorption rate. The cumulative extent of desorption for the three PAHs suggested that the desorption step was rate limiting for biodegradation. The degree of

partitioning was found to be dependent on their solubility and diffusivity in the aqueous phase. A realistic adsorption-reaction-desorption mechanism suggested a time dependent degradation of the PAHs describing the adsorption of the solute on the soil particle surface.

The exponential nature of the experimental biodegradation kinetics data for naphthalene, anthracene and pyrene was fitted with a kinetic model for both single and multisubstrate catalysis using the twin concepts of rate-determining step (RDS) and steady state approximation (SSA). This model predicted the experimental profile of the biodegradation behaviour: an initial rapid decrease in the concentration of the PAHs followed by a significantly slower rate of degradation. The RDS model gave a better prediction as its reaction rate constant (k) closely fitted the experimental values. Prediction by the SSA model was not feasible as a comparative analysis of both single and multisubstrate results show that the SSA overestimates the biodegradation rates.

The method of temporal moment (MOM) and a nonlinear least square curve-fitting program CXTFIT were used to estimate the transport parameters and degradation rate constants. Estimation of the transport parameters and the pore-water velocity, V for a non-reactive solute was aided by the use of only the first normalized moment. The dispersion

coefficient, D , first order degradation rate constant (λ) and the retardation factor (R) were estimated using both first and second normalized moments. The observed results suggest that naphthalene would elute first before pyrene and anthracene, in the following order: naphthalene > pyrene > anthracene.

The solution to these model equations was achieved by the use of the backward finite difference scheme. The estimated transport parameters and diffusivities were used to reduce the dimensionality of the search process. Results obtained showed that naphthalene was more selectively degraded than pyrene and anthracene. The residual concentration of these PAHs in the axial and radial directions were: naphthalene ($1.16\text{E-}5$ and 1.48mg/l); pyrene ($3.11\text{E-}4$ and 1.58mg/l) and anthracene ($7.67\text{E-}4$ and 1.61mg/l). The resultant effect is the occlusion of these compounds within the fissures and cavities of the soil particles, which renders them not readily bioavailable and thus inaccessible to microbial degradation.

The developed approach in this research work thus shows the practical effects of intrinsic kinetics, rate-limited desorption and mass transfer resistances on the outer surface and within the pores of the soil particle.

NOMENCLATURE

E	Enzyme
C	Contaminant hydrocarbon
k	Reaction rate constant
J	Flux of rate-limiting substrate into the biofilm ($\text{mol/m}^2.\text{s}$)
A	Biofilm surface area (m^2)
b	Specific decay or maintenance-respiration coefficient (hr^{-1})
D_f	Molecular diffusivity within biofilm (m^2/day)
C_b	Concentration of rate-limiting substrate in the bulk liquid (mg/l)
L_f	Thickness of biofilm (L)
X_f	Bacterial density in biofilm (M_g/L^3)
Y	True yield of bacterial mass per unit of substrate mass utilized (mg/mg)
k_s	Saturation constant
C_f	Concentration of substrate within the biofilm
B_f	Bioavailability Factor
k_b	First-order rate coefficient for biodegradation
k_i	Inhibition constant
μ_{\max}	Maximum specific growth rate
θ	Standard biofilm time dimension T ($2/Yk$)
τ	Standard biofilm dimension L ($2K_s/D_f k X_f$) ^{1/2}
V	Pore water velocity (m/day)
D	Dispersion Coefficient (m^2/day)
k_f	Mass transfer coefficient for external film diffusion (m/day)
C_{oi}	Initial concentration of contaminant i at $t = 0$
C_i	Concentration of contaminant i in the external pellet surface i.e. Opening of the Pores (mg/l)

C_{si}	Concentration of contaminant i in the solid phase (mg/l)
C_{pst}	Concentration of contaminant i in the fluid phase within the pore of soil particle
ε_p	Porosity of soil
ε_p	Particle porosity (void fraction in particles)
r	distance from the centre of the particle (cm)
R	Radius of soil particle (cm)
z	Axial distance (cm)
t	time (days)
λ	first order degradation rate (min^{-1})
R	Retardation factor
ε	Coefficient of deviation
RRE	Relative Error
z_T	Length of soil column (cm)
T	Total experimental time (days)

Dimensionless parameters

$\tau = t/T$	dimensionless time
$\bar{C} = C_i/C_{oi}$ or C_{si}/C_{oi}	dimensionless concentration
α, β, γ	constants defined by equation (4.15)
ψ, η, ϕ	constants defined by equation (4.16)
$Z = z_T/z$	dimensionless depth

TABLE OF CONTENTS

Title	i
Certification	ii
Declaration	iii
Dedication	iv
Acknowledgement	v-vi
Abstract	vii-ix
Nomenclature	x-xii
Table of Contents	xiii-xiv
List of Tables	xv
List of Figures	xvi-xvii
List of Appendices	xviii
 Chapter One Introduction	 1-7
1.1 Theoretical Framework of Study	7-12
1.2 Motivation of Research Work	12-13
1.3 Purpose of Study	14-15
1.4 Research Questions	15
1.5 Implications of Research Work	16-17
1.6 Scope and Limitation of Research Work	17-18
1.7 Significance of Research	18-19
 Chapter Two Literature Review	 20-27
2.1 Adsorption – Reaction – Desorption in Bioremediation Processes	27-32
2.2 Equilibria: Adsorption Isotherms	32-34
2.3 Model Isotherms	34
2.3.1 Langmuir Isotherm	34-35

2.3.2	Freundlich Isotherm	35-36
2.3.3	Brunauer, Emmett and Teller (BET) Equation	36
2.4	Use of Biosurfactants in Soil Remediation	36-40
2.5	Biodegradation Kinetics	40-43

Chapter Three Model Development for Steady State

	for Biofilm Kinetics	44
3.1	Kinetic and Molecular Diffusion in Interface Film	44
3.1.1	Intrinsic Kinetics using Rate-Determining Step	44-45
3.1.2	Single Substrate Catalyzed Reaction	45-47
3.1.3	Multisubstrate Catalyzed Reaction	47-48
3.1.4	Coupling Kinetics and Molecular Diffusion	48-50
3.1.5	Intrinsic Kinetics using Steady State Approximation	50-52
3.1.6	Coupling Kinetics and Molecular Diffusion	52-54
3.2	Kinetic Model of Biofilm at Steady State	54-59
3.3	Development of Mathematical Model for Macro and Microporous Systems	60-63
3.4	Model Development for Macro and Microporous Systems	63
3.4.1	Macroporous Systems	64-67
3.4.2	Microporous Systems	67-72

Chapter Four Materials and Methods

		73
4.1	Materials	73-74
4.2	Instruments	74
4.3	Soil	75
4.4	Experimental Set-up	75-78
4.5	Methods	78-80
4.6	Kinetic Experiments	80-82

4.7	Microbial Analysis	82-84
4.8	Characterization	84
4.8.1	Morphological Characteristics	84
4.8.2	Gram's Stain	85
4.9	Cultural Characteristics	85
4.9.1	Biochemical Characteristics	85-89
4.10	Microbial Growth Study	89
4.11	Soil Characterization	90-94
4.12	Parameters from Experimental Investigation	95
4.13	Parameters needed for Simulation	95-96
4.14	Software	97-98
4.15	Numerical Solution and Analysis	99-108
Chapter Five	Results	109-110
5.1	Soil Characterization	110-112
5.2	Microbial Analysis	112-119
5.3	Analysis of Oxygen Uptake and Carbon (iv) Oxide Evolution Data	120-123
5.4	Analysis of Adsorption and Desorption Data	124-143
5.5	Biodegradation Study	145-145
5.6	Kinetic Models	145-149
5.7	Estimation of Transport and Degradation Parameters	150-151
5.8	PAHs Breakthrough Curves	151-156
5.9	Simulation Plots for a Non Steady-State Model	157-164
5.10	Model Validation	165-168
Chapter Six	Discussions	169-182

Chapter Seven	Contributions to Knowledge	183-184
Chapter Eight	Conclusions and Recommendations	185
8.1	Conclusions	185-186
8.2	Recommendations	186-187
References		188-203
Appendices		204-256

LIST OF TABLES

Tables	Contents	Page
5.1	Some properties of investigated PAHs	110
5.2	Soil characteristics	111-112
5.3	Kinetics of substrate utilization	119
5.4	Isotherm constants for adsorption and desorption for the contaminant PAHs	131
5.5	Biokinetic constants for contaminant PAHs	144
5.6	Kinetic constants for contaminant PAHs with model fits	146
5.7	Comparison of the pore-water velocity and dispersion coefficients obtained from methods of temporal moments and CXTFIT curve fitting program	150
5.8	Comparison of the degradation and transport parameters for the contaminant PAHs	151
5.9	Estimated values of the parameters for the solution of the modelling equations	157
5.10	Residual concentration of contaminant PAHs in both axial and radial directions	158
5.11	Relative error between the two kinetic models and experimental data	165

LIST OF FIGURES

Figures	Title	Page
3.1	Schematic of a cell surrounded by a biofilm	57
4.1	Schematic representation of experimental set-up	77
4.2	Schematic representation of serial dilution method	84
5.1-5.6	Mineralization of naphthalene by pure microbial Isolates	113-118
5.7	Net cumulative carbon (iv) oxide evolution from the reactor spiked with a mixture of naphthalene, anthracene and pyrene	121
5.8	Oxygen uptake in microcosm reactor	122
5.9	Net cumulative oxygen uptake in microcosm reactor	123
5.10-5.12	Adsorption kinetics for naphthalene, anthracene and pyrene	125-127
5.13-5.15	Desorption kinetics for naphthalene, anthracene and pyrene	128-130
5.16-5.18	Freundlich adsorption isotherms for naphthalene, anthracene and pyrene	132-134
5.19-5.21	Langmuir adsorption isotherms for naphthalene, anthracene and pyrene	135-137
5.22-5.24	Freundlich desorption isotherms for naphthalene, anthracene and pyrene	138-140

5.25-5.27	Langmuir desorption isotherms for naphthalene, anthracene and pyrene	141-143
5.28	Variation of concentration of PAHs against time	147
5.29	Simulated concentration of single substrate model against time	148
5.30	Simulated concentration of multisubstrate model against time	149
5.31-5.34	Comparison of MOM and CXTFIT simulated breakthrough curves for tracer, naphthalene, anthracene and pyrene using experimental data	153-156
5.35-5.37	Variation of concentration of anthracene, pyrene and naphthalene with time and depth	159-161
5.38-5.40	Variation of concentration of anthracene, naphthalene and pyrene with time and radial direction	162-164
5.41-5.42	Experimental and simulated degradation of naphthalene, anthracene and pyrene in a soil microcosm reactor (axial and radial directions)	167-168

LIST OF APPENDICES

Appendix	Content	Page
A	Experimental data from soil microcosm reactor for biodegradation studies	204-206
B	Respirometric bioreactor data for oxygen uptake and carbon (iv) evolution kinetics	207-211
C	Adsorption and desorption kinetic data obtained from experiment	212-217
D	Cultural, morphological and biochemical characterization of microbial colonies. Microbial growth study	218-225
E	Standard interpretational rules generally accepted for tropical and subtropical soils	226-227
F	Independent estimation of the transport parameters needed for the simulation of the non steady-state modelling the macroporous and microporous soil systems	228-229
G	Simulation of the concentration profile for the kinetic model	230-232
H	Determination of the concentration profiles at different time steps in both axial and radial directions using the inverse matrix method	233-250
I	Microsoft Excel Template showing the concentration of contaminant PAHs in the axial and radial directions of flow	251-256

CHAPTER ONE

1.0

INTRODUCTION

Large amounts of petroleum and petroleum products are discharged into the environment as a result of exploration, production, transportation, refining and utilization. Despite careful handling and containment, there are possibilities that some may spill into the soil through blow-outs, accidents, sabotage, corrosion, equipment malfunction, operators/maintenance errors, rupture of oil pipelines, operational discharges and natural causes (rain, flood, soil erosion). It is estimated that 1.7 to 8.8 million metric tons of petroleum are released annually into the global environment (Leahy and Colwell, 1990).

Polycyclic aromatic hydrocarbons (PAHs) constitute a large group of organic contaminants, which consist of two or more fused aromatic rings in various structural configurations (Blumer, 1976). They are commonly found as constituents of heavy fuel, tar and creosote, for which reason they are often identified at gas works and coal gasification sites and from anthropogenic sources such as heat and power generation, coke production, catalytic cracking, carbon-black production and use, incineration, landfills/waste disposal, wood treatment and preservation, refining and distillation of crude oil (Bos *et al.*, 1984; Wilson and Jones, 1993). However, aside their presence in contaminated sites, it should be

noted that they are found everywhere although usually in low concentration as a result of the incomplete combustion of fossils. The background level of these chemicals is expected to further increase in the future because many of these PAHs are rather persistent in the environment even under aerobic conditions. Their high octanol-water partitioning coefficient values also show that they are not very mobile (Jones *et al.*, 1989). The long-term effect of the presence of aromatic hydrocarbons in the environment has become one of the major environmental concerns of the petroleum and other process industries.

Since the 1970s, there has been a growing concern about the general state of health of the environment by the Nigerian public as a result of the widespread releases of PAHs, whether accidental or intentional, into soil systems ranging from surface soils to deep aquifers. Consequently, both engineers and scientists have been mobilized into a search for the technology that will effectively clean up contaminated soils at reasonable cost. The development of effective clean up technology to reduce the levels of these hydrocarbon contaminants in order to meet environmental regulation standards is therefore a continuing subject of research. Most of the important chemical reactions encountered in bioremediation studies are catalytic and in the majority of these processes, the catalysts are enzymes from microorganisms.

In Nigeria, as a result of increasing daily activities within the petroleum industry, polycyclic aromatic hydrocarbons input into the environment have similarly increased greatly (Naagbanton, 1999, Asuquo *et al.*, 2004). Generally, the Nigerian environment has been subjected to a barage of sustained and unmitigated pollution of its air, land and sea. Some of the spills have been known to seep into the ground and contaminate ground water. Many in the Delta region have complained that water from freshly sunk boreholes showed evidence of oil contamination. This makes the water undrinkable even after some treatment. The other problem with oil spill is that areas that have been known to be fertile for farming in the past have suddenly become barren or are getting close to being so. The mangrove forest is slowly withering away and the agricultural industry is suffering. This is particularly sad because the natives, who used to make their living through subsistent farming, have to look elsewhere (Akpofure *et al.*, 2007; Nwilo and Badejo, 2001; Kinigoma, 2001). The various input sources of oil spills include the following: pipeline (trunk, delivery, gathering line), flowstation, tank farm, drilling site, well head, pumping stations, refinery, natural sources, offshore oil production marine transport, municipal etc. There have also been instances, where vandals have allegedly caused oil leaks. It was reported on November 27, 1998, (This Day Newspaper), that one thousand five hundred (1,500) barrels of oil leaked in the Santa Barbara River Crossing in Bayelsa State, where

Shell Petroleum Development Company, which is the largest oil company in Nigeria accounting for about 50% of oil production was conducting operations. It has therefore become imperative and very desirable to decontaminate quickly and safely locations that have had shock loading of petroleum or petroleum products.

Consequent upon this, concerted efforts have been made to understand the fate, transport and reactions of this group of compounds in aqueous-solids/sediments matrix. To this end, bioremediation, which can best be described as the optimization of biodegradation (Bluestone, 1986; Nwachukwu, 2001; Ayotamuno, 2006; Ayotamuno; 2007), has become successful over the years in harnessing the natural activity of microorganisms for the performance of beneficial functions that have greatly enhanced our standard of living? This is not remotely far from the fact that the process can be an effective option to reclaim PAH-contaminated sites due to its relatively low cost and limited impact on the environment.

The microorganisms exposed to these anthropogenic substances have sometimes responded by acquiring new genes for degradation of these compounds, either for detoxification or to enable the microbe use the contaminant as a source of energy to meet metabolic needs (Gunnison *et*

al., 1997, Adenipekun *et al.*, 2005). The use of the microbes as catalysts in bioremediation, particularly in Nigeria has been to essentially increase the rate of degradation so as to eliminate as quickly as possible, both long and short term effects of these contaminants that compromise the integrity of the environment (Odu, 1981; Layokun *et al.*, 1987; Amadi and Antai, 1991; Odokuma and Dickson, 2003; Oboh, 2006; Ojo, 2006).

The process of biodegradation of PAH impacted soils/sediment matrix is complex and involves the diffusion of contaminants in the porous soil matrix, adsorption to the soil surface, biodegradation in the biofilm existing on the soil particle surface and in the large pores as well as in the bound and free water phase after desorption from the soil surface (Tabak and Govind, 1997; Knightes, 2000). The type of reactor now forms the basis of many new bioremediation techniques. To be commercially viable, it has become imperative to obtain the best performance from the reactor. Thus the emphasis is on the need for more accurate design parameters and methods.

Generally, the overwhelming reported literatures and articles have specified clean-up techniques for PAH contaminated sites using bacterial cultures, pure strains or strains in association (Boldrin *et al.*, 1993; Banerjee *et al.*, 1995; Caldini *et al.*, 1995; Bouchez *et al.*, 1996; Ahn *et*

al., 1999; Reardon *et al.*, 2002). The few available reports on the modelling of PAH degradation (Tabak and Govind, 1997; Rogers and Reardon, 2000) have however, been unable to perform optimally relative to availability, mobility, toxicity and concentration of polycyclic aromatic hydrocarbons in the soil system ranging from surface soils to deep aquifers.

The development of the mathematical model carried out in this research work is based on the fundamental principle of conservation of mass or material balance. It takes into consideration the gas-liquid interface film and the biofilm between liquid and solid interface. It also accounts for the interparticle, intraparticle and interphase mass transport. The effects of axial dispersion in the fluid phase and transport resistances are not neglected. It responds to the pressing research needs for bioremediation with the underlying task of determining the factors, which govern bioavailability. The technique for selecting efficient design methods and/or parameters depends on the development of realistic models for the mathematical description of the process. Thus, this research work is focused on the modeling of the biodegradation of polycyclic hydrocarbon compounds with emphasis on:

- i. bioavailability
- ii. mobility (transport)

- iii. toxicity
- iv. concentration with respect to both time and distance (axial and radial directions) and
- v. PAH disappearance

Solving these problems by obtaining the parameters implicated would provide a comprehensive information and database on the rate and extent of biodegradation with a view to averting considerably, the prolonged effects of polycyclic aromatic hydrocarbon contamination on the environment.

A computational scheme for the solution of the model equations for the case of one-dimensional convective-diffusive mass transfer occurring in the subsurface is presented here for macroporous and microporous systems. The proposed methodology is sensitive to changes in the concentration of contaminant with time as a function of the axial and radial directions of flow.

1.1 Theoretical Framework of Study

This research work focuses on the development of suitable models for the evaluation of bioavailability and biodegradation parameters in contaminated aqueous-solids/sediments matrix, based on the following theoretical concepts:

(a) The development of kinetic expressions following the methods used in the derivation of rate equations for synthetic catalysts. This is hinged on the twin concepts of rate-determining step (RDS) and steady state approximation (SSA). These concepts are used in conjunction with mass transport, where the rate of mass transfer by diffusion is assumed to be governed by Fick's Law (Treybal, 1981; Susu, 1997; Coulson and Richardson, 2000; Bird *et al.*, 2005; Fogler, 2006).

(b) The theory of convective and diffusive transfer of solutes in both axial and radial directions of flow. Convective mass transport in swarms of particles is a commonly encountered process in a wide range of industrial and scientific applications such as fluidized beds, separation processes, catalytic and non-catalytic fluid-solid reactions (Coutelieris *et al.*, 2004). Convection is due to fluid flow while dispersion is due to solute movement/transport.

(c) Equilibrium adsorption and desorption described using both the Freundlich and Langmuir isotherm relationships (McCabe, *et al.*, 1993; Susu, 2000).

(d) Application of the method of temporal moments (MOM) and a computer software program CXTFIT version 2.0 to estimate solute transport with equilibrium sorption and first order degradation (Toride *et al.*, 1995; Pang *et al.*, 2003).

(e) Use of dimensional analysis in the conversion of a partial differential

equation modeling a physical system into a dimensionless equation and resolution of the equation by the Finite Difference Scheme (Sun and Levan, 1995).

The concept of RDS in a reacting system is one method of simplifying the rate expression. It proposes that in a sequence of elementary steps, one step is postulated to be rate-determining and that all the other steps in the sequence of reaction are assumed to be in quasi-equilibrium. Consequently, only that step is kinetically significant being the slowest, as only its rate constant appears in the rate expression. The catalyst which in this case is a homogenous enzyme is perceived to be present in two forms either as free enzyme E or combined in an appreciable extent to form intermediate enzyme-substrate complex (ES).

Two films are implicated: Interface film between dissolved oxygen and the substrate, and the biofilm between the substrate phase and aggregates of microorganisms attached to the soil particle.

Chemical reactions occur through intermediates and these intermediates (in the form of atoms and free radicals and other short-lived species) are conceived to be adsorbed species with mobility to search for energetically favourable sites for subsequent conversion into final state (products), prior to desorption. The SSA allows a procedure where the intermediates

whose concentrations are low, are assumed to be negligible during the course of the reaction since at steady state, their rate of production is equal to their rate of consumption.

In assessing the concentration, availability and toxicity of the contaminant in the subsurface soil, the theory of convective and diffusive transfer of solutes in both axial and radial directions of flow is incorporated in the development of mathematical models. Adsorption and desorption are the primary processes in the evaluation of bioavailability and mass transfer is the mechanism of movement from the fluid phase to the surface of the soil particle. The equilibrium adsorption and desorption reactions were described by the basic correlations developed by Freundlich and Langmuir. The correlations were used to describe the surface adsorption of the solutes and their subsequent desorption from the soil surface. Sorption of contaminant tends to separate the direct contact between microorganisms and contaminants, which is necessary for biodegradation to occur. The practical effect of the adsorption and desorption rate, is that it controls the overall reaction rate. The transport (mobility) of contaminant solute therefore is significantly dependent on two possible scenarios: fast sorption/desorption and slow sorption/desorption.

The interplay between degradation and sorption is brought to focus, as

issues such as the bioavailability of subsurface contaminants become the subject of discourse. The method of temporal moments (MOM) solutions and the nonlinear leastsquare curve-fitting program CXTFIT which is described as a parameter optimization method were other concepts, which were useful in the estimation of the transport parameters: (i) pore-water velocity V , (ii) dispersion coefficient D , (iii) degradation parameters, (iv) retardation factor R and (v) first order degradation rate.

The MOM solutions are based on the assumptions that local equilibrium is established instantaneously during solute transport in a homogenous porous medium and that sorption could be linear and reversible. The CXTFIT assumes convective-dispersion (or advective-dispersive) transport, in a one-dimensional flow.

The transport model described using second order partial differential equations involve functions of two real variables (x, y) , where x, y represent z, t and r, t respectively. By applying the backward finite difference scheme, we can compute every domain point (x, y) selected at random. This is achieved by laying a rectangular grid over the domain and evaluating $f(x, y)$ at the grid point- the points of intersection of the lines parallel to the x -axis and the lines parallel to the y -axis.

The mathematical formulations for the macroporous and microporous systems are based on constant coefficients of dispersion, diffusion,

constant porosities, and that the microbes have uniform size and homogenous structure.

1.2 Motivation of Research Work

The discharge of petroleum and petroleum products into the environment as a result of exploration, production, transportation, refining and utilization and the consequent pollution has adverse ecological effect in oil-producing areas of the world. In Nigeria, due to the daily increasing activities of the petroleum industry, the petroleum hydrocarbon input into the environment has increased tremendously. Analysis of these spillages shows that there is the possibility that some may enter the soil environment through blow-outs, accidents, sabotage, rupture of oil pipelines, equipment failure, maintenance error, corrosion and natural causes.

There is a dearth of knowledge on the mechanisms of sequestration, transport and fate of polycyclic aromatic hydrocarbons (PAHs) in soils. This is hinged on the fact that the rate and extent of PAH removal are dependent on the number of aromatic rings, molecule topology or pattern of ring linkage, contaminant-soil (or sediment) contact time and to a large extent on soil properties (Bosset and Bartha, 1986; Guthrie and Pfaender 1988; Evans and Krug 2002; Spark 2003; Reddy and Angelo 2003;

Oleszczuk and Baran 2003; Galinada and Yoshida 2004; Shor *et al.*, 2004; de Lucas *et al.*, 2005).

The frequency of discharge of these groups of compounds into the environment, particularly land, and their build-up compromises the quality of the environment. This has resulted in a high level of awareness of the potential negative effects on man. These effects apart from the degradation of the ecosystem, also results in commodity loss, loss to the communities that depend on such lands for their livelihood and economic loss due to spill clean up cost.

The development of remedial techniques to deal with these contaminant solutes and assess their behaviour over relatively long spatial and temporal scales seem to be the only viable solution or management strategy to maintaining the integrity of the environment. In the light of the limitations arising from the expensive and cumbersome nature of experimental studies over sufficiently long distances and /or time periods, theoretical models are thus required to describe the process of bioremediation. Data on availability, transport and degradation, which are limited, will be generated and used for the design of the equipment for the treatment process.

1.3 Purpose of Study

The purpose of this research work is to assess the potential of ex-situ bioremediation in a microcosm reactor as a clean up technique for contaminated soils using theoretical models. The research work shall achieve the following objectives:

- (i) Design and fabrication of a soil microcosm reactor for evaluating bioavailability and biodegradation of PAHs in contaminated aqueous-solid systems.
- (ii) Application of the concept of rate-determining step and steady state approximation useful for describing the kinetics of synthetic catalysis in evolving a suitable biodegradation kinetics model at the gas-liquid interface for both single and multisubstrate enzyme catalysis.
- (iii) Development of steady state biofilm kinetics model for interactions between the substrate and aggregates of microorganisms attached to the soil particle.
- (iv) Development of mathematical models for macroporous and microporous systems at non-steady state to ascertain bioavailability and fate (toxicity) of the remaining contaminant PAHs.
- (v) Application of the methods of temporal moment solutions (MOM) and a nonlinear least square curve-fitting program for estimating the transport parameters involving equilibrium sorption and first

order degradation of PAHs.

1.4 Research Questions

The following research questions will guide this research work:

- (i) What are the current bioremediation techniques and their shortcomings in terms of concentration, availability and toxicity of contaminants?
- (ii) How does the present research work differ from works of previous researchers?
- (iii) Are there enough data for relating bioavailability and biodegradation of contaminant PAHs? Do the parameters-availability, mobility (transport) and toxicity- correlate with the concentration of contaminants in the soil?
- (iv) How well do the theoretical predictions from the model compare with experimental measurements from the soil microcosm reactor in terms of convenience and applicability in solving biodegradation problems in real time and space?
- (v) Would the developed models be universally applicable to all bioremediation systems?

1.5 Implications of Research Work

This research work has the following significance:

- (i) The understanding of the basic principles in the development of theoretical models for substrate bioavailability and biodegradation of contaminants in aqueous-solids/sediment matrix and the development of applicable models.
- (ii) Models for one-dimensional convective-diffusive mass transfer occurring in the subsurface and kinetic-diffusive equations are presented.
- (iii) Applicability of the developed models in predicting the level of contaminants in the micropores of the soil matrix.

These following activities are essential in realizing the above objectives: ..

- (a) The design and fabrication of a bench scale soil microcosm reactor for the treatment of polycyclic aromatic hydrocarbon compounds, which serves as a benchmark for bioremediation studies.
- (b) Prediction of the distribution of contaminants in both axial and radial directions with intraparticle, interparticle and interphase mass transport.
- (c) The knowledge and understanding derived from this research work bring to the fore, the mechanism of bioavailability, mobility, toxicity and contaminant concentration in aqueous-

solids/sediments matrix for detailed pilot and full-scale design of soil microcosm reactors treating single and multisubstrate organic contaminants.

1.6 Scope and Limitation of Research Work

This research work is limited to the development of a systematic protocol for evaluating bioavailability and biodegradation of contaminant polycyclic aromatic hydrocarbon in the soil matrix. The work is covered within the scope presented below:

1. Detailed literature review of polycyclic aromatic hydrocarbon biodegradation in soils/sediments matrix.
2. Model development for steady state biofilm kinetics and the non-steady state macroporous and microporous systems.
3. Design and fabrication of a soil microcosm reactor as a first step in the kinetic protocol for evaluating substrate bioavailability and biodegradation in contaminated aqueous-solids/sediments matrix.
4. Characterization of soil to provide insight into the physicochemical properties of the soil.
5. Studies on soil microcosm reactor to provide acclimated soils and to determine primary biodegradation by providing average biodegradation rates of soil contaminants.
6. Studies on abiotic sorption/desorption kinetics and equilibria of the

contaminants using soil slurry systems.

7. Numerical simulation for bioavailability and biodegradation parameters in contaminated aqueous-solids/sediments matrix.
8. Testing and validation of theoretical models with data from experiments.

1.7 Significance of Research Work

This research work focused on the potential application of bioremediation as a means of effective clean up of contaminated soils in the Niger-Delta and other regions where there are oil and gas activities in Nigeria. The significance of the research work includes:

1. The development of a mass transfer-limited numerical model for the restoration process occurring in the surface and subsurface soil during bioremediation
2. Application of the developed model in the investigation of the effects of sorption and bioavailability on the rates of biodegradation. This approach shows the effects of rate-limited desorption on bioavailability and it does not over estimate the biodegradation rate.
3. The quantitative parameters (measured, calculated and estimated) represent a valuable pool of information to the Federal Ministry of Environment through its regulatory and control agencies in their

functions and duties with a view to containing and remediating contaminated sites.

4. The estimated transport and degradation parameters form the basis for predicting the bioavailability, mobility and toxicity of the contaminants in the soil.
5. The data for the biodegradable contaminants within the soil matrix following treatment provide an insight into the degree of bioaccumulation and immobilization of individual PAH within the soil micropores.

CHAPTER TWO

2.0

LITERATURE REVIEW

Polycyclic aromatic hydrocarbons (PAHs) originate from both natural and anthropogenic sources such as terrestrial deposit of coals, atmospheric input as a result of incomplete combustion (wood burning, forest fire, fossil fuel, and coke oven), oil seeps and spills, highway dust associated with vehicle exhaust. They are also constituents of the exhaust from lawn mowers and charcoal grills. The pure PAHs usually exist as colorless, white or pale yellow-green solids (Keith and Telliard, 1979; Freeman and Cattell, 1990; Schwarzenbach *et al.*, 1993). The simplest and commonest of this group of compounds is naphthalene, which consists of two benzene rings fused together. Other PAHs include anthracene, pyrene, phenanthrene, benzo[a]pyrene (BaP), to list but a few. They are used in the manufacture of phthalic anhydride (used in dye making), lubricants, vermicides, antiseptic and insecticide especially in mothballs, wood preservative, coating for water storage tanks to prevent rust and as a soil fumigant. They are also used commercially to make pesticides, pharmaceuticals and plastics (Xu and Obbard, 2003).

Generally, an increase in the size and angularity of a PAH molecule results in a concomitant increase in hydrophobicity and electrochemical stability (Blumer, 1976).

Despite their widespread distributions, PAHs can be ultimately deposited and persisted in sediment (as sink) in the aquatic system. This is due largely to the fact that most PAHs sorb strongly to sediment organic matter because of their high hydrophobicity and are resistant to bacterial degradation under anoxic environment. However, when environmental conditions become favourable, PAHs will be released to the overlying water as long-term source and pose potential threat to water quality and aquatic ecosystem via bioaccumulation in food chains (Jones *et al.*, 1989).

Interest in the biodegradation mechanisms and environmental fate of polycyclic aromatic hydrocarbons (PAHs) is prompted by their ubiquitous distribution and their potentially deleterious effects on human health. They exhibit toxic properties at low concentrations and several have been listed as priority pollutants to be monitored in industrial effluents, natural waters, soils and sediments (Karthikeyan and Bhandari, 2001). On exposure at high levels (above 10ppm), headaches, fatigue, and nausea occur while if ingested, they have the potential to cause hemolytic anemia, a condition that involves the breakdown of red blood cells (Volkova, 1983). Chronic effects arising from long term exposure to these compounds can lead to reproductive defects including foetal damage and decreasing fertility, damage to the kidneys and liver. Higher

incidences of cancer, lung and skin tumor have been reported for people who have been occupationally exposed to these compounds (Day-Barker *et al.*, 1985; Sorsa, 1992).

Biological treatment techniques for remediating soils contaminated with hazardous organic compounds (polycyclic aromatic hydrocarbons) are gaining public acceptance as increasing numbers of effective bioremediation processes have been developed (Okerentugba and Ezeronye, 2003; Ebuehi *et al.*, 2005; Okoh, 2006). The potential of bioremediation is almost boundless. Tremendous studies have been made over a relatively short time, both in the discovery of novel biochemical mechanisms and the development and/or refinement of innovative reactor designs (Heitkamp *et al.*, 1987; Wilson and Jones, 1993). It is understood that the initial step in the aerobic catabolism of a PAH molecule by bacteria occurs via oxidation of the PAH to a dihydrodiol by a multicomponent enzyme system. These dihydroxylated intermediates may then be processed through either an ortho cleavage type or a meta cleavage type of pathway, leading to central intermediates such as protocatechuates and catechols, which are further converted to tricarboxylic acid intermediates (van der Meer *et al.*, 1992; Kanaly and Harayama, 2000).

In many applications, bioremediation methods can be cost effective compared to other alternatives such as thermal or physical/chemical treatment methods. Laboratory and field studies have been used to demonstrate the effectiveness of bioremediation in cleaning up PAH contaminated sites (Mahaffey *et al.* 1988, Mueller *et al.*, 1989; Onig and Bower, 1990). The method depends on the ability of indigenous microbes to degrade organic contaminants in their vicinity, provided conditions suitable for biodegradation can be created in the contaminated site. The application of microorganisms for remediation of environmental problems has aroused considerable interest in recent years with the growth of the biotechnology industry.

Various types of microorganisms capable of oxidizing petroleum hydrocarbons and related compounds (directly or by co-oxidation) are widespread in nature. Over two hundred species of bacteria, yeasts and filamentous fungi have been shown to metabolize one or more hydrocarbon compounds ranging in complexity from methane to compounds of over forty carbon atoms (Zobell, 1973). Microbial activities in hydrocarbon impacted sites are well documented (Jabson *et al.*, 1972; Atlas, 1981; Bakers and Morita, 1983; Bewley *et al.*, 1989; Leahy and Colwell, 1990; Atlas, 1991; Chunga and King 2001). In the

process of utilizing these hydrocarbons as energy sources, they are broken down to carbon (iv) oxide, water and a number of intermediates. Independent research results by Hong-gyus (1990) and Boonchan *et al.* (2000) have shown that microorganisms capable of mineralizing petroleum hydrocarbons are present in almost any conceivable soil environment. Microbial biodegradation of polycyclic aromatic hydrocarbons (PAHs) during the process of bioremediation can be constrained by lack of appropriate nutrients, low bioavailability of the contaminants to the microbial biomass, or scarcity of PAH-biodegrading microorganisms (Xu and Obbard, 2004). However, an accelerated biodegradation can be achieved by manipulating the substrate microenvironment, such as by adding nutrients (Oh *et al.*, 2001) enhancing aerobic status i.e. oxygen availability (Symons *et al.*, 1995), introducing microbial inoculum and/or exploiting the presence in the soil of hydrocarbon degrading species of microorganisms (Rahman *et al.*, 2002; Tam *et al.*, 2002), enhancing PAH availability (Barkay *et al.*, 1999; Duke *et al.*, 2000; Bogan *et al.*, 2003), or by co-metabolism, a term which describes the process whereby a microorganism utilizes a readily degradable substrate as the carbon (energy) source to degrade an organic compound that it is unable to use as a sole carbon (energy) source (Zhang *et al.*, 1998). In addition, the degradation pathway is found to be dependent on water, temperature, pH and inorganic nutrients.

The fate of hydrocarbon spill in the soil/sediment environment is determined by the apparently complex physical and chemical alterations occurring with time. Reliable predictions of the fate and transport of PAHs in soils under various conditions are critical for proper prompt remediation, risk assessment and influences the environmental acceptability of treated soils.. The rates of these changes are influenced by a variety of abiotic environmental parameters, as well as the physicochemical properties inherent to the PAH itself including molecular structure which depend on the molecular volume, presence of co-solutes (hydrocarbon mixtures), presence of active groups (Burwood and Speers, 1974) and thermodynamic stability of the PAHs (Mueller *et al.*, 1989). Extensive studies have been conducted to evaluate sorption and desorption kinetics of PAHs in soils and sediments (Peters *et al.*, 1999; Rockne *et al.*, 2002; Loor *et al.*, 1996). These works, however, failed to address solute transport based on convective-diffusive mass transfer occurring in the subsurface. Sorption of contaminants to mineral and organic surfaces controls contaminant bioavailability and hence the rate and extent of biodegradation. Hatzinger and Alexander (1995) prescribed the phenomenon of aging in which it was found that the biodegradation rates of organic compounds decreased with increasing age in both high and low organic matter soils. They attributed this to the fact that a slow sorption following the initial rapid and reversible sorption was

responsible for the chemical fraction that was very resistant to desorption.

Studies on contaminant sequestration and bioavailability as reported by Alexander (1995) indicate:

- (i) That the aging process results in the movement of contaminant to the interior of soil particles thereby becoming sequestered;
- (ii) The availability of some contaminants decline with decreasing periods of time because they become sequestered and
- (iii) Concentration of contaminants as determined by solvent extraction is not an appropriate predictor of availability and toxicity.

The availability, mobility and toxicity of contaminants in the soil is a function of its measured concentration and the mechanism of distributing the contaminants into surfaces and into pores of individual soil particles, the chemical properties of the soil, the time of contact between contaminants and soil (i.e. aging) and the type and extent of treatment of soil (Alexander, 2000). As a result of the very low water solubility and high octanol-water partitioning coefficient (k_{ow}), they tend to sorb to the organic matter in the soil instead of being solubilized in the infiltrating water and through this be transported downward to the groundwater reservoirs. The sorption process is thus counteractive to efficient biodegradation because it decreases bioavailability since the compounds

due to sorption will be located in microporous areas of the soil inaccessible to the bacteria (Zhang *et al.*, 1998). Walter *et al.*, (1992) further showed that sorption of organic pollutants onto soil organic matter significantly affects biodegradability as well as biotoxicity. PAHs have also been reported to be partitioned or incorporated more or less reversibly into the humic substances of the soil after partial degradation and thereby become even more immobilized in the soil (Kastner *et al.*, 1999; Ressler *et al.*, 1999).

Development of the treatment process would therefore involve the selection of appropriate pollutant-degrading microorganisms and suitable reagents, optimization of the chemical supplements required to achieve effective biodegradation in microcosm systems and finally, optimization of the physical conditions most conducive to microbial activity in the field (Bewley *et al.*, 1989)

2.1 Adsorption-Reaction-Desorption in Bioremediation Processes

Adsorption is a physical separation process in which certain compounds of a fluid phase are transferred to the surface of a solid adsorbent (McCabe *et al.*, 1993). The separation is dependent on one component in a mixture being more readily adsorbed than the other components. The adsorption process takes place in three steps: macrotransport,

microtransport and sorption. Macrotransport involves the movement of the organic material through the water to the liquid-solid interface by advection and diffusion. Microtransport involves the diffusion of the organic material through the macropore system of the soil particle to the adsorption sites in the micropores and submicropores of the soil particle.

The adsorption which results from the influence of Van der Waals forces is essentially physical in nature. Due to the fact that the forces are not strong, the adsorption may be easily reversed. However, in some systems, additional forces bind adsorbed molecules to the solid surface. These are chemical in nature involving the exchange or sharing of electrons, or possibly molecules forming atoms or radicals. In such cases, the term chemisorption is used to describe the phenomenon (Coulson and Richardson, 2006). This is less easily reversed than physical adsorption, and regeneration may be a problem.

Adsorption equilibrium is a dynamic concept achieved when the rate at which molecules adsorb unto a surface is equal to the rate at which they desorb. The theoretical adsorption capacity of the soil for a particular contaminant solute can be determined by calculating its adsorption isotherm.

Unlike absorption, in which solutes diffuse from the bulk of a gas to the

bulk of a liquid phase, in adsorption, molecules diffuse from the bulk of a fluid to the surface of a solid adsorbent, forming a distinct adsorbed phase (Coulson and Richardson, 2006). Solid surfaces tend to attract components of gases and liquids surrounding them. These components often collect as monolayer or sometimes as multilayers on the surfaces. In most, but not all cases, the adsorbent (the solid) bind the components (adsorbates) reversibly so that the adsorbents can be reused. Most solids (adsorbents) are very porous and most of their surface area is the interior of the adsorbent. Thus, the adsorption process consists of the sequence of mass transfer operations whereby the solute is transported into the interior of the adsorbent where it is adsorbed.

During bioremediation, the adsorption of the contaminant solutes is followed by a chemical reaction, leading ultimately to the transformation of the adsorbates and finally the release or desorption of the products of the metabolic process (Lapinskas, 1989).

In this study, the solid adsorbents are the spherical soil particles in which indigenous microorganisms present are perceived to play the role of a catalyst pellet in an irreversible reaction. Adsorption takes place primarily on the walls of the pores or at specific sites inside the particle. The overall reaction rate is influenced by the intrinsic kinetics, mass transfer resistance within the pores of the soil particles and resistance to mass

transfer of the solute (contaminant) to the outer surface of the particles (Coulson and Richardson, 2000).

In general, the concentration of the contaminant will decrease from C_o in the bulk of the fluid to C_i at the surface of the particle, to give a concentration driving force of $(C_o - C_i)$. Hence, within the pellet, the concentration will fall progressively from C_i with distance from the surface. This presupposes that no distinct adsorbed phase is formed in the pores.

The process of adsorption has been described as one of the most important chemical processes in soils (Brady and Weil, 1999, Sparks, 2003). It determines the quantity of plant nutrients, metals, pesticides and other organic chemicals retained on soil surfaces and is therefore one of the primary processes that affects the transport of nutrients and contaminants in soil. Both physical and chemical forces are involved in the adsorption of solutes from solution. The physical forces include van der Waal forces and electrostatic interactions between ion or dipole and surfaces (ion exchange), while the chemical forces include inner sphere complexation that involved a ligand exchange mechanism, covalent bonding and hydrogen bonding. The surface of a solid represents an interface between the gas or solution phase and mineral crystal. It consists

of discrete sites and each one individually participates in a reaction resulting in sorption (Sposito, 1994). Sorption can be affected by a number of factors which include surface area, mineral surface properties, organic carbon and the organic carbon distribution coefficient (k_{oc}), solubility of solutes, temperature, pH and salinity (Weissenfels *et al.*, 1992; Rockne *et al.*, 2002; Kukkonen, 2003).

When a fluid containing sorbates flows through the soil/sediment matrix, the sorbates are transferred from the flowing stream to the pore fluid at the outer surface of the particles by the mechanism of film diffusion (Treybal, 1981). Inside the particles, sorbates diffuse in the pore fluid by the mechanism of pore diffusion and are adsorbed onto the internal surface through a transfer process of solid diffusion (McCabe *et al.*, 1993; Fogler, 2006). The mass transfer kinetics of a contaminant from the bulk liquid phase to the solid phase is influenced by the presence of the solute and maybe the rate-limiting step in some instances. The mass transfer steps during the adsorption process may be described as follows:

- within the flowing fluid stream, the solute is transported by diffusion in both axial and radial directions,
- the contaminant solute is transferred from the bulk liquid phase to the liquid film surrounding the surface of the adsorbent (in this case soil particle),
- the contaminant flow via the liquid film to the interstitial voids,

pore diffusion through the voids in the solid particle and finally adsorption of the contaminant onto the soil particles.

- after adsorption, the contaminant solute may be transported along the surface or through the solid phase by diffusion.

2.2 Equilibria: Adsorption Isotherms

An isotherm is the relationship that shows the distribution of an adsorbate (material adsorbed) between the adsorbed phase (that adsorbed on surface of adsorbent) and the solution phase at equilibrium keeping the temperature constant (McCabe *et al.*, 1993; Coulson and Richardson, 2006). The capacity of an adsorbent for a particular adsorbate involves the interaction of three properties: the concentration, C , of the adsorbate in the fluid phase, the concentration C_s , of the adsorbate in the solid phase and the temperature of the system. In the mathematical description of adsorption and reaction processes in porous media, the choice of the applicable adsorption isotherm is very crucial to system specification.

Linear isotherms are used for dilute systems where linearity prevails while the Freundlich and Langmuir isotherms are applicable to adsorption and reaction systems in which concentrated media are encountered and hence they are described as non-linear adsorption isotherms. For gases, the concentration is usually given in mole percent or as a partial pressure,

while for liquids; the concentration is often expressed in mass units, such as microgram, milligram or gram. The concentration of the adsorbate on the solid is given as mass adsorbed per unit mass of original adsorbent.

For a typical isotherm shape, the ordinate-abscissa coordinate system is applicable where the mass adsorbed/weight of solid (ordinate) is plotted against the equilibrium concentration of adsorbate in solution after adsorption (abscissa). The linear isotherm goes through the origin and the amount adsorbed is proportional to the concentration in the fluid. On the one hand, isotherms that are convex upward are called favourable, because a relatively high solid loading can be obtained at low concentration in the fluid; while on the other hand, an isotherm that is concave upward is called unfavourable because relatively low solid loadings are obtained. Concave upward isotherms lead to long mass-transfer zones in the bed. However, if the adsorption isotherm is favourable, mass transfer from the solid back to the fluid phase has characteristics similar to those for adsorption with an unfavourable isotherm.

The limiting case of a very favourable isotherm is irreversible adsorption, where the amount adsorbed is independent of concentration down to very low values. All systems show a decrease in the amount adsorbed with an

increase in temperature. The adsorbate can thus be removed by raising the temperature. However, desorption requires a much higher temperature when the adsorption is strongly favourable or irreversible than when the isotherms are linear.

2.3 Model Isotherms

There are three generally recognized mathematical relationships that were developed to describe the equilibrium distribution of a solute between the dissolved (liquid) and adsorbed (solid) phases. These relationships help interpret the adsorption data obtained during constant temperature tests, referred to as adsorption isotherms. They include the following:

2.3.1 Langmuir Isotherm

The Langmuir adsorption isotherm equation was derived on the basis of the following assumptions:

- (i) Fixed individual sites exist on the surface of the adsorbent
- (ii) Each of these sites is capable of adsorbing one molecule, resulting in a layer of one molecule thick over the entire adsorbent surface
- (iii) All sites adsorb the adsorbate equally
- (iv) Adsorption is reversible.

It is defined by the expression

$$\frac{x}{m} = \frac{abC_e}{1 + bC_e} \quad (2.1)$$

Where $\frac{x}{m}$ = amount adsorbed per unit weight of adsorbent (soil).

a, b = empirical constants

C_e = equilibrium concentration of adsorbate in solution after adsorption.

The constants in the Langmuir isotherm can be determined graphically

using the equation $C_e / \left(\frac{x}{m} \right) = \frac{1}{ab} + \frac{1}{a} C_e$.

Where $C_e / \left(\frac{x}{m} \right)$ is the ordinate, C_e , abscissa, $\frac{1}{ab}$ and $\frac{1}{a}$ are the intercept and slope respectively.

2.3.2 Freundlich Isotherm

The Freundlich isotherm equation assumes that:

- (i) The adsorbent has a heterogenous surface composed of adsorption sites with different adsorption potentials.
- (ii) Each class of adsorption sites adsorbs molecules as in the Langmuir equation.

This isotherm equation is the most widely used. Freundlich in 1926 (McCabe *et al.*, 1993), showed that an adsorption study data could be correlated using an equation of the form:

$$\frac{x}{m} = kC^{1/n} \quad (2.2)$$

where x is the amount of solute adsorbed, m (mg), mass of adsorbent (mg) C , the concentration of adsorbate remaining in solution after

adsorption is complete i.e. at equilibrium (mg/l). k , n are empirical constants that must be determined experimentally for each solute type and temperature. A plot of $\log \frac{x}{m}$ against $\log C$, gives a straight line with slope $\frac{1}{n}$ and intercept k .

2.3.3 Brunauer, Emmett and Teller (BET) Equation

The third adsorption isotherm model is the BET equation. It assumes that

- (i) Adsorbent surface is composed of fixed individual sites
- (ii) Molecules can be adsorbed more than one layer thick on the surface of the adsorbent
- (iii) The energy required to adsorb the first particle layer is adequate to hold the monolayer in place.

2.4 Use of Biosurfactants in Soil Remediation

Many organic contaminants of interest tend to sorb onto soil such that only a small fraction of the compound may actually be in the bulk water phase. Over long contact time, the sorbing pollutants slowly diffuse into the organic and inorganic matrix and likely form bound residues (Bouwer *et al.*, 1997).

The accumulation of contaminants in fissures and cavities within

subsurface soils renders them inaccessible to microorganisms and their enzymes, thus, limiting the bioavailability of these contaminants for microbial utilization. The practical effect of the resulting slow diffusion of contaminants within the soil aggregates, coupled with other kinetic limitations of desorption, results in a concomitant decrease in the rate of removal of the contaminant. Sorption and transport processes which ultimately determine the fate of PAHs can be affected by surfactants due to admicellar sorption, which is the partitioning of components between an aqueous phase and an adsorbed surfactant phase. Results from several studies suggest that non-aqueous phase compound dissolution in saturated porous media is positively dependent on the interstitial water velocity (Imhoff *et al.*, 1994; Seagren and Moore, 2003; Chrysikopoulos *et al.*, 2003). However, surfactants may also retard the transport of contaminants due to the partitioning of the contaminants to an adsorbed surfactant phase. Enhanced apparent solubility of contaminant PAHs was found to be significantly dependent on the critical micelle concentration (CMC). No enhanced solubility of PAH was detected at surfactant concentrations below the CMC (Koeppel, 1997). The influence of surfactant on the sorption of hydrophobic components by both solubilization and admicellar sorption has also been documented by Brown (2007). From the result of the liquid chromatography study, the presence of surfactants in the mobile phase at submicellar concentrations

was found to increase the retardation of certain solutes, but decreased retardation when used at supramicellar concentrations.

Facilitated bioavailability resulting from the use of surfactants refers to the ability of an organism to have access to pools of non-labile chemical. Mechanisms proposed for this ability include the release of biosurfactants, direct mining of adsorbed chemical and alteration of interfacial chemistry and passive effects of attached biofilms on molecular diffusion (Pignatello and Li, 2006). Results of their investigation revealed that the ability of nutrients to accelerate degradation of bioavailable PAHs by native cells indicated that the persistence of PAHs for many decades at the site was likely due to nutrient-limited natural attenuation. It was thus suggested that the application of surfactants promotes facilitated bioavailability of PAHs in the soil to indigenous microorganisms. Zhu *et al.*, (2004) examined the sorption behaviour of PAHs (solutes) in soil-water systems containing surfactants for better understanding of the fate of contaminants in natural systems and the feasibility of using surfactants for remediation of contaminated soils. Their report showed that the ratio of apparent sorption coefficients to the intrinsic coefficients, varied from greater to less than one depending on the system.

The prospects for the use of biosurfactants in soil remediation are dependent on the capacity of these compounds to enhance the solubility and thus promote the movement of non-aqueous phase solids and liquids whose dissolution are very slow and mass-transfer limited (Vogler and Chrysikopoulos, 2004). Literature findings have revealed that surfactants are implicated in facilitating or enhancing the dissolution of PAHs in aqueous phase liquids with the concomitant increase in biodegradation rates, applied for stimulating the dissolution of non-aqueous phase liquids initially present in soil, the dissolution of solid contaminants and the desorption and transport of soil-sorbed contaminants (Pennel *et al.*, 1993; Mason and Kueper, 1996; Fortin *et al.*, 1997; Brown *et al.*, 1999; Brown and Jaffe, 2006). A closely related aquifer remediation technology involves the use of surfactants that can reduce the surface tension and also enhance the dissolution and mobilization of dense nonaqueous phase (DNAP) compounds. Addition of synthetic surfactant resulted in increased mobility and solubility of PAHs, which is essential for effective microbial degradation (Tiehm, 1994). In recent times, Urum and Pekdemir (2004) evaluated the ability of aqueous biosurfactants solutions for possible applications in washing crude oil contaminated soil. They reported that oil removal was due to mobilization caused by the reduction of surface and interfacial tensions. The study suggested that knowledge of surfactants behavior across different systems is paramount before their

use in the practical application of oil removal.

2.5 Biodegradation Kinetics

The process of the biodegradation of contaminants in the soil/sediment matrix is complex and involves the diffusion of contaminants in the porous soil matrix, adsorption to the soil surface, biodegradation in the biofilm existing on the soil surface and in the large pores as well as in the bound and free water phase after desorption from the soil surface. The availability, mobility and toxicity of contaminant PAHs in the soil is not a function of its measured concentration, but depends on the physical/chemical mechanisms of distributing the chemicals onto surfaces and into pores of individual soil particles, chemical properties of the soil, molecular size, i.e., the number of aromatic rings, molecular topology or the pattern of ring linkage, the time of contact between chemicals and soil (i.e. aging), the type and extent of treatment of soil (Alexander, 1995; Carmichael and Pfaender, 1997; Kanaly and Harayama, 2000; Gosh *et al.*, 2001; Oleszczuk and Baran, 2003; Shor *et al.*, 2004).

Extensive work has been done on the kinetics of biodegradation. The most celebrated is the Michaelis-Menten kinetics 1913 (Levenspiel, 1999; Fogler, 2006) in which the rate of degradation was correlated with time. The mechanism of biodegradation of PAHs is dependent on the structural

configuration of the compounds, environmental conditions and the microbial species (Guthrie and Pfaender 1988; Lamoureux *et al.*, 1999; Oleszczuk and Baran, 2003). Effective bioremediation can thus reduce contaminant concentration in soil to a level where they are postulated to no longer pose an unacceptable risk to the environment. This represents environmentally acceptable end points (EAEs); i.e. they no longer harm ecological receptors or human health. The chemicals that remain in soil thus exhibit reduced toxicity and leachability compared to chemicals freshly added to soils.

The kinetics of research studies on effective biotreatment of PAHs in the soil environment indicates that contaminants are biodegraded by indigenous soil microbiota to a “plateau” concentration (Tabak and Govind, 1997). Some of the interpretations of important experimental results show that:

- i. Only limited biological activities exist within the intraparticle pores;
- ii. Many species of bacteria are known to bio-degrade only the more soluble polycyclic aromatic hydrocarbons;
- iii. Many organic contaminants of interest tend to sorb onto soils so that only a small fraction of the compound may actually be in the water phase;

- iv. Prolonged exposure of these contaminants in fissures and cavities within subsurface solids renders them inaccessible to microorganisms and their systems, and also decreases their bioavailability; and
- v. The constituents of contaminant at the site are likely less available for microbial utilization because they reside on the surface or in the pores of the soil particle.

There is no systematic methodology in the open literature (as far as the author knows) that quantitatively determine biodegradation kinetics of PAHs in compacted soil systems. However, a systematic multilevel protocol using soil slurry, wafer and column reactors has been developed to determine the biokinetic parameters for toxic organic pollutants (Tabak and Govind, 1997; Reardon *et al.*, 2002). Chemicals, which become transported to micropores of soil particles, are bounded to humic solids. The longer the contaminant remains in soil, the less rapidly it is removed by solvents. Sorption entails slow and continuing diffusion to remote sites of solid particles and that desorption involves a very slow diffusion from remote sites to surface of soil particles. More precisely, it can be presupposed that the solute is first adsorbed on the surface, where a heterogeneous reaction takes place and its products, which are supposed to be inactive and of very low concentration, are desorbed into the fluid.

The adsorption is assumed to take place on vacant sites that are normally distributed over the solid surface, whereas the overall rate of the process is determined from basic thermodynamics (Coutelieres *et al.*, 2004).

Assessing the availability of the remaining contaminant is a critical issue which influences the environmental acceptability of treated soil. Therefore, information is still needed to correlate the effect of treatment of soil contaminated with hydrocarbons on the concentration, mobility and toxicity of these organics. The patterns of disappearance as indicated by Tabak and Govind (1997) showed a rapid decline of concentration of PAHs during the initial stage of bioremediation followed by a declining rate of reduction of chemicals that ultimately approaches zero over time. The extent of contaminant removal and final concentrations achieved, differed among different soils.

Substrates interactions were observed in biodegradation kinetics of PAH mixtures and the best model to describe these interactions is a multisubstrate model. Results from multi-substrate models (Guha *et al.*, 1999; Knightes, 2000) indicate that the biodegradation rates of the more degradable and abundant compounds are reduced due to competitive inhibition, but enhanced biodegradation of the more recalcitrant PAHs occurs due to simultaneous biomass growth on multisubstrates.

CHAPTER THREE

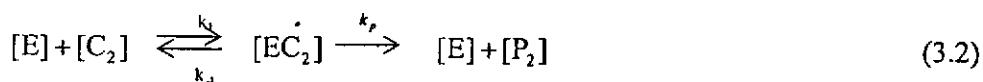
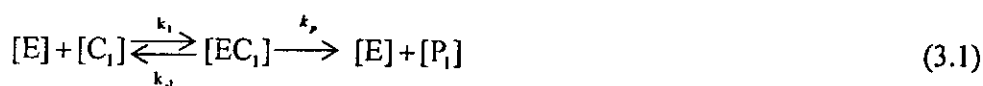
3.0 MODEL DEVELOPMENT FOR STEADY STATE BIOFILM KINETICS

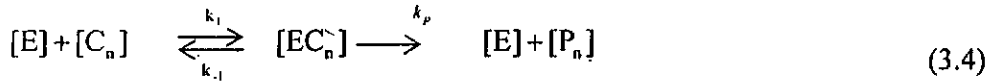
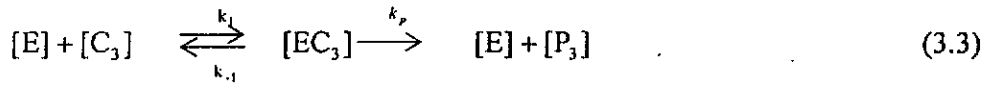
3.1 Kinetic and Molecular Diffusion in the Interface Film

Generally, the kinetics of an enzyme catalyzed reaction of a given contaminant (substrate) such as petroleum hydrocarbons can be presented along the twin concepts of rate-determining step and the steady state approximation (Susu, 1997; Fogler, 2006). Consider, for an example, the following enzyme-catalyzed reaction scheme where a substrate, C, reacts with an enzyme, E, to form an enzyme-substrate complex EC, to yield a product, P; the enzyme is recovered, like a true catalyst. Two reactive schemes will be used in deriving the kinetics of this simple reaction. The first uses the concept of rate-determining step and the second uses the steady state approximation.

3.1.1 Intrinsic Kinetics using Rate-Determining Step

The kinetic sequence is given below:





The mathematical formulations for both single and multisubstrate enzyme catalyzed reactions are developed below.

3.1.2 Single Substrate Catalyzed Reaction

The rate of product formation depends on the dissociation of product forming complex, and by simple kinetic scheme, the rate of reaction is given by:

$$r = k_p [EC] \quad (3.5)$$

A material balance on the enzyme distribution in the reacting system yields:

$$[E_t] = [E] + [EC] \quad (3.6)$$

Combining equations (3.5) and (3.6),

$$\frac{r}{[E_t]} = \frac{k_p [EC]}{[E] + [EC]} \quad (3.7)$$

The dissociation constant k_s can be expressed as the ratio of the rate constant k_1 and k_{-1} :

$$k_s = \frac{k_1}{k_{-1}} = \frac{[E][C]}{[EC]} \quad (3.8)$$

$$[EC] = \frac{[E][C]}{[k_s]} \quad (3.9)$$

Substituting equation (3.9) into equation (3.7), yields:

$$\frac{r}{[E_t]} = \frac{\frac{k_p[C][E]}{k_s}}{[E] + \frac{[C][E]}{k_s}} \quad (3.10)$$

By appropriate mathematical approach, equation (3.10) becomes:

$$\frac{r}{k_p} = \frac{[E_t][C][E]}{k_s[E] + [C][E]} \quad (3.11)$$

$$\frac{r}{k_p[E_t]} = \frac{[C][E]}{[E](k_s + [C])} \quad (3.12)$$

But the rate of formation of product will be maximal when the total enzymes form a complex. Hence,

$$k_p[E_t] = r_{\max} \quad (3.13)$$

Therefore, substituting (3.13) into (3.12), we have:

$$\frac{r}{r_{\max}} = \frac{[C]}{k_s + [C]} \quad (3.14)$$

For a single hydrocarbon, equation (3.14) becomes:

$$r = \frac{r_{\max}[C]}{k_s + [C]} \quad (3.15)$$

But the rate of hydrocarbon degradation is:

$$r = \frac{dC_t}{dt} \quad (3.16)$$

Hence combining equation (3.15) and (3.16) and on rearrangement, we have:

$$r_{\max} dt = \left(\frac{k_s + [C]}{[C]} \right) dC \quad (3.17)$$

Equation (3.17) can be expressed as

$$r_{\max} dt = \sum_{i=1}^n \left(1 + \frac{k_s}{C} \right) dC \quad (3.18)$$

For a single substrate system,

$$r_{\max} dt = \left(\frac{k_{s_i}}{C_i} + 1 \right) dC_i \quad (3.19)$$

On integration, equation (3.19) yields:

$$r_{\max} t = k_s \ln \frac{C_0}{C_0 - C} + (C_0 - C) \quad (3.20)$$

3.1.3 Multisubstrate Catalyzed Reaction

Multi-substrate feed (a mixture of hydrocarbons) has been found to be present during petroleum spill. Consequently, the velocity at any given time is the sum of the velocities contributed by degrading microbes.

Therefore, from equation (3.19), the rate can be represented as:

$$\frac{dC_i}{dt} = \frac{r_{\max 1} [C_1]}{k_{s1} + [C_1]} + \frac{r_{\max 2} [C_2]}{k_{s2} + [C_2]} + \dots + \frac{r_{\max n} [C_n]}{k_{sn} + [C_n]} \quad (3.21)$$

Equation (3.21) can be re-written as:

$$\frac{dC_i}{dt} = \sum_{i=1}^n \frac{r_{\max i} [C_i]}{k_{si} + [C_i]} \quad (3.22)$$

Let $r_{\max}^* = \sum r_{\max i}$

$$\frac{dC_i}{dt} = r_{\max i}^* \sum_{i=1}^n \frac{[C_i]}{k_{Si} + [C_i]} \quad (3.23)$$

and r_{\max}^* is given by:

$$r_{\max}^* dt = \frac{dC_i}{\sum_{i=1}^n \frac{[C_i]}{k_{Si} + [C_i]}} \quad (3.24)$$

Integrating both sides of equation 3.24, we have

$$\begin{aligned} r_{\max}^* t &= \sum [k_{Si} \ln C_i + C_i]_0^n \\ r_{\max}^* t &= \sum k_{Si} \ln \left[\frac{C_n}{C_0} \right] - [C_0 - C_n] \end{aligned} \quad (3.25)$$

For all values of $i = 1 \text{---} n$

3.1.4 Coupling Kinetics and Molecular Diffusion

Recall Fick's law of molecular diffusion,

$$\frac{D_r d^2[C]}{dx^2} = \frac{d[C]}{dt} + r \quad (3.26)$$

At steady state, $dC/dt = 0$

Therefore,

$$\frac{D_r d^2[C]}{dx^2} - r = 0 \quad (3.27)$$

From equation (3.27):

$$D_r d^2[C] = r dx^2 \quad (3.28)$$

Integrating both sides of equation (3.28),

$$D_r d[C] = r dx$$

$$\text{Thus, } \frac{D_r d[C]}{dx} = r \quad (3.29)$$

Therefore, substituting equation (3.29) into equation (3.27), we have:

$$\frac{D_r d^2[C]}{dx^2} - \frac{d[C]}{dx} = 0 \quad (3.30)$$

Equation (3.30) can be resolved by the method of solution as applied by Jenson and Jeffreys (1966); Coulson and Richardson (2000).

Thus,

$$[C] = A + Be^x \quad (3.31)$$

Similarly, for a multisubstrate catalyzed reaction, equation (3.30) holds and the same method of solution as in the single substrate catalyzed reaction applies.

Therefore,

$$[C] = A + Be^x + \frac{(i-1)}{x} - 1 \quad (3.32)$$

For all values of $i = 1 \dots n$

The constants A and B in equation (3.31) and (3.32), can be solved for by using the following boundary conditions:

$$\text{At } x = 0, \quad C = C_0$$

$$x = L, \quad C = 0$$

Thus

$$A = \frac{1}{2} \left[\frac{C_0 e^L}{e^L - 1} + C_0 \right] \quad (3.33)$$

$$B = \frac{-C_0}{2(e^L - 1)} \quad (3.34)$$

Substituting the values of A and B into equation (3.31), we have:

$$C = \frac{1}{2} \left[\frac{C_0 e^L}{e^L - 1} + C_0 \right] - \left[\frac{C_0 e^x}{2(e^L - 1)} \right] \quad (3.35)$$

Equation (3.33) describes the model equation for a single substrate catalyzed reaction in the interface film.

In the same way, substituting A and B into equation (3.32)

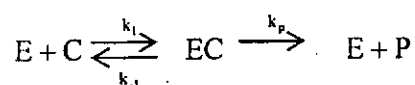
$$C = \frac{1}{2} \left[\frac{C_0 e^L}{e^L - 1} + C_0 \right] - \left[\frac{C_0 e^x}{2(e^L - 1)} \right] + \frac{n-1}{x} - 1 \quad (3.36)$$

$n \neq 0$

Equation (3.36) above describes the model equation for a multisubstrate catalyzed reaction in the interface.

3.1.5 Intrinsic Kinetics using Steady state approximation

Using the elementary steps for the biodegradation of the hydrocarbon components and applying the steady state approximation technique for deriving the rate expression,



$$\frac{d[P]}{dt} = k_p [EC] \quad (3.37)$$

Enzyme conservation $E_T = E + EC$

$$\frac{d[EC]}{dt} = k_1[E][C] - k_{-1}[EC] + k_p EC \quad (3.38)$$

By the steady state approximation,

$$\frac{d[EC]}{dt} = 0 \quad (3.39)$$

The reactive intermediate concentration is so small and as such, it can be assumed that the rate of change is negligible and hence zero or its rate of change is assumed to be at equilibrium with the reactants (Susu, 1997; Levenspiel 1999; Bailey and Ollis, 1977).

Eliminating $[E]$ in equation (3.38), we have:

$$k_1[C][E_T] - [EC] = k_{-1}[EC] + k_p[EC]$$

$$k_1[C][E_T] - k_1[C][EC] = k_{-1}[EC] + k_p[EC]$$

$$k_1[C][E_T] = k_1[C][EC] + k_{-1}[EC] + k_p[EC]$$

and

$$EC = \frac{k_1[C][E_T]}{(k_{-1} + k_p) + k_1[C]} \quad (3.40)$$

Putting equation (3.40) into equation (3.37), we have:

$$\frac{d[P]}{dt} = \frac{k_p k_1 [C][E_T]}{(k_{-1} + k_p) + k_1 [C]}$$

and

$$\frac{d[P]}{dt} = \frac{k_p [E_T][C]}{\left(\frac{k_{-1} + k_p}{k_1} \right) + [C]} = \text{rate of reaction for single substrate} \quad (3.41)$$

Let $\frac{k_{-1} + k_p}{k_1} = \text{constant } M$ (usual form of Michaelis - Menten constant)

$$\frac{d[P]}{dt} = \frac{k_p [E_T][C]}{M + [C]}$$

Therefore, the rate of reaction is given by the rate of disappearance of the reactant or the rate of production of the product of reaction:

$$r = \frac{-d[C]}{dt} = \frac{d[EC]}{dt} = \frac{d[P]}{dt} \quad (3.42)$$

For multi-substrate reaction scheme, the rate of reaction is given by:

$$r = \frac{\sum_{i=1}^n k_p [E_T][C_i]}{\frac{k_{-1} + k_p}{k_1} + \sum_{i=1}^n C_i} \quad (3.43)$$

3.1.6 Coupling Kinetics and Molecular Diffusion

Equations (3.41) and (3.43) when incorporated into the equation of Fick's law of molecular diffusion gives:

$$D_r \frac{d^2 C}{dx^2} - \frac{k_p [E_T][C_0]}{\left(\frac{k_{-1} + k_p}{k_1} \right) + [C_0]} = 0 \quad (3.44)$$

Rearrangement yields:

$$D_r \frac{d^2 C}{dx^2} - \frac{k_p [E_T][C_0]}{M + [C_0]} = 0 \quad (3.45)$$

Further,

$$\frac{D_r d^2 C}{dx^2} = \frac{k_p [E_T] [C_0]}{M + [C_0]} \quad (3.46)$$

Integration of equation (3.46) yields:

$$D_r \int dC = \frac{k_p [E_T] [C_0]}{M + [C_0]} \int dx \quad (3.47)$$

Solution of equation (3.47) yields:

$$D_r C = \frac{k_p [E_T] [C_0]}{M + [C_0]} x \quad (3.48)$$

And rearrangement of equation (3.48) yields:

$$C = \left(\frac{k_p [E_T] [C_0]}{M + [C_0]} \right) \frac{x}{D_r} \quad (3.49)$$

Equation (3.49) represents the model equation for a single substrate catalyzed reaction.

Similarly, for a multisubstrate catalyzed reaction,

$$C = \sum_{vi} \left(\frac{V_{max} [C_i]}{M + [C_i]} \right) \frac{x}{D_r} \quad (3.50)$$

Equation (3.50) is rearranged to yield:

$$C = \frac{V_{max} \sum_{vi} [C_i]}{M + \sum_{vi} [C_i]} \frac{x}{D_r} \quad (3.51)$$

The selection of which relationship will be applicable in any specific case will be determined by how well the prediction of experimental data mirrors the simulated prediction.

3.2 Kinetic Model of Biofilm at Steady State

A direct impact of sorption on biodegradation is the reduction of organic contaminants in the bulk water phase. For a microorganism assumed spherical, with a spherical shape and radius R , a relatively stagnant zone of thickness L , is assumed to surround a microbial cell. At steady state, the rate of substrate utilization within the cell must be equal to the rate of substrate transport into the cell. We also utilize the concept of minimum substrate concentration (C_{\min}) introduced by Rittman and McCarty (1980).

This defines a critical cell concentration below which the biofilm will have a negative growth rate and above which it will have a positive growth rate; the biofilm can thus grow beyond the monolayer limit, until it reaches its steady state thickness. A biofilm is described as a layer-like aggregation of microorganisms attached to a solid surface. The rate of substrate utilization is dependent on the mass of biofilm present. It is intuitive that the mass of biofilm will be large when the substrate concentration in the bulk liquid is high since the bacteria will be able to capture chemical energy and convert some partially to cell mass at a fast

rate. Conversely, when the substrate concentration is low, the rate of energy capture becomes low and at sufficiently low concentration, the rate of energy capture may be less than the rate of energy expenditure required to sustain the viability of the bacteria. The task therefore is to define a minimum bulk contaminant concentration that will allow a steady state monolayer to exist. This objective can be achieved by establishing the relationship showing the interdependence between contaminant utilization and the rate of contaminant transport.

Due to the specific sequence of elementary steps encountered during diffusion of compounds, geometric and mass transfer restrictions are likely to occur. These cause most bacteria to be present in the external surface of soil particles and in the bulk aqueous phase (Rittman and McCarty, 1980). Since only limited biological activities exist within the intraparticle pores, the influence of mass transfer on biodegradation therefore becomes important and this has been characterized by a single parameter, bioavailability as given by Bouwer *et al.*, 1997.

The contaminant and oxygen consumption rates are considered important parameters characterizing a biological reaction. This is because they have been proposed as a means of adaptive control of biodegradation process taking place in a perfectly mixed bioreactor (Babary, 1999). However, it

is not adequate to simply transfer sufficient oxygen to the bulk liquid medium in cell systems. Oxygen must also be transferred from the bulk liquid to the cells. For instance, the transfer of oxygen must be achieved from a gas bubble through the liquid medium to the micropores of the cells. The resistance to oxygen transfer as well as the oxygen transfer rate from the gas phase to the inside of the micropores has been reported (Coosen, 2002). In order to ensure the survival of the cells in the micropores, the oxygen transfer rate must be greater than (or at least equal to) the oxygen consumption rate of cells inside the pores.

At steady state, the rate of contaminant utilization within the biofilm must be equal to the rate of contaminant transport into the biofilm, (Wami and Ogoni, 1997) , yielding the equation:

$$\frac{4}{3} \pi R^3 \frac{1}{Y} \frac{\mu_{\max} C_i}{K_s + C_i} = 4 \pi R^2 D_s \left. \frac{dC}{dr} \right|_{r=R} \quad (3.52)$$

This balance assumes that the Monod specific growth rate with constant yield factor and contaminant diffusion through the stagnant region (biofilm) is presumed to be governed by Fick's law (Bailey and Ollis, 1977). A mass balance on biofilm surrounding the cell is shown in Figure 3.1 below.

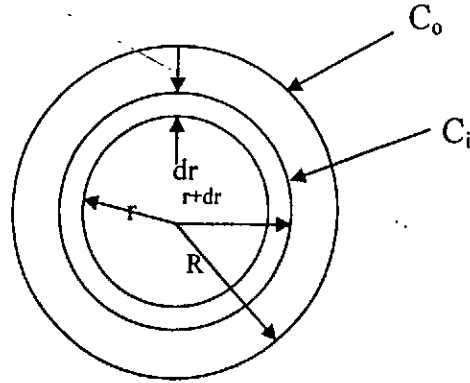


Fig. 3.1: Schematic of a cell surrounded by a biofilm

Steady state mass balance between r and $r + dr$ gives,

$$\frac{d}{dr} \left(r^2 \frac{dC}{dr} \right) = 0 \quad (3.53)$$

Since no reaction occurs in this biofilm, equation (3.53) implies that:

$$r^2 \frac{dC}{dr} = \text{constant} = c_1 \text{ within the film.} \quad (3.54)$$

Integrating equation (3.54), we have:

$$\frac{-c_1}{r} + c_2 = C \quad (3.55)$$

The constants c_1 and c_2 are evaluated by use of the boundary conditions:

$$\left. \begin{array}{l} \text{At } r = R, C = C_i \\ \text{At } r = R + L, C = C_0 \end{array} \right\} \quad (3.56)$$

Where C_0 = concentration of substrate in the bulk medium surrounding the biofilm, and

C_i = concentration of contaminant in the biofilm

Substituting the known values of r into equation (3.55), we have

$$C = (C_o - C_i) \frac{(R+L)R}{L} \quad (3.57)$$

Recalling equation (3.54), we have:

$$\begin{aligned} \left. \frac{dc}{dr} \right|_{r=R} = \frac{c_i}{r^2} &= (C_o - C_i) \left(\frac{R^2 + RL}{L} \right) \frac{1}{R^2} = \frac{R(R+L)}{R^2 L} \\ &= (C_o - C_i) \frac{R+L}{RL} \end{aligned} \quad (3.58)$$

Therefore, putting the value of $\left. \frac{dc}{dr} \right|_{r=R}$ into equation (3.52), gives:

$$\frac{(\mu_{\max} \frac{R}{3} Y) C_i}{k_s + C_i} = \frac{D_r (R+L)}{RL} (C_o - C_i) \quad (3.59)$$

Equation (3.59) is then evaluated to get C_i in terms of C_o .

But the rate of substrate utilization is given by Atkinson (1974) and Fogler (2006) as:

$$r_s = \frac{3}{R} D_r \frac{(R+L)}{RL} [C_o - C_i(C_o)] \quad (3.60)$$

Therefore, expressing C_i in terms of C_o i.e. $C_i(C_o)$,

$$C_i = \frac{1}{(\mu_{\max} \frac{R}{3} Y) D_r (R+L)} \left(\frac{D_r (R+L) C_o (\mu_{\max} \frac{R}{3} Y) \times k_s (D_r (R+L)) + RL (\mu_{\max} \frac{R}{3} Y)}{RL (\mu_{\max} \frac{R}{3} Y) - D_r (R+L) C_o} \right) \quad (3.61)$$

Thus, C_i in equation (3.61) when substituted into equation (3.60) gives the rate of substrate utilization (r_s) as:

$$r_s = \frac{3}{R} D_r \frac{(R+L)}{RL} \left(C_o - P \left(\frac{Q \times k_s (D_r (R+L)) + RL (\mu_{\max} R/3 Y)}{RL (\mu_{\max} R/3 Y) - D_r (R+L) C_o} \right) \right) \quad (3.62)$$

Equation (3.62) describes the model equation for the steady state biofilm kinetics.

C_0 is assumed to be C_{\min} and P and Q are given by:

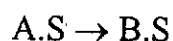
$$P = \frac{1}{(\mu_{\max} R/3 Y) D_r (R+L)} \quad (3.63)$$

$$Q = D_r (R+L) C_o (\mu_{\max} R/3 Y) \quad (3.64)$$

3.3 Development of Mathematical Model for Macroporous and Microporous Systems

A reactant once adsorbed onto a surface, is capable of reacting in a number of ways to form the reaction product (Fogler, 2006):

1. That the surface reaction may be a single-site mechanism in which only the site upon which the reactant is adsorbed is involved in the reaction. For example, an adsorbed molecule of A may isomerize (or perhaps decompose) directly upon the site to which it is attached:



2. That the surface reaction may be a dual-site mechanism in which the adsorbed reactant interacts with another site (either unoccupied or occupied) to form the product. For example, adsorbed A may react with an adjacent vacant site to yield a vacant site and a site on which the product is adsorbed:



Another example of a dual site mechanism is the reaction between two adsorbed species:



Adsorption and desorption are primary processes in the evaluation of bioavailability, and mass transfer is the mechanism of solute movement

from the fluid phase to the surface of the soil particle. The removal of contaminants by adsorption/desorption is an important step in biodegradation processes occurring in soil/sediment matrix. The design and analysis of treatment systems for the process thus require considerations for multicomponent, non-linear reaction rate expression, non-linear adsorption/desorption phenomena and the contributions of intraparticle and interparticle mass transport in the flow system.

Generally, in the discussion of rate laws and catalytic reaction steps, the effects of diffusion (mass transfer) limitations or resistance on the overall rate of processes involving both chemical reactions and mass transfer have been neglected. Two types of diffusion resistances that are applicable: (i) external resistance which is the diffusion of the reactants or products between the bulk fluid and the external surface of the soil particle, and (ii) internal resistance which is the diffusion of the reactants or products between external surface of soil particle (pore mouth) and the interior of the soil particle. The intraparticle diffusion becomes important depending on the relative values of the chemical reaction rate term and the rate of diffusion or mass transfer step (Fogler, 2006). The development of the mathematical models used in this research work, recognized the limitations highlighted above and in addition, did not fail to account for axial dispersion effects, and convective and diffusive

transfer (Bird *et al.*, 2005). Convective mass transport in swarms of particles is a commonly encountered process in a wide range of industrial and scientific applications such as fluidized beds, separation processes, filters, catalytic and non-catalytic fluid-solid reactions (Coutelieris *et al.*, 2004). The model incorporates the contributions of radial transport (pore and surface diffusion), and film resistance. The important assumptions made in the formulation of the model are: (i) constant coefficients of dispersion and diffusion, (ii) constant porosities, (iii) that the spherical soil particles have uniform size and homogeneous structure, (iv) that the intraparticle diffusion takes place in the fluid within the pores of the particles, (v) radial variations, (vi) mass transfer from the fluid stream to the ends of the soil particles is taken to be negligible in order to avoid the difficulty of treating two-dimensional diffusion within the soil particles, (vii) pore diffusion is assumed to occur in the radial direction (i.e. direction perpendicular to the direction of flow).

A material balance applied to the contaminant carried by the flowing fluid stream (macroporous system) was carried out. The mass balance of adsorbate in the pore fluid and on the soil particle surface was also carried out. A resultant differential equation defining the pore and surface concentrations inside the particles (microporous system) as a function of the radius of the soil particle and time was similarly derived. The

unsteady state model for macroporous and microporous systems thus helps to predict the concentration of contaminant in the axial and radial directions, given the concentration-time data from experiment. The model accounts for contaminant transport through a homogenous, porous media in a one-dimensional uniform flow by considering convection, dispersion, linear equilibrium sorption and first order degradation. The equations are intended for the purpose of simulating results from two fundamental processes that characterize environmental phenomena, convection due to fluid flow and dispersion/diffusion due to solute movement/transport in the subsurface.

3.4 Model Development for Macroporous and Microporous Systems

The essential assumptions made are:

1. Constant coefficient of diffusion
2. Constant porosities
3. Radial variations
4. That the microorganisms have uniform size and homogenous structure
5. That the intraparticle diffusion takes place in the fluid within the pores of the particles.

3.4.1 Macroporous System

The following assumptions were made:

1. The rate of mass transfer of the contaminant in the direction of flow of the flowing fluid stream is assumed to occur by diffusion governed by Fick's law:

$$J_{Li} = -D \frac{\partial c_i}{\partial z} \quad (3.65)$$

2. The rate of mass transfer from the bulk conditions of the fluid stream to the external pellet surface (the opening of the pores) is given by:

$$r_{Li} = K_f a (C_i - X_i)_{r=R} \quad (3.66)$$

3. A material balance on contaminant i over the time period from t to t + Δt over the element of volume of the adsorption bed, from z to z + ∂z is represented thus:

$$\begin{aligned} & (\text{Input at } z) - (\text{output at } z + \partial z) + (\text{Generation due to chemical} \\ & \text{reaction}) - (\text{Rate of transfer into solid phase}) = \text{Accumulation over} \\ & \text{time period} \end{aligned} \quad (3.67)$$

The input and output are defined by the sum of the convective and diffusive mass transfer at z and z + ∂z respectively:

Input at $z = VAC_i|_z + \varepsilon_b AJ_{Li}|_z$

Convective Diffusive
Transfer Transfer

$$= VAC_i|_z + (-\varepsilon_b AD \frac{\partial c_i}{\partial z}|_z) \quad (3.68)$$

Output at $z + \partial z = VAC_i|_{z+\partial z} + \varepsilon_b AJ_{Li}|_{z+\partial z}$

$$= VAC_i|_{z+\partial z} + (-\varepsilon_b AD \frac{\partial c_i}{\partial z}|_{z+\partial z}) \quad (3.69)$$

$$\text{Mass transfer rate into the particle} = \frac{3(1 - \varepsilon_b)}{R} D_f \left(\frac{\partial x_i}{\partial r} \Big|_{r=R} \right) A \partial z \quad (3.70)$$

Accumulation in the fluid phase in the elemental volume can be expressed as

$$= \varepsilon_b A \partial z \left(\frac{\partial C_i}{\partial t} \right) \quad (3.71)$$

since there is no reaction in the bulk fluid, i.e. all reactions take place on the catalyst surface, the reaction term is therefore equal to zero.

Incorporating equation (3.68) through equation (3.71) into equation (3.67), we have:

$$\begin{aligned}
& VAC_i \Big|_z + \left(-\varepsilon_b AD \frac{\partial C_i}{\partial z} \Big|_z \right) - VAC_i \Big|_{z+\partial z} - \left(-\varepsilon_b AD \frac{\partial C_i}{\partial z} \Big|_{z+\partial z} \right) - \frac{3(1-\varepsilon_b)D_f A \partial z}{R} \left(\frac{\partial x_i}{\partial r} \Big|_{r=R} \right) \\
& = \varepsilon_b A \partial z \left(\frac{\partial C_i}{\partial t} \right)
\end{aligned} \tag{3.72}$$

Collecting terms in equation (3.72) yields;

$$\varepsilon_b AD \left(\frac{\partial C_i}{\partial z} \right)_{z+\partial z} - \left(\frac{\partial C_i}{\partial z} \right)_z - VA(C_i|_{z+\partial z} - C_i) - \frac{3(1-\varepsilon_b)D_f A \partial z}{R} \left(\frac{\partial x_i}{\partial r} \Big|_{r=R} \right) = \varepsilon_b A \partial z \left(\frac{\partial C_i}{\partial t} \right) \tag{3.73}$$

Applying the mean value theorem of differential calculus to the first two terms on the LHS of equation (3.73) and taking the limits as $\partial z \Rightarrow 0$, we have:

$$\varepsilon_b AD \left(\frac{\partial^2 C_i}{\partial z^2} \right) \partial z - VA \left(\frac{\partial C_i}{\partial z} \right) \partial z - \frac{3(1-\varepsilon_b)D_f A \partial z}{R} \left(\frac{\partial x_i}{\partial r} \Big|_{r=R} \right) = \varepsilon_b A \partial z \left(\frac{\partial C_i}{\partial t} \right) \tag{3.74}$$

Dividing equation (3.74) by $\varepsilon_b A \partial z$, we have:

$$D \frac{\partial^2 C_i}{\partial z^2} - \frac{V}{\varepsilon} \frac{dC_i}{dz} - \left(\frac{1-\varepsilon}{\varepsilon} \right) \left(\frac{3}{R} \right) D_f \left(\frac{\partial x_i}{\partial r} \Big|_{r=R} \right) = \frac{\partial C_i}{\partial t} \tag{3.75}$$

Equation (3.75) thus gives a generalized model expression for a macroporous system.

However, if a linear (film diffusion) model for interphase mass transfer is assumed, we would have

$$D_f \left(\frac{\partial x_i}{\partial r} \right) = K_{f,i}(C_i)_{r=R} \tag{3.76}$$

Substituting equation (3.76) into (3.75), we obtain:

$$D \frac{\partial^2 C_i}{\partial z^2} - \frac{V}{\varepsilon_b} \frac{\partial C_i}{\partial z} - \left(\frac{1 - \varepsilon_b}{\varepsilon_b} \right) \left(\frac{3}{R} \right) k_{\beta} (C_i)_{r=R} = \frac{\partial C_i}{\partial t} \quad (3.77)$$

Equation (3.77) represents the model equation for a macroporous system using a film diffusion model. The LHS of the equation expresses the physical process while the RHS expresses the intrinsic rate which can not be accurately predicted and as such must be measured experimentally.

The initial and boundary conditions are:

$$i. \quad C_i = C_{oi} \text{ at } t \leq 0, \quad z_T \geq z \geq 0 \quad (3.78)$$

ii. Inlet condition ($z = 0, t \leq 0$):

$$C_{oi} + D \frac{\partial C_i}{\partial z} = C_i \quad (3.79)$$

iii. Outlet condition ($z = z_T, t > 0$):

$$\left. \frac{\partial C_i}{\partial z} \right|_{z=z_T} = 0 \quad (3.80)$$

3.4.2 Microporous System

In the analysis for microporous systems, the following assumptions are made:

1. The rate of mass transfer of the contaminant in the direction of flow of the aqueous phase by diffusion occurs by Fick's law.

$$J = -D \frac{\partial C_i}{\partial x} \quad (3.81)$$

2. The rate of mass transfer from the bulk conditions of the aqueous phase to the external surface of solid/soil sediment is given by ;

$$r = KA(C_i - C_{si}) \quad (3.82)$$

A material balance on the contaminant over the time period from t to $t + \Delta t$ is taken to be

Input at x – output at x + generation due to chemical reaction- rate of transfer into solid phase

$$= \text{Accumulation over the time period } \Delta t \quad (3.83)$$

Let $x = r$ = radial distance

$$\text{Input at } r = 4\pi r^2 (\epsilon_p J_{pi} + Js_i) \quad (3.84)$$

$$\text{Output at } r + \Delta r = 4\pi r^2 (\epsilon_p J_{pi} + Js_i)_{r+\Delta r} \quad (3.85)$$

$$\text{Generation due to chemical reaction} = 4\pi r^2 \partial r R \quad (3.86)$$

$$\text{Rate of transfer into solid phase} = k(C_{pst} - C_{si}) 4\pi r^2 \partial r \quad (3.87)$$

$$\text{Accumulation} = 4\pi r^2 \epsilon_p \partial r \frac{\partial x_i}{\partial t} + 4\pi r^2 \partial r \frac{\partial C_{si}}{\partial t} \quad (3.88)$$

Pore diffusion is faster than a parallel mechanism of solid diffusion, therefore,

$$\therefore J_{pi} \gg J_{si}, \text{ as } J_{si} \text{ tends to zero}$$

Physical adsorption is assumed to be exceedingly fast, such that a state of equilibrium exists between the pore-fluid concentration, X_i , and the adsorbed phase concentration, C_{si} . Thus C_{si} can be replaced by C_{si}^* , where C_{si}^* is the amount of contaminant i adsorbed per unit volume of the particle at equilibrium with a fluid phase concentration, X_i , in a solution containing n contaminants.

Therefore, two material balance equations can be written:

- (i) for the fluid phase in the pore of the particle, and
- (ii) for the solid phase.

For the pore fluid inside the particle, a modified form of the material balance equation of equation (3.83) applies. On the one hand, there is no reaction term as no chemical reaction takes place in the pore fluid. All reactions take place on the catalyst surface. On the other hand, there is transfer of material from the pore-fluid to the solid surface. The rate of this mass transfer is dependent on the concentration difference between the fluid phase and solid phase.

A modified form of equation (3.83) can be written thus:

$$\begin{aligned}
 &(\text{Input at } r) - (\text{Output at } r + \partial r) + (\text{Rate of transfer from the pore-fluid to} \\
 &\text{the solid phase}) = \text{Accumulation in the pore-fluid over time period, } \Delta t)
 \end{aligned}
 \tag{3.89}$$

Thus, substituting the known terms in equation (3.84) through (3.88) into equation (3.89), we have

$$4\pi r^2 (\varepsilon_p D_{pi} \frac{\partial x_i}{\partial r}) - (-4\pi r^2 \varepsilon_p D_{pi} \frac{\partial x_i}{\partial r}) - 4\pi r^2 \partial r k_f (C_{psi} - C_{si}) = 4\pi r^2 \partial r \varepsilon_p \frac{\partial x_i}{\partial t} \quad (3.90)$$

In equation (3.90), the accumulation term on the solid phase is not included in the material balance since the solid phase is not within the system boundary.

Applying the mean value theorem of differential calculus to the first two terms on the LHS of equation (3.90) and taking limits as ∂r tends to zero, we have

$$\frac{\partial}{\partial r} \left(4\pi r^2 \varepsilon_p D_{pi} \frac{\partial x_i}{\partial r} \right) \partial r - 4\pi r^2 \partial r k_f (C_{psi} - C_{si}) = 4\pi r^2 \varepsilon_p \partial r \frac{\partial x_i}{\partial t} \quad (3.91)$$

Dividing equation (3.91) by $4\pi r^2 \partial r$ yields:

$$\frac{\varepsilon_p}{r^2} \frac{\partial}{\partial r} \left(r^2 D_{pi} \frac{\partial x_i}{\partial r} \right) - k_f (C_{psi} - C_{si}) = \varepsilon_p \frac{\partial x_i}{\partial t} \quad (3.92)$$

Equation (3.92) describes the model equation for pore-fluid diffusion in a microporous system.

For the solid phase material balance, another modification of equation (3.83) applies:

(Input at r) - (Output at $r + \partial r$) - (Rate of transfer from the pore fluid to the solid phase) + (Generation due to chemical reaction) = (Accumulation on the solid surface over time period Δt) (3.93)

$$\begin{aligned} & \left(-4\pi r^2 \varepsilon_p D p_{si} \frac{\partial C_{si}}{\partial r} \right) \Big|_r - \left(-4\pi r^2 \varepsilon_p D p_{si} \frac{\partial C_{si}}{\partial r} \right) \Big|_{r+\partial r} + k_f (C_{psi} - C_{si}) 4\pi r^2 \partial r + 4\pi r^2 \partial r R \\ & = 4\pi r^2 \partial r \frac{\partial C_{si}}{\partial t} \end{aligned} \quad (3.94)$$

Applying the mean value theorem of differential calculus to the LHS of equation (3.94) taking limits as $\partial r \rightarrow 0$, and dividing by $4\pi r^2 \partial r$, we have:

$$\frac{\varepsilon_p}{r^2} \frac{\partial}{\partial r} \left(r^2 D p_{si} \frac{\partial C_{si}}{\partial r} \right) + k_f (C_{psi} - C_{si}) + R = \frac{\partial C_{si}}{\partial t} \quad (3.95)$$

But, $C_{psi} = C_{si}^*$ at equilibrium

Equation (3.95) represents the model equation for solid phase diffusion in a microporous system.

The initial and boundary conditions are:

$$(i) \quad C_{si}(r, t) = C_{si}(r) \text{ at } t \leq 0, \quad 0 \leq r \leq R \quad (3.96)$$

$$(ii) \quad \left. \frac{\partial C_{si}}{\partial r} \right|_{r=R} = 0 \quad 0 \leq r \leq R, \quad t \geq 0 \quad (3.97)$$

There is no inlet condition for equation (3.95). The film mass transfer coefficient (k_f), pore-water velocity (V) and dispersion coefficient (D) must be determined independently for the solution of the equations for macroporous and microporous systems.

The successful predictions of the fate and transport of solutes in the subsurface is hinged on the availability of accurate transport parameters. These significantly help in assessing the behaviour of solutes over

relatively long spatial and temporal scales, since the feasibility of experimental measurements can be cumbersome and not cost effective. The use of numerical models in predicting solute concentrations prior to the application of management strategies is rapidly generating considerable interest because of the concerns for the quality of the subsurface environment.

CHAPTER FOUR

4.0 MATERIALS AND METHODS

The experimental approach involved the use of soil microcosm as a first step in the kinetic protocol for evaluating substrate bioavailability and biodegradation in contaminated aqueous-soil/sediment matrix.

Data on oxygen uptake and carbon dioxide evolution were collected from the microcosm reactor. These data served as a means of assessing the microbial activities in the soil. The abiotic sorption and desorption kinetics and equilibria of the contaminants were determined using soil slurry systems. Soil-core samples were taken at appropriate time intervals and analyzed using standard solvent extraction and gas chromatography methods to determine the concentration of the contaminants in the soil. Microbial analysis was also carried out to determine the population count, types of colonies, maximum specific growth rate and true yield of bacterial mass per unit of substrate mass utilized.

4.1 Materials

The polycyclic aromatic hydrocarbons used (naphthalene, anthracene and pyrene) were purchased from Harrison and Harrison Laboratories Co. Ltd in Lagos, Nigeria. The culture media used were Potato Dextrose Agar (for fungi enumeration) and Nutrient Agar (for bacteria enumeration).

The Minimal salts medium consisted of the following K_2HPO_4 , KH_2PO_4 , $MgSO_4$, $NaCl$, $CaCl_2$ and NH_4NO_3 . Trace elements solution was prepared using MgO , $CaCO_3$, $FeSO_4 \cdot 7H_2O$, $ZnSO_4 \cdot 7H_2O$, $MgSO_4 \cdot 4H_2O$, $CuSO_4 \cdot 5H_2O$, H_3BO_3 , and HCl . Other chemicals used were: potassium hydroxide, calcium hydroxide, pyrogallol, and mercuric chloride. All reagents used were of analytical grade. Distilled water was used for solution, sample preparation and dilution.

4.2 Instruments

The oxygen uptake was determined using a reagent bottle connected to a UV/V spectrophotometer. The carbon dioxide evolution was measured using a GC-120 orsat gas analyzer. Solvent extraction was carried out using n-hexane and dichloromethane (HPLC grade). A Hewlett Packard gas chromatography (HP 5890 series 11) was used for the determination of the concentration of the polycyclic aromatic hydrocarbons. The gas chromatography is equipped with flame ionization detector (FID) and nitrogen was used as carrier gas at a pressure of 60-65psi. The injector and detector temperatures were 250°C and 320°C, respectively. The column temperature was 40-300°C programmed at 10°C/min with computer interphase and a chem. station.

4.3 Soil

Soil sample (2000kg) collected from unimpacted zones at field 17 (uncultivated) in the Nigerian Institute for Oil Palm Research (NIFOR), near Benin City; Edo State, Nigeria was used. The sampling was done in the dry season around a sampling point to a depth of 0-15cm. The bulk composite soil sample was first analyzed for the presence of polycyclic aromatic hydrocarbons and thereafter put in a sterile black polyethylene bag sealed and stored in a refrigerator prior to analysis.

4.4 Experimental Set-Up

The experimental set-up (see Figure 4.1) consisted of a microcosm reactor, oxygen cylinder fitted with high pressure valves, leachate holding tank, high pressure refrigerated nutrient tank, a control system made up of programmable timer and a solenoid valve, an oxygen analyzer bottle and an Orsat Gas Analyzer. The microcosm reactor was 60.96cm height by 30.48cm width by 25.4cm length, with a holding capacity of 30litres. It was constructed using a 20mm thick plastic glass (transparent) material. Medical grade oxygen from an oxygen bottle flowed through a rotameter (Arm field Technical Education Co. Ltd., CEM-RG 3675) to the reactor. The leachate tank with dimensions of 30.48cm height by 30.48cm width

by 30.48cm length was made with same material as the microcosm reactor.

The refrigerated tank was constructed from a stainless steel material (20.32cm depth by 30.48cm height by 30.48cm width). It had a holding capacity of 15litres. The experimental set up and was equipped with a control system, which comprised solenoid valve (3/8 diameter tube, temperature between 40°C to 105°C, pressure of 46 bar. Also fitted to the reactor, were a pressure gauge, a digital multimeter (8900 series, model; AVD890C4) and a 400watts centrifugal pump (Stuart Turner Ltd., model no 34973/18, RPM 2800, 800watts). An air conditioner type of foam filter enclosed in a stainless steel material with dimensions (22.86cm height by 7.62cm depth by 7.62cm width) was used.

A 100ml oxygen absorption bottle and an Orsat (GC-120) gas analyzer containing a carbon dioxide absorption bottle were connected to the soil microcosm reactor.

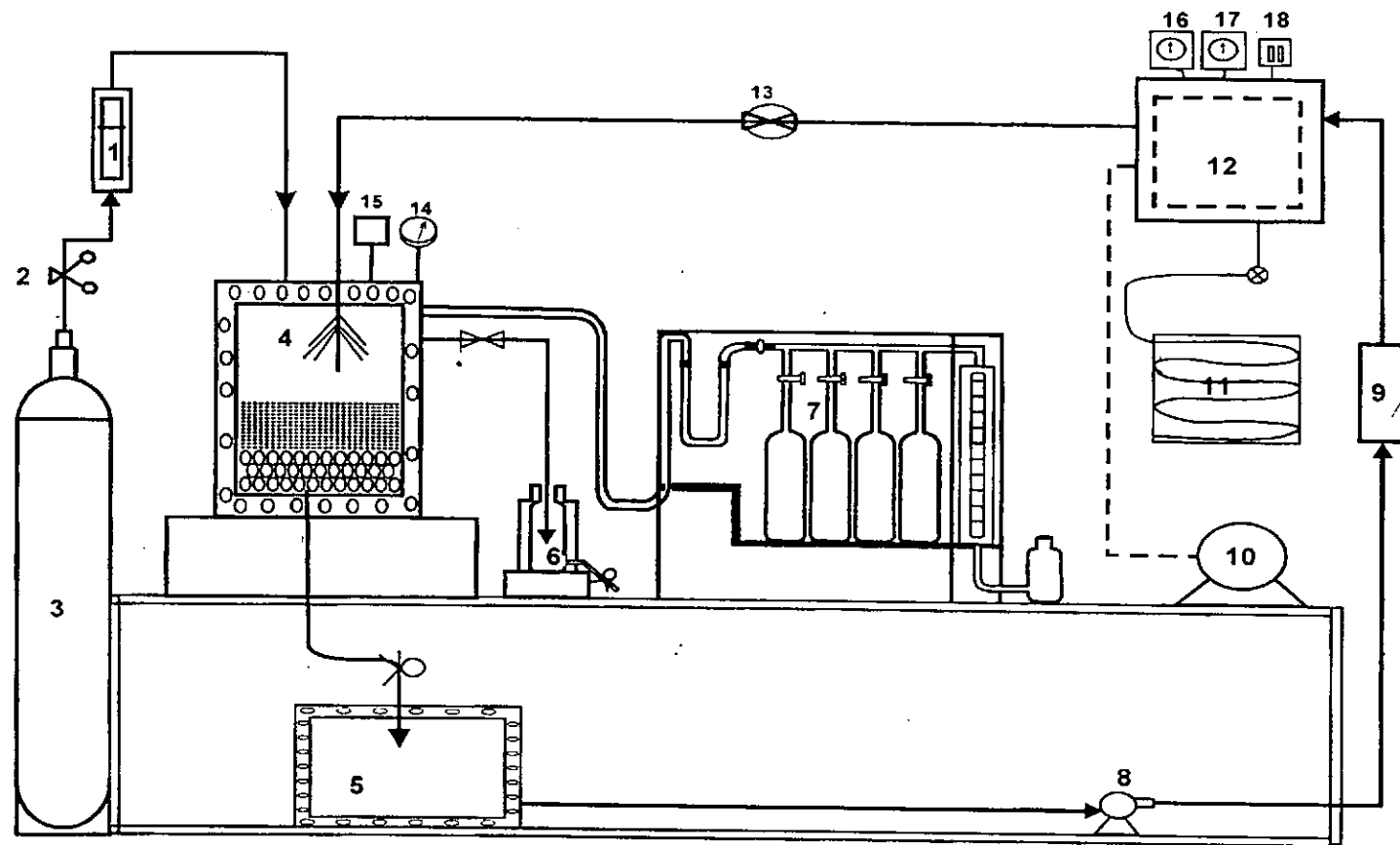


Fig 4.1: Schematic representation of experimental setup

Key: (1) Rotameter, (2) Regulator, (3) Oxygen bottle, (4) Microcosm reactor, (5) Leachate holding tank, (6) Oxygen absorption bottle, (7) Orsat gas analyzer, (8) Pump, (9) Filter, (10) Compressor, (11) Condenser, (12) Refrigerated nutrient tank, (13) Solenoid valve, (14) Pressure gauge, (15) Digital multimeter, (16) Delay timer, (17) Programmable timer, (18) Electrical switch.

The following precautions were taken to reduce to the barest minimum any incidence of possible microbial contamination and other inhibitory substances:

- (i) The entire system was effectively sterilized.
- (ii) Medical grade oxygen was used instead of air, which contains some amount of carbon dioxide.
- (iii) Distilled water was used.
- (iv) Samples for microbial and contaminant hydrocarbons analysis were stored at a temperature below 4°C until the commencement of analysis.

4.5 Methods

(a) Soil Microcosm

The contaminant hydrocarbons used for the study included naphthalene, anthracene and pyrene. 1kg unimpacted surface and subsurface soils were excavated and placed inside the microcosm. The soil was spiked with a mixture of the contaminant hydrocarbons (200mg each) dispersed in 2 litres of water containing a 0.02% surfactant sodium hexametaphosphate, SHMP (Koeppel *et al.*, 1997) and nutrients (straw, sawdust, and poultry dung). Another reactor was also set up and used as a control. A constant flow rate of oxygen was then sent into the two reactors. The temperature

and pressure of the microcosm reactors were monitored throughout the period of experimentation using a digital multimeter and pressure gauge.

Thereafter, samples were taken on a weekly basis and analyzed using solvent extraction and gas chromatography methods to determine the concentration of contaminants. The oxygen uptake and carbon (iv) oxide evolution measurements were also carried out.

(b) Oxygen Uptake Determination

The absorbent (100ml) in the absorption bottle consisted of one volume of a 1% (w/v) aqueous solution of pyrogallol with three volumes of a 30% (w/v) aqueous solution of potassium hydroxide. Opening the stopcock connecting the absorption bottle to the microcosm reactor absorbed oxygen. Sample gas was drawn into the absorbent solution and the amount of oxygen not consumed was determined colorimetrically using a UV/V spectrophotometer (Spectronic 21D), at a wavelength of 605nm. Sampling was done every 5days.

(c) Determination of Carbon dioxide

The determination of carbon dioxide evolved was carried out using Orsat Gas Analyzer. The absorption vessel was charged with 100ml calcium hydroxide as the absorbent. The leveling bottle was filled with a

confining liquid (5% sulphuric acid solution containing a few drops of methyl orange indicator. The levelling bottle was raised to the top of the analyzer, with the 3-way cock at the end of the manifold opened. The burette was filled with water up to the capillary tube and air was removed from the connecting tube using a rubber bellows pump. With the 3-way cock suitably set, sample gas was drawn into the burette by lowering the levelling bottle until the water meniscus reaches the lowest graduation mark of the burette. The stopcock connecting the burette to the absorption vessel containing calcium hydroxide was opened and the level bottle raised. The level bottle was lowered again and the gas brought into the burette until the absorbent in the vessel reaches the mark just above the top of the vessel.

The operation was repeated until absorption was complete as was evidenced when the meniscus in the level bottle was at the same level with that in the burette. The burette reading was recorded. Sampling was done every 10 days.

4.6 Kinetic Experiments

(i) Sorption

The sorption study was done in a soil slurry system. The soil sample was initially air dried and soil aggregates broken by a wooden mallet before

sieving. The experiment was conducted using the soil fraction, which passed a sieve up to 2.00 mm. 50g of the soil sample was placed in the reaction chamber and mixed with 250 ml of distilled water containing 10mg of the contaminant (naphthalene) and 1ml of mercuric chloride saturated solution to minimize biodegradation. A magnetic stirrer (Gallenkamp, England) regulated at a speed of 1300 rev/min was used to ensure adequate mixing of the soil suspension in the reaction chamber, which contains a magnetic follower encased in polypropylene. The stirring speed was maintained at a minimum to reduce abrasion of the soil. The slurry suspension was sampled after 0, 2, 4, 6, 8, 10, 12, 14, 16, 20 and 36 hours (Tabak and Govind, 1997). After the predefined period had elapsed, the suspension was centrifuged (Polite 350) and withdrawn using a 10ml syringe connected to a filter membrane, which prevents soil particles from entering the sample.

(ii) Desorption

Desorption studies were conducted by first adsorbing naphthalene in the soil until equilibrium was attained. This was achieved by mixing 250ml distilled water with 50g of air dried soil and 10mg of naphthalene. After adsorption equilibrium was attained, the sample was diluted with an equal volume of water and with 1ml of mercuric chloride saturated solution to inhibit biodegradation. The slurry suspension was sampled after 0, 4, 8,

16, 24, 48, 72, 96 and 120 hours (Tabak and Govind, 1997). After the predefined time had elapsed, the slurry was centrifuged and withdrawn by means of a syringe.

The samples from the adsorption and desorption experiments were stored in a freezer prior to solvent extraction using n-hexane and dichloromethane (HPLC grade) and GC analysis.

The processes in 4.6 (i) and (ii) were repeated for anthracene and pyrene.

4.7 Microbial Analysis

a. Sterilization: All the glasswares, were sterilized using the hot air- oven (Phoenix; Harrow Scientific Ltd, model 53L, serial no 526-05) at 160°C for 2 hours. The media were also sterilized using an autoclave (Portable Universal Electricity model, working pressure 1.05kg.cm² and temperature 121°C) at 120°C for 15 minutes.

b. Enumeration of Bacteria and Fungi Colonies (Using the Pour Plate Method)

The most probable number of the bacteria and fungi colonies was determined using the Pour Plate Method described by Gerhardt *et al.*, 1994.

From the 100ml stock sample, 1ml was taken and serially diluted to obtain a 10^{-5} dilution as shown in Figure 4.2. 1ml of the 1st test tube (10^{-1}) was pipetted into the corresponding 1st plate to obtain a 10^{-1} dilution. Using fresh pipettes, same amount was taken from the 2nd, 3rd, 4th and 5th test tubes respectively to obtain the desired dilutions (10^{-2} , 10^{-3} , 10^{-4} and 10^{-5}). The procedure above was repeated for the enumeration of fungi colonies.

Molten NA (containing 0.5ml fulcin) and PDA (containing 0.5ml streptomycin and penicillin) were poured into the plates and rotated for even distribution. Thereafter, the plates were allowed to set or solidify. Upon this, the NA plates were incubated for 24 hours, inverted (using Sanyo Incubator MIR-252) to avoid water of condensation at 37°C while PDA plates were incubated at 28°C for 72 hours.

After 24 hours of incubation for NA plates, the emergent colonies were counted and only counts of 30-300 colonies were considered as significant colonies. The uninoculated plates served as control.

Similarly, the fungi plates were counted after 72 hours and the colonies recorded.

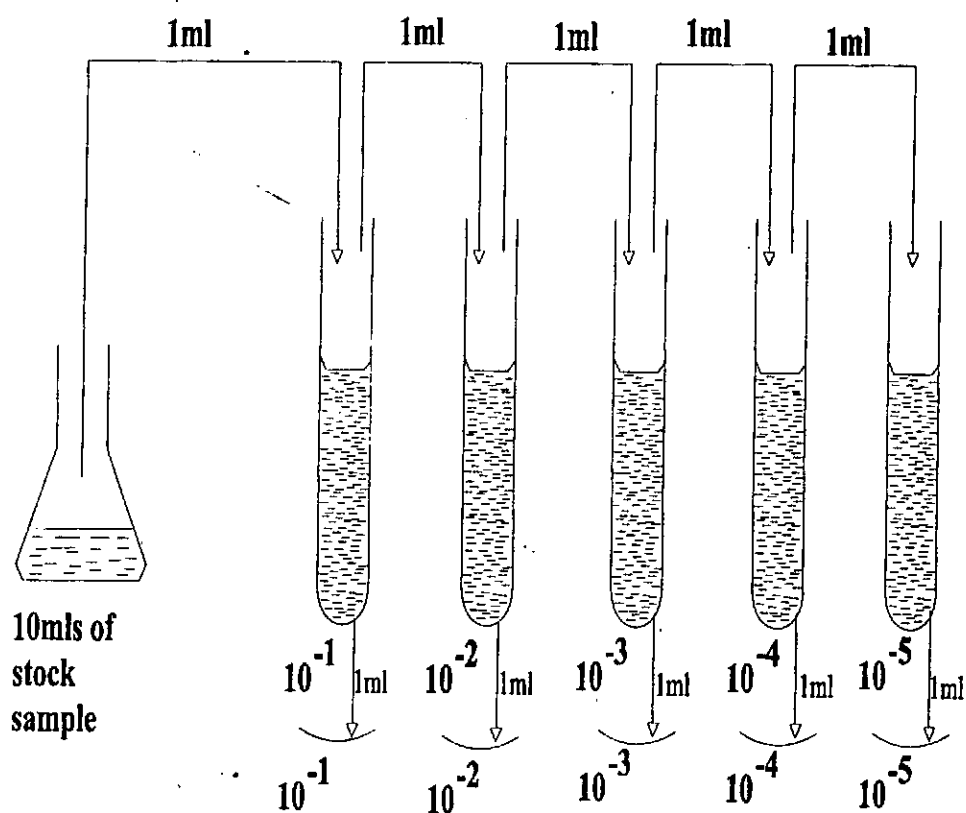


Figure 4.2: Schematic representation of serial dilution

4.8 Characterization

Sub culturing of isolates was based on their cultural and morphological characteristics.

4.8.1 Morphological Characteristics

The morphological characteristics were determined by using staining reactions – the gram stain.

4.8.2 Gram's Stain

A smear of the bacteria culture was prepared on a clean slide. This was air-dried and heat fixed. The heat fixed cultures were then stained using the gram staining technique and observed under the oil immersion objective of a light microscope. Crystal violet solution was used to stain the smear for 1 minute after which the stain was washed off with water and immersed in Lugol's iodine solution for 1 minute. The slide was again washed in water, decolorized for 30seconds with alcohol-acetone. These again were washed off with water and finally counter stained with Safranin dye for 30seconds, washed with water and air-dried. The slide was observed under a microscope.

4.9 Cultural Characteristics

The characterization of the culture was determined for each organism by culturing isolate on nutrient agar and visually observing their cultural characteristics.

4.9.1 Biochemical Characteristics

(i) Methyl Red Test

5ml of glucose phosphate peptone water medium was inoculated with the organism and incubated at 37°C for 48hours. 5 drops of 0.5% methyl red

(v) Catalase Test

A light inoculum of the organism was added to about 3 drops of 3% hydrogen peroxide on a slide. The production of gas or bubbles indicated positive results.

(vi) Motility Test

10ml of a semi-solid agar was dispersed in test tubes and left to set in a vertical position. The tubes were inoculated with the test organisms with a straight wire, making a single stab down the center of the tube to about half the depth of the medium. The tubes were incubated at 37°C and examined at intervals of 6 hours, 2 and 6 days. Motile bacteria swarm and gave a diffuse hazy growth that spread throughout the medium rendering it slightly opaque. Non motile bacteria generally gave growth that was confined to the stab line and the surrounding medium remaining transparent.

(vii) Oxidase Test

The oxidase test depends on the presence in bacteria of certain oxidases that will catalyze the transport of electrons between electron donors in the bacteria and a redox dye, tetraethyl-p-phenylene-diamine hydrochloride. A 1% solution of this dye prepared and stored in a dark bottle (shelf life is 2 weeks at 4°C. Few drops of the 1% dye solution were added to a

piece of Whatman filter paper in a Petri dish, using a glass rod or platinum loop. A smear of the test organism was made on the impregnated filter paper. A purple coloration was produced within 5-10 seconds by oxidases organisms.

(viii) Sugar Fermentation

15g of peptone water powder was dissolved in 1000ml of water to prepare peptone water solution. 1g of lactose, glucose, sucrose; mannitol was added to 100ml of peptone water. A suitable indicator, 2ml of bromothymol blue was also added. 5ml of each sugar medium was inoculated with the test organism using a sterile loop. The cultures were incubated at 37°C for up to one week. The utilization of the sugars by an organism was indicated by the presence of acid and gas. Acid production was indicated by the change of color from purple to yellow, while gas production was indicated by the presence of gas bubbles collected in inverted Durham tubes.

(ix) Coagulase Test

Nutrient broth was used to cultivate the test organisms for 24 hours. 0.2ml of oxalate plasma was pipetted into a fresh test tube and 0.8ml of the broth culture containing the organism was added to it. The culture was mixed gently and incubated at 37°C for 24 hours and observed for

clotting by tilting the tube. Clotting of the tube contents or fibrin clot in the tube gave a positive coagulase test.

(x) Citrate Utilization Test

3ml of Kosar's citrate medium was inoculated with organism and incubated at 37°C for up to 4 days, checking daily for turbidity and/or blue color, which indicated positive test.

The results of the investigations on the microbial enumeration are presented in Tables D.1 to D.4 in Appendix D.

4.10 Microbial Growth Study

Microbial degradation of naphthalene by soil microbial isolates

The growth rate of the microbes and their utilization of substrates were studied using a minimal salt medium. The bacteria and fungi isolated from the soil were used as test microbes and naphthalene as the test substrate. The experiment was performed in a 500ml shake flasks containing 100ml minimal salt medium and incubated on a rotatory shaker 200 rpm at 30°C. Samples were periodically taken (2hours interval) and the growth rate was determined turbidometrically at an optical density (OD) of 436nm, with a UV/V spectrophotometer (Spectronic 21D). Portions of the samples were centrifuged and the supernatant were analyzed for the mineralization of naphthalene by gas chromatography.

4.11 Soil Characterization

The soil was characterized to determine soil moisture content, clay, sand and silt content, percent organic matter, soil pH, cation exchange capacity, bulk density, and nutrients in soil.

1. Soil Moisture Determination

This was determined by gravimetric method. A weighed soil moisture can (container) was filled with the sample submitted to the laboratory and weighed to obtain the wet weight. The can filled with soil was put into the oven and dried at 105°C to constant weight. The dried soil and can were reweighed and the moisture content calculated as below:

Wt of empty can	= 4.6768g
Wt of empty can + wet soil	= 6.6762g
Wt of wet soil	= 1.9994g
Wt of can + dry soil	= 6.5805g
Wt of dry soil	= 1.9037g
Wt of moisture	= 0.0957g
%Moisture	= 5.027g

2. Bulk Density Determination

This expresses the ratio of the mass of dried soil to its total volume (solids and pores together) and is given as

$$P_b = M_s / (V_s + V_a + V_w) = \frac{M_s}{V}$$

Where M_s = mass of soil

V_s = volume of solids

V_a = volume of air

V_w = volume of gravimetric water

20g of soil was transferred into a measuring cylinder and the cylinder tapped several times to compact the soil. The volume was read and the bulk density calculated as

$$\frac{20}{16} = 1.25$$

3. Total Porosity

To determine the total porosity, it was necessary to determine the particle density (P_s) as described by Hilliel (1982).

Wt of empty pycnometer W_a = 24.6g

Wt of pycnometer + soil W_s = 34.6g

Wt of pycnometer + soil + water (W_{sw}) = 81.1g

Wt of pycnometer filled with water (W_w) = 75.2g

Density of water in g/cc at

Observed temperature (d_w) = 0.988

$$\text{Particle density } D_p = \frac{d_w(W_s - W_a)}{(W_s - W_a) - (W_{sw} - W_w)} = P_s$$

Therefore,

$$\begin{aligned}\therefore \text{Porosity} &= 1 - \frac{\text{Bulk density}}{\text{Particle density}} \\ &= \frac{P_b}{P_s} = 0.481\end{aligned}$$

4. Particle Size Distribution

Mechanical analysis of the soil was carried out by the hydrometer method after the destruction of organic matter with hydrogen peroxide (Day, 1965).

50g of the air dried soil was weighed into a 600ml beaker. 50ml of distilled water was added followed by 10ml of 30ml volume H_2O_2 . The suspension was heated on a hot plate until frothing stopped and the liquid almost dried. The soil was then transferred into a milk shake cup with baffles. 100ml of water and 20ml of 20% sodium hexametaphosphate solution (algon) was added to the cup and the suspension stirred for 30minutes. The suspension was then transferred into a 1 litre measuring cylinder with a jet of water from wash bottle and the volume brought to mark with distilled water.

The suspension was agitated vigorously to ensure thorough mixing and exactly 40seconds from when agitation stopped, a hydrometer reading was taken and the temperature of the suspension was also recorded. The suspension was left undisturbed on the bench. At the end of 24hours,

another hydrometer and temperature readings were taken. The various particle sizes were calculated as below:

$$\% \text{ Sand} = 100 - \text{Corrected 40sec hydrometer reading} \times \frac{100}{50}$$

$$\% \text{ Clay} = \text{Corrected 2hours hydrometer reading} \times \frac{100}{50}$$

$$\% \text{ Silt} = 100 - (\% \text{ Sand} + \% \text{ Clay})$$

5. pH (1:1) H₂O

The hydrogen ion concentration of the soil was determined using a Corning (model 260T) glass electrode pH meter.

30g of 2mm air dried sample was weighed into a 100ml beaker and 30ml of distilled of distilled water was added. The suspension was stirred intermittently for 30minutes and the pH was measured using a glass electrode pH meter after the meter had been standardized with pH buffer 4.0 and 7.0 solutions.

6. Organic Carbon (Org C %)

Organic carbon content of the soil was determined by the chromic acid wet oxidation procedure as described by Black, 1965.

7. Organic Matter

This was determined by multiplying the % organic carbon value by a factor of 1.724.

8. Total Nitrogen

The total N content of the soil was extracted by the micro Kjeldahl procedure and the ammonium in the extract assayed by the alkaline-phenate colorimetric method (Fiore and O'Brien, 1968).

9. Available phosphorous

This was extracted from 5g air dried soil using 35ml of Bray and Kurtz, 1945, (0.03N NH_4F + 0.025N HCl) solution and the P in the extract was determined by the ascorbic acid blue colour procedure of Murphey and Riley (1962).

10. Cation Exchange Capacity (CEC)

The CEC of the soil was determined by extracting the cations with 1N NH_4OAc (ammonium acetate pH 7) and then determining Ca and Mg by the EDTA volumetric procedure and K and Na by flame photometry. Exchangeable acidity was extracted with 1N KCl solution and an aliquot titrated with 0.1N NaOH solution using phenolphthalein indicator. CEC was calculated as the sum of Ca + Mg + K + Na + EA in cmol/kg.

4.12 Parameters from Experimental Investigation

The parameters obtained from the experimental investigation included the following:

- (a) Breakthrough (concentration-time) data for both the non-reactive solute (biosurfactants) and the contaminant PAHs.
- (b) Adsorption/Desorption Isotherms: The batch adsorption and desorption kinetics and equilibria data on the contaminants were fitted to Freundlich and Langmuir isotherm equations. The diffusivities, isotherm exponents and mass transfer coefficients were obtained.
- (c) Six microbial isolates were identified in the study. Four were of the bacteria group while two belonged to the fungi group. The maximum growth rates and the corresponding specific decay coefficients were determined to help ascertain the metabolic response i.e. the level of toxicity of the PAHs on the microbes or the suitability of the PAHs for the microbes.

4.13 Parameters needed for simulation

The modeling equations of an unsteady state system for the soil microcosm reactor contain a number of parameters, which must be estimated for a reasonable solution of the equations. The constant

transport parameters D_{Li} , V , k_{fi} and D_{pi} needed for the simulation, of the biodegradation process, were estimated independently in order to reduce the dimensionality of the search process. The D_{Li} and V for the non reactive solute (surfactant) were obtained using the MOM of Das and Kluitenberg (1996), also reported by Pang *et al.*, (2003) and the CXTFIT software, version 2, as described by Toride *et al.*, (1995). The film mass transfer coefficient was determined from the experimental data on adsorption/desorption, using the following relationship (Tabak and Govind, 1997):

$$k_{fi} = 0.32 \frac{D_{pi}^{2/3}}{D_f} V^{1/3} \text{Re}_{dp}^{3/4} \left[\frac{D_i^{1/2} d_p^{-3/4}}{D_f^{1/2} H_L^{1/4}} \right] \quad (4.1)$$

The pore diffusivities D_{pi} may also be estimated from literature (Perry and Green, 1998):

$$D_{pi} = \frac{E_p}{T} \left[\frac{3}{4\bar{r}} \left(\frac{\pi m}{2R\theta_A} \right)^{1/2} + \frac{1}{D_f} \right]^{-1} \quad (4.2)$$

While the diffusivity of the fluid phase D_f may be obtained from the correlation of Wilke Chang, reported by Bird *et al.* (2005):

$$D_f = 7.4 \times 10^{-8} \frac{\sqrt{\psi_B M_B T}}{\mu V_A^{0.6}} \quad (4.3)$$

4.14 Software

A computer software program CXTFIT version 2.0 described by Toride *et al.* (1995) was applied. The Program assumes one-dimensional flow and estimates parameters by fitting the parameters to observed laboratory/experimental or field solute transport data. In this study, the program was used to solve direct problems where it predicted solute distribution against time. In addition, it can also be used to solve the inverse problems by minimizing an objective function, which consists of the sum of the squared differences between observed and fitted concentrations.

The governing equation to which the software had been applied may be described by the following partial differential equations (Toride *et al.* 1995):

$$R \frac{\partial c}{\partial t} = D \frac{\partial^2 c}{\partial x^2} - V \frac{\partial c}{\partial x} - \lambda C \quad (4.4)$$

The initial and boundary conditions were given as

$$c(x, 0) = 0 \quad 0 < x < \infty \quad (4.5)$$

$$c(0, t) = c_0 \quad 0 < t \leq t_0 \quad (4.6)$$

$$c(0, t) = 0 \quad t_0 < t < \infty \quad (4.7)$$

$$c(\infty, t) = 0 \quad 0 < t < \infty \quad (4.8)$$

The solutions of the degradation rate constant (λ) and retardation factor (R) were obtained using the expressions (Pang *et al.*, 2003):

$$R = \frac{(\mu_1 - 0.5t_0)\sqrt{V^2 + 4D\lambda}}{x} \quad (4.9)$$

and

$$\lambda = \frac{V^2}{4D} \left[\left(1 - \frac{2D}{xV} \ln \frac{M_o}{C_o t_o} \right)^2 - 1 \right] \quad (4.10)$$

The n th temporal moment of a concentration distribution at a location x was defined by Kucera, (1965) and Valocchi, (1985) and described by Pang *et al.*, (2003) as:

$$M_n = \int_0^{\infty} t^n C(x, t) dt \quad (4.11)$$

and the n th normalized moment of the distribution was defined as:

$$\mu_n = \frac{M_n}{M_o} = \frac{\int_0^{\infty} t^n C(x, t) dt}{\int_0^{\infty} C(x, t) dt} \quad (4.12)$$

Equations (4.11) and (4.12) may be used to obtain experimental temporal moments from concentration breakthrough curves.

The pore water velocity (V) and dispersion coefficient (D) are estimated in order to calculate R and λ from equations (4.9) and (4.10).

$$V = \frac{x}{\mu_1 - 0.5t_0} \quad (4.13)$$

and

$$D = \frac{V^3}{2x} \left(\mu_2 - \mu_1^2 - \frac{t_0^2}{12} \right) \quad (4.14)$$

4.15 Numerical Solution and Analysis

The numerical method adopted for the solution of the second-order partial differential equations in equations (3.75) and (3.95) is the Backward Finite Difference Scheme also called Fully Implicit Method. This method is preferred to the central or forward difference methods because its truncation error is of the second order, and it often involves implicit method of solution, which is stable and valid for any chosen interval. Both terms on the R.H.S and L.H.S of the equations have the unit of concentration. The scheme involves the discretization of both depth (z) and time (t) simultaneously into mesh or grid points with constant intervals. The z - t plane is subdivided into equal time steps, $\Delta\tau = k$, and depth step, $\Delta z = h$. The domain of the function is overlaid by a grid whose mesh size is of h units, in the z direction and k units in the τ direction. The value of the function (z, τ) at the i, j^{th} grid point is denoted as $f_{ij} \equiv f(ih, jk)$. The values of the expression are required to be found at the grid points as:

$$\begin{array}{ccccccc}
 & & \text{---} & & \text{---} & & \text{---} & & \text{---} & & \text{---} \\
 & & \text{---} & f_{i-1,j+1} & f_{i,j+1} & f_{i+1,j+1} & \text{---} & & & & \\
 & & \text{---} & f_{i-1,j} & f_{i,j} & f_{i+1,j} & \text{---} & & & & \\
 & & \text{---} & f_{i-1,j-1} & f_{i,j-1} & f_{i+1,j-1} & \text{---} & & & &
 \end{array}$$

The value of the first derivative with respect to x at the point (x_i, y_j) on the grid overlaying the function domain is found

$$\begin{array}{cccccc}
0 & 0 & 0 & 0 & 0 & 0 \\
0 & 0 & 0 & 0 & 0 & 0 \\
0 & 0 & 0 & 0 & 0 & 0 \\
0 & 0 & 0 & 0 & 0 & 0
\end{array}$$

$$\Delta \tau = k, \quad \Delta z = h$$

The representative mesh point $p(i,j)$ is

$$z = i h \text{ and } \tau = j k$$

where

$$i, j = 0, 1, 2, 3, \dots, N$$

hence

$$C_p = C(ih, jk) = C_{i,j}$$

The backward finite difference scheme is valid and converges for all values of k/h^2 i.e. $k/h^2 \geq 0$. This is known as the stability criterion. To allow for more flexibility of the result to the equations, the following dimensionless variables are used:

$$Z = \frac{z}{z_r} \tag{4.15}$$

Z = dimensionless depth

$$\tau = \frac{t}{T} \tag{4.16}$$

τ = dimensionless time

$$\bar{C} = \frac{C_i}{C_{oi}} \quad (4.17)$$

\bar{C} = dimensionless concentration

$$\alpha = D, \beta = \frac{V}{\varepsilon_b}, \gamma = \left(\frac{1 - \varepsilon_b}{\varepsilon_b} \right) \frac{3}{R} k_r \quad (4.18)$$

$$\eta = \frac{k}{\alpha}, \quad \psi = \frac{1}{\alpha}, \quad \varphi = \frac{R + kC_p}{\alpha} \quad (4.19)$$

subject to

$$\bar{C} = \bar{C}_{oi} \quad 1 > z > 0, \tau = 0 \quad (4.20)$$

$$\bar{C}(z, 0) = 1, \quad \tau = 0 \quad (4.21)$$

$$\bar{C} = \bar{C}_{oi} \quad 1 > r > 0, \tau = 0 \quad (4.22)$$

$$\bar{C}(r, 0) = 1, \quad \tau = 0 \quad (4.23)$$

Therefore, non dimensionalizing equations (3.75) and (3.95), yields:

$$\frac{\partial \bar{C}}{\partial \tau} = \alpha \frac{\partial^2 \bar{C}}{\partial z^2} - \beta \frac{\partial \bar{C}}{\partial z} - \gamma(\bar{C}_i) = 1 \quad (4.24)$$

$$\psi \frac{\partial \bar{C}}{\partial \tau} = \frac{\partial^2 \bar{C}}{\partial r^2} + \frac{\partial \bar{C}}{\partial r} - \eta \bar{C} + \varphi = 1 \quad (4.25)$$

Discretizing equations (3.75),

$$C = C_{i,j} \quad (4.26)$$

$$\frac{\partial C}{\partial z} = \frac{C_{i,j+1} - C_{i,j}}{h} \quad (4.27)$$

$$\frac{\partial^2 C}{\partial z^2} = \frac{C_{i,j-1} - 2C_{i,j} + C_{i,j+1}}{h^2} \quad (4.28)$$

$$\frac{\partial C}{\partial t} = \frac{C_{i,j+1} - C_{i,j}}{k} \quad (4.29)$$

$$h = 0.015, k = 7$$

Combining these computational molecules, substituting equations (4.26) through 4.29 and the values of α , β , γ , \bar{C} , \bar{C}_i , into equation (4.24) result in composite molecule that represent the differential equations.

$$C_{i-1,j+1} - 2C_{i,j+1} + C_{i+1,j+1} = -2.49 \times 10^{-3} C_{i,j} + 1.49 \times 10^{-3} C_{i+1,j} \quad (4.30)$$

The composite computational molecule is applied to the grid points. This will convert the system of partial differential equations to a system of linear simultaneous equations. These conditions are represented in Table H.1 shown in Appendix H. In the table, $C_{1,1}, C_{2,1}, C_{2,2}, C_{3,1}$, are all unknown to be computed. For every time step, nine unknowns need to be solved simultaneously from the resulting nine equations. That is, to solve for the various concentration values in $j=1$ row, nine equations result. Substituting the initial and boundary values into equation (4.30) will give the following:

For $j = 0$

$$i=1, j=0, \quad C_{0,1} - 2C_{1,1} + C_{2,1} = (-2.49C_{1,0} + 1.49C_{2,0}) \times 10^{-3}$$

$$\text{but } C_{1,0} = 0, \quad C_{2,0} = 0, \quad C_{0,1} = 99.7$$

$$-2C_{1,1} + C_{2,1} = -99.7 \quad (4.31)$$

$$i=2, j=0$$

$$C_{1,1} - 2C_{2,1} + C_{3,1} = 0 \quad (4.32)$$

$$i=3, j=0$$

$$C_{2,1} - 2C_{3,1} + C_{4,1} = 0 \quad (4.33)$$

$$i=4, j=0$$

$$C_{3,1} - 2C_{4,1} + C_{5,1} = 0 \quad (4.34)$$

$$i=5, j=0$$

$$C_{4,1} - 2C_{5,1} + C_{6,1} = 0 \quad (4.35)$$

$$i=6, j=0$$

$$C_{5,1} - 2C_{6,1} + C_{7,1} = 0 \quad (4.36)$$

$$i=7, j=0$$

$$C_{6,1} - 2C_{7,1} + C_{8,1} = 0 \quad (4.37)$$

$$i=8, j=0$$

$$C_{7,1} - 2C_{8,1} + C_{9,1} = 0 \quad (4.38)$$

$$i=9, j=0$$

$$C_{8,1} - 2C_{9,1} + C_{10,1} = 0$$

$$\text{but } C_{10,1} = 0$$

$$C_{8,1} - 2C_{9,1} = 0 \quad (4.39)$$

These nine simultaneous equations were solved to obtain concentration values in the next time step, i.e., $j=1$. These linear simultaneous equations are solved using the inverse matrix method. The matrix method

involves the arrangement of the system of equations to the form having the matrix variables X, coefficients A and right hand side constant matrix (r.h.s). This is simply stated as

$$AX = R$$

$$X = A^{-1} R$$

A = Coefficient matrix,

R = R.H.S constant matrix and

X = Solution matrix

This resulting coefficient matrix is a tridiagonal matrix. To ease computation of the resultant sets of algebraic equation, the Microsoft Excel template is used. The inverse of the coefficient matrix is computed and then multiplied with the constant matrix. The procedure is shown below:

$$\begin{bmatrix} -2 & 1 & 0 & 0 & 0 & 0 & 0 & 0 & 0 \\ 1 & -2 & 1 & 0 & 0 & 0 & 0 & 0 & 0 \\ 0 & 1 & -2 & 1 & 0 & 0 & 0 & 0 & 0 \\ 0 & 0 & 1 & -2 & 1 & 0 & 0 & 0 & 0 \\ 0 & 0 & 0 & 1 & -2 & 1 & 0 & 0 & 0 \\ 0 & 0 & 0 & 0 & 1 & -2 & 1 & 0 & 0 \\ 0 & 0 & 0 & 0 & 0 & 1 & -2 & 1 & 0 \\ 0 & 0 & 0 & 0 & 0 & 0 & 1 & -2 & 1 \\ 0 & 0 & 0 & 0 & 0 & 0 & 0 & 1 & -2 \end{bmatrix} \begin{bmatrix} C_{1,1} \\ C_{2,1} \\ C_{3,1} \\ C_{4,1} \\ C_{5,1} \\ C_{6,1} \\ C_{7,1} \\ C_{8,1} \\ C_{9,1} \end{bmatrix} = \begin{bmatrix} -99.7 \\ 0 \\ 0 \\ 0 \\ 0 \\ 0 \\ 0 \\ 0 \\ 0 \end{bmatrix}$$

Solving:

$$\begin{bmatrix} C_{1,1} \\ C_{2,1} \\ C_{3,1} \\ C_{4,1} \\ C_{5,1} \\ C_{6,1} \\ C_{7,1} \\ C_{8,1} \\ C_{9,1} \end{bmatrix} = \begin{bmatrix} -2 & 1 & 0 & 0 & 0 & 0 & 0 & 0 & 0 \\ 1 & -2 & 1 & 0 & 0 & 0 & 0 & 0 & 0 \\ 0 & 1 & -2 & 1 & 0 & 0 & 0 & 0 & 0 \\ 0 & 0 & 1 & -2 & 1 & 0 & 0 & 0 & 0 \\ 0 & 0 & 0 & 1 & -2 & 1 & 0 & 0 & 0 \\ 0 & 0 & 0 & 0 & 1 & -2 & 1 & 0 & 0 \\ 0 & 0 & 0 & 0 & 0 & 1 & -2 & 1 & 0 \\ 0 & 0 & 0 & 0 & 0 & 0 & 1 & -2 & 1 \\ 0 & 0 & 0 & 0 & 0 & 0 & 0 & 1 & -2 \end{bmatrix}^{-1} \begin{bmatrix} -99.7 \\ 0 \\ 0 \\ 0 \\ 0 \\ 0 \\ 0 \\ 0 \\ 0 \end{bmatrix}$$

The solution obtained for the first time step is as shown below.

$$\begin{bmatrix} C_{1,1} \\ C_{2,1} \\ C_{3,1} \\ C_{4,1} \\ C_{5,1} \\ C_{6,1} \\ C_{7,1} \\ C_{8,1} \\ C_{9,1} \end{bmatrix} = \begin{bmatrix} 89.73 \\ 79.76 \\ 69.79 \\ 59.82 \\ 49.85 \\ 39.88 \\ 29.91 \\ 19.94 \\ 9.97 \end{bmatrix}$$

Other time steps i.e. $j=1, 2, 3, \dots, 9$ are solved using similar procedure.

Similarly, discretizing equation (3.95),

$$C = C_{i,j} \quad (4.40)$$

$$\frac{\partial C}{\partial r} = \frac{C_{i+1,j} - C_{i,j}}{h} \quad (4.41)$$

$$\frac{\partial^2 C}{\partial r^2} = \frac{C_{i-1,j} - 2C_{i,j} + C_{i+1,j}}{h^2} \quad (4.42)$$

$$\frac{\partial C}{\partial t} = \frac{C_{i+1,j} - C_{i,j}}{k} \quad (4.43)$$

$$h=0.001, k=7$$

Substituting equations 4.40 through 4.43 and the values of ψ , η , ϕ into equation 4.25 \Rightarrow

$$C_{i-1,j+1} - 3.4C_{i,j+1} + C_{i+1,j+1} = -1.18C_{i,j} - 0.2C_{i+1,j} - 0.74 \quad (4.44)$$

Applying same principle as in equation (4.30) and substituting initial and boundary conditions, we have

For $j=0$

$$i=1, j=0 \quad C_{0,1} - 3.4C_{1,1} + C_{2,1} = -1.18C_{1,0} - 0.2C_{2,0} - 0.74$$

but $C_{1,0} = 0$, $C_{2,0} = 0$, $C_{0,1} = 99.7$

$$-3.4C_{1,1} + C_{2,1} = -100.44 \quad (4.45)$$

$i=2, j=0$

$$C_{1,1} - 3.4C_{2,1} + C_{3,1} = -0.74 \quad (4.46)$$

$i=3, j=0$

$$C_{2,1} - 3.4C_{3,1} + C_{4,1} = -0.74 \quad (4.47)$$

$i=4, j=0$

$$C_{3,1} - 3.4C_{4,1} + C_{5,1} = -0.74 \quad (4.48)$$

$i=5, j=0$

$$C_{4,1} - 3.4C_{5,1} + C_{6,1} = -0.74 \quad (4.49)$$

$i=6, j=0$

$$C_{5,1} - 3.4C_{6,1} + C_{7,1} = -0.74 \quad (4.50)$$

$i=7, j=0$

$$C_{6,1} - 3.4C_{7,1} + C_{8,1} = -0.74 \quad (4.51)$$

$$i=8, j=0$$

$$C_{7,1} - 3.4C_{8,1} + C_{9,1} = -0.74 \quad (4.52)$$

$$i=9, j=0$$

$$C_{8,1} - 3.4C_{9,1} + C_{10,1} = -0.74$$

$$\text{but } C_{10,1} = 0$$

$$C_{8,1} - 3.4C_{9,1} = -0.74 \quad (4.53)$$

These set of simultaneous equations are also resolved by applying the same procedure described for the macroporous system. Therefore, we have,

$$\begin{bmatrix} -3.4 & 1 & 0 & 0 & 0 & 0 & 0 & 0 & 0 \\ 1 & -3.4 & 1 & 0 & 0 & 0 & 0 & 0 & 0 \\ 0 & 1 & -3.4 & 1 & 0 & 0 & 0 & 0 & 0 \\ 0 & 0 & 1 & -3.4 & 1 & 0 & 0 & 0 & 0 \\ 0 & 0 & 0 & 1 & -3.4 & 1 & 0 & 0 & 0 \\ 0 & 0 & 0 & 0 & 1 & -3.4 & 1 & 0 & 0 \\ 0 & 0 & 0 & 0 & 0 & 1 & -3.4 & 1 & 0 \\ 0 & 0 & 0 & 0 & 0 & 0 & 1 & -3.4 & 1 \\ 0 & 0 & 0 & 0 & 0 & 0 & 0 & 1 & -3.4 \end{bmatrix} \begin{bmatrix} C_{1,1} \\ C_{2,1} \\ C_{3,1} \\ C_{4,1} \\ C_{5,1} \\ C_{6,1} \\ C_{7,1} \\ C_{8,1} \\ C_{9,1} \end{bmatrix} = \begin{bmatrix} -100.44 \\ -0.74 \\ -0.74 \\ -0.74 \\ -0.74 \\ -0.74 \\ -0.74 \\ -0.74 \\ -0.74 \end{bmatrix}$$

Solving:

$$\begin{bmatrix} C_{1,1} \\ C_{2,1} \\ C_{3,1} \\ C_{4,1} \\ C_{5,1} \\ C_{6,1} \\ C_{7,1} \\ C_{8,1} \\ C_{9,1} \end{bmatrix} = \begin{bmatrix} -3.4 & 1 & 0 & 0 & 0 & 0 & 0 & 0 & 0 \\ 1 & -3.4 & 1 & 0 & 0 & 0 & 0 & 0 & 0 \\ 0 & 1 & -3.4 & 1 & 0 & 0 & 0 & 0 & 0 \\ 0 & 0 & 1 & -3.4 & 1 & 0 & 0 & 0 & 0 \\ 0 & 0 & 0 & 1 & -3.4 & 1 & 0 & 0 & 0 \\ 0 & 0 & 0 & 0 & 1 & -3.4 & 1 & 0 & 0 \\ 0 & 0 & 0 & 0 & 0 & 1 & -3.4 & 1 & 0 \\ 0 & 0 & 0 & 0 & 0 & 0 & 1 & -3.4 & 1 \\ 0 & 0 & 0 & 0 & 0 & 0 & 0 & 1 & -3.4 \end{bmatrix}^{-1} \begin{bmatrix} -100.44 \\ -0.74 \\ -0.74 \\ -0.74 \\ -0.74 \\ -0.74 \\ -0.74 \\ -0.74 \\ -0.74 \end{bmatrix}$$

The solution obtained for the first time step is as shown below:

$$\begin{bmatrix} C_{1,1} \\ C_{2,1} \\ C_{3,1} \\ C_{4,1} \\ C_{5,1} \\ C_{6,1} \\ C_{7,1} \\ C_{8,1} \\ C_{9,1} \end{bmatrix} = \begin{bmatrix} 32.782 \\ 11.018 \\ 3.9399 \\ 1.6375 \\ 0.8875 \\ 0.64 \\ 0.5485 \\ 0.4849 \\ 0.3603 \end{bmatrix}$$

The results showing the numerical solutions to the non-steady state model (axial and radial directions) for the contaminant PAHs used in this study are given in Tables I.1 to I.3 and I.4 to I.6 in Appendix I. A 3-dimensional plot showing the detailed distribution and variation in composition of the contaminant solutes in time and space (position) are presented in Chapter Five.

CHAPTER FIVE

5.0

RESULTS

The results of the experimentation and computation analysis of the modelling equations of the bioremediation of PAH contaminated surface and subsurface soils are now presented. A case study of ex-situ technique in a soil microcosm reactor is used. The potential for the indigenous microbes to mineralize the PAHs have been exploited. The level of microbial activities in the soil was assessed by measuring the net cumulative oxygen uptake and carbon (iv) oxide evolution. The information on the aqueous-phase concentration alone on the PAHs was inadequate to predict risk likely to occur from exposure to PAHs. This is because it ignores the bioavailability of the contaminants. The mass transfer-limited numerical model developed was therefore used to explore the possible effects of sorption and bioavailability on biodegradation rates. A comparative analysis of the theoretical predictions from the model with data from laboratory experiments provided the basis for the choice of the applicable and suitable parameters for correlating bioavailability and biodegradation. Some of the properties of the PAHs under investigation in this research work are listed in Table 5.1 below. These properties are relevant in the study of the behaviour of these chemicals.

Table 5.1 Some properties of investigated PAHs*

Properties	Naphthalene	Anthracene	Pyrene
Molecular formula	C ₁₀ H ₈	C ₁₄ H ₁₀	C ₁₆ H ₁₀
Molecular weight (g/mol)	128	178	202
Density (g/cm ³)	1.14	1.099	1.271
Melting point (°C)	80.5	217.5	145-148
Boiling point (°C)	218	340	404
Aqueous solubility (g/m ³)	0.93	0.07	0.14

*Adapted from Zander *et al.*, (1993), Perry's Handbook of Chemical Engineers' (1998) and Oleszczuk and Baran, (2003).

The details of the results of the studies carried out for the mineralization of the mixture of polycyclic aromatic hydrocarbons in this research work are presented and discussed below.

5.1 Soil Characterization

Soil structure controls the effective delivery of air, water and nutrients and as such is an important factor primarily considered for a successful bioremediation process. The result of the soil analysis for the level of PAH-contamination prior to the spiking of the soil with naphthalene, anthracene and pyrene, showed that there was no PAH present in the soil. Consequent upon this, the soil used for this study was characterized and the results of its physicochemical properties are as shown in Table 5.2.

The soil was characterized as sandy-clay in the ratio 85:14%. The most dominant particle size was between 0.35-2.00 mm with fewer than 5% greater than 2.00mm. The pH value of the soil was 3.98 as it was characterized by a high level of exchangeable acidity ($\text{Al}^{3+} + \text{H}^+$). The organic content in the soil was 2.44% (carbon) and 4.19% (organic matter). The total cation exchange capacity of the soil was 3.65 cmol/kg while the nitrogen and available phosphorus content were 0.114% and 6.65mg/kg, respectively. The values of ammonium acetate-exchangeable Ca, Mg, K and Na were 0.65 cmol/kg, 0.14 cmol/kg, 0.12 cmol/kg and 0.08 cmol/kg, respectively. The standard interpretation generally adopted for tropic and subtropical soils are given in Appendix E (Soil Survey Manual, 1975).

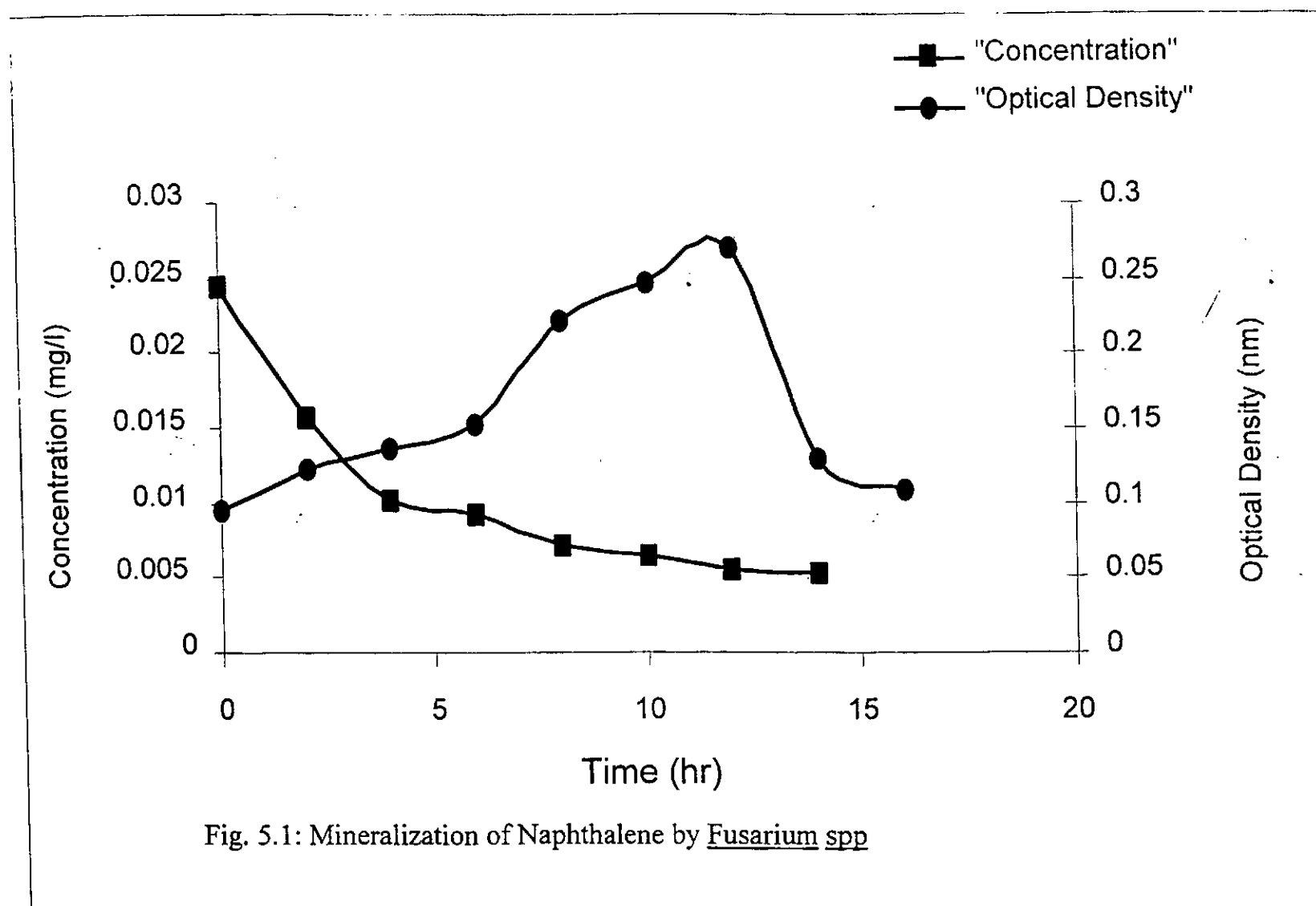
Table 5.2: Soil Characteristics

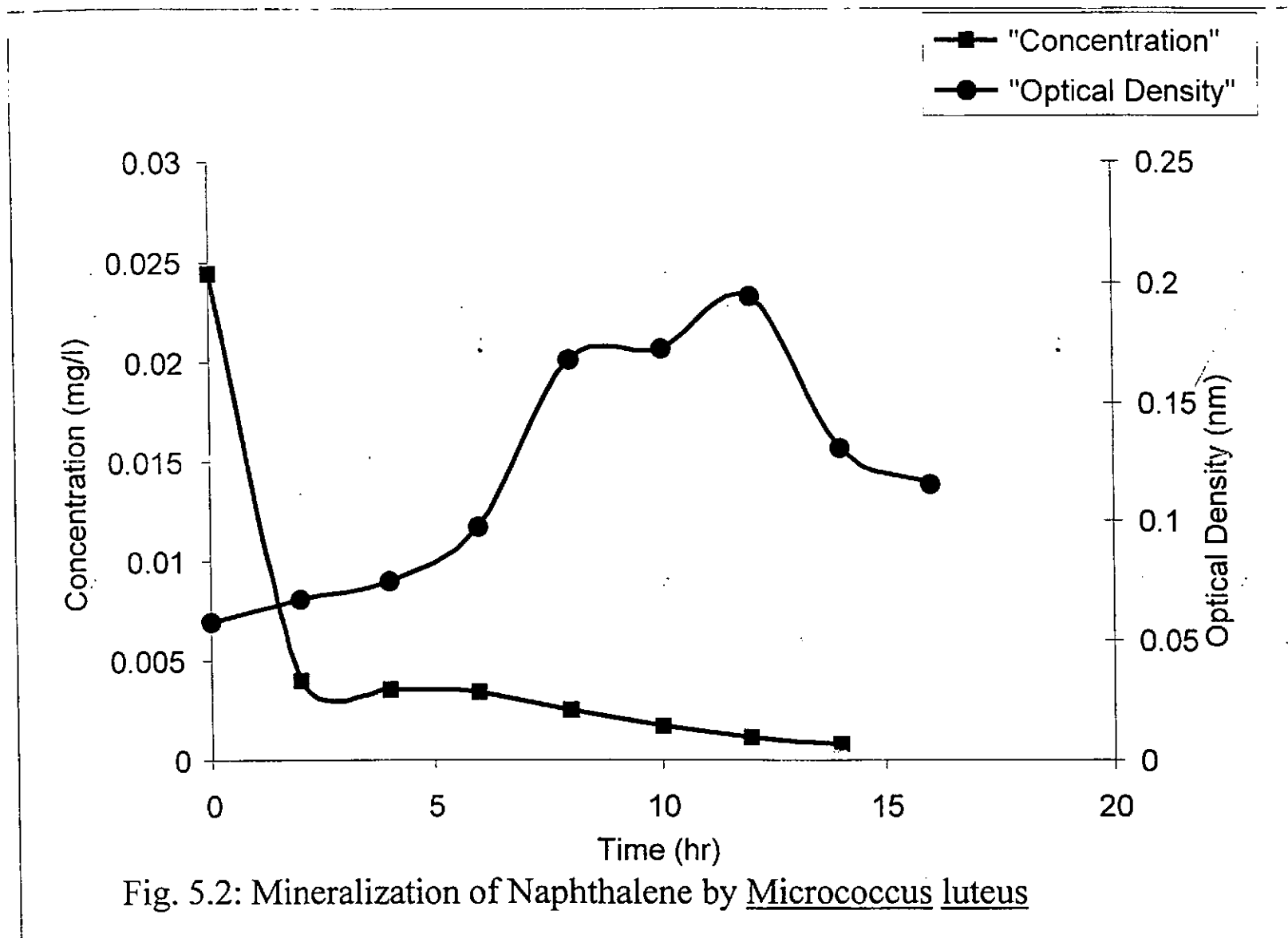
Soil moisture (%)	5.027
Bulk density	1.25
Total porosity	0.481
Particle size (%)	
Sand	85
Silt	1
Clay	14
pH (1:1) H_2O	3.98
Organic Carbon (%)	2.44
Organic Matter (%)	4.19
Total Nitrogen (%)	0.114
Available Phosphorus (mg/Kg)	6.65

Exchangeable Bases (cmol/kg)	
Ca ⁺⁺	0.65
Mg ⁺⁺	0.14
K ⁺	0.12
Na ⁺	0.08
Exchangeable Acidity (Al ³⁺ + H ⁺)	2.66
CEC (cmol/kg)	3.65

5.2 Microbial analysis

Mineralization of a solution of crystalline naphthalene resulted in increased biomass concentration as indicated by the batch growth curve of a microbial culture shown in Figures 5.1, 5.2, 5.3, 5.4, 5.5 and 5.6. All the microbes used for the study showed the same growth pattern characterized by an initial lag or induction period (region 1), followed by a rapid and an exponential increase in biomass growth (region 2), a stationary/static period (region 3) and finally, the decay phase (region 4).





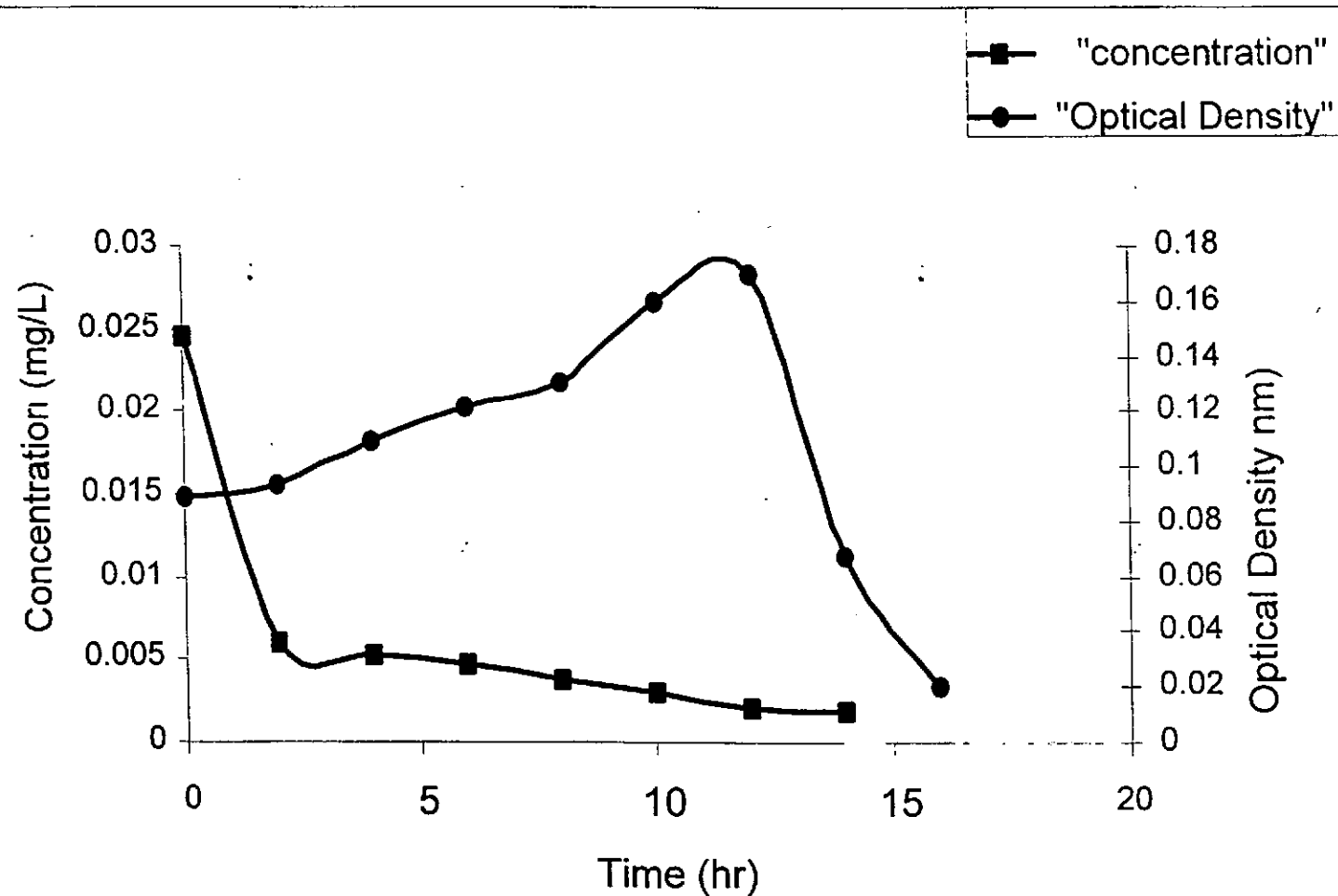


Fig. 5.3: Mineralization of Naphthalene by Bacillus luteus

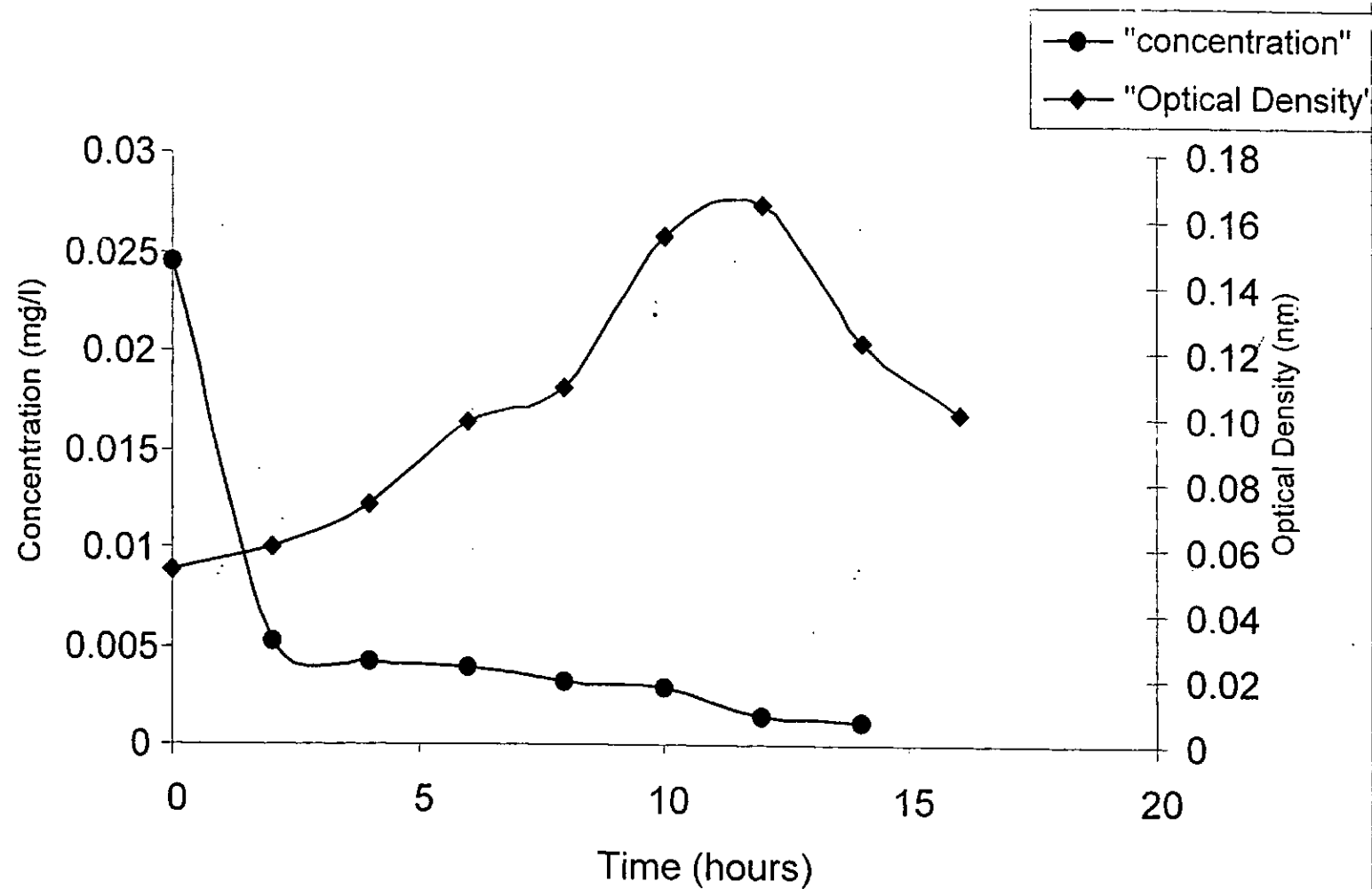


Fig. 5.4: Mineralization of Naphthalene by Bacillus sphaericus

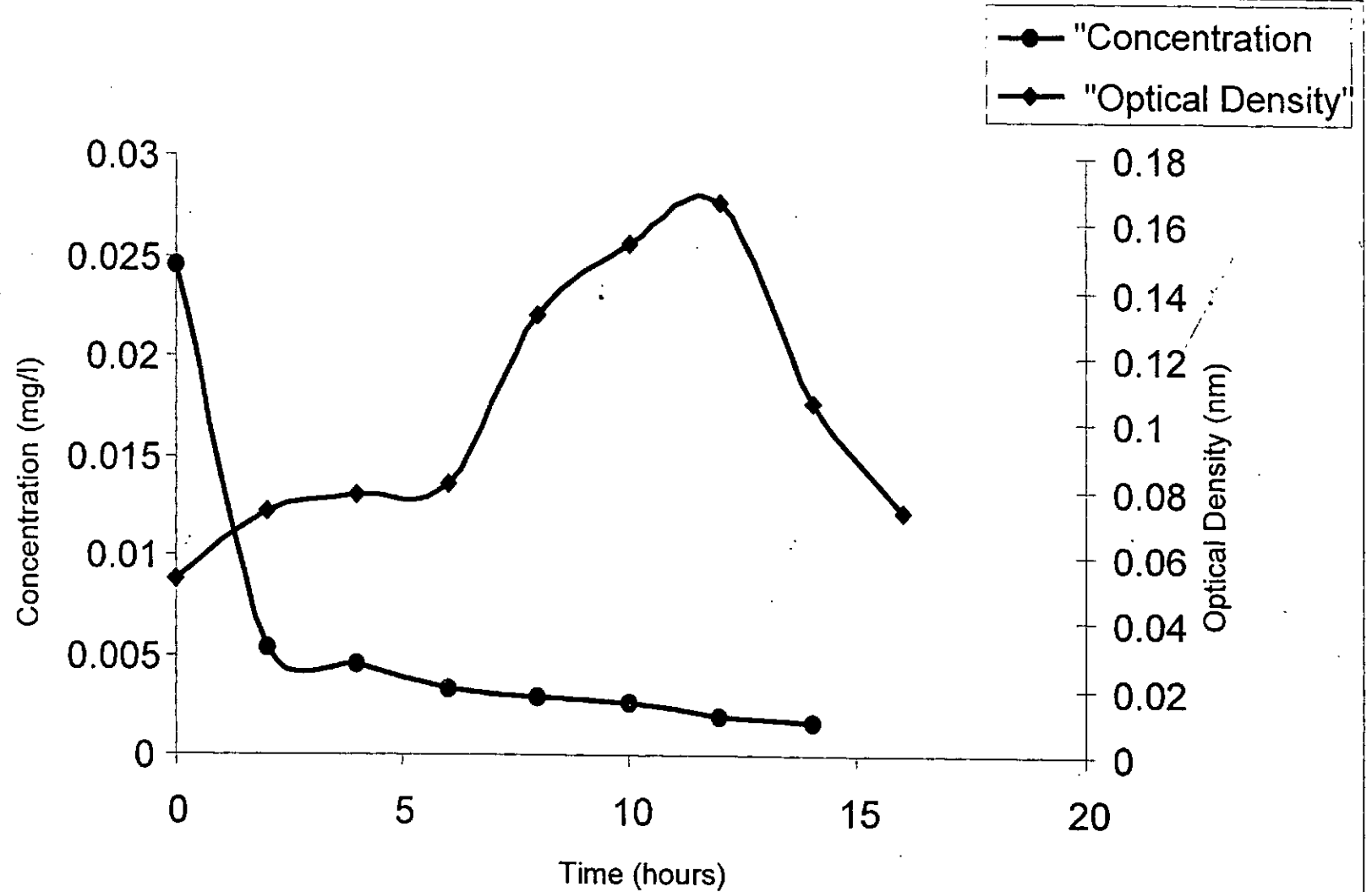
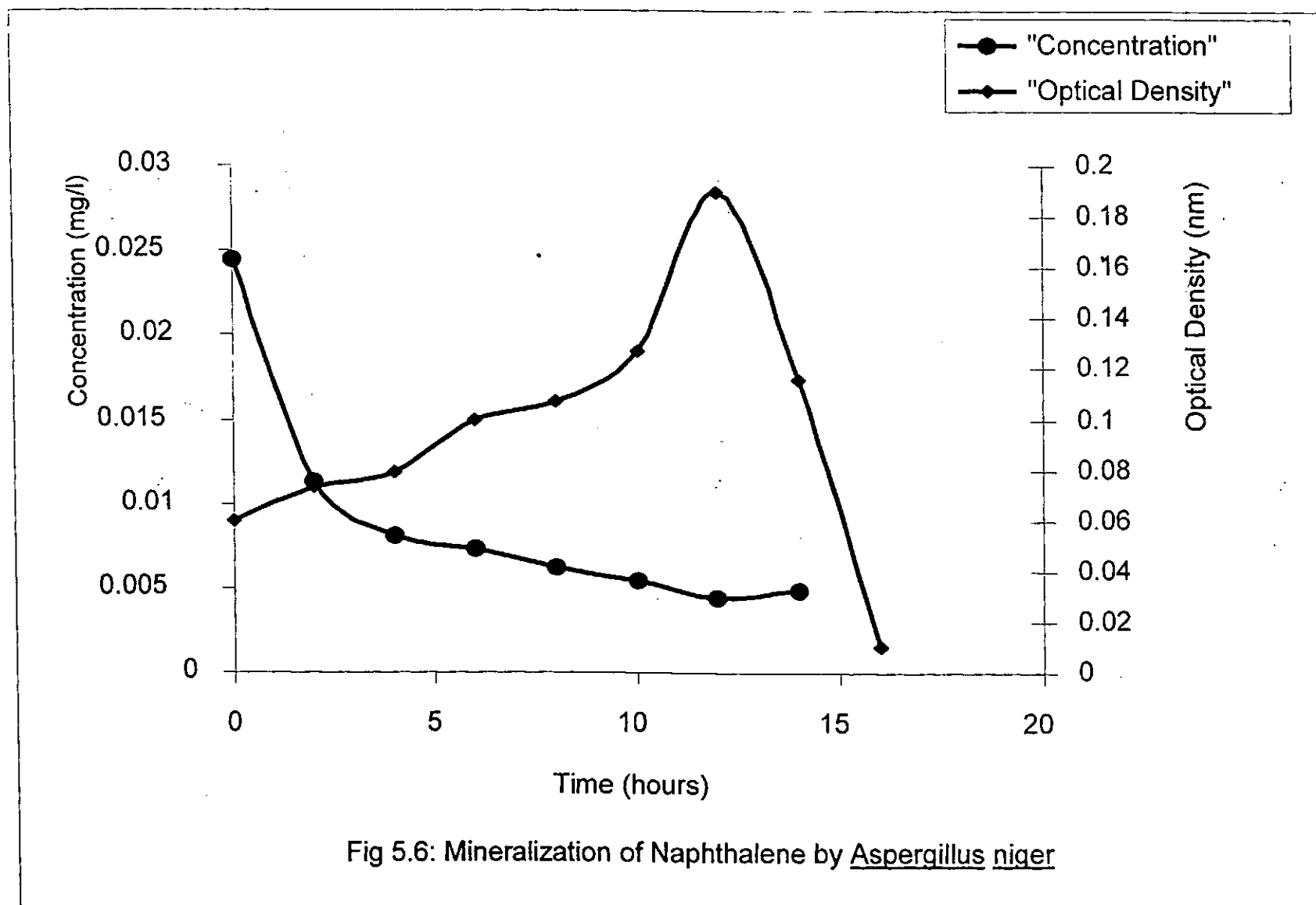


Fig. 5.5: Mineralization of Naphthalene by Klebsiella pneumonia



The microbial growth and substrate consumption rates were determined from the results of the batch experiments on substrate limiting microbial degradation using the performance equation described by Monod and reported by Levenspiel (1999). These are shown in Table 5.3.

Table 5.3: Kinetics of substrate utilization

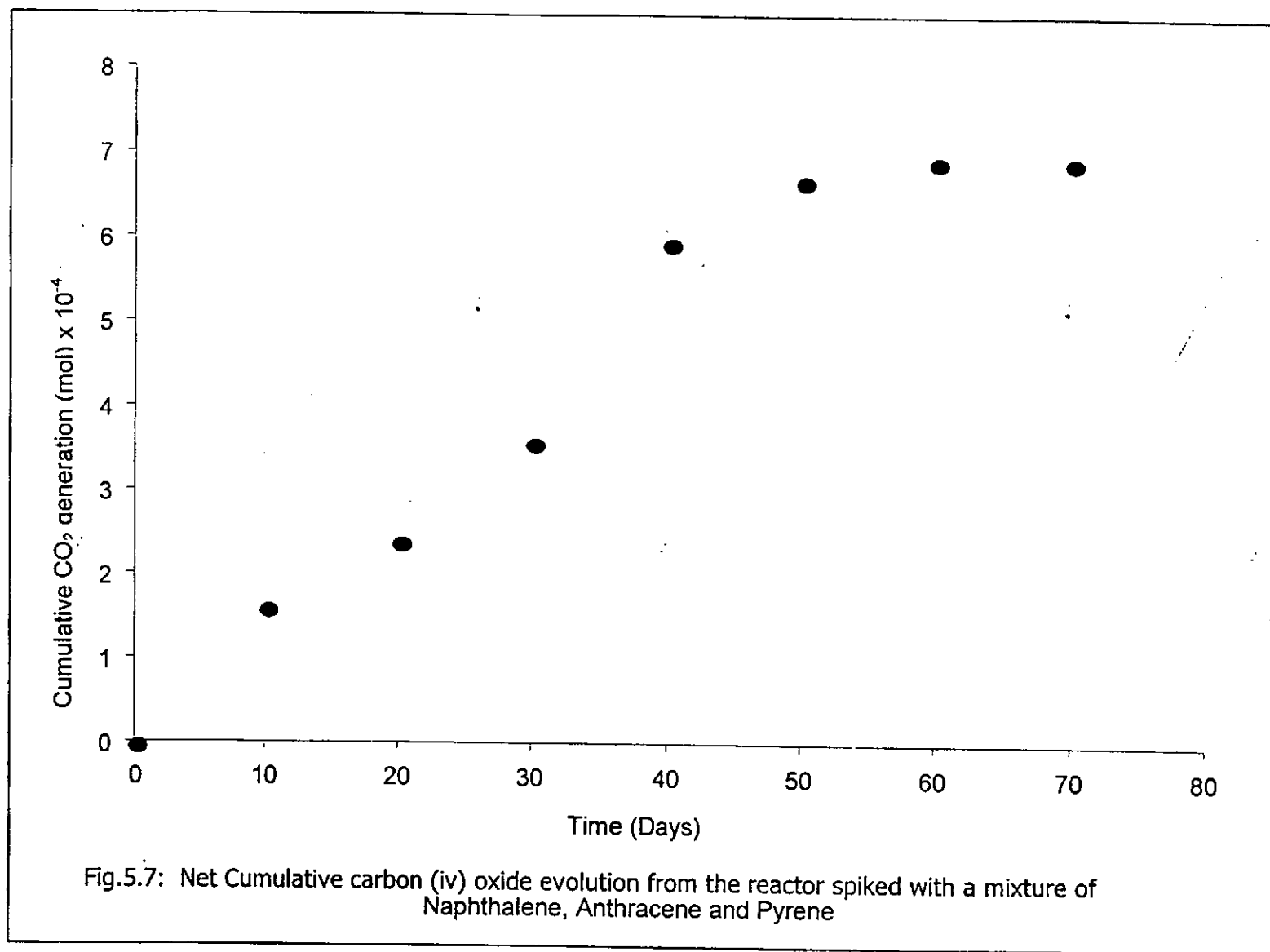
Microorganism	Maximum specific growth rate μ_{\max} (hr ⁻¹)	Biomass yield Y (kg)	Saturation constant k_s (kgm ⁻³)
<u>Bacillus luteus</u>	0.095	0.349	0.028
<u>Bacillus sphaericus</u>	0.165	0.272	0.0343
<u>Micrococcus luteus</u>	0.177	0.222	0.046
<u>Klebsiella pneumonia</u>	0.88	0.271	0.034
<u>Fusarium sp</u>	0.108	0.139	0.195
<u>Aspergillus niger</u>	0.126	0.243	0.061

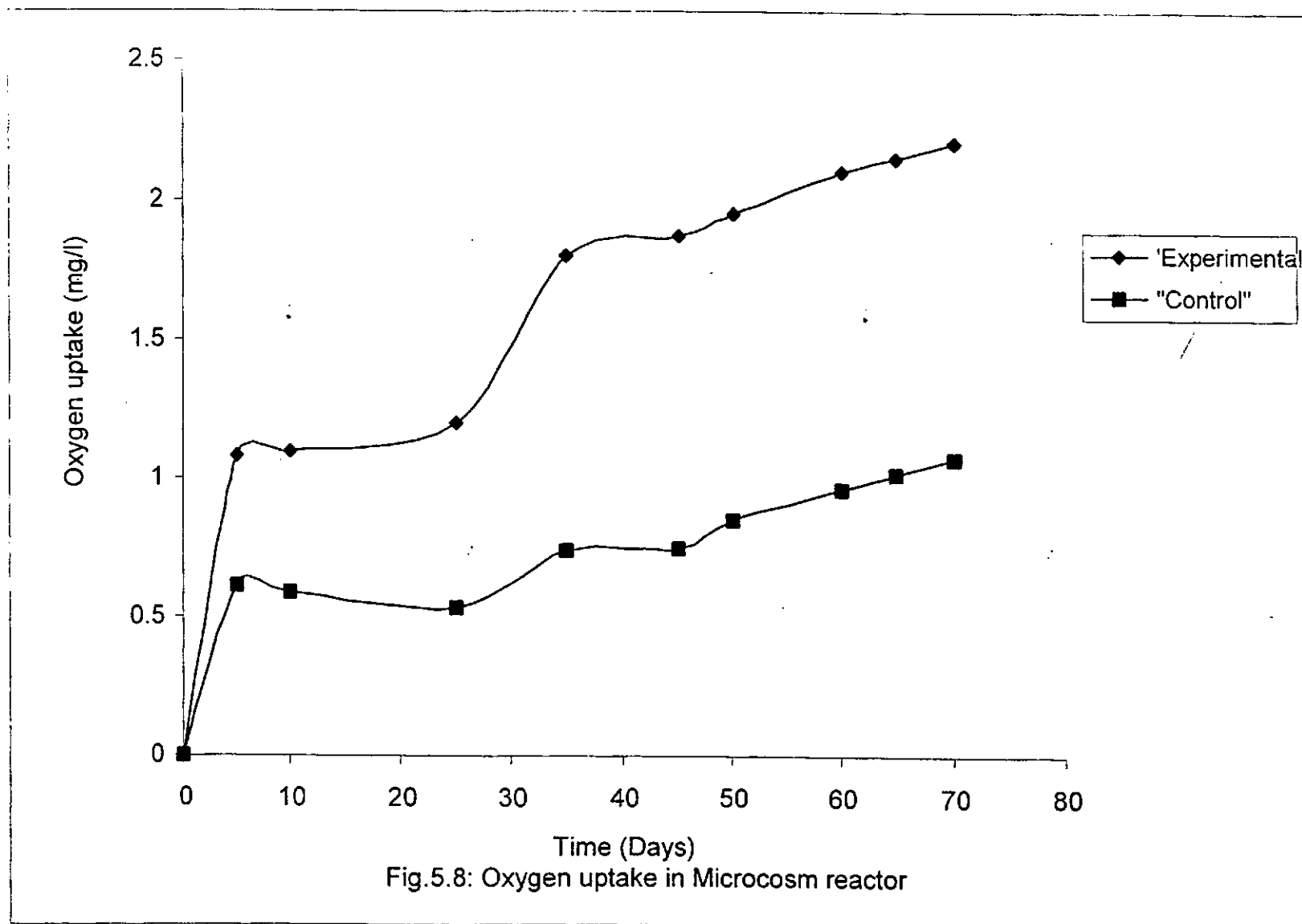
The maximum specific growth rate and biomass yield are dependent on the saturation constant. The saturation constant (k_s) measures the metabolic ability of the organism to utilize naphthalene as carbon and energy sources. A high k_s is indicative of a low affinity for the substrate by the microbe.

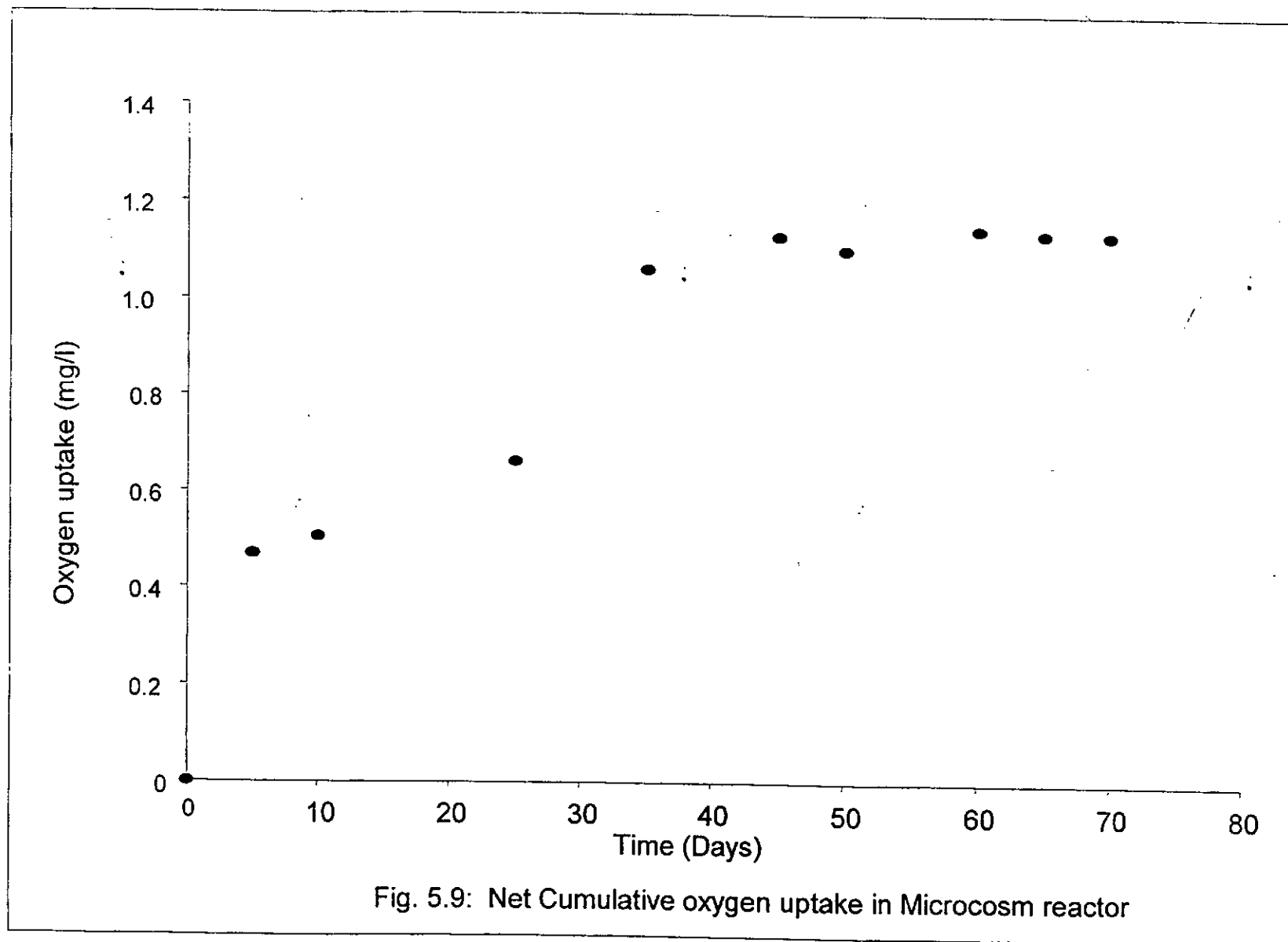
5.3 Analysis of Oxygen Uptake and Carbon (iv) Oxide

Evolution Data

Respirometric studies were conducted to measure the level of microbial activity and for quantitating PAH biodegradation rates in the soil microcosm reactor. Figures 5.7, 5.8 and 5.9 show the net cumulative oxygen consumed and carbon (iv) oxide generated with time. The cumulative oxygen uptake in the control reactor was due mainly to the degradation of soil organic matter resulting from normal soil respiration. It provides an insight on organic matter degradation, which also occurs in the experimental reactor when the PAHs are present.

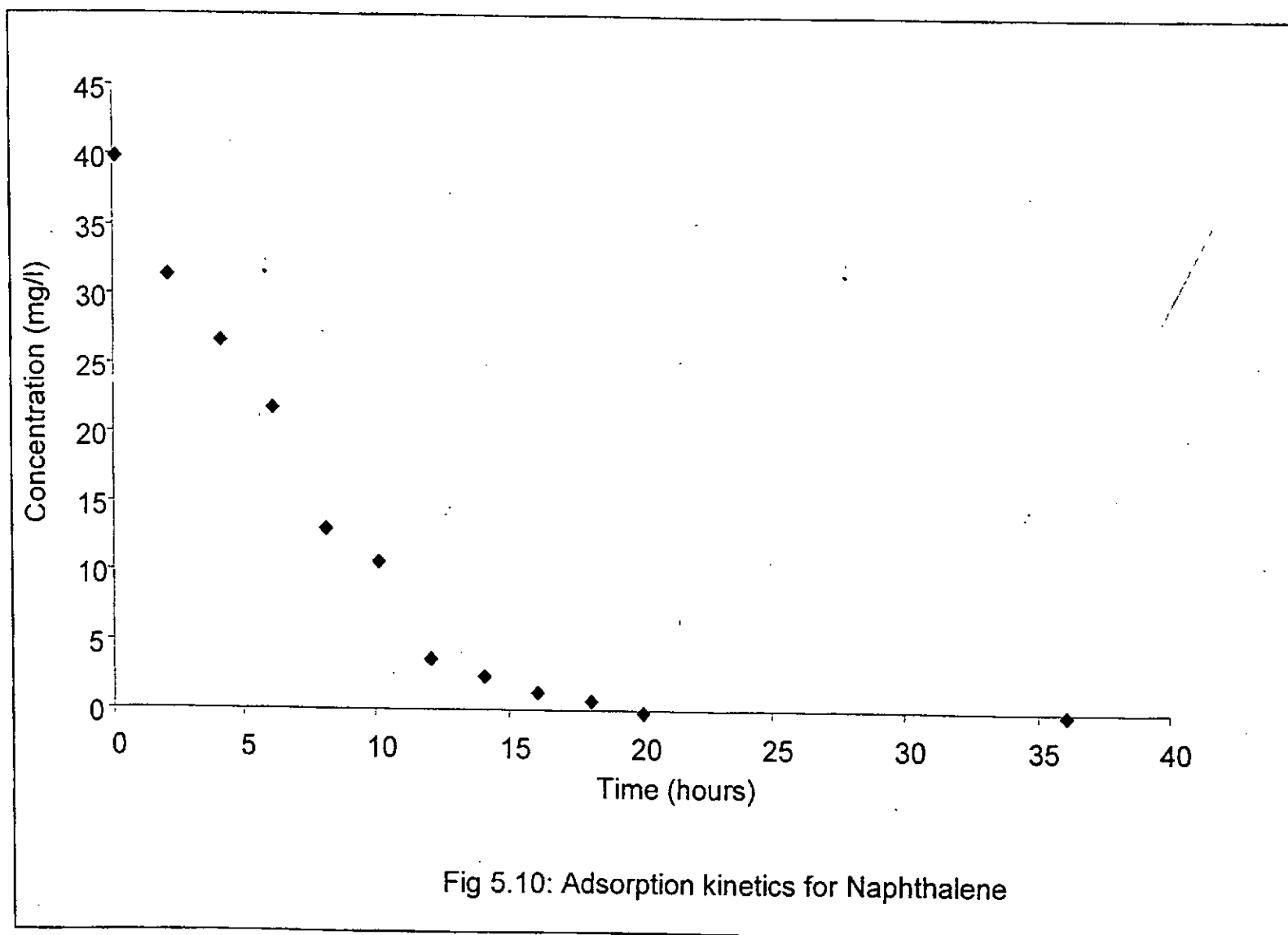


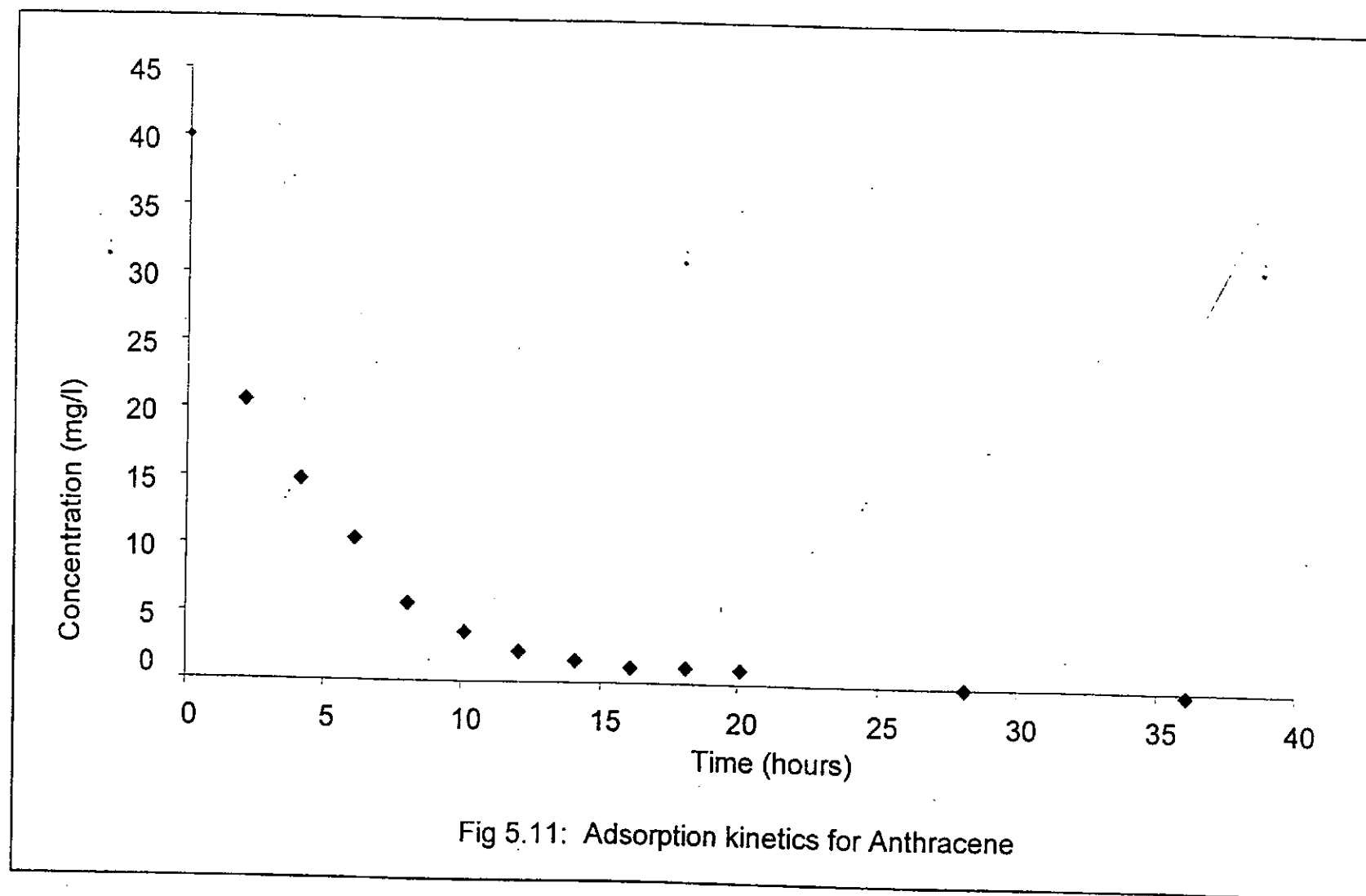


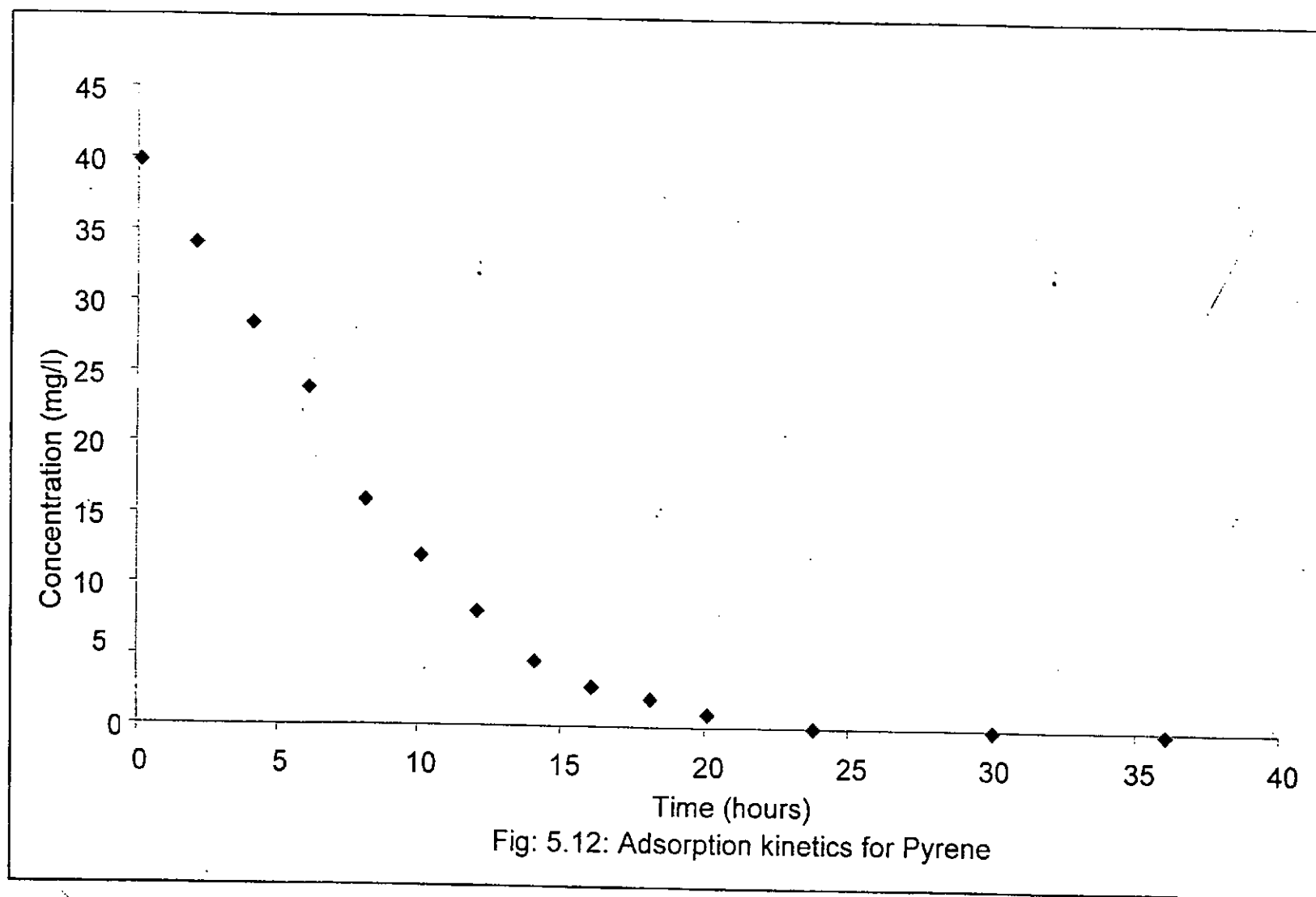


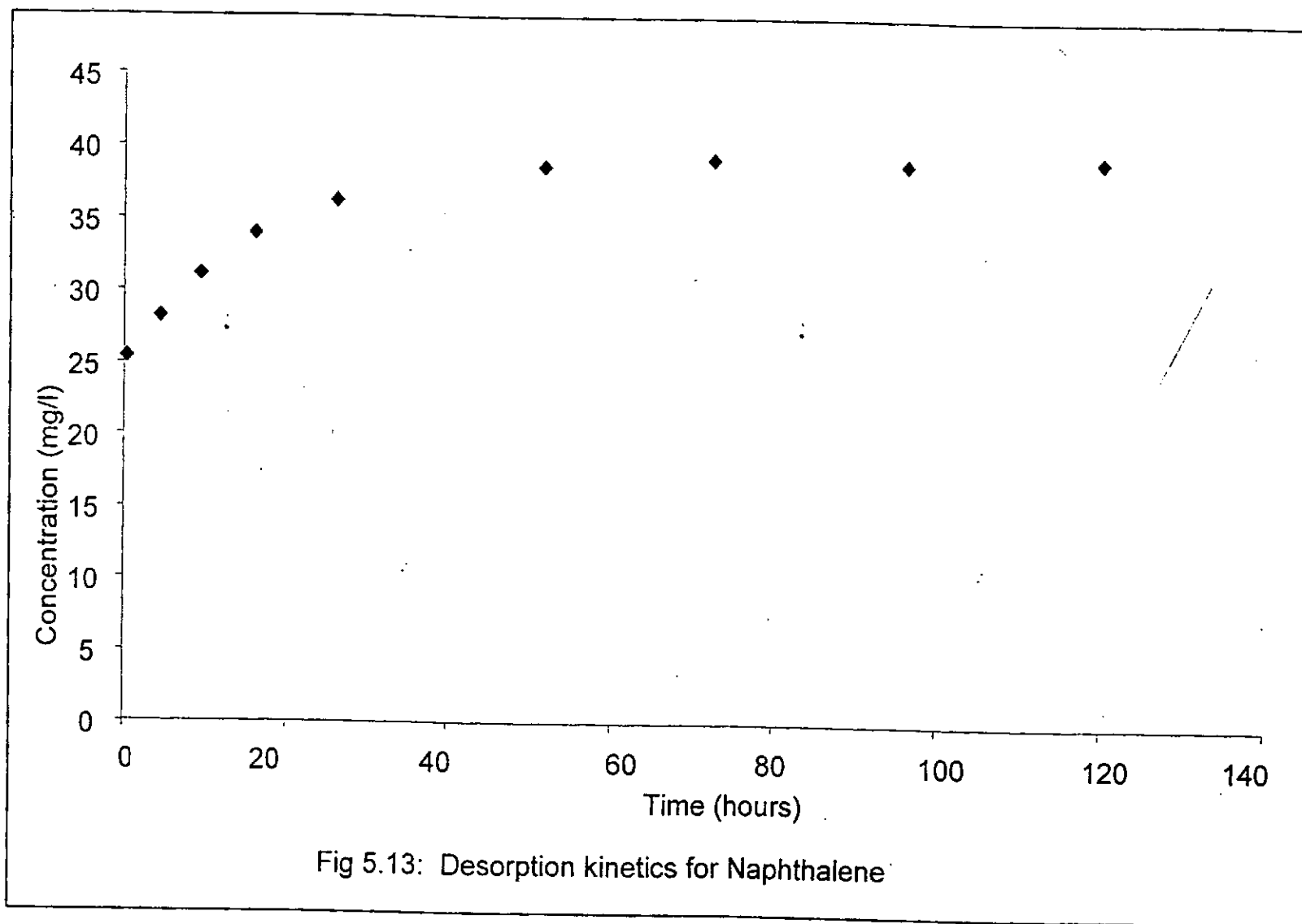
5.4 Analysis of Adsorption and Desorption Data

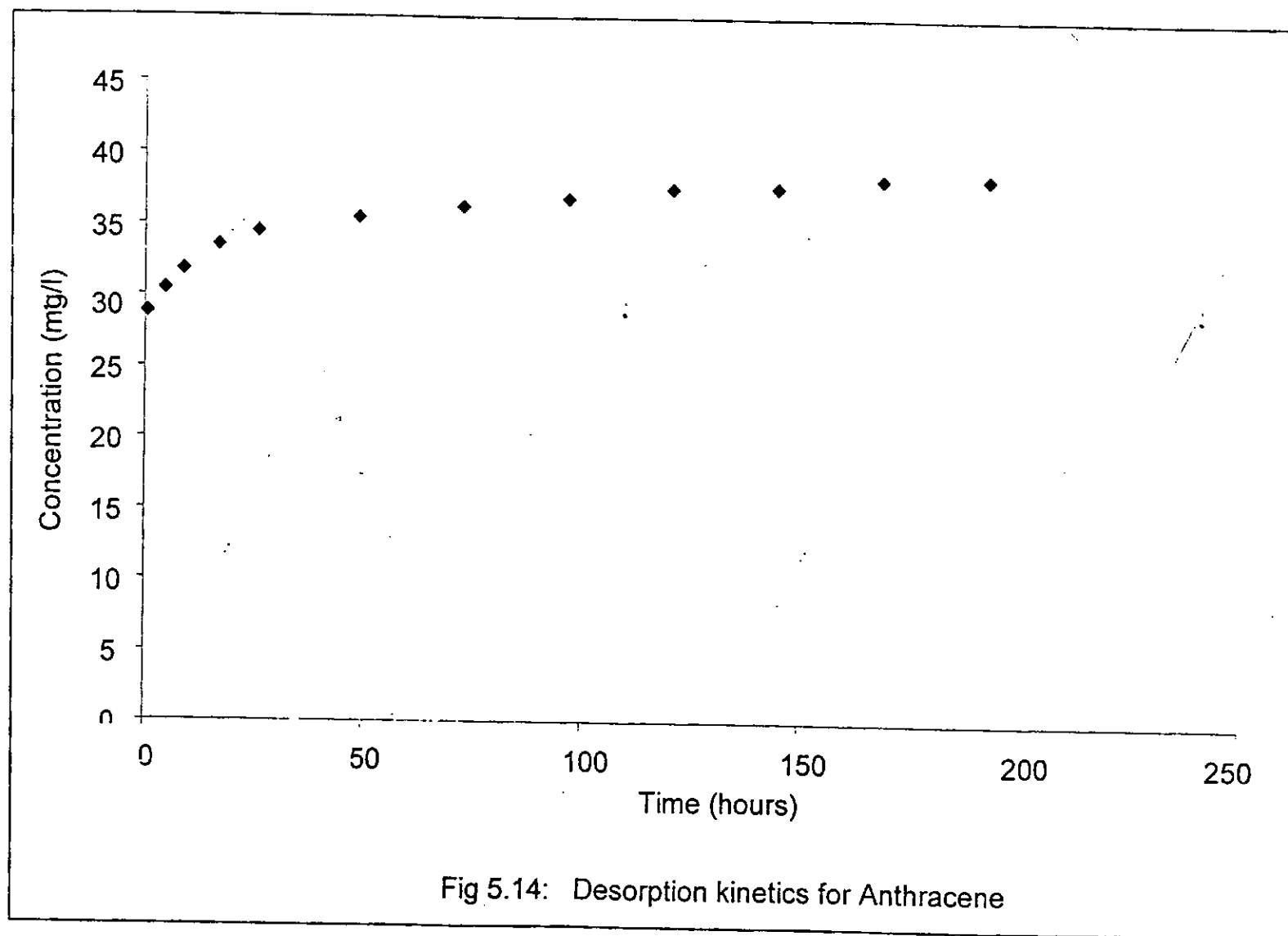
The batch adsorption/desorption kinetics using the test contaminants were characterized by a biphasic pattern, a fast step followed by a slow, diffusive near constant step. Analysis of the experimental results shown in Figures 5.10, 5.11, 5.12, and 5.13, 5.14, 5.15 showed that equilibrium was attained in about 20 hours (naphthalene), 24hours (pyrene), 28hours (anthracene) and 60hours (naphthalene), 120hours (pyrene), 144hours (anthracene) for adsorption and desorption, respectively. The observed slowly desorbing fraction maybe attributed to the effect of intraorganic matter and hindered pore diffusion mechanisms.











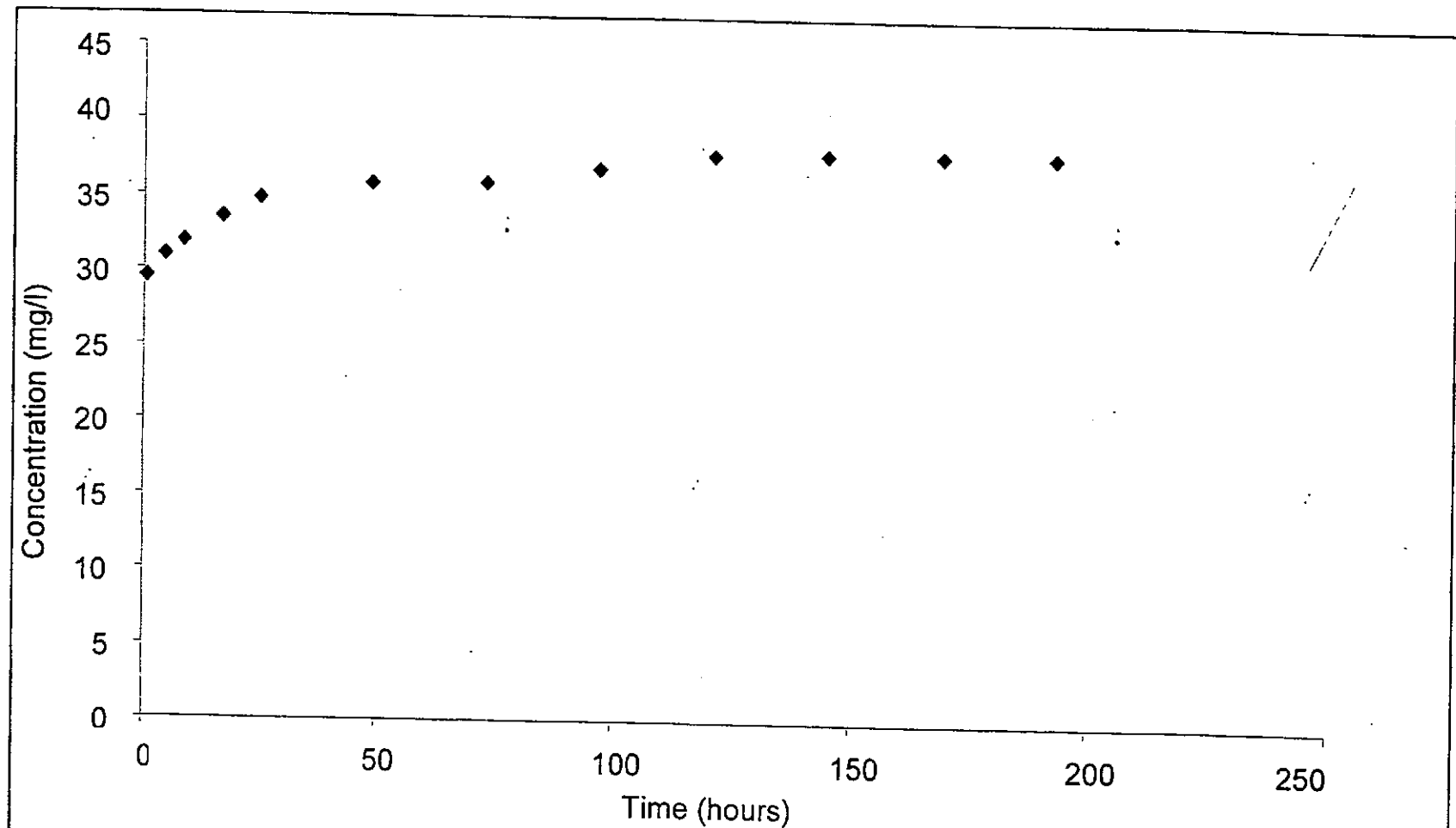


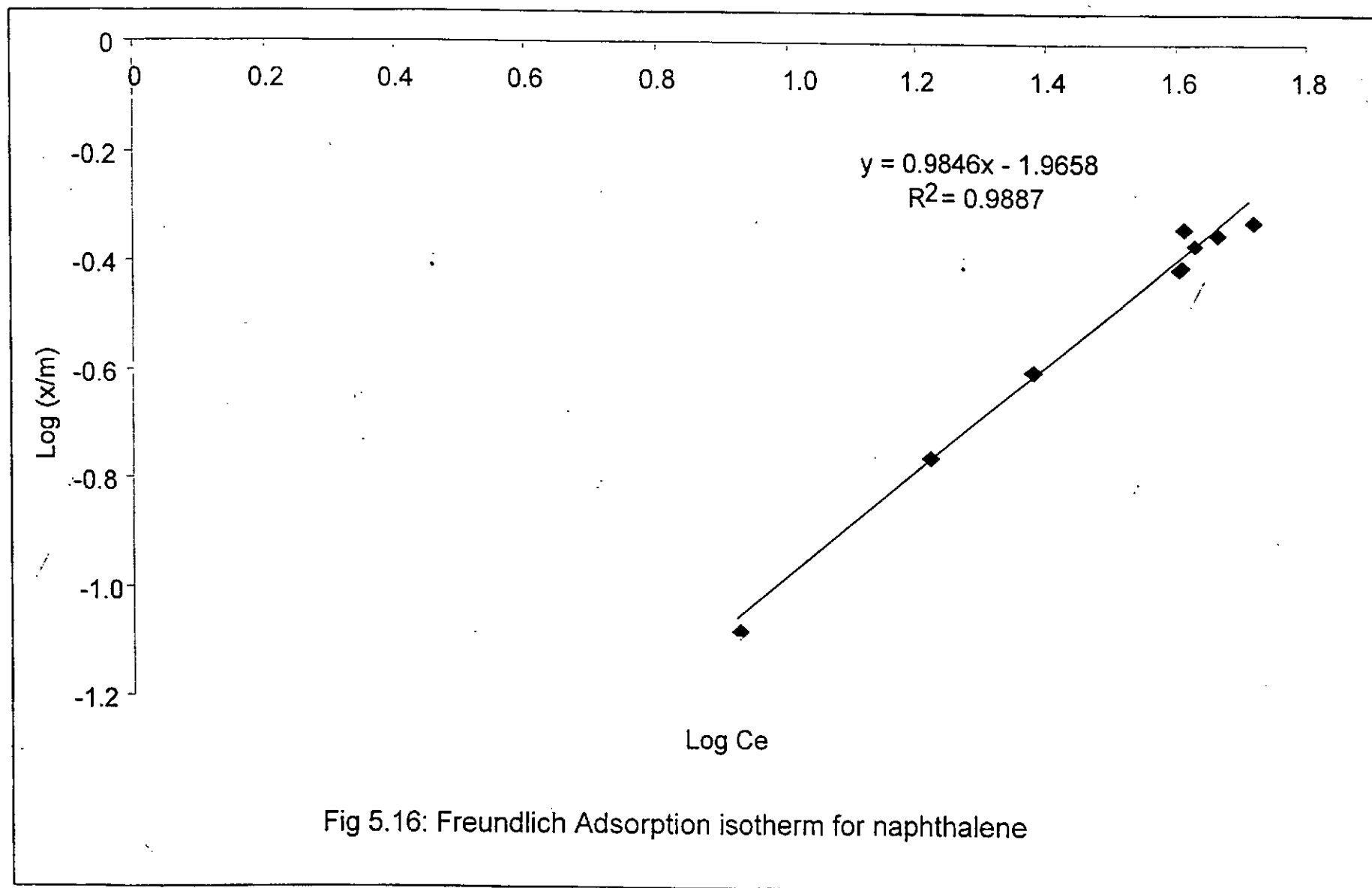
Fig 5.15: Desorption kinetics for Pyrene

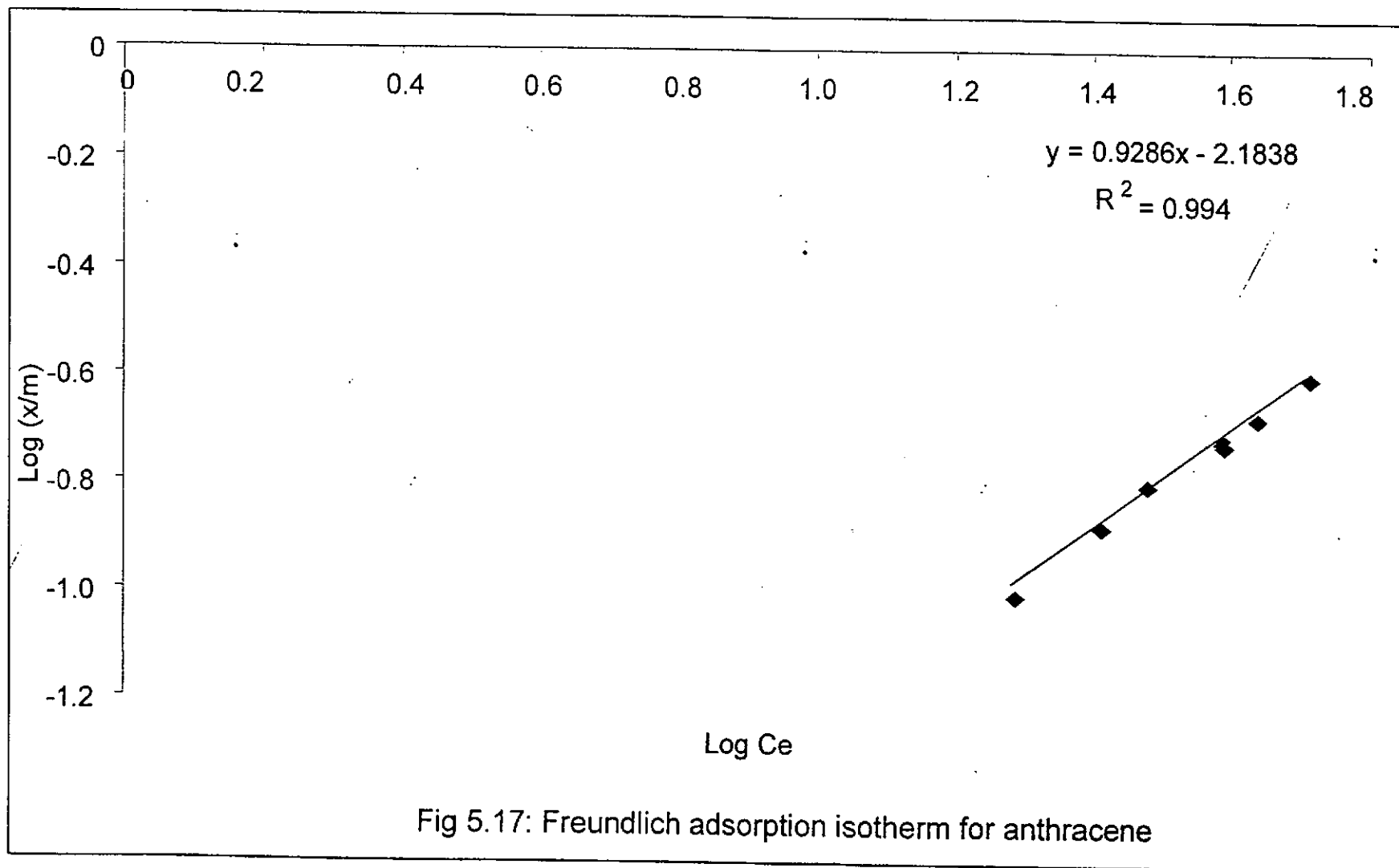
A summary of the result obtained from the application of the linearized Freundlich and Langmuir isotherms on the experimental data from the soil slurry reactor is given in Table 5.4.

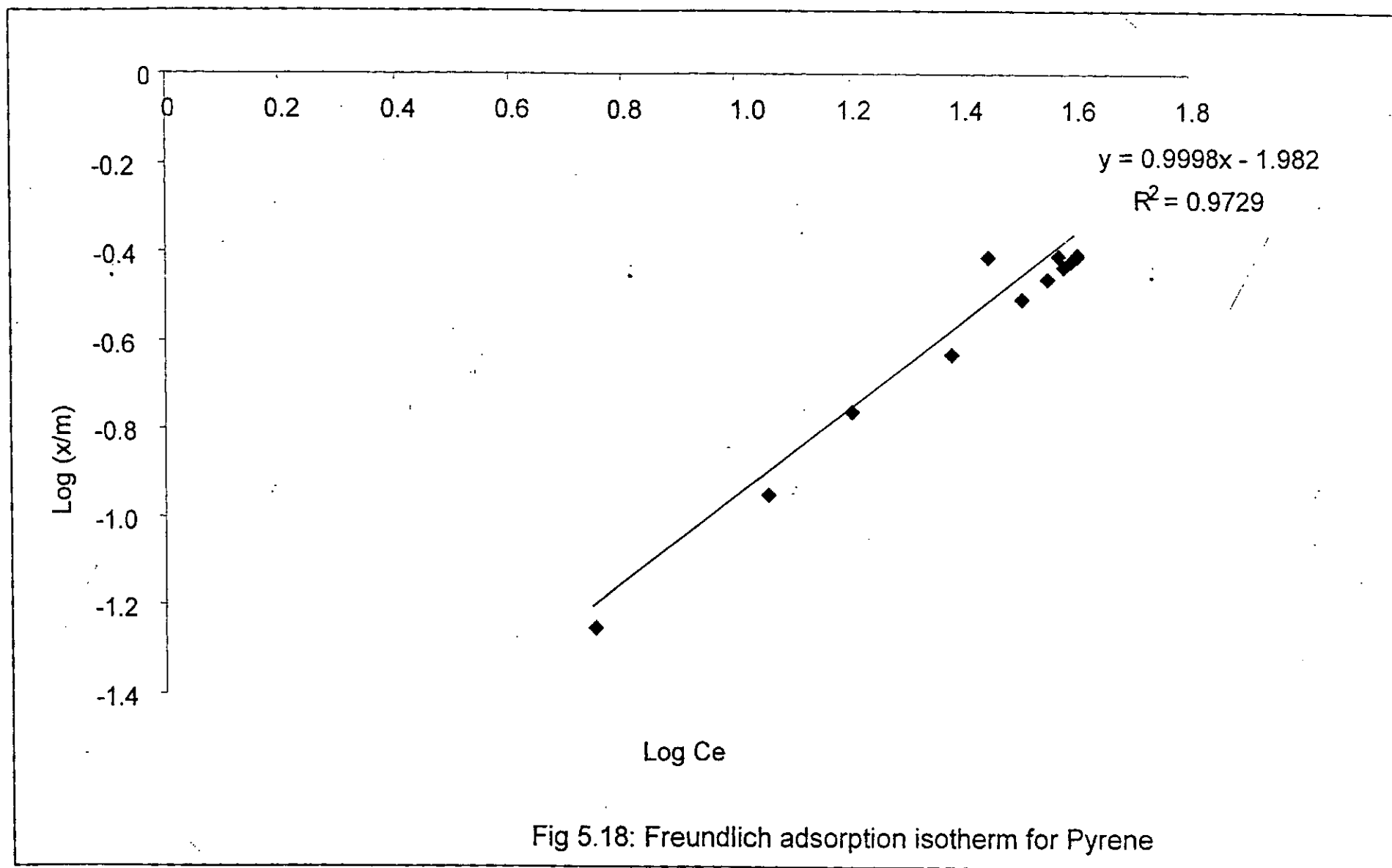
Table 5.4 Isotherm constants for adsorption and desorption for the contaminant PAHs

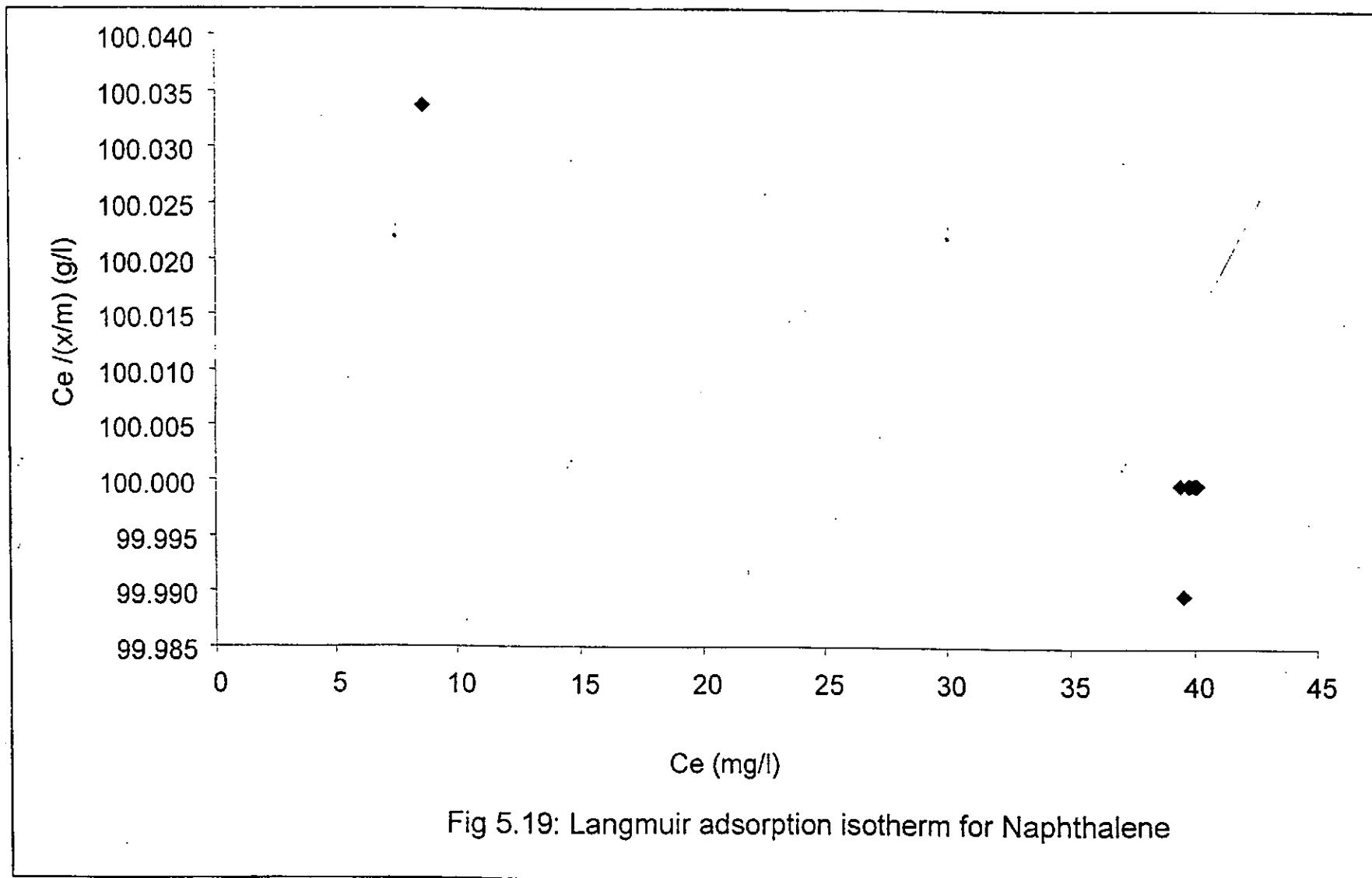
Constants	Naphthalene	Anthracene	Pyrene
Freundlich isotherm			
1/n (adsorption)	0.984	0.9286	0.9998
1/n' (desorption)	0.9695	0.9890	0.9932
K _a	0.010819	0.006549	0.010423
K _d	0.008913	0.0101719	0.010233
Langmuir isotherm			
1/a (adsorption)	-0.0011	-0.308	0.0005
1/a' (desorption)	-1.4499	-0.0026	-0.0011
K _a	9.84E+99	1.349E+99	9.572E+99
K _d	22583.95501	9.984E+99	1.096E+100

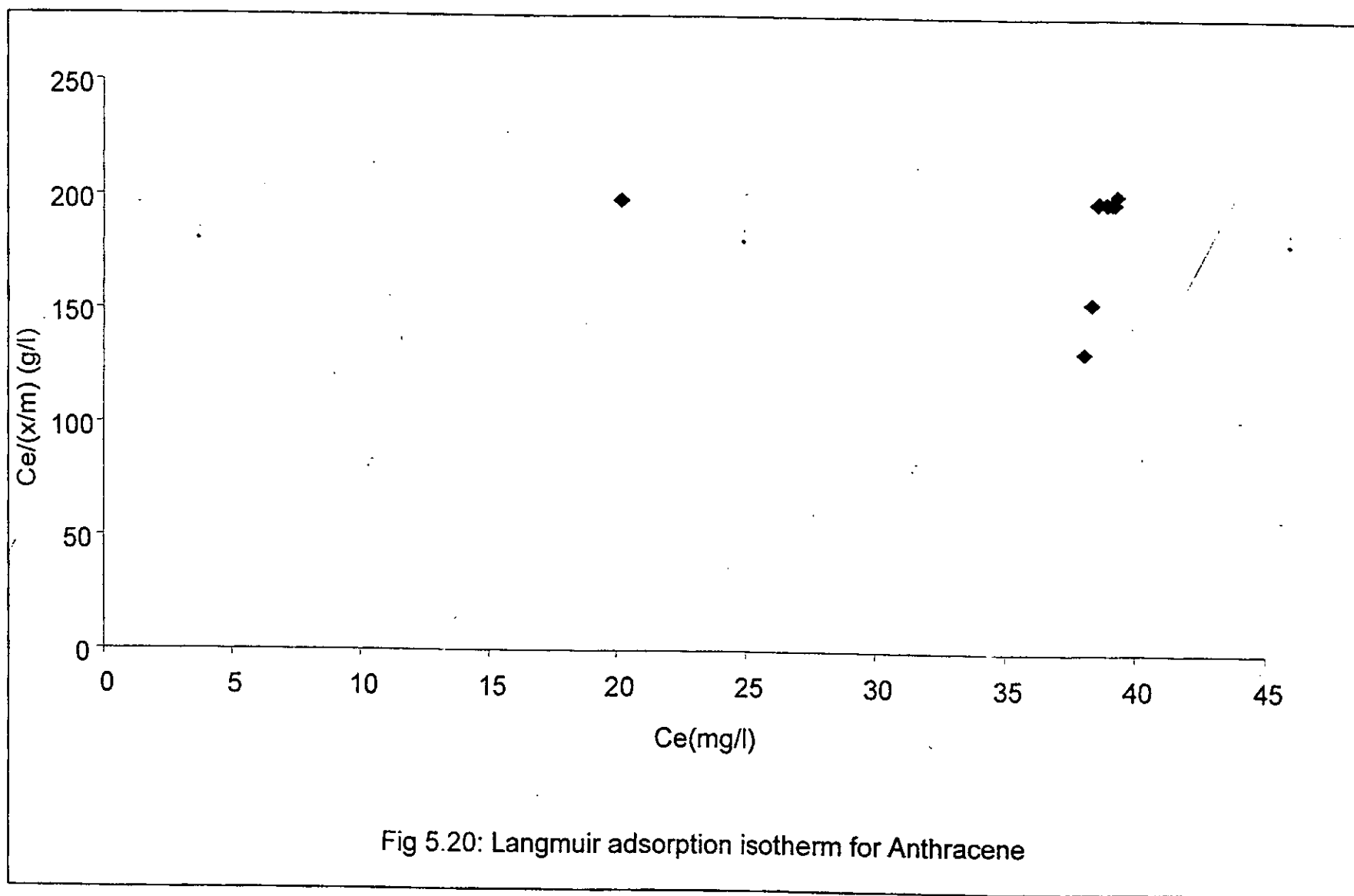
An acceptable and reasonable straight-line correlation was achieved with the Freundlich model as shown in Figures 5.16, 5.17, 5.18, 5.22, 5.23 and 5.24 for adsorption and desorption respectively.

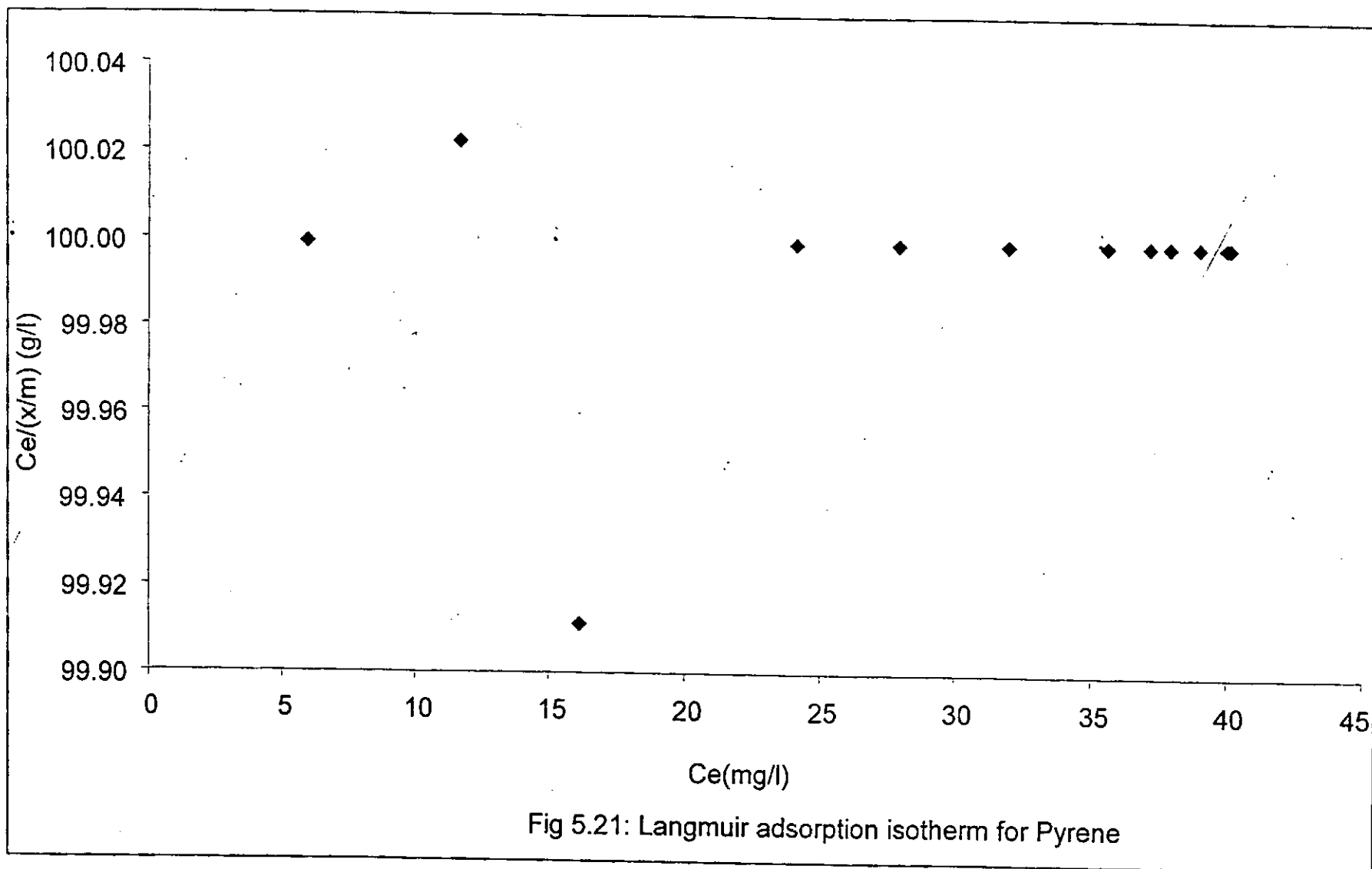












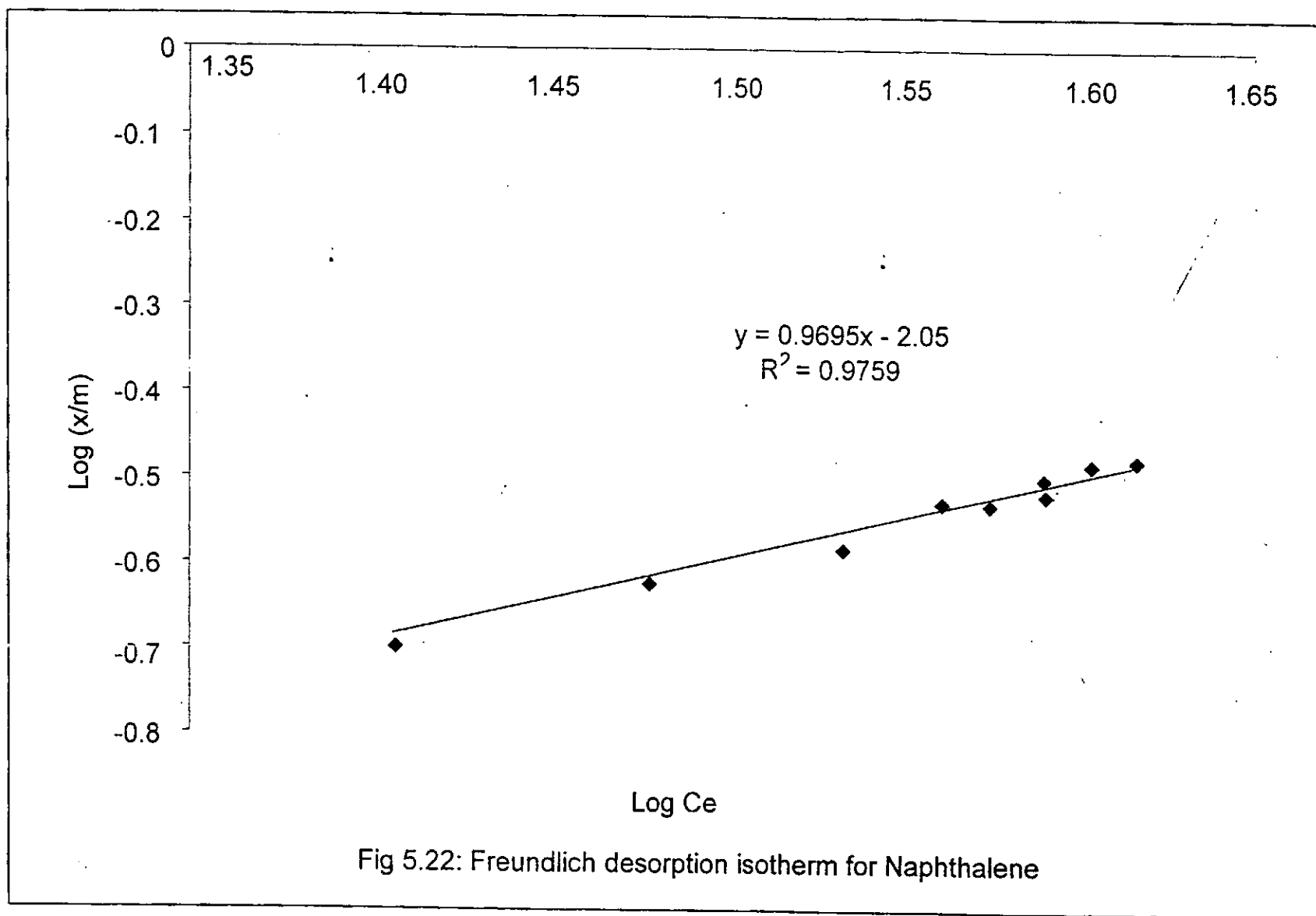


Fig 5.22: Freundlich desorption isotherm for Naphthalene

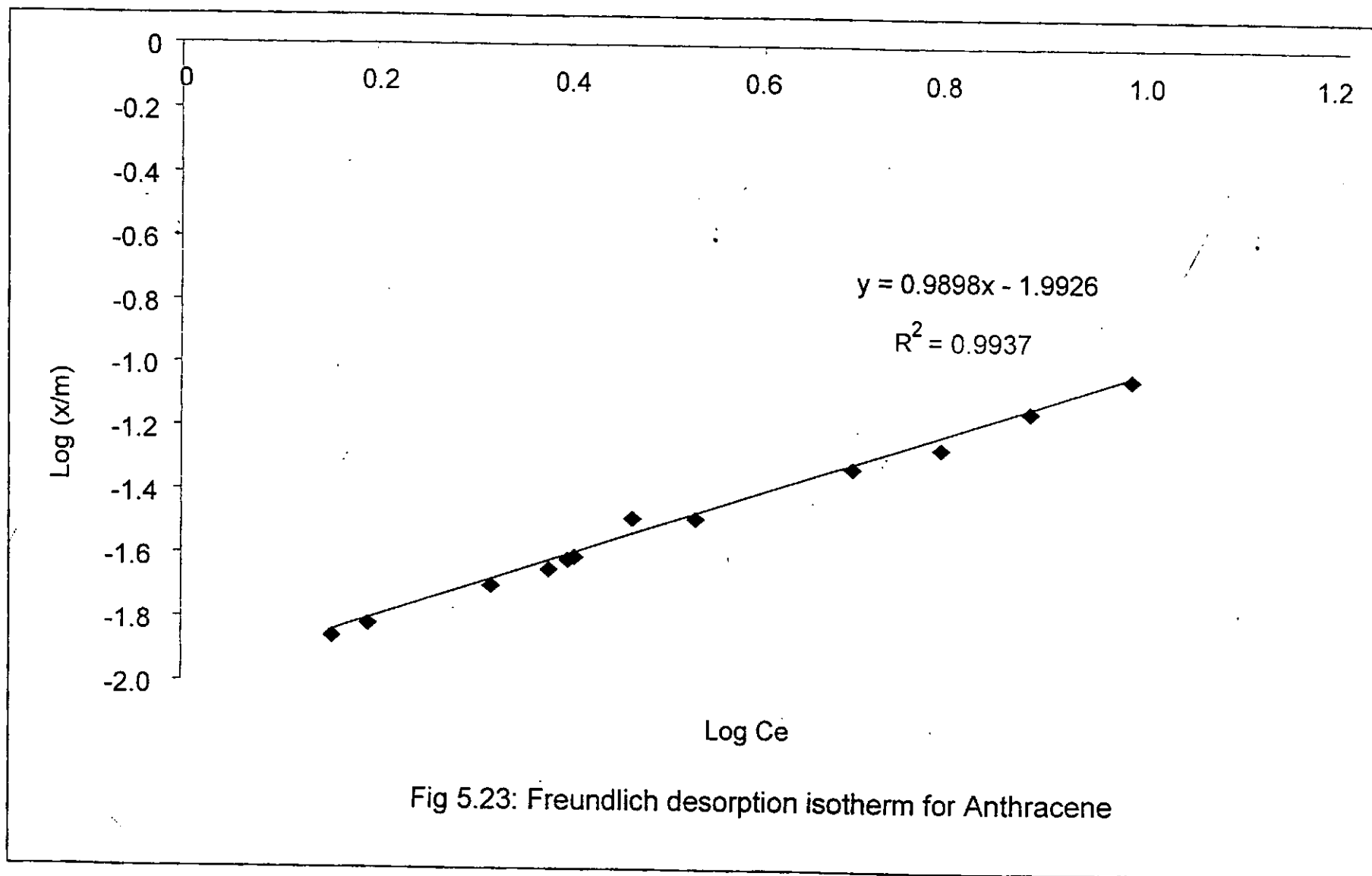
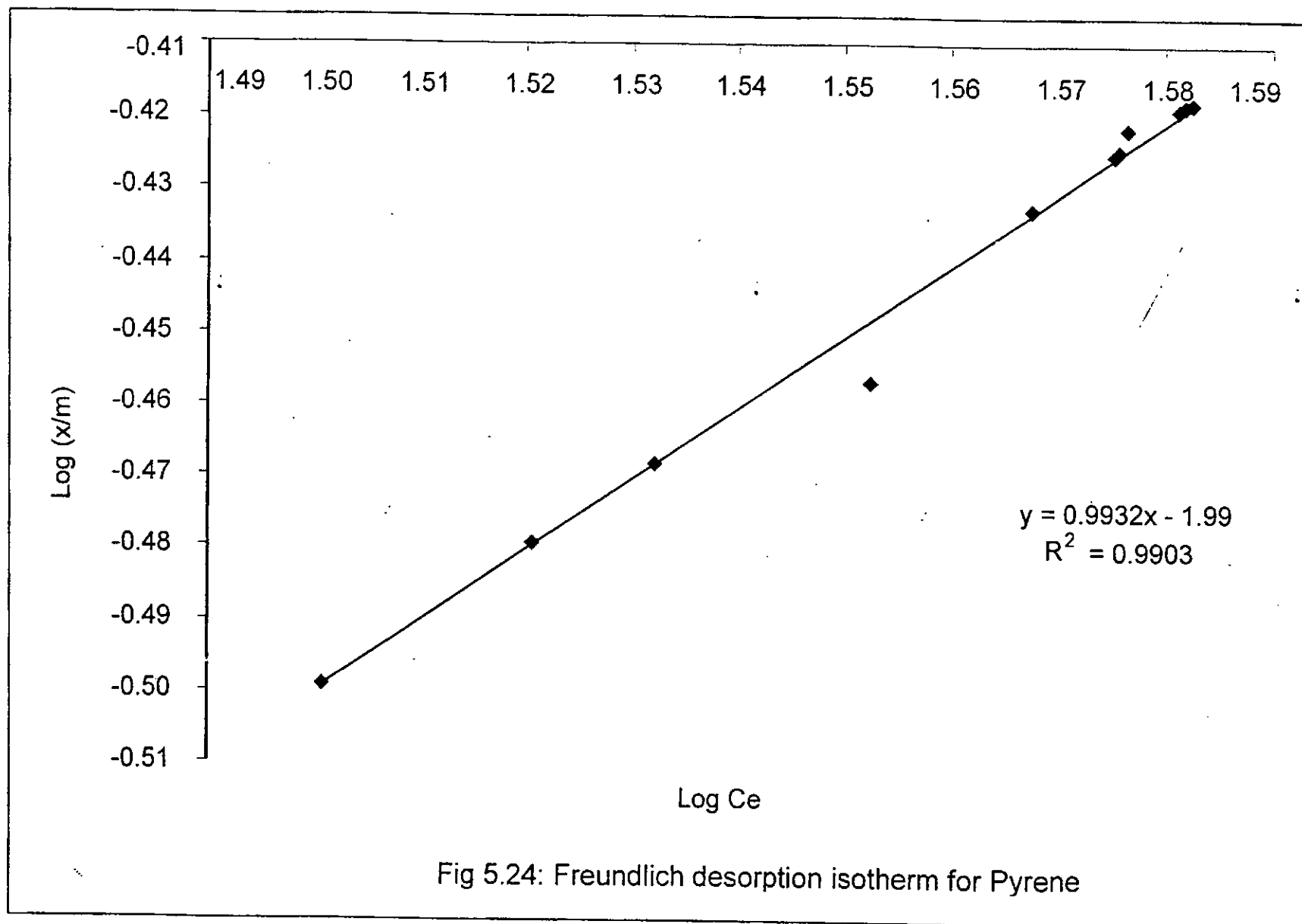
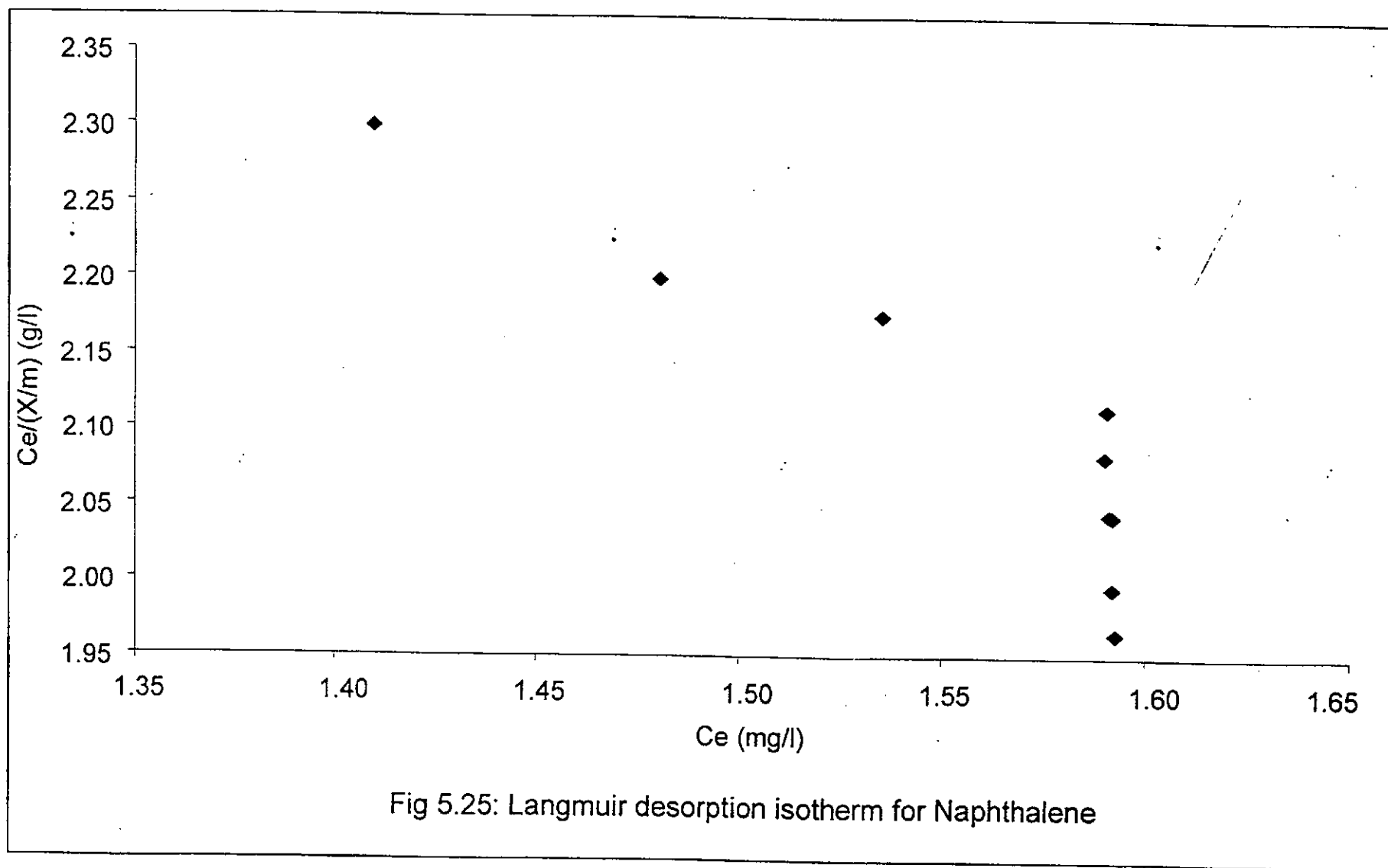
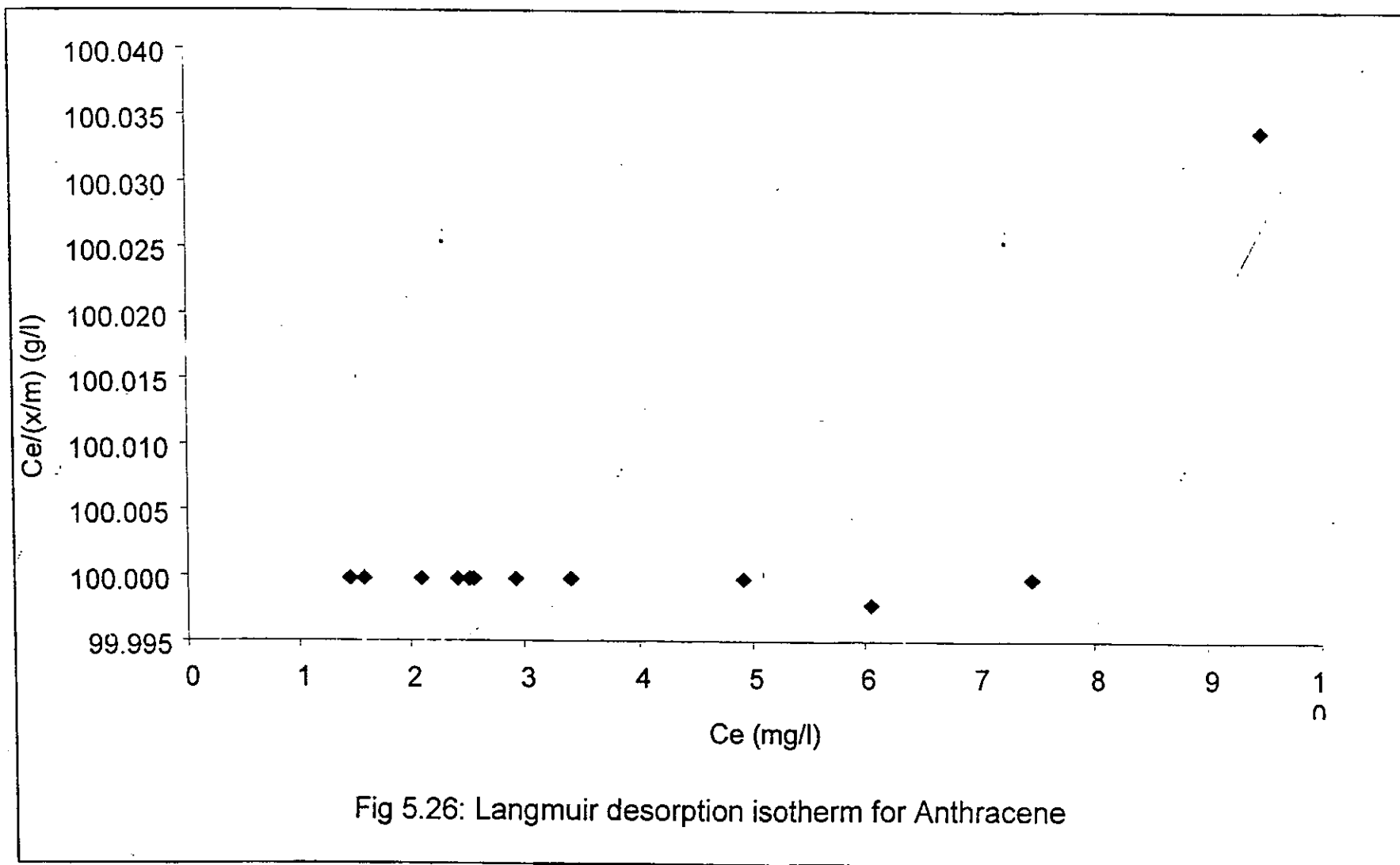
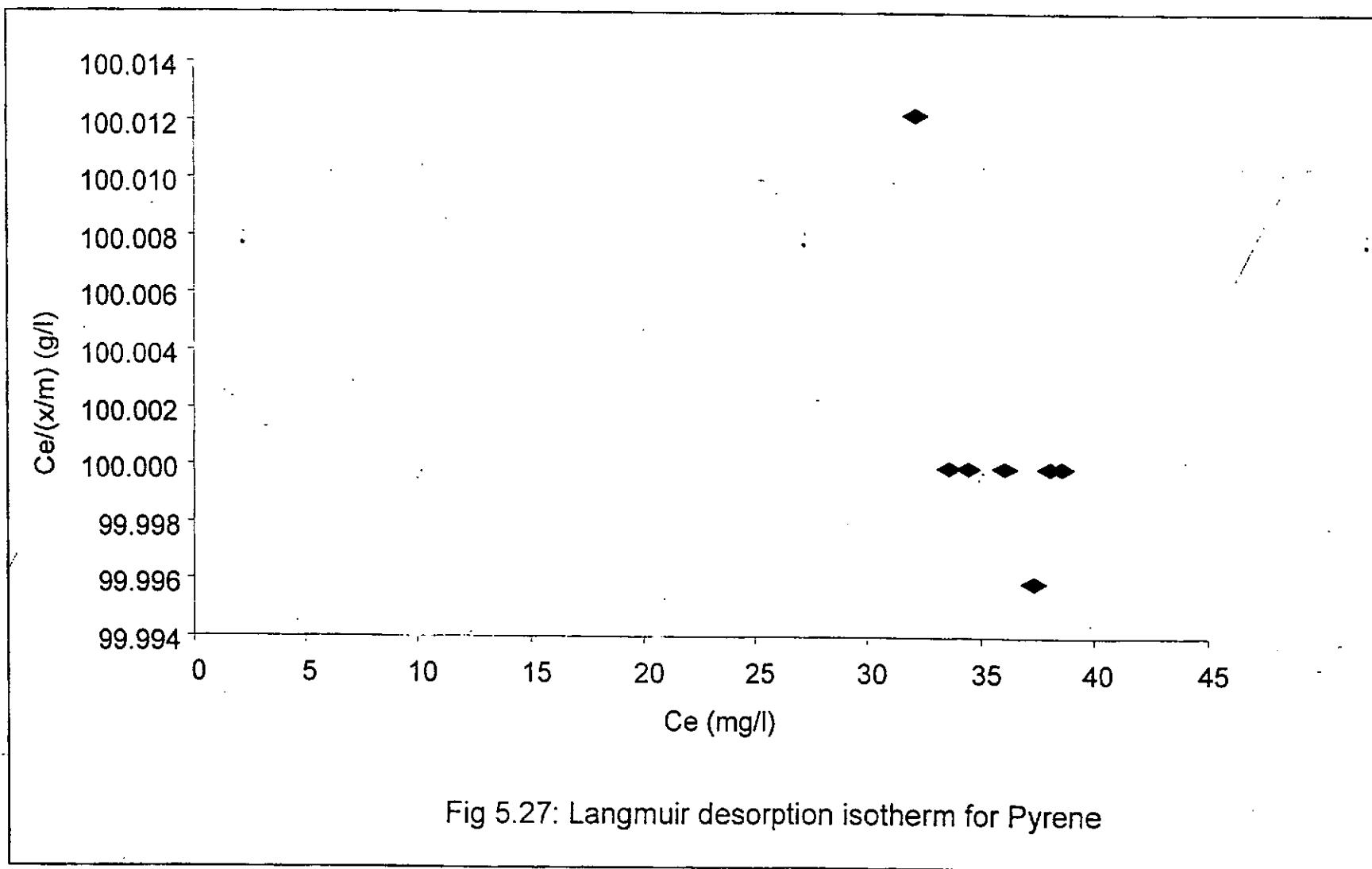


Fig 5.23: Freundlich desorption isotherm for Anthracene









5.5 Biodegradation Study

The result of the experimental study on the mineralization of naphthalene, anthracene and pyrene as functions of time using indigenous microbes in a soil microcosm reactor, are shown in Figures 5.28.

The biokinetic parameters for each of the three PAHs were estimated using the celebrated Michaelis-Menten kinetic equation via the Lineweaver-Burk plot for rate against concentration of contaminant. The results are shown in Table 5.5.

Table 5.5: Biokinetic constants for contaminant PAHs

Constants	Naphthalene	Anthracene	Pyrene
V_{\max} (moles/l.min)	0.0028	0.015	0.0023
K_m (M)	0.00314	0.0468	0.0035

These parameters V_{\max} and K_m were estimated using the celebrated Michaelis-Menten kinetics via the Lineweaver Burk reciprocal plots. The Lineweaver-Burk reciprocal plot is simply a linear transformation of the basic velocity of the Michaelis-Menten kinetic equation. The K_m which is Michaelis constant is a pseudo-equilibrium constant expressing the relationship between the actual steady state concentration rather than the

equilibrium concentrations. It measures the strength of the ES complex. Low K_m indicates strong binding while a high K_m indicates weak binding. V_{max} is not a constant of the enzyme in the reaction, but defines the maximal velocity that would be observed when the entire enzyme is present as an intermediate ES. Both parameters provide a means of comparing enzyme activity from different microorganisms during degradation. They actually help to characterize the enzymes by determining whether enzyme A is identical to enzyme B or whether they are different.

5.6 Kinetic models

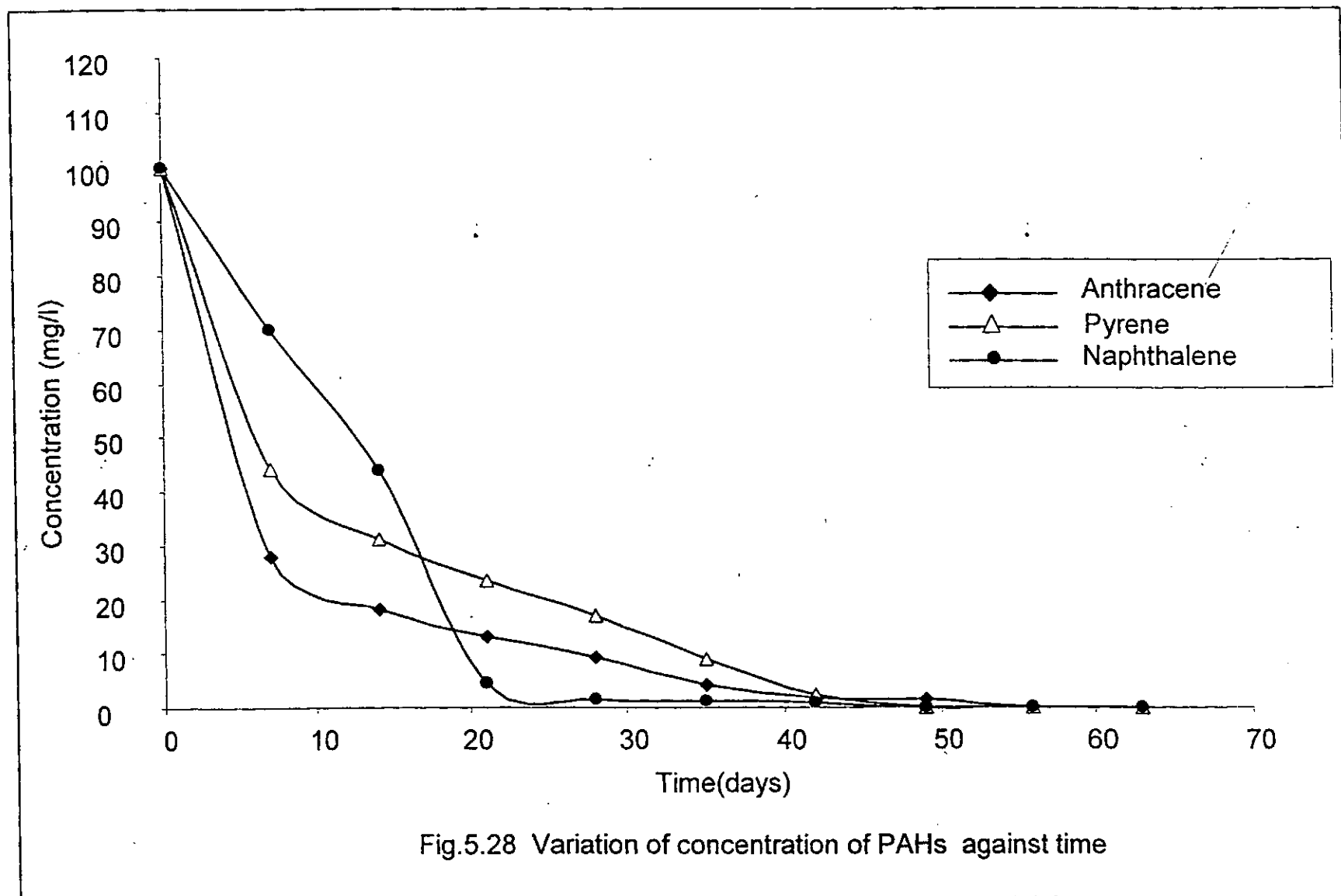
The experimental data from the soil microcosm reactor was used to simulate the change in PAH concentration in contaminated soil as a function of time, for both single and multisubstrate catalysis. The detailed procedure for calculating the concentration profile using the kinetic models for both single and multisubstrate catalyzes biodegradation process are presented in Appendix G. Figures 5.29 and 5.30 show the simulated concentration plots using both rate-determining step and steady state approximation methods.

The rate constant k for the degradation of the experimental PAHs with model fits is as shown in Table 5.6.

Table 5.6: Kinetic constants for contaminant PAHs
with model fits

	k (min ⁻¹)
Naphthalene	0.029
Anthracene	0.014
Pyrene	0.019
Single Substrate RDS Model	0.06
Multi Substrate RDS Model	0.069
Single Substrate Steady State Approximation Model	51.487
Multi Substrate Steady State Approximation Model	12.05

The reaction rate constant k approximates the fraction of the substrate present that is converted to product per small increment of time. The results imply that approximately 2.9%, 1.9% and 1.4% of naphthalene, pyrene and anthracene present in the microcosm reactor at zero time would be utilized in a minute if the velocity of the reaction remained constant for the period.



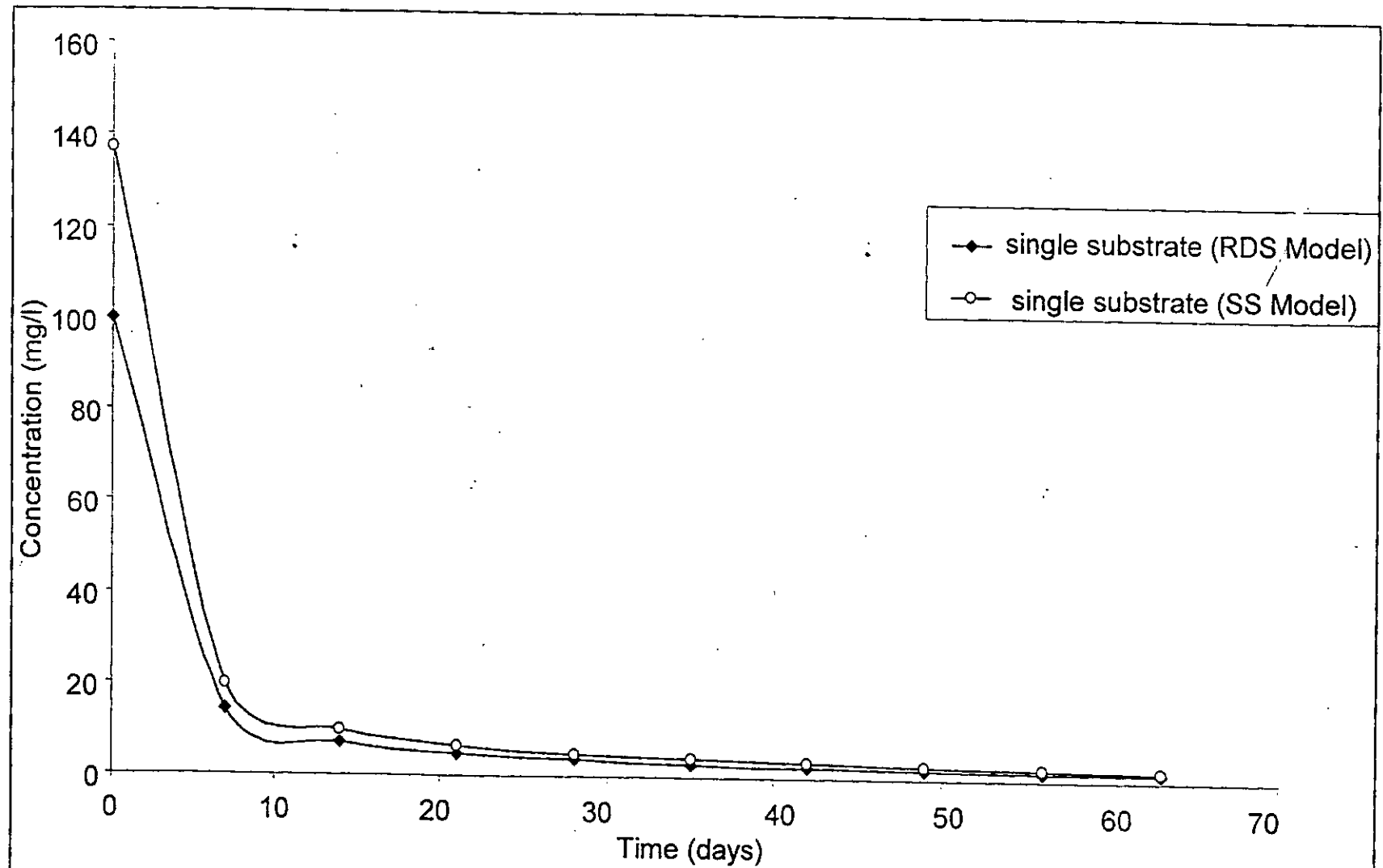
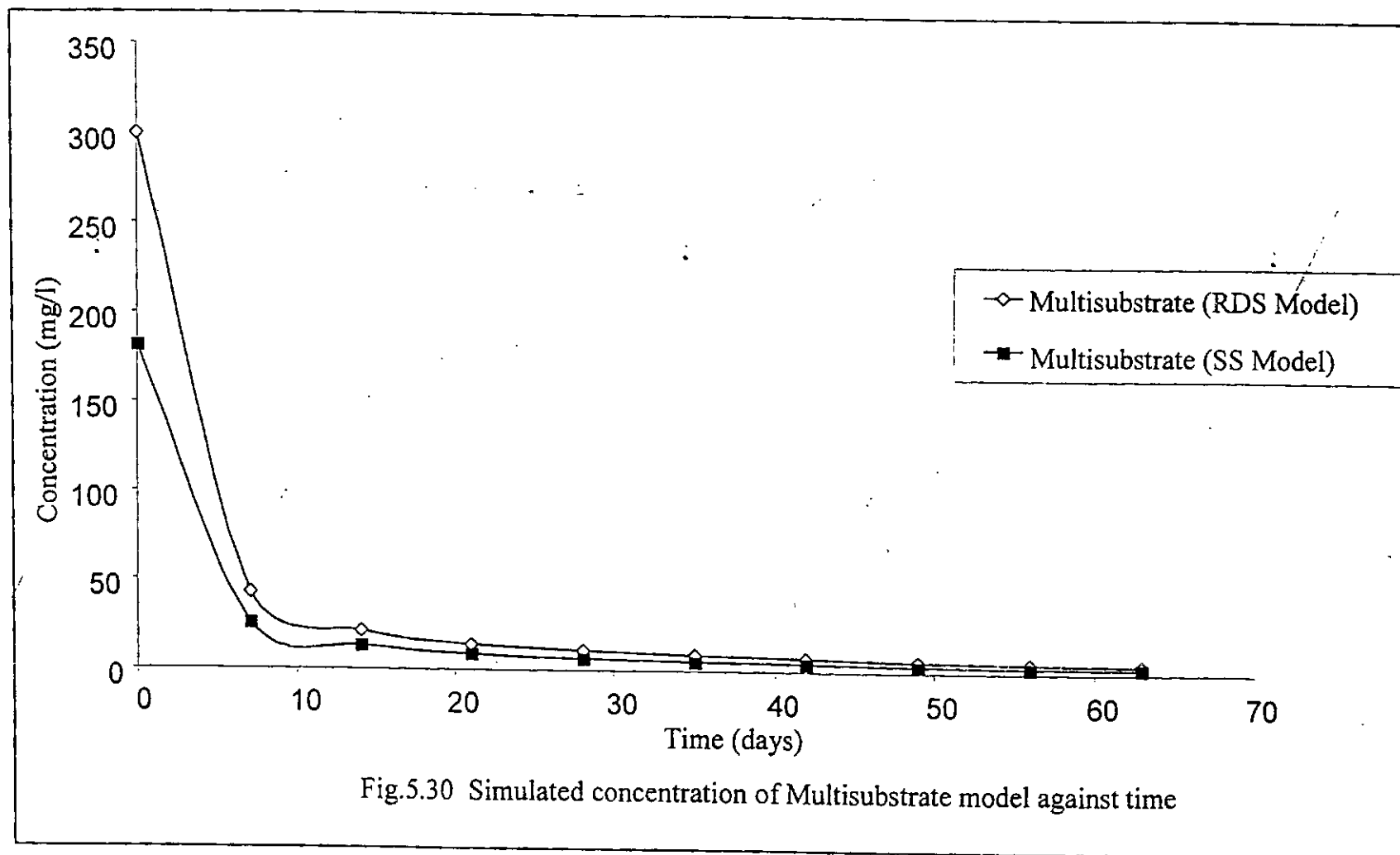


Fig.5.29 Simulated concentration of single substrate model against time



5.7 Estimation of Transport and Degradation Parameters

The method of temporal moments (MOM) described by Das and Kluitenberg, 1996 which interprets solute transport with linear equilibrium sorption and first order degradation and the analytical solutions of a transport model CXTFIT version 2.0 described by Toride *et al.*, (1995) were comparatively used to analyze the experimental data from the soil microcosm with a view to estimating the transport parameters (pore-water velocity, V and dispersion coefficient, D) using non-reactive solute and the degradation parameters (retardation factor R and first order degradation rate λ) of the contaminant PAHs. The results are shown in Tables 5.7 and 5.8.

Table 5.7 Comparison of the Pore-water velocity and Dispersion coefficient obtained from Methods of temporal Moments and CXTFIT curve fitting program.

Experimental data of the study (sandy soil microcosm reactor)

Tracer	V (m/day)			D (m ² /day)		
	MOM	CXTFIT	ϵ	MOM	CXTFIT	E
CO ₂	2.15	2.24	-0.04	2.79	2.47	0.11

Table 5.8: Comparison of the Degradation and Transport parameters for the Contaminant PAHs

PAHs	R			Δ (per day)		
	MOM	CXTFIT	ϵ	MOM	CXTFIT	E
Naphthalene	25.77	20.23	0.21	3.54	4.22	-0.19
Anthracene	41.62	28.43	0.32	1.21	2.05	-0.69
Pyrene	35.66	25.89	0.27	2.25	3.26	-0.45

Where $\epsilon = \frac{\text{MOM}_{\text{value}} - \text{CXTFIT}_{\text{value}}}{\text{MOM}_{\text{value}}}$

The solution took into consideration the interplay of degradation and sorption. By using a coefficient of deviation ϵ , the similarity and disparity of the results obtained from MOM and CXTFIT curve-fitting for each parameter could be compared. The difference can be attributed to the fact that the CXTFIT curve-fitting results that are based on minimizing the sum of square deviations are dominated by high-data points (as all the data points are assigned an equal weight by CXTFIT); while the MOM-estimated value is a function of the difference between the second moment and first moment squared.

5.8 PAHs Breakthrough Curves

The variation of the relative concentration with time obtained for the experimental PAHs and non-reactive solute (tracer) using the MOM and non-linear least square curve-fitting program CXTFIT are illustrated in

Figures 5.31 to 5.34.

The breakthrough profiles were characterized by an initial low level of normalized concentration C/C_o , naphthalene was zero throughout the 40hr period, tracer was zero for 1hour, pyrene was zero for 3hours and anthracene was zero for 5hours. The experiments were carried out in a water medium at a flow rate of 8.06 ml/min^{-1} . This low profile was followed by a sharp but rather steep ascent to the exhaustion point as depicted by the smooth and sigmoid shape and a subsequent decline in C/C_o values.

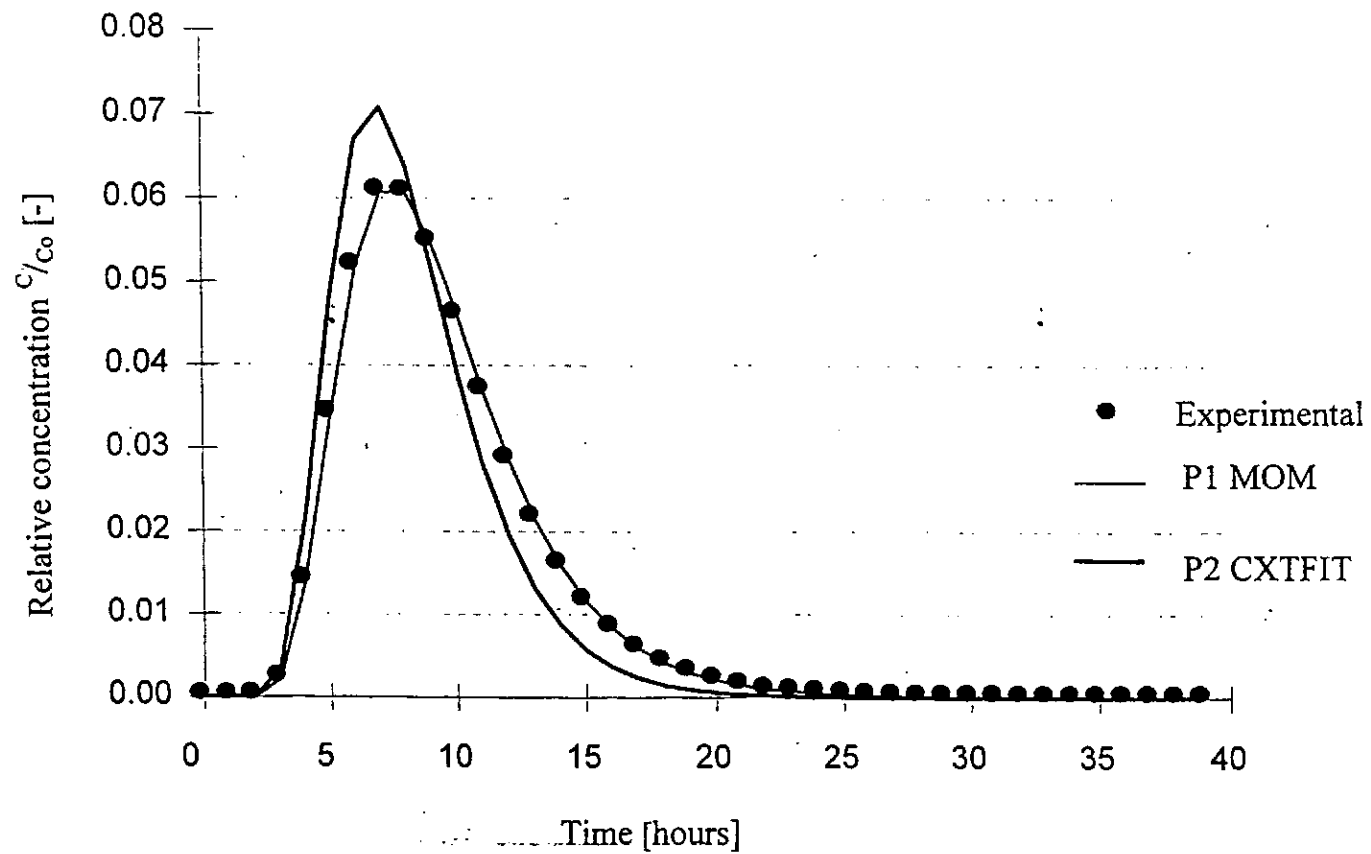


Fig 5.31: Comparison of MOM and CXTFIT simulated breakthrough curves for Tracer using experimental data.

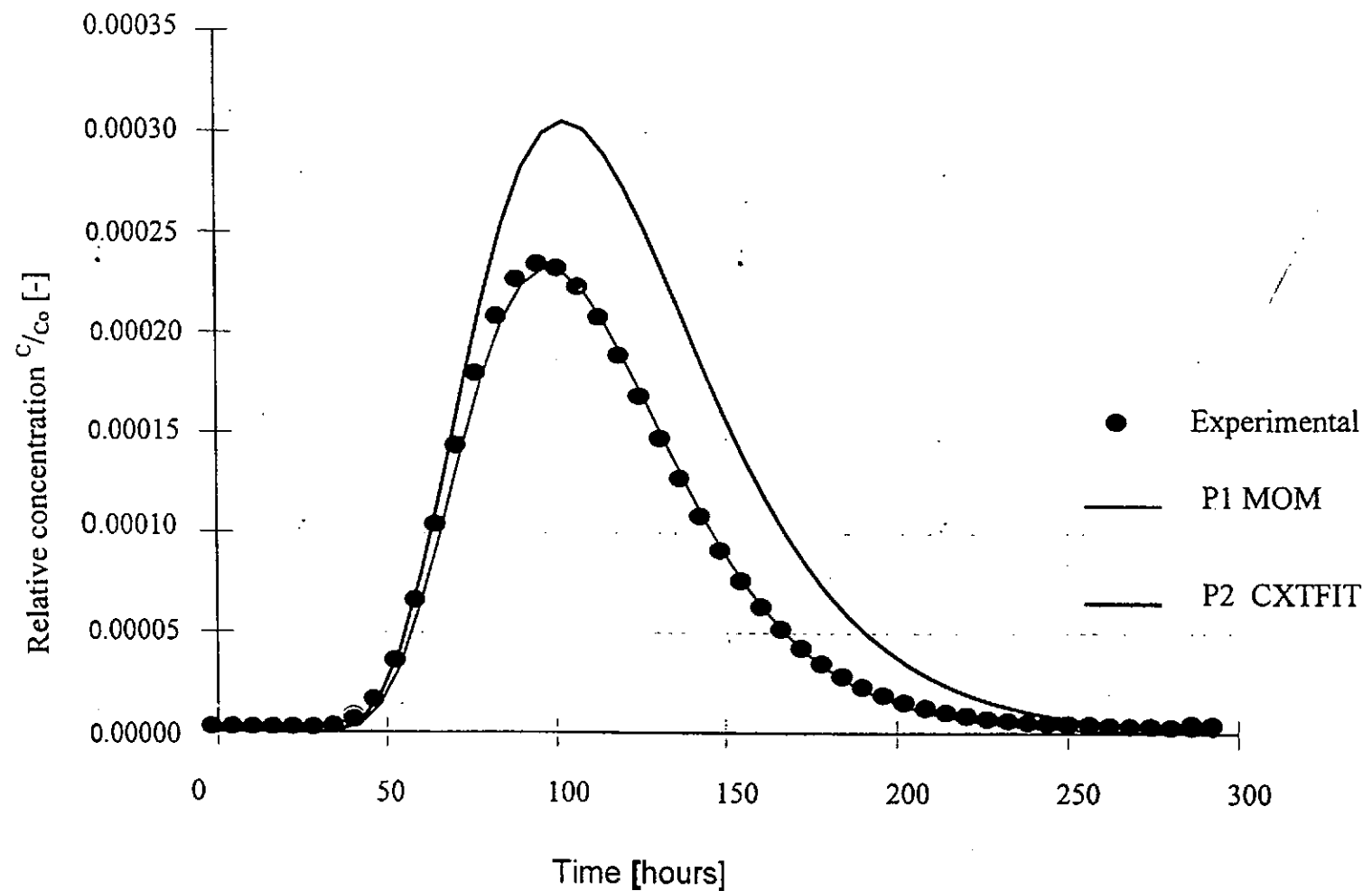


Fig.5.32: Comparison of MOM and CXTFIT simulated breakthrough curve for Naphthalene using experimental data.

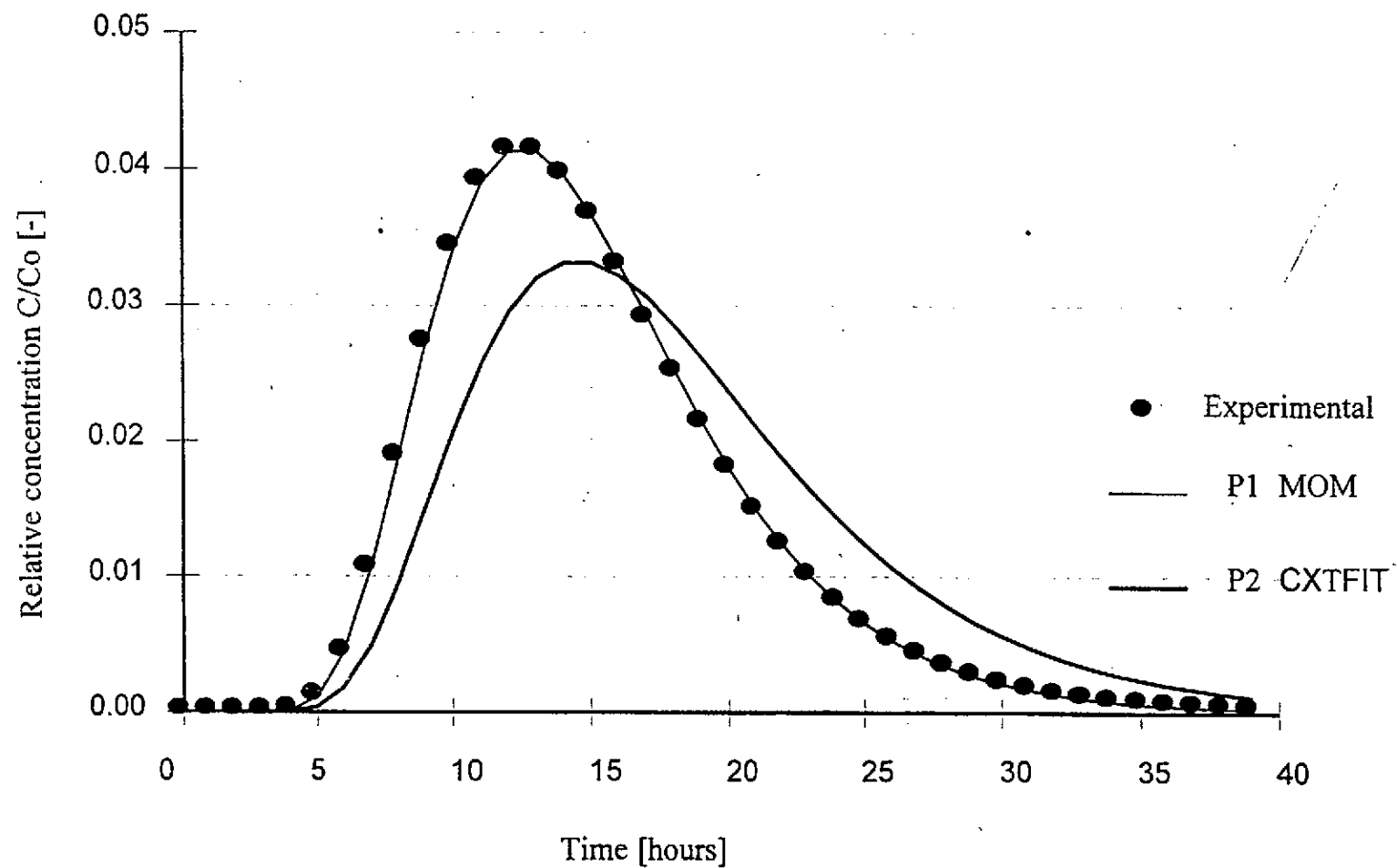
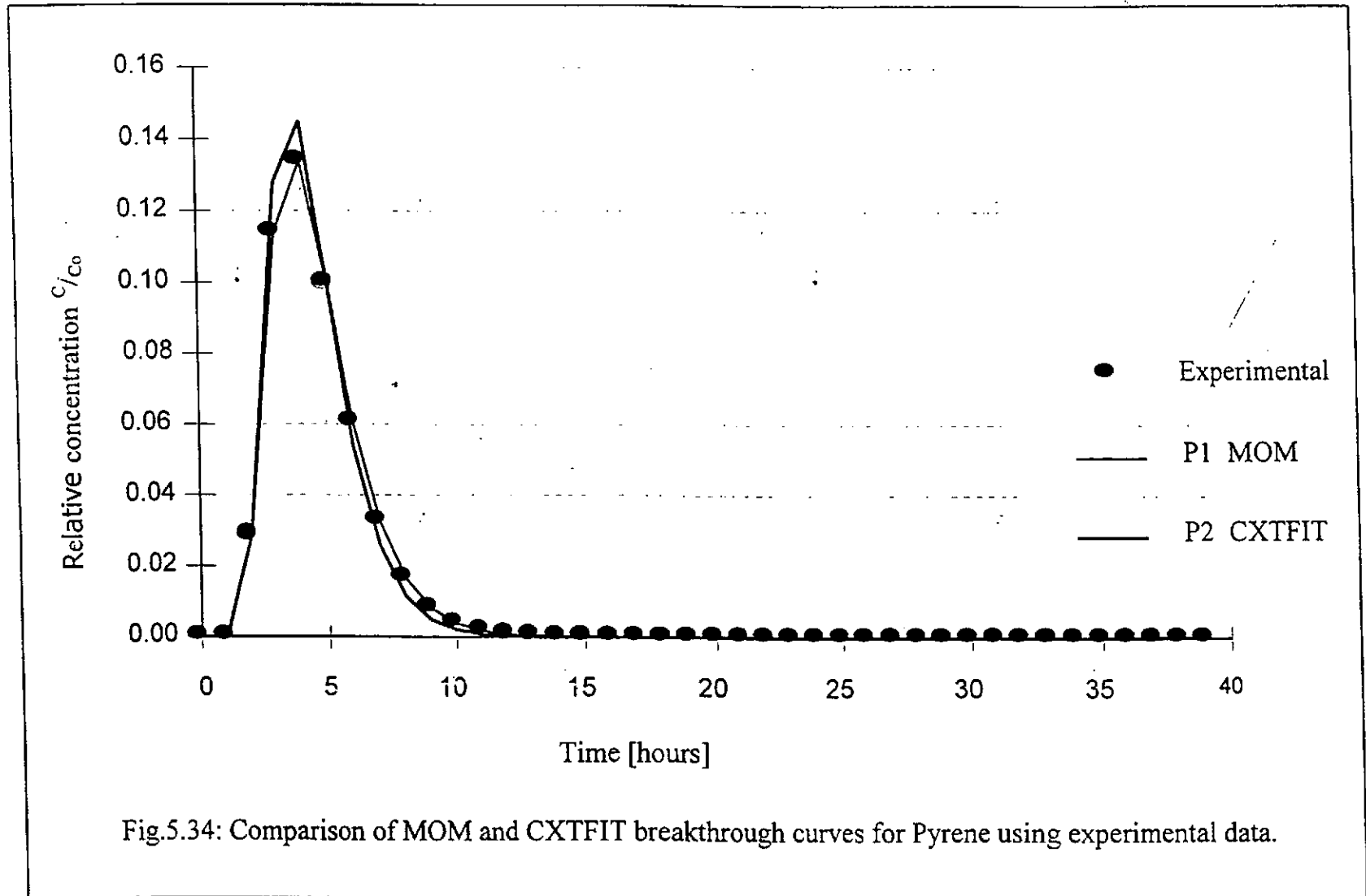


Fig.5.33: Comparison of MOM and CXTFIT simulated breakthrough curve for Anthracene using experimental data.



5.9 Simulation Plots for the Non-Steady State Model

The differential equations modelling the non- steady state macroporous and microporous systems of the soil matrix contain many parameters which must be estimated to achieve a reasonable solution of the equations. The constant transport parameters k_f , D_p and D_f are independently estimated to reduce the dimensionality of the search process. The summary of the estimated values of these parameters are shown in Table 5.9.

Table 5.9: Estimated values of the parameters for the solution of the modelling equations

Parameters	Naphthalene	Anthracene	Pyrene
k_f (m/day)	1.924E-3	1.72E-3	1.689E-3
D_p (m ² /day)	8.61E-6	8.59E-6	8.567E-6
D_f (m ² /day)	7.28E-5	6.10E-5	6.08E-5

Generally, the estimated diffusivities in soil, D_p , were found to be much slower than diffusivities in water for the contaminant PAHs used. The film mass transfer coefficient was determined from the experimental data on adsorption/desorption and the resistance to transfer was significantly high for the three PAHs compared to the diffusivities. The results showing the numerical solutions to the non-steady state model for macroporous system (axial direction of flow) and microporous system

(radial direction of flow) for the contaminant PAHs used in this study are given in Tables I.1 to I.6 in Appendix I.

These results are depicted using 3-dimensional plots shown in Figures 5.35 to 5.40. The profiles which are similar for the tested PAHs show the detailed distribution and variation in composition of the contaminants in time and position (i.e. both axial and radial directions of flow). Typically, it was characterized by an initial rapid drop in concentration which was followed by a slower rate of decrease in the concentration of the contaminant PAHs.

Given the initial and boundary conditions, the model predicted a residual concentration shown in Table 5.10 for the tested PAHs present in the soil microcosm reactor. Results depicted that for macroporous and microporous systems with C , z , r as dependent variables, the residual concentrations were in the order naphthalene < pyrene < anthracene.

Table 5.10: Residual concentration of contaminant PAHs in both axial and radial directions

PAHs	Axial (mg/l)	Radial (mg/l)
Naphthalene	1.1159E-5	1.4782
Anthracene	7.67E-4	1.6086
Pyrene	3.11E-4	1.5771

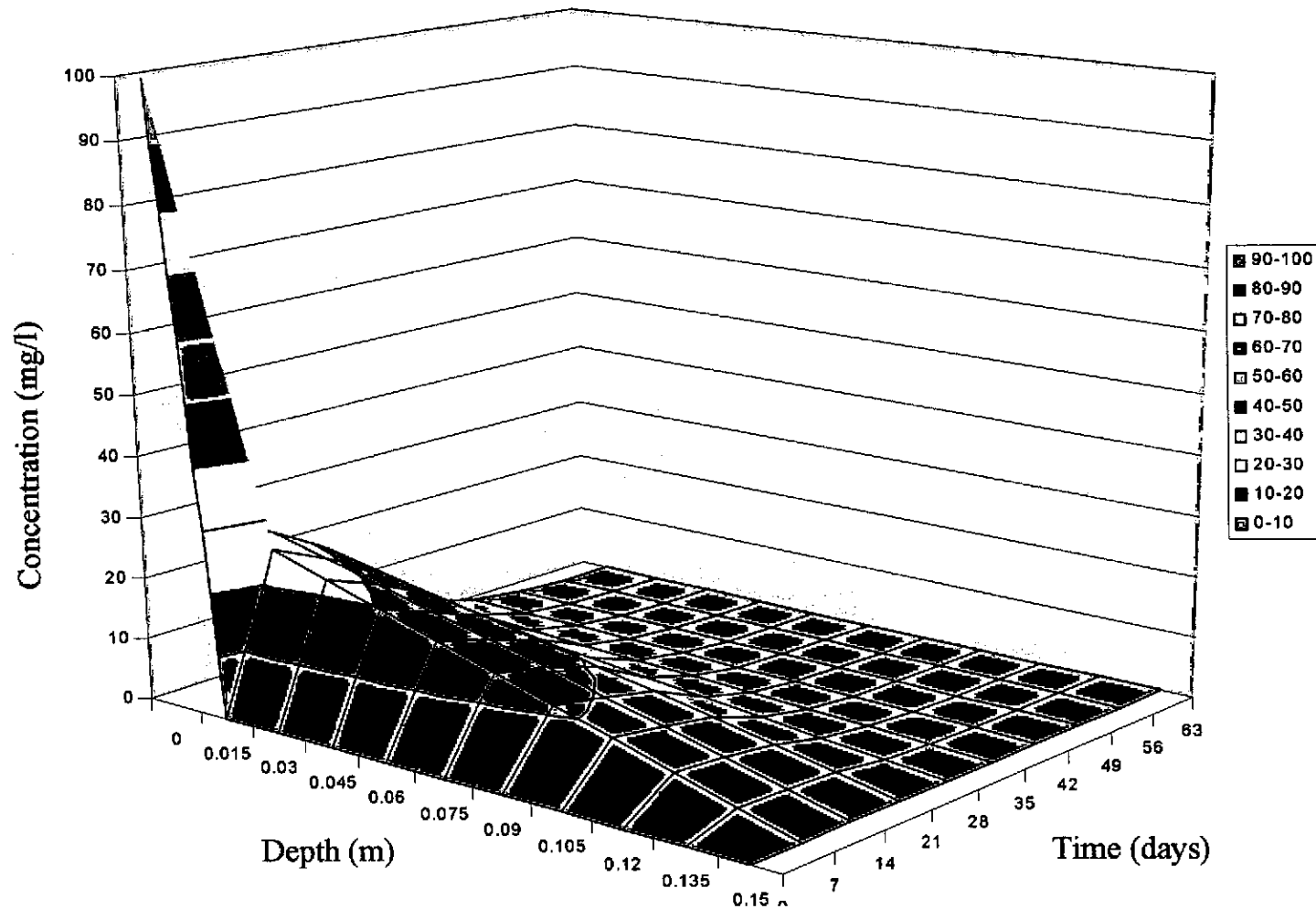


Fig 5.35 Variation of concentration of Anthracene with time and depth

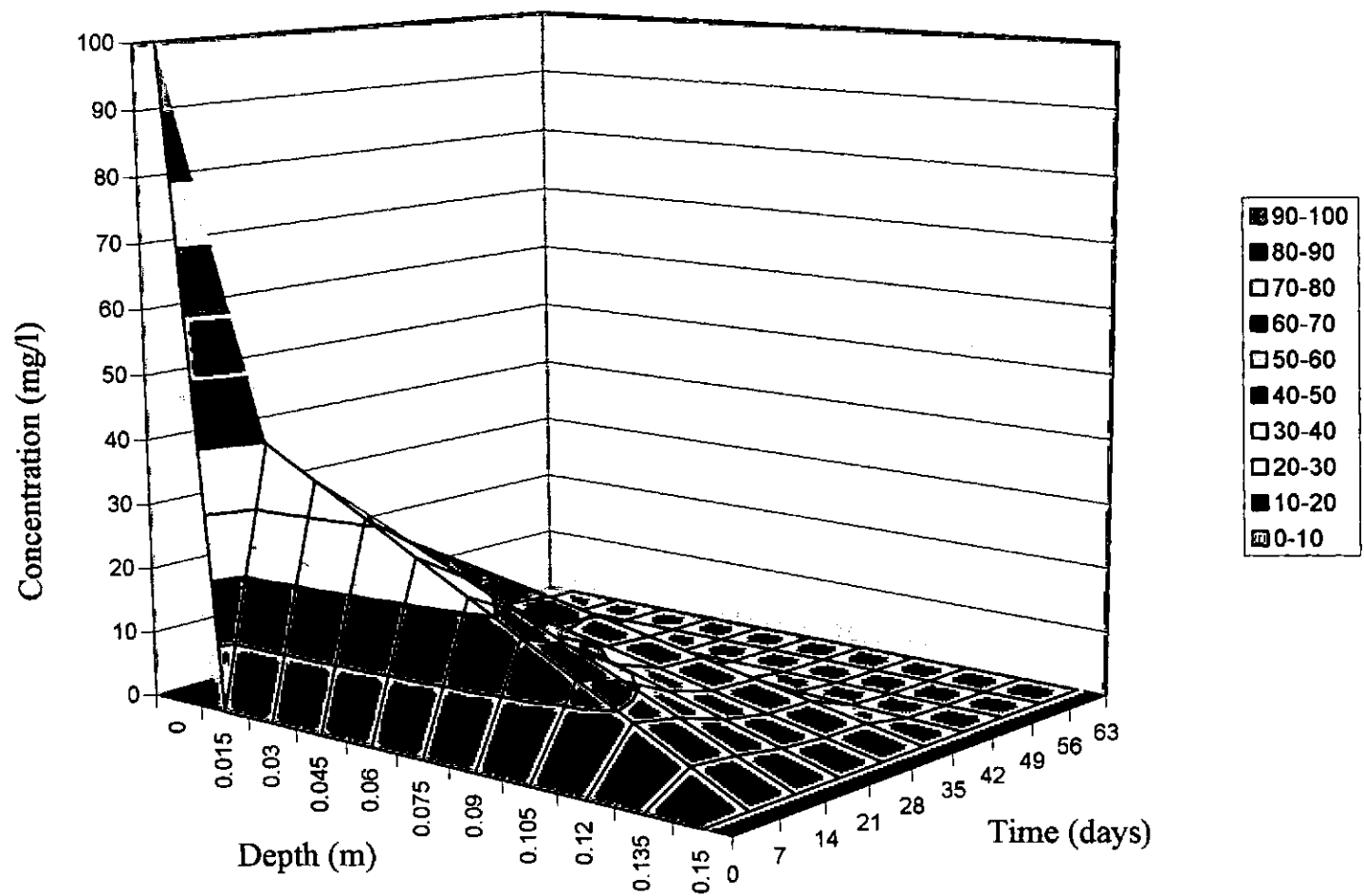


Fig 5.36: Variation of Concentration of Pyrene with time and depth

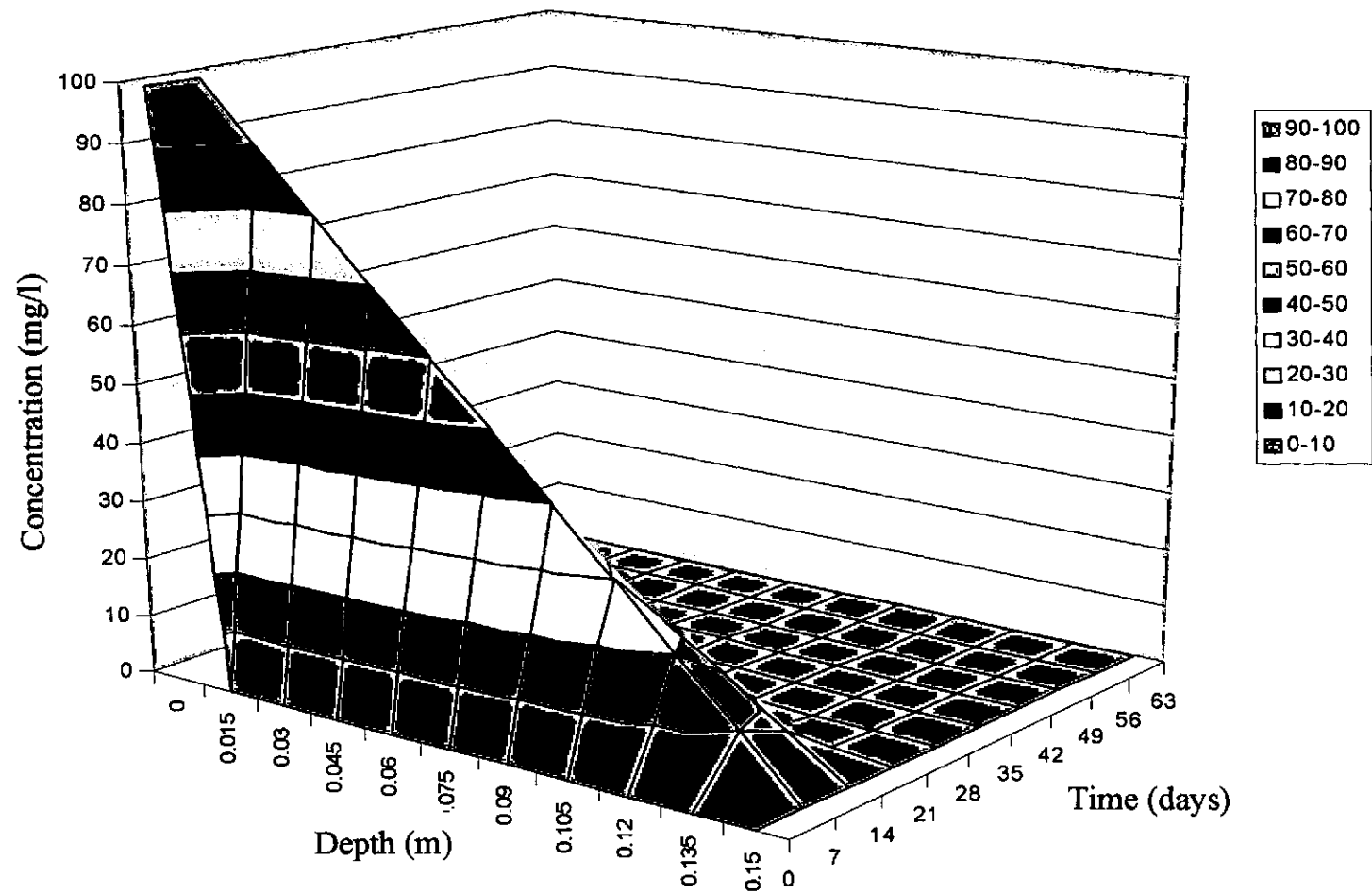


Fig 5.37: Variation of Concentration of Naphthalene with time and depth

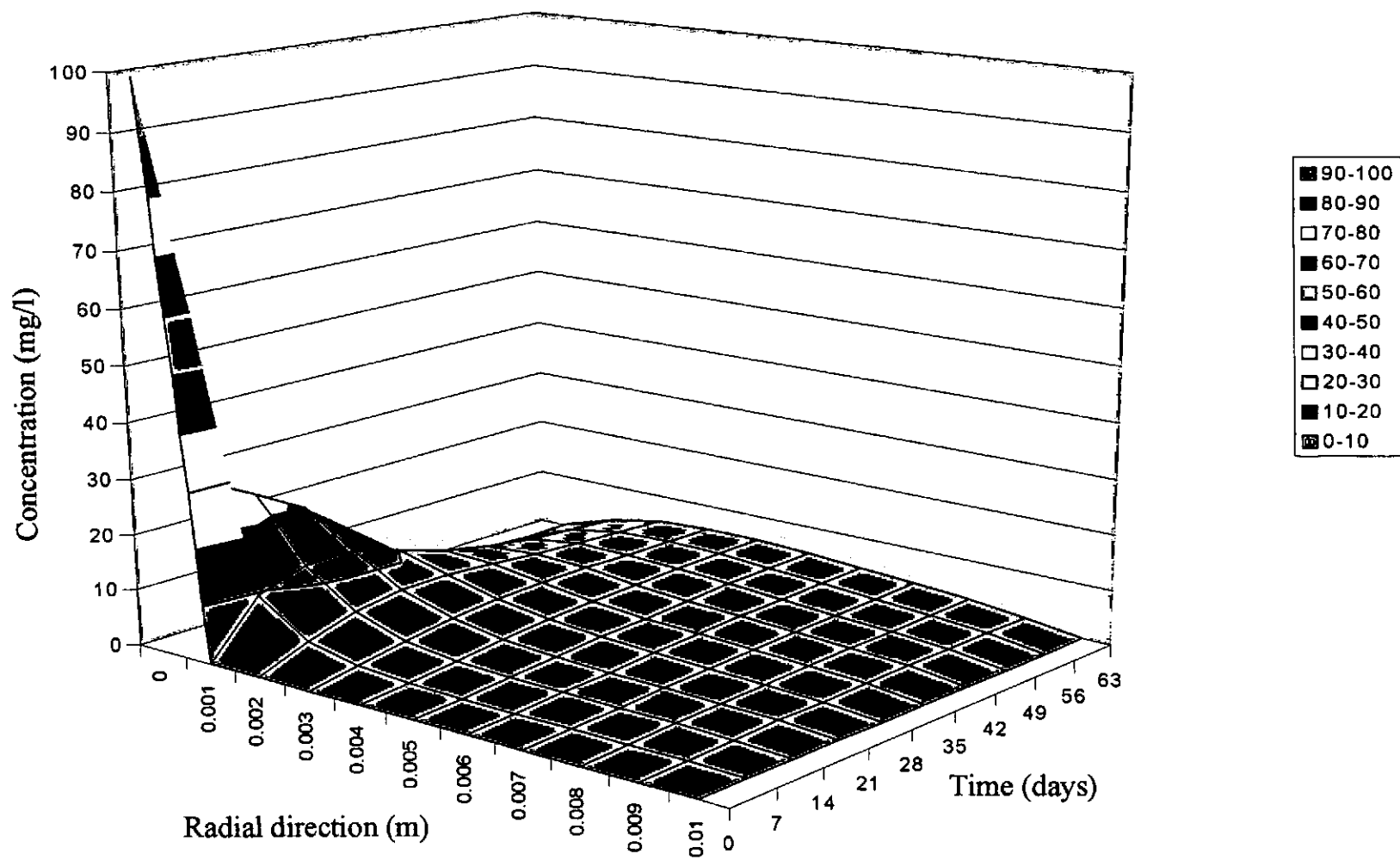


Fig 5.38: Variation of Concentration of Anthracene with time and radial direction

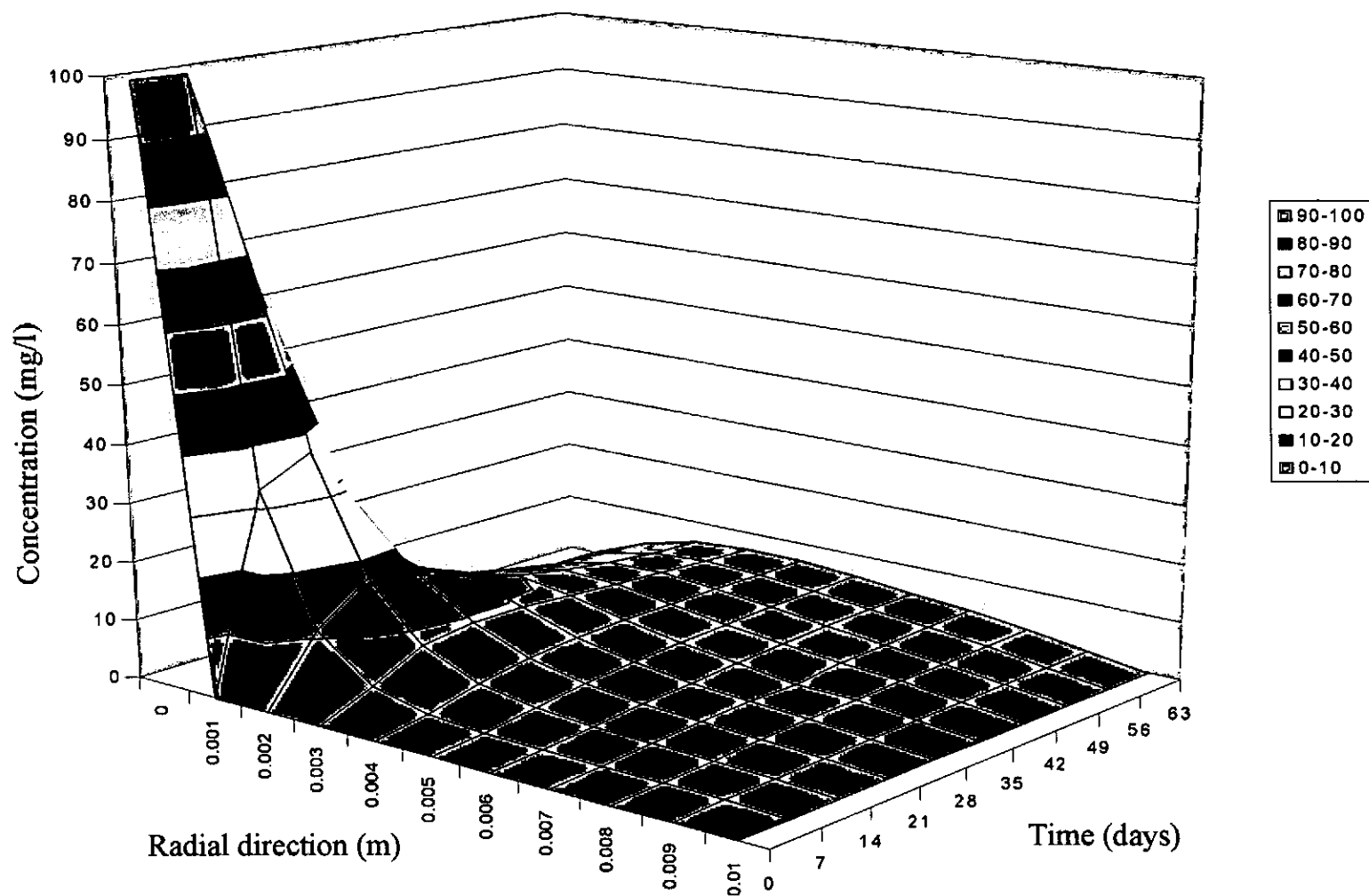


Fig 5.39: Variation of Concentration of Naphthalene with time and radial direction

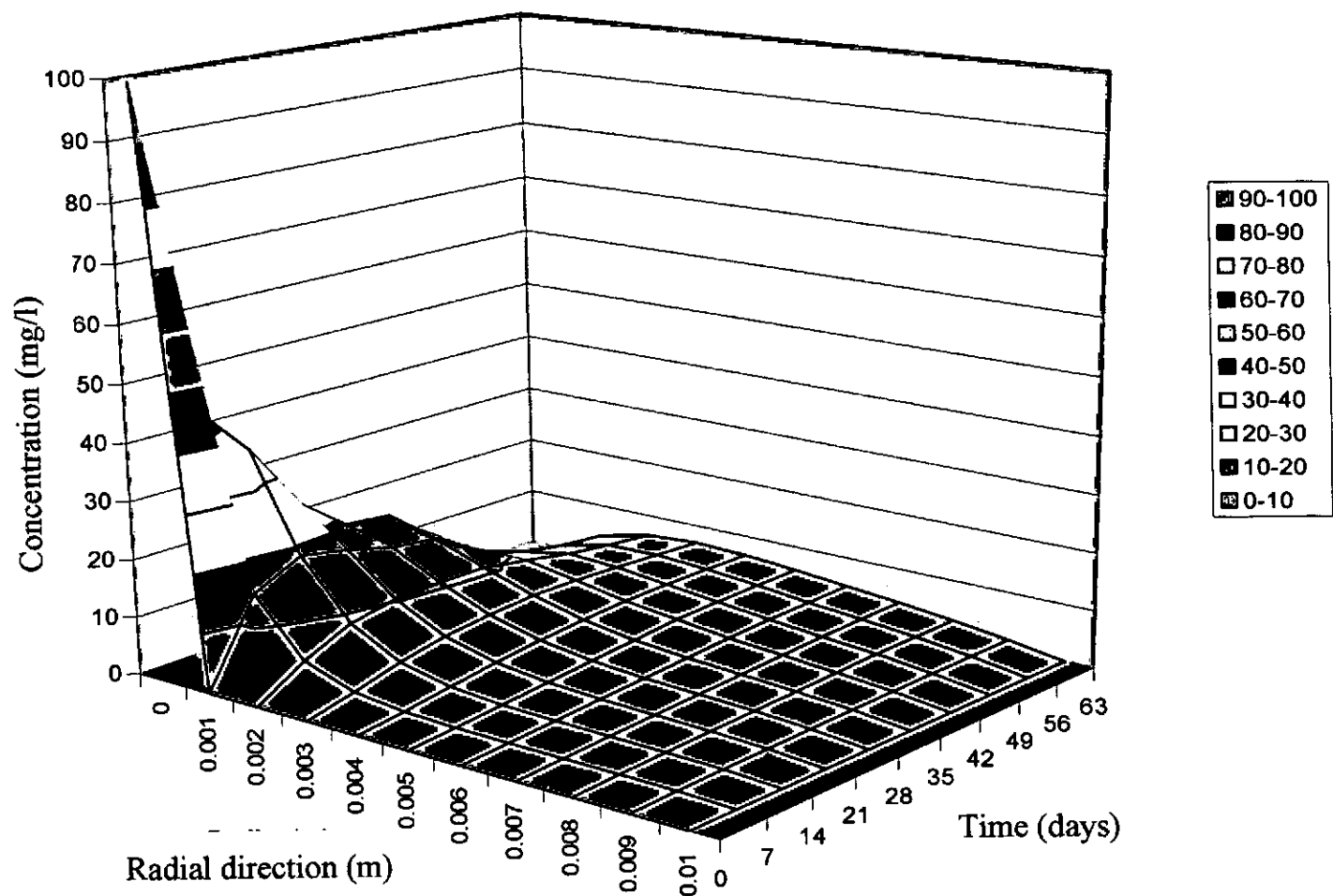


Fig 5.40: Variation of Concentration of pyrene with time and radial direction

5.10 Model Validation

The kinetic and mass transfer-limited numerical models formulated in this research work were validated using data from experiment. These data were obtained from the bench-scale soil microcosm reactor designed and fabricated for this study. The investigated reaction was the degradation of a mixture of naphthalene, anthracene and pyrene using enzymes from the indigenous microorganisms as catalyst. The developed models have been run for the same experimental conditions and the simulated and experimental results and profiles have been compared.

In the validation of the kinetic model, two sets of model simulation were carried out. The simulated effectiveness factor of the rate-determining step and steady state approximation model was depicted using a relative error (RRE) method to show the goodness of fit between the experimental data and the model. The result is presented in Table 5.11.

Table 5.11: Relative Error between the two Models and Experimental data

Rate Determining Step		Steady State Approximation	
Single substrate	Multi substrate	Single substrate	Multi substrate
0.0651	0.065	0.133	0.1364

$$RRE = \frac{\sqrt{\sum_{i=1}^m [\text{mod}(t_i) - \text{Exp}(t_i)]^2}}{m \text{Exp}(t_i)}$$

where:

Mod (t_i) = value determined from the model at time t_i

Exp (t_i) = experimental value at time i

m = number of experimental points

The RRE show the deviation of the simulated results from the experimental data.

The non-steady state model developed for macroporous and microporous systems which had a number of variables whose numerical values were independently estimated was validated to assess the variation of the simulated composition of naphthalene, anthracene and pyrene with exposure time within the soil matrix. A comparison of the experimental and simulated results for both systems is shown in Figures 5.41 and 5.42.

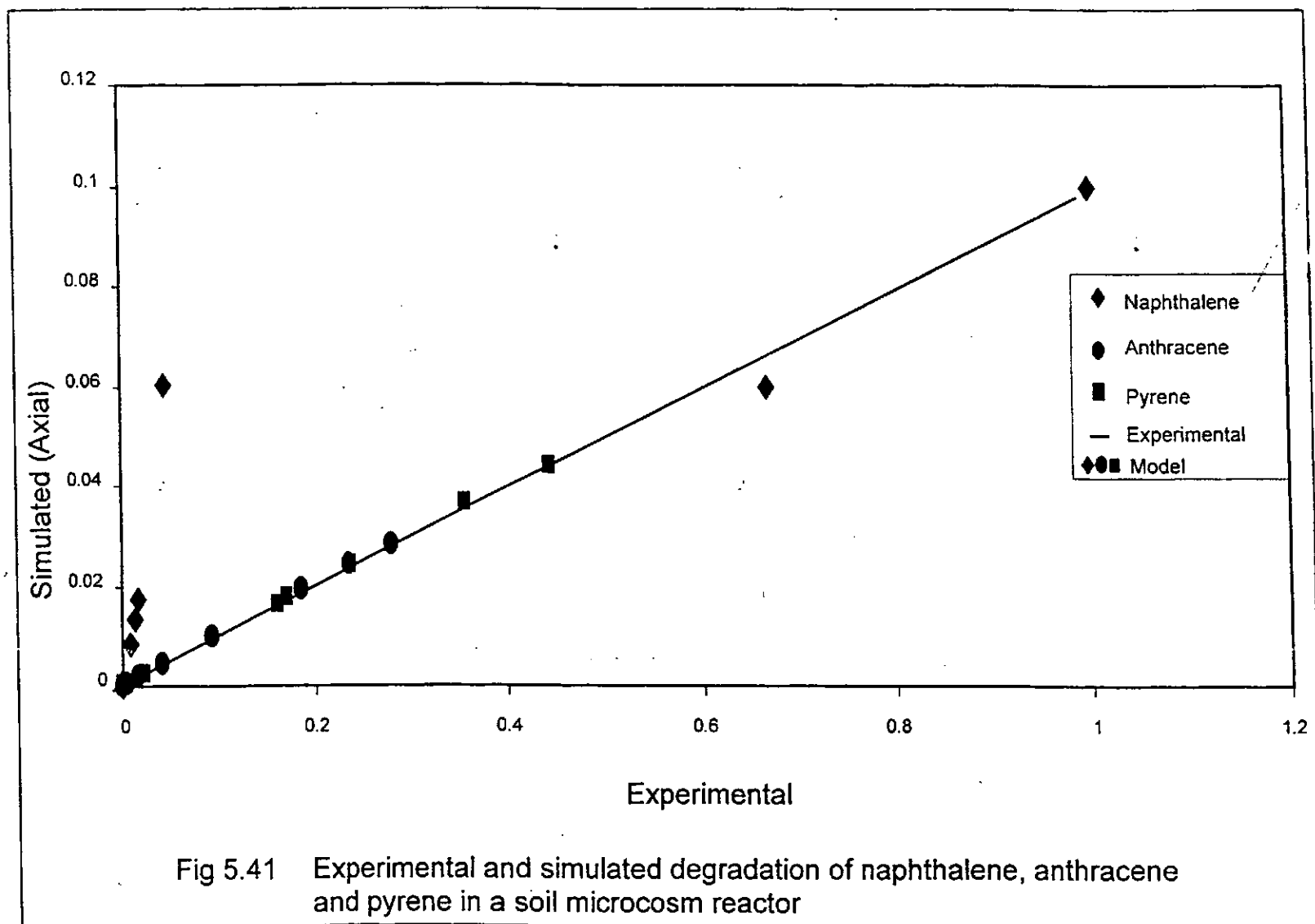
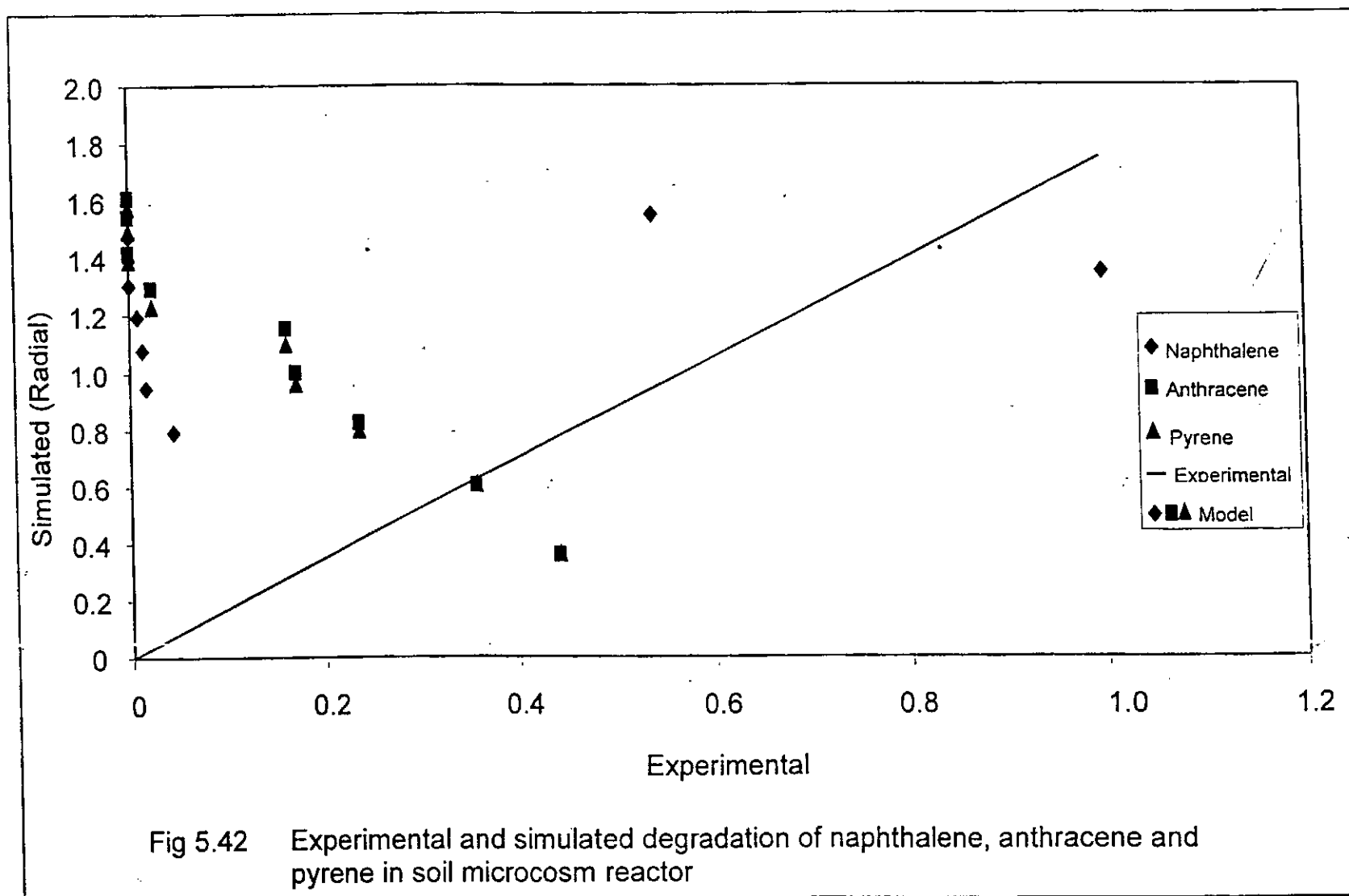


Fig 5.41 Experimental and simulated degradation of naphthalene, anthracene and pyrene in a soil microcosm reactor



CHAPTER SIX

6.0 DISCUSSIONS

The experiments conducted in this study provide a deep understanding of the insight on the degradation kinetics of a mixture of naphthalene, anthracene and pyrene as model polycyclic aromatic hydrocarbons (PAHs) in aqueous-soil matrix. The salient characteristics of the uncontaminated soil used showed that the soil was highly porous with a particle size distribution in the ratio 85%: 14%: 1% for sand, clay and silt respectively. The microbial activities which would have been impeded as a result of the low moisture content (5%) of the soil were enhanced by the addition of water which provided an aqueous environment suitable for the degradation process. The cation exchange capacity of the soil was within the recommended value of 5 cmol/kg for sandy soil low in organic matter. This is especially significant because decaying organic matter shrinks and swells and encourages micro fauna which create or widen openings in the soil thus improving infiltration and aeration. The level of exchangeable acidity as reflected by the pH implied that the soil was very acidic. This, therefore, portends a reducing environment. The redox condition necessary to enhance microbial activity and hence the degradation of the PAHs in the soil was achieved through the use of oxygen which functioned as electron donor. The low nitrogen and low-to-

moderate available phosphorus in the soil accounted for the low nutrient level which was however, supplemented with straw, sawdust and poultry dung as prescribed by the organization for economic cooperation and development (OECD).

In order to demonstrate the remarkable insight on the mineralization of PAHs by a group of microorganisms under aerobic conditions, naphthalene was used as a model PAH. The observed lag/induction phase is more or less a warming up stage and it was as a result of the shock to the microbes of finding themselves in a new substrate environment. A rapid and an exponential increase in biomass growth (cell multiplication) followed this. During this phase, the microbes had become adapted to the new conditions. The stationary/static phase was unpronounced probably due to limiting substrate, increase in temperature as a result of increased cell yield, or the presence of electron acceptor (due to the presence of co-metabolites) which limits the cell growth rate. The eventual dying of the cells characterized the decay phase. This was predicated on the incidence of substrate exhaustion/depletion due to increase in cell crowding. In addition, the accumulation of toxic materials/by-products of metabolism (product poisoning) may also have been responsible for the drop in cell growth. From Table 5.3, the microbial growth and consumption rates estimated using the Monod kinetics showed that all the microbes used in

this study exhibited a high metabolic affinity for naphthalene.

As a means of assessing the level of microbial activities in relation to biodegradation kinetics in the soil, the soil samples in the microcosm reactor was used as a source of acclimated microbiota for measuring oxygen uptake respirometrically to determine biodegradation kinetics and carbon (iv) oxide evolution kinetics. Figure 5.7 showed the net cumulative carbon (iv) oxide evolution, i.e., actual carbon (iv) oxide evolution from microcosm minus the carbon (iv) oxide evolution from the control reactor spiked with only the OECD nutrients. The results showed that after impacting the soil with a mixture of PAHs, the net cumulative carbon (iv) oxide evolution depicted in Figure 5.7, increased and attained a plateau concentration with a carbon (iv) oxide limit of 6.925×10^{-4} moles ($30.47 \times 10^{-3} \text{g}$) within 60 days of contact time. Similarly, the net cumulative oxygen uptake curve (Figure 5.9) also showed an equilibrium time of 60 days. This suggested that a reasonable degree of PAH acclimation was achieved in the soil microcosm within the exposure time.

Analysis of the results on the batch adsorption/desorption kinetics and equilibria indicated that the desorption rate was slower than the adsorption rate (Figures 5.10 to 5.15). The cumulative extent of desorption for the three PAHs tested suggested that the desorption step was the rate limiting for biodegradation as diffusion in the pores may

have been retarded by surface adsorption effects on soil organic carbon. The overall effect was therefore the lowering of the aqueous phase concentration of the contaminant PAHs thereby rendering them not readily bioavailable to the microorganisms. The biodegradation will thus in the long run be controlled by the slow desorptive and diffusive mass transfer into biologically active areas. Comparing the adsorption/desorption equilibration time with the biodegradation acclimation time as given by the net carbon (iv) oxide evolution and oxygen uptake data shown in Figures 5.7 and 5.9, affirms that adsorption/desorption equilibrium was achieved prior to the onset of biodegradation in soil. From these experimental results, a realistic adsorption-reaction-desorption mechanism can be adduced and this would suggest that a time dependent degradation of the PAHs describes the adsorption of solute on the particle surface instead of an assumption of instantaneous adsorption.

By using the linearized Freundlich and Langmuir isotherm equations to describe equilibrium adsorption and desorption at the external surface and the internal pore of the soil particle, an acceptable and reasonable straight-line correlation was achieved with the Freundlich model as shown in Figures 5.16, 5.17, 5.18, 5.22, 5.23 and 5.24. The magnitude of its adsorption capacity (n), an indication of system suitability as given in

Table 5.4 was found to be positive, greater than 1 and within the limit defined by Treybal (1981), as representing favourable adsorption conditions. The estimated coefficients of adsorption and desorption suggest that both processes are in equilibrium. In contrast, the Langmuir isotherm was found to be inappropriate being characterized by negative adsorption/desorption intensities, curvilinear and irreversible plots. The ambiguous coefficient of adsorption and desorption obtained further confirmed the unsuitability of the isotherm.

Representative experimental biodegradation kinetics data for naphthalene, anthracene and pyrene is shown in Figure 5.28. The exponential nature of the curves strongly indicates that the disappearance of the PAHs was not linear with time. Using the best-fit kinetic parameters obtained from the cumulative oxygen uptake experimental data for the microcosm reactor; equations 1 to 4 were used to simulate the change in PAHs concentration in a contaminated soil as a function of time.

The results for both single and multisubstrate catalysis using the twin concepts of rate-determining step and steady state approximation are as shown in Figures 5.29 and 5.30. The typical hockey-stick curves obtained is an indication of an initial, rapid decrease in the concentration

of the PAHs, followed by a significantly slower rate of degradation. This may be attributed to oxygen diffusion limitation in the microcosm. At the onset, oxygen diffuses rapidly in the upper section of the microcosm and thereafter, a slower rate in the lower section. In addition, the incidence of refraction of the contaminants may also have been responsible for the observed exponential decay pattern. Approximately 98.4% of the naphthalene, 82.98% anthracene and 89.67% pyrene contained in the microcosm had been degraded within 33 days of exposure.

The extent of degradation of the PAHs tested was found to be dependent on the molecular weight, solubility and diffusivity in water as given in Tables 5.1 and 5.9. The increasing order of molecular weight would have suggested a progressive decrease in the degradation rate but their diffusivity/transfer rate and solubility in water present some degree of variation, which explains the observed preferential decay of one PAH over the other. Anthracene exhibits a lower solubility in water and hence it was not readily available for utilization by the indigenous microbes present in the soil. The effects of these limitations are reflected in the estimated biokinetic and kinetic parameters calculated based on all measured quantities as shown in Tables 5.5 and 5.6. From the results, using the numerical values of V_{max} and K_m , the following observations were adduced: that the enzyme showed significantly high catalytic

potential on the substrates, given the estimated rate constant of the degradation process, the enzymes catalyzing the breakdown of naphthalene and pyrene had very close attributes and that there was a weak binding between anthracene and the enzymes catalyzing its breakdown as indicated by the K_m value. The K_m indicates the relative suitability of alternate substrate of a particular enzyme.

The estimated reaction rate constant k of the experimental PAHs with the simulated results is shown in Table 5.6. The objective of the simulation was to obtain the attainable reaction rate constant (k) of the biodegradation process. The RDS model gave a better fit as its k value closely fitted the experimental values. Prediction by the SSA model was not feasible as its k values for both single and multisubstrate catalysis deviated widely from experimental data. Comparing the simulated and experimental results show that the SSA overestimates the biodegradation rates. This observation can be attributed to the existence of intermediates at steady state usually present at such small concentrations that its rate of change in the mixture can be assumed to be zero or negligible. The RDS model was therefore chosen because the differences in the model fits were small and its prediction of mixture experiments were more enhanced.

As part of this research work, the method of temporal moments which interprets solute transport with linear equilibrium sorption and first order degradation was applied to analyze the experimental data from the soil microcosm. The solution took into consideration, the interplay of degradation and sorption. In addition, the experimental data were also fitted to the analytical solutions of a transport model CXTFIT curve-fitting program described by Toride *et al.*, (1995). The two methods were comparatively used to estimate the transport parameters: the pore-water velocity and dispersion coefficient using the non-reactive solute, the retardation factor and the degradation rate constant of the contaminant solutes. In the results shown in Table 5.7 and 5.8, the lower order of magnitude (one order) observed for the coefficient of deviation of V when compared with those for D , R and λ , was attributed to the fact that only the first normalized moment is required to estimate V for a non-reactive solute.

Conversely, estimation of D , R and λ required both the first and second moments, hence the marked deviation for those parameters. This observation was found to be consistent with the reported values of Leij and Dane, (1992) and Pang *et al.*, (1998) where it was noted that the higher the order of the moments, the less stable the calculation. The

higher values of D obtained using MOM when compared with the least squares curve-fitting showed that the first moment calculation is positively influenced by calculation in the BTC tail. This is predicated on the fact that the MOM estimated values is a function of the difference between the second moment and the first moment squared. R is a dimensionless parameter which describes the bioavailability (the accessibility of a chemical for assimilation and possible toxicity) of one PAH relative to another and it increases with increasing solute hydrophobicity. The results in Table 5.8 showed that naphthalene had lowest retardation factor with a corresponding higher degradation rate constant. The observed trend is similar to the estimates from the Michaelis-Menten kinetics. The implication of this result is significant as it affirms that the biodegradation of the contaminant PAHs is a function of their bioavailability. In agreement with Oleszczuk and Baran (2003), the finding can be attributed to the aqueous solubility, diffusivity and mobility of each PAH.

The comparative analysis of the concentration breakthrough curves in the contaminant transport studies for non-reactive solute (tracer) and the experimental PAHs using the MOM and CXTFIT, presented in the profiles of Figures 5.31 to 5.34, showed that they both fit the experimental breakthrough curve; although the MOM had better fit. This

was because with MOM, no assumptions about the initial conditions for the experiment were required. The profiles showed that the non-reactive solute attained its maximum concentration in 5 hours, pyrene in 17 hours and anthracene in 30 hours. The time as at exhaustion, i.e., at the peak of C/C_o profiles, indicate the breakthrough time. The observed result suggest that naphthalene would elute first followed by pyrene and anthracene. This behaviour can again be attributed to the differences in their properties such as aqueous solubility, molecular weight and diffusivity in water. The drop in the C/C_o peaks may be as a result of the weakening of the hydrogen-carbon bonds with time. This weakening, which results from the solubility of the contaminants, promotes diffusive mechanism, facilitates the transport of the compound and thus enhances its availability in solution. The dissolution of the tracer is of utmost benefit for the reaction because it promotes the degradation process by enhancing the solubility and bioavailability of the recalcitrant PAHs.

However, naphthalene was observed to solubilize completely almost at the start of the experiment. This suggests that its solubility and transport were not facilitated by the presence of the surfactant. This behavior can be attributed to its physical properties when compared to the other PAHs in the soil matrix (see Table 5.1), as aqueous solubility for naphthalene

was highest at 0.93 (Perry and Green, 1998). Furthermore, the breakthrough time which was completely zero throughout the 40hour duration affirms the literature report by Pang *et al.*, 2003 which showed that an increasing degradation rate results in a shift of the BTC centre of mass to the left i.e. λ and μ_1 are inversely related.

The marked variation in time between pyrene and anthracene in spite of the fact that pyrene has a higher molecular weight may be attributed to the differences in their structural configuration, the very low solubility of anthracene and the close diffusivity exhibited between anthracene and pyrene. Anthracene has a linear structure in which the benzene rings are tightly fused together while pyrene has a tetrahedral structure in which the rings are loosely fused. This creates porosity within the interstitial spaces between the rings making it susceptible for microbial attack. The results, therefore, implicates pattern of ring linkage and molecule topology as factors which could be considered as very important in the study of the kinetics of PAH degradation.

The transport parameters, V and D , obtained from the temporal moment solutions and the independently estimated diffusion parameters, k_f , D_p and D_f were used for the resolution of the dimensionality of the non-steady state model. A reasonable agreement was observed between

the experimental data on the concentration-time behaviour and the model predictions for the PAHs depicted by the 3-dimensional profiles shown in Figures 5.35 through 5.40. The lower diffusivities obtained in the soil when compared to diffusivities in water further suggest that diffusion in the pores of the soil may have been retarded by surface adsorption/desorption effects on soil organic carbon, mineral surfaces and interstitial voids within the micropores and submicropores of the soil particle. The mass transfer coefficient was significantly high for the PAHs compared to the diffusivities and this can be directly attributed to their aqueous solubility. Thus low solubility will account for low transfer/diffusion rate.

A critical appraisal of the values from the axial and radial directions of flow revealed that there was a consistent decrease in the concentration of the PAHs with time in the axial direction. In contrast, with increasing contact time, more PAHs were found within the soil particle pores than on the soil particle surface in the radial direction. This observation was found to be consistent with the findings of Tabak and Govind (1997), Bouwer *et al.*, (1997), Zhang *et al.*, (1998) and Chunga and King (2001), which confirmed that more microbial activities take place on the soil particle surface than within the pores. This therefore suggested that with prolonged contact time, PAHs become occluded within the micropores

(fissures and cavities) of the soil particles, making them not bioavailable and thus inaccessible to microbial degradation. A summary of the simulated results as given by the residual concentration in Table 5.10 showed that the decay rate was faster in the macroporous system than in the microporous system, that the concentration of naphthalene was lower in both systems followed by pyrene and anthracene in that order. These results affirmed the fact that the microbial utilization of pyrene and anthracene for metabolic activities were greatly limited by their resistance to mass transfer between the fluid phase and the soil matrix occasioned by their low aqueous solubility. Finally, the result confirmed that naphthalene was more selectively mineralized in the microcosm reactor than pyrene and anthracene.

The result of the validation of the kinetic model gave a 6.5% and 13.5% deviation for the rate-determining step and steady state approximation method respectively. This implied that prediction by the rate-determining step closely approximates the data from experiment. Generally, the numerical solution of the non-steady state model for the macroporous system gave a reasonable agreement with the experimental data as shown in Figure 5.41 with an average deviation of less than 5%. The deviation from experimental data for the microporous system was over 7%. This deviation from linearity observed in the scattered plot of Figure 5.42 for

the microporous system, can be attributed to the inability of obtaining experimental measurement values for the initial condition within the pores of the soil particles.

CHAPTER SEVEN

7.0 CONTRIBUTIONS TO KNOWLEDGE

The formulations and solution approach adopted in this research work differ significantly from previous attempts at the study of the kinetics of biodegradation of polycyclic aromatic hydrocarbons. These differences are now elucidated below:

1. The first major difference is the ability to locally design and fabricate a microcosm reactor equipped with the conditions suitable for ex-situ mineralization of a mixture of PAHs.
2. The kinetic formulation was developed following the methods used in the derivation of rate equations for synthetic catalyst. This kinetic formulation was coupled with the mass transport expression governed by Fick's first law of diffusion. They provided insight into the degradation of both single and combined polycyclic aromatic hydrocarbon mixture in the surface and subsurface soils. The implication of this is important. Normally in an event of a spill, it is rare to find a single hydrocarbon in the contaminated soil. The model formulated permits the determination of the rates of bioremediation of both single and a mixture of hydrocarbons.
3. The non-steady state model accounted for the intraparticle and interphase mass transport. The solution approach showed the

distribution and composition of these contaminants in three dimensions, viz, axial and radial distances with time. This obviates the need for experimental measurements over relatively long distances or spatial and temporal scales and/or time periods. This is a departure from the existing models of Loo *et al.* (1996), Tabak and Govind (1997), Peters *et al.* (1999), Rogers and Reardon (2000) and Rockne *et al.* (2002).

4. The application of the method of temporal moments solution and a nonlinear least square curve-fitting program CXTFIT version 2.0 in estimating a retardation factor R and degradation rate constant (using data from laboratory experiments), demonstrate the efficacy of the solution from this research work in predicting the biodegradation rate as a direct function of the transport (mobility) and bioavailability of the contaminant solute.
5. The generated data on availability, mobility and degradation, which hitherto have been limited, can be utilized for the design of reactors for the treatment process. The data constitutes a major source of information for the environmental practitioners in the oil and gas industries who are constantly faced with the problem of petroleum and petroleum product spill.

CHAPTER EIGHT

8.0 CONCLUSIONS AND RECOMMENDATIONS

8.1 Conclusions

In this work, reasonable fit were obtained between the rate-determining step model and the experimental biodegradation kinetics data. The rate-determining step has been shown to be a more reliable model for showing the substrates interaction within the soil system. The rate of degradation of contaminants was found to be determined by only one step in the sequence of elementary steps. Prediction by the steady-state model was found to be very poor as it overestimates the biodegradation rate.

From the adsorption/desorption equilibration and biodegradation acclimation time, it can be affirmed that adsorption/desorption equilibrium was achieved prior to the onset of biodegradation in the soil slurry reactor. Desorption studies showed the lowering of the aqueous phase concentration of the contaminant PAHs.

Results of the detailed non-steady state model, which accounts for the intraparticle, and interphase mass transport developed for both macro and microporous systems showed that long-term exposure of PAHs was characterized by a progressive bioaccumulation and immobilization of the

PAHs from the soil particle surface towards the pores of the soil particle. This suggested PAH occlusion in the micropores of the soil particle. Empirical data and numerical simulations thus suggest that biodegradation will be limited by contaminant sorption to soil organic matter.

From the results of the degradation and transport parameters obtained using the method of temporal moments and the nonlinear least squares curve-fitting program, the temporal moment solutions have been satisfactorily verified in this study. It was found to be capable of providing an additional and useful means of parameter estimation for transport involving equilibrium sorption and first order degradation.

8.2 Recommendations

The application of the non-steady state model to other reactor systems and soil types is recommended for future research. This will assist to evaluate the reductions in contaminant concentrations that can be achieved over time and space in such systems to correlate the reductions to availability, mobility and/or toxicity.

The need for the use of surfactant in soil remediation is recommended. The future research work will include investigating the effects of the

presence of surfactants on the rates of biodegradation of PAHs, the competing effects of solubilization, admicellar sorption and sorption of contaminants during bioremediation. This could help to determine the suitability of surfactants to facilitate transport and mobility of soil contaminants.

Due to the significant challenges that confront efforts to model real world biodegradation kinetics, in which mixed substrates and mixed cultures are the rule, it is recommended that mathematical models be developed to predict the effect and level of substrate interactions and inhibitions during bioremediation. Furthermore, the interactions between microbial species in a mixed culture for biodegradation kinetics are also recommended for investigation.

REFERENCES

- Ahn, Y., Sanseverino, J. and Sayler, G.S. (1999). *"Analyses of polycyclic aromatic hydrocarbon-degrading bacteria isolated from contaminated soils."* Biodegradation, 10: 149-157.
- Akpofure, E.A., Efere, M.L. and Ayawei, P. (2007). Integrated grass root post-impact assessment of acute damaging effects of continuous oil spills in the Niger Delta January 1998-January 2000, in: Oil spillage in Nigeria's Niger Delta, Urhobo Historical Society.
- Alexander, M. (1995). Sequestration and bioavailability of organic compounds in soil in: Bioavailability and biodegradation kinetics protocol for organic pollutant compounds to achieve environmentally acceptable endpoints during bioremediation. Annals of the New York Academy of Sciences. The New York Academy of Sciences, New York, 829: 36-61.
- Alexander, M. (2000). *"Ageing, bioavailability and overestimation of risk from environmental pollutants."* Environmental Science and Technology, 34: 4259-4265.
- Amadi, A. and Antai, S.P. (1991). *"Degradation of bonny medium crude oil by microbial species isolated from Oshika-Oyekama oil polluted area."* Int. J. Biochemphysics, 1: 10-14.
- Asuquo, F.E., Ewa-oboho, I., Asuquo, E.F. and Udo, P.J. (2004). *"Fish species used as biomarker for heavy metal and hydrocarbon contamination for Cross River, Nigeria."* The Environmentalist, 24: 1-2.
- Atkinson, B. (1974). Biochemical Reactors, Pion Limited, London, 80-84.
- Atlas, R.M. (1981). *"Biodegradation of petroleum hydrocarbons: Environmental perspective."* Microbiology Rev. 45: 180-209.

- Atlas, R.M. (1991). "*Microbial hydrocarbon degradation of oil spills.*" J. Chem. Technol. Biotechnol., 52: 149-156.
- Ayotamuno, M.J., Kogbara, R.B., Ogaji, S.O. and Probert, S.D. (2006). "*Bioremediation of a crude oil polluted soil ay Portharcourt, Nigeria*". Applied Energy, 83: 1249-1257.
- Ayotamuno, M.J., Okparanma, R.N., Nweneka, E.K., Ogaji, S.O.J. and Probert, S.D. (2007). "*Bioremediation of a sludge containing hydrocarbons*". Applied Energy, 84: 936-943.
- Babary, J. P. (1999) "*New boundary conditions and adaptive control of fixed bed bioreactors.*" J. Chem. Eng. and Processing, 38: 35-44.
- Bailey, J.E. and Ollis, D.F. (1977). Biochemical Engineering Fundamentals McGraw-Hill Book Company, 90-95.
- Bakers, J.H. and Morita, R. (1983). "*A note on the effects of crude oil on microbial activities in a stream sediment.*" Environmental Pollution, 17: 175-185.
- Banerjee, D.K, Fedorak, P.M, Hashimoto, A., Masliyah, J.H., Pickard, M.A. and Gray, M.R. (1995). "*Monitoring the biological treatment of anthracene-contaminated soil in a rotating-drum bioreactor.*" Appl. Microbiol. Biotechnol., 43: 521-528.
- Bewley, R.J.F. (1986). A microbiological strategy for the decontamination of polluted soil in: Contaminated soil, (eds J.W. Assink and W.J. Van den Brink), Dordrecht: Martinus Nijhoff, 759-768.
- Bird, R.B., Stewart, W.E. and Lightfoot, E.N. (2005). Transport Phenomena, John Wiley and Sons, Inc. 2nd edition, 528-530.
- Black, C.A. (1965). Organic carbon determination by the chromic acid wet oxidation method. Methods of Soil Analysis. 1372 - 1376

Bluestone, M. (1986). "Microbes to the rescue" Chemists Week 139:

17-34.

Blumer, M. (1976). "Polycyclic aromatic hydrocarbons in nature." Sci. Am., 234: 35-45.

Bogan, B.W., Trbovic, V. and Paterek, J.R. (2003). "Inclusion of vegetable oils in Fenton's chemistry for remediation of PAH-contaminated soils." Chemosphere, 50: 15-21.

Boldrin, B., Tiehün, A. and Fritzsche, C. (1993). "Degradation of phenanthrene, fluorine, fluoranthene and pyrene by a mycobacterium sp." Appl. Environ. Biotechnol., 59: 1927-528.

Boonchan, M.L., Sudarat, B. and Grant, A.S. (2000). "Degradation of high molecular weight polycyclic aromatic hydrocarbon by defined fungi-bacteria cocultures." Applied and Environmental Microbiology, 66: 1007-1019.

Bos, R.P., Theuws, J.L.G., Leijdekkers, C.M. and Henderson, P.T. (1984). "The presence of the mutagenic polycyclic aromatic hydrocarbons benzo(a)pyrene and benz(a)anthracene in creosote Pl." Mutat. Res., 130: 153-158.

Bossert, I.D. and Bartha, R. (1986). "Structure biodegradability relationships of polycyclic aromatic hydrocarbons in soil." Bull. Environ. Contam. Toxicol., 37: 490-495.

Bouchez, M., Blanchet, D. and Vandecasteele, V. P. (1996). "The microbiological fate of polycyclic aromatic hydrocarbons. Carbon and oxygen balances for bacterial degradation of model compounds." Appl. Microbiol. Biotechnol., 45: 556-561.

Bouwer, E.J., Zhang, W., Liza, P.W. and Durant, N.D. (1997). In: Bioremediation of surface and subsurface contamination. Annals of the New York Academy of Sciences. The New York Academy of

- Sciences, New York, 829:103-117.
- Brady, N.C and Weil, R.R. (1999). The nature and properties of soil, Prentice Hall, Upper Saddle River, New Jersey, 12th edition, 446-474.
- Brakay, T., Navon-Venezia, S., Ron, E.S. and Rosenberg, E. (1999). *"Enhancement of solubilization and biodegradation of polyaromatic hydrocarbons by bioemulsifier Alasan."* Appl. Environ. Microbiol., 65: 2697-2702.
- Bray, R.H. and Kurtz, I.T. (1945). *"Determination of total organic and available form of phosphorus in soil."* Soil. Sci., 59: 39-45.
- Brown, D.G., Guha, S. and Jaffe, P.R. (1999). *"Surfactant-enhanced biodegradation of a PAH in a soil slurry reactor."* Bioremediation J., 3: 269-283.
- Brown, D.G. and Jaffe, P.R. (2006). *"Effects of non-ionic surfactants on the cell surface hydrophobicity and apparent Hamaker constant of a sphingomonas sp."* Environ. Sci. Technol., 40: 195-201.
- Brown, D.G. (2007). *"Relationship between micellar and hemi-cellar processes and the bioavailability of surfactant-solubilized hydrophobic organic compounds."* Environ. Sci. Technol., 41: 1194-1199.
- Burwood, R. and Speers, G.C. (1974). *"Photo oxidation as a factor in the environmental dispersal of crude oil."* Estuarine and Coastal Mar. Sci., 2: 117-135.
- Caldini, G., Cenci, G., Manenti, R. and Morozzi, G. (1995). *"The ability of an environmental isolate Pseudomonas fluorescens to utilize chrysene and other four-ring polynuclear aromatic hydrocarbons."* Appl. Microbiol. Biotechnol., 44: 225-229.
- Carmichael, L.M and Pfaender, F.K. (1997). *"Polynuclear aromatic hydrocarbon metabolism in soils: relationship to soil*

- characteristics and pre exposure.*" Environ. Toxicol. Chem., 16: 666-675.
- Chunga W.K. and King, G.M. (2001). *"Isolation, characterization and polyaromatic hydrocarbon degradation potential of aerobic bacteria from marine macrofaunal burrow sediments."* Appl. Environ Microbiol., 67: 5585-5592.
- Chrysikopoulos, C.V., Hsuan, P.Y., Fyrrillas, M.M. and Lee, K.Y. (2003). *"Mass transfer coefficient and concentration boundary layer thickness for a dissolving NAPL pool in porous media."* J. Hazardous Materials, B97: 245-257.
- Coosen, M.A. (1991). *"Experimental and modelling studies of mass transfer in microencapsulated cell systems."* Tropical J. Pharmaceutical Res., 1: 3-14.
- Coulson, J.M and Richardson, J.F. (2000). Chemical Engineering, John Wiley and Sons, New York, 6th edition, 1: 626-642.
- Coulson, J.M and Richardson, J.F. (2006). Chemical Engineering, John Wiley and Sons, New York, 5th edition, 2: 970-989.
- Couteliers, F.A., Burganos, V.N. and Payatakes, A.C. (2004). *"Model of adsorption-reaction-desorption in a swarm of spheroidal particles."* AIChE J., 50: 779-785.
- Day, O.R. (1965). *"Particle Fractionation and particle size analysis"* in: *Methods of Soil Analysis*. Am. Soc. Agron., 9: 545-567.
- Day-Barker, P., Sambuco, C.P. and Forbes, P.D. (1985). *"Development of an animal model to study the phytotoxic effects of anthracene and UV in skin and ocular tissues."* Photochem. Photobiol., 41: 23-27.
- de Lucas, A., Rodriguez, L., Villasenor, J. and Fernandez, F.J. (2005). *"Biodegradation kinetics of stored wastewater substrate by a mixed microbial culture."* Biochem. Eng. J., 26: 191-197.

- Duke, N.C., Burns, K.A., Swannell, R.P.J., Dalhaus, O. and Rupp, R.J. (2000). *"Dispersant use and a bioremediation strategy as alternate means of reducing impacts of large oil spills on mangroves: the Gladstone field trials."* Mar. Pollut. Bull., 41: 403-412.
- Ebuchi, O. A., Abibo, I. B., Shekwolo, P. D., Sigismund, K. I., Adoki, A. and Okoro, I. C. (2005). *"Remediation of crude oil contaminated soil by enhanced natural attenuation technique"*. Journal of Applied Science and Environmental Management, 9: 103-106.
- Fiore, J. and O'Brien, J.E. (1968). Ammonia Determination by Automatic Analysis. Wastes Engineering, 33, 352.
- Fogler, H.S. (2006). Elements of Chemical Reaction Engineering. Prentice-Hall of India Private Limited, New Delhi, 3rd edition, 383-386, 581-616.
- Fortin, J., Jury, W.A. and Anderson, A. (1997). *"Enhanced removal of trapped non-aqueous phase liquids from saturated soil using surfactant solutions."* J. Contam. Hydrol., 24: 247-258.
- Freeman, D.J. and Cattell, F.C.R. (1990). *"Woodburning as a source of atmospheric polycyclic aromatic hydrocarbons."* Environ. Sci. Technol., 24: 1581-1585.
- Galinada, W.A. and Yoshida, H. (2004). *"Intraparticle diffusion of phosphate in-OH type strongly basic ion exchanger."* AIChE J., 50: 2806-2815.
- Gerhardt, P., Murray, E.G.R., Wood, A.W. and Krieg, R.N. (1994). Methods for General and Molecular Bacteriology. ASM Press Washington, 790-791.
- Gosh, U., Talley, J.W. and Luthy, R.G. (2001). *"Particle-scale investigation of PAH desorption kinetics and thermodynamics from sediment."* Environ. Sci. Technol., 35: 3468-3475.
- Guha, S., Peters, C.A. and Jeff, P.R. (1999). *"Multisubstrate*

- biodegradation kinetics of naphthalene, phenanthrene and pyrene mixture.*" Biotechnol Bioeng., 65: 491-499.
- Gunnison, D., Fredrickson, H.L., Kaplan D.L., Allen, A.L., Mello C.M., Walker, J.E., Myrick, G., Evans, W.E. and Ochman, M. (1997). Application of continuous technology for the development of explosives-degrading microorganisms. in: Bioremediation of Surface and Subsurface Contamination. Annals of the New York Academy of Sciences. The New York Academy of Sciences, New York, 829, 230-241.
- Guthrie, E. A. and Pfaender, F.K. (1998). "*Reduced pyrene bioavailability in microbially active soils.*" Environ. Sci. Technol., 32: 501-508.
- Hatzinger, P.B. and Alexander, M. (1995) "*Effects of aging of chemicals in soil on their biodegradability and extractability.*" Environ. Sci. Technol., 29:537-545.
- Heitkamp, M.A., Freeman, J.P and Cerniglia, C.E. (1987). "*Naphthalene biodegradation in environmental microcosms: estimates of degradation rates and characterization of metabolites.*" Appl. Environ. Microbiol., 53: 129-136.
- Hillel, D. (1982). Introduction to Soil Physics Academic Press Inc. Ltd. London, U.K. 47-54.
- Hong-gyu, S. and Bartha, R. (1990). "*Effects of petroleum fuel spills on the microbial community of soil.*" Appl. Environ. Microbiol. 56: 646-651.
- Imhoff, P.T., Jaffe, P.R. and Pinder, G.G. (1994). "*An experimental study of complete dissolution of nonaqueous phase liquid in saturated porous media.*" Water Resour. Res., 30: 307-315.
- Jabson, A., Cook, F. and Westlake, D. (1972). "*Microbial utilization of crude oil.*" Appl. Microbiol., 23: 1082-1089.

- Jenson, V. G. and Jeffreys, G. V. (1966). Mathematical methods in Chemical Engineering. Academic Press Inc. London and New York 3rd edition, 41-49.
- Jones, K.C., Stratford, J.A., Waterhouse, K.S., Furlong, E.T., Giger, W., Hites, R.A., Schaffner, C. and Johnston, A.E. (1989). "*Increases in the polynuclear aromatic hydrocarbon content of an agricultural soil over the last century.*" Environ. Sci. Technol., 23: 95-101.
- Kanally, R.A. and Harayama, S. (2000). "*Biodegradation of high-molecular-weight polycyclic aromatic hydrocarbons by bacteria.*" J. of Bacteriol., 182: 2059-2067.
- Karthikeyan, R. and Bhandari, A. (2001). "*Anaerobic biotransformation of aromatic and polycyclic aromatic hydrocarbons in soil microcosms: A review.*" J. of Hazardous Substance Research, 3: 1-7.
- Kastner, M., Streibich, S., Beyrer, M., Richnow, H.H. and Fritsche, W. (1999). "*Formation of bound residues during microbial degradation of [¹⁴C] anthracene in soil.*" Appl. Environ. Microbiol., 65: 1834-1842.
- Keith, L.H. and Telliard, W.A. (1979). "*Priority pollutants: a perspective view.*" Environ. Sci. Technol., 13: 416-423.
- Kinigoma, B.S. (2001). "*Effects of drilling fluid additives on the Niger Delta environment: A case study of the Soku oil fields.*" J. Appl. Sci. Environ., 5: 57-61.
- Koeppel, C., Popovic, M. and Bajpai, R.K. (1997). Microbial migration in soil in: bioremediation of surface and subsurface contamination in: bioremediation of surface and subsurface contamination, Bajpai Sciences, the New York Academy of Sciences, New York, 829, 250-262.
- Knightes, C.D. (2000). Mechanisms governing sole-substrate and

- multisubstrate biodegradation kinetics of polycyclic aromatic hydrocarbons PhD Dissertation. Princeton University, Princeton, NJ.
- Krug, S and Evans, J. R.G. (2002). "*Reaction and Transport Kinetics for Depolymerization with a porous Body.*" *AIChE J.*, 48: 1553-1540.
- Kukkonen, J.V.K., Landrum, P.F., Mitra, S., Gossiaux, D.C., Gunnarsson, J. and Weston, D. (2003). "*Sediment characteristics affecting the desorption kinetics of select PAH and PCB congeners for seven laboratory spiked sediments.*" *Environ. Sci. Technol.*, 37: 4656-4663.
- Lapinskas, J. (1989). "*Bacterial degradation of hydrocarbon contamination in soil and groundwater.*" *Chemistry and Industry*, 4: 784-789.
- Lamoureux, E.M. and Brownawell, B.J. (1999). "*Chemical and biological availability of sediment-sorbed hydrophobic organic contaminants.*" *Environ. Toxicol. Chem.*, 18: 1733-1741.
- Layokun, S.K., Umoh, E.F. and Solomon, A. (1987). "*Kinetic model for the degradation of dodecane by pseudomonas flourescens isolated from Warri in Nigeria.*" *J. of the Nig. Soc of Chem. Engrs.*, 6: 49-52.
- Leahy, J. and Colwell R. (1990). "*Microbial degradation of hydrocarbons in the environment.*" *Microbiological reviews*, 54: 305-395.
- Leij, F.J and Dane, J.J (1992). "*Moment method applied to solute transport with binary and ternary exchange*". *Soil Sci. Soc. Am. J.*, 56: 667-674.
- Levenspiel, O. (1999). Chemical Reaction Engineering, John Wiley and Sons Inc., 3rd edition, 65-67, 623 – 641.
- Loor, Y., Strom, P.F. and Farmer, W. J. (1996). "*The effect of sorption on*

- phenanthrene bioavailability.* J. Biotechnol., 51: 221-227.
- Mahaffey, W.R., Gibson, D.T. and Cerniglia, C.E (1988). "*Bacterial oxidation of chemical carcinogens: formation of polycyclic aromaticacids from benz[a] anthracene.*" Appl. Environ. Microbiol., 54: 2415-2423.
- Mason, A.R. and Kueper, B.H. (1996). "*Numerical simulation of surfactant-enhanced solubilization of pooled DNAPL.*" Environ. Sci. Technol., 30: 3205-3212.
- McCabe, W.L., Smith, J.C. and Harriott, P. (1993). Unit operations of Chemical Engineering McGraw-Hill Inc., 5th edition, 814-832.
- Mueller, J.G., Chapman, P.J. and Pritchard, P.H. (1989). "*Action of a fluoranthene-utilizing bacterial community on polycyclic aromatic hydrocarbon components of creosote.*" Appl. Environ. Microbiol., 55: 3085-3090.
- Murphy, J., and Riley, J., (1962). "*A Modified Single Solution for the Determination of Phosphate in Natural Waters.*" Anal Chim. Acta, 27:31.
- Naagbantton, P. (1999). "*Shell's oil spills in Bille, in Niger Delta's River State.*" An Environmental Rights Action (ERA) Report, Benin City, Nigeria, 24: 1-5.
- Nwachukwu, S.C.U. (2001). "*Bioremediation of sterile agricultural soils polluted with crude petroleum by application of the soil bacterium, Pseudomonas putida, with inorganic nutrient supplementation.*" Current Microbiology, 42: 231-236.
- Nwilo, P.C. and Badejo, O.T. (2001). "*Soil sediment and water: Impacts Of oil spills along the Nigerian coast.*" The Association for Environmental Health and Sciences (AEHS).
- Oboh, B. O., Ilori, M. O., Akinyemi, J. O. and Adebuseye, S. A. (2006). "*Hydrocarbon degrading potentials of bacteria isolated from a*

Nigerian bitumen (Tarsand) deposit". Nature and Science, 4(3):
51 - 57.

- Odokuma, L.O. and Dickson, A.A. (2003). *"Bioremediation of crude oil polluted tropical rain forest soil."* Global J. of Environmental Sciences, 2: 29-40.
- Odu. C.T.I. (1982). *"Microbiology of soil contaminated with petroleum hydrocarbon: Extent of contamination and some soil and microbial properties after contamination."* J. Inst. Petroleum, 58: 201-208.
- Oh, Y.S., Sim, D.S. and Kim, S.J. (2001). *"Effects of nutrients on crude oil biodegradation in the upper interstitial zone."* Mar. Pollut. Bull., 42: 1367-1372.
- Ojo, O. A.(2006). *"Petroleum hydrocarbon utilization by native bacterial population from a wastewater canal Southwest Nigeria".* African Journal of Biotechnology, 5: 333-337
- Okerentugba, P. O. and Ezeronye, O. U. (2003). *"Petroleum degrading potential of single and mixed microbial cultures isolated from rivers and refinery effluent in Nigeria".* African Journal of Biotechnology, 2: 288-292.
- Okoh, A. I.(2003). *"Biodegradation of Bonny light crude oil in soil microcosms by some bacterial strains isolated from crude oil flow stations saver pits in Nigeria".* African Journal of Biotechnology, 2: 104-108.
- Oleszczuk, P. and Baran, S. (2003). *"Degradation of individual polycyclic aromatic hydrocarbons (PAHs) in soil polluted with aircraft fuel."* Polish J. Environ. Studies, 12: 431-437.
- Onig, S.K and Bowers, A.R. (1990). *"Steady state analysis for biological treatment of inhibitory substrates."* J. Environ. Eng., 116: 1013-1028.
- Pang, L., Gottz, M. and Close, M. (2003). *"Application of the method of*

- temporal moments to interpret solute transport with sorption and degradation.*" J. Contaminant Hydrology, 60: 123-134.
- Perry, R.H. and Green, D.W. (1998). Perry's Chemical Engineers Handbook, 7th Edition. McGraw-Hill Inc.
- Pennel, K.D., Abriola, L.M. and Weber, W.J., Jr. (1993). "*Surfactant-enhanced solubilization of residual dodecane in soil columns. Experimental investigation.*" Environ. Sci. Tech., 27: 2332-2339.
- Peters, C.A., Knightes, C.D. and Brown, D.G. (1999). "*Long term composition dynamics of PAH-containing NAPLs and implications for risk assessment.*" Environ. Sci. Technol., 33: 4499-4507.
- Pignatello, J.J. and Li, J. (2006). "*Facilitated bioavailability of PAHs to native soil bacteria promoted by nutrient addition.*" American Geophysical Union, Fall meeting, H331-05.
- Rahman, K.S.M., Thahira-Rahman, J., Lakshmanaperumalsamy, P. and Banat, I.M. (2002). "*Towards efficient crude oil degradation by a mixed bacterial consortium.*" Bioresour. Technol., 85: 257-261.
- Reardon, K.F., Mosteller, D.C., Rogers, J.B., Duteau, N. and Kim, K. (2002). "*Biodegradation kinetics of aromatic hydrocarbon mixtures by Pure and mixed bacterial cultures.*" Environmental Health Perspectives, 110: 1005-1011.
- Reddy, K. R and Angelo, D. E. (2003). "*Effect of aerobic and anaerobic conditions on chlorophenol sorption in wetland soils.*" Am. J. Soil Sci Soc., 67: 784-787.
- Ressler, B.P., Kneifel, H. and Winter, J. (1999). "*Bioavailability of polycyclic aromatic hydrocarbons and formation of humic acid-like residues during bacterial PAH degradation.*" Appl. Microbiol. Biotechnol., 53: 85-91.
- Rittmann, B.E. and McCarty, P.L. (1980). "*Model of steady-state biofilm kinetics.*" Biotechnol. Bioeng., 22: 2343-2357.

- Rockne, K.J., Shor, L.M., Young, L.Y., Taghon, G.L. and Kosson, D.S. (2002). *"Distributed sequestration and release of PAHs in weathered sediment: The role of sediment structure and organic carbon properties."* Environ. Sci. Technol., 36: 2636-2644.
- Rogers, B. and Reardon, K.F. (2000). *"Modeling substrate interactions during the biodegradation of mixtures of toluene and phenol by Burkholderia sp. JS 150."* Biotechnol. Bioeng., 70: 428-435.
- Schwarzenbach, E.J., Steinberg, C.E. and Schneider, J.R. (1993). *"Physical and chemical properties of polycyclic aromatic hydrocarbons."* Appl. Microbiol. Technol., 36: 401-410.
- Seagren, E.A. and Moore, T.O. (2003). *"Nonaqueous phase liquid pool dissolution as a function of average pore water velocity."* J. Environ. Eng. (ASCE), 129: 786-791.
- Segel, I.H. (1975). Biochemical Calculations, John Wiley and Sons Inc., 2nd Edition, 214-246, 326-329.
- Shor, L.M., Kosson, D.S., Rockne, K.J., Young, L.Y. and Taghon, G.L. (2004). *"Combined effects of contaminant desorption and toxicity on risk from PAH contaminated sediments."* Risk Analysis, 24: 1109-1119.
- Spark, D. L. (2003). Environmental soil Chemistry, Academic Press, 2nd edition, 150-152; 207-209.
- Sposito, G. (1994). Chemical equilibria and kinetics in soils John Wiley and Sons, New York, 40-46, 139-142.
- Soil Survey Manual (1975). Soil taxonomy: A basic system of soil classification for making and interpreting soil surveys. Agric Handbook 436, Dept of Agriculture, Washington D.C.
- Sorsa, M. (1992). *"Genotoxic effects and chemical composition of four creosotes"* Mutation Res., 278: 1-9.
- Sun, L.M. and Levan, M.D. (1995). *"Numerical solutions of*

diffusion equations by the finite differences method: Efficiency improvement by iso-volumetric spatial discretization. " Chem. Eng. Sci., 50: 163.

Susu, A. A. (1997). Chemical kinetics and heterogeneous catalysis CJC Press, Nigeria Limited, 49-83.

Susu, A.A. (2000). "*Mathematical modelling of fixed bed adsorption of aromatics and sulphur compounds in kerosene deodorization.*" Chemical Engineering Processing, 39: 485-497.

Symons, B.D., Linkenheil, R., Pritchard, D., Shanker, C.A. and Seep, D. (1995). "*In-situ groundwater aeration of polycyclic aromatic hydrocarbons.*" in: Effects of nutrients on crude oil biodegradation in the upper interstitial zone." Mar. Pollut. Bull., 42: 1367-1372.

Tabak, H.H. and Govind, R. (1997). Bioavailability and biodegradation kinetics protocol for organic pollutant compounds to achieve environmentally acceptable endpoints during bioremediation in: bioremediation of surface and subsurface contamination. Annals of the New York Academy of Sciences. The New York Academy of Sciences, New York, 829, 36-61.

Tam, N.F.Y., Guo, C.L., Yau, W. and Wong, Y.S. (2002). "*Preliminary study on biodegradation of phenanthrene by bacteria isolated from mangrove sediments in Hong Kong.*" Mar. Pollut. Bull., 45: 316-324.

Tiehm, A. (1994). "*Degradation of polycyclic aromatic hydrocarbons in the presence of synthetic surfactants.*" Appl. Environ. Microbiol., 60: 258-263.

Toride, N., Leij, F.J. and Van Genuchten, M.T. (1995). "*The CXTFIT code for estimating transport parameters from laboratory or field version 2.0.* in: Application of the method of temporal moments to

- interpret solute transport with sorption and degradation."* J. Contaminant Hydrology 60, 123-134.
- Treybal, R.E. (1981). Mass-Transfer Operations. McGraw-Hill Book Company, 3rd Edition.
- Urum, K. and Pekdemir, T. (2004). "*Evaluation of biosurfactants for crude oil contaminated soil washing.*" Chemosphere 57, 1139-1150.
- van der Meer, J.R., de Vos, W.M., Harayama, S. and Zehnder, A.J.B. (1992). "*Molecular mechanisms of genetic adaptation to xenobiotic compounds.*" Microbiol. Rev., 56: 677-694.
- Vogler, E.T. and Chrysikopoulos, C.V. (2004). "*An experimental study of acoustically enhanced NAPL dissolution in porous media.*" AICHE J., 50: 3271-3280.
- Volkova, N.I. (1983). Anthracene and derivatives. in: Encyclopaedia of occupational health and safety, Parmeggiani ed. International labour office, Geneva, 162-163.
- Walter, D.W., Hans-Jurgen, K. and Joseph, L. (1992). "*Adsorption of polycyclic aromatic hydrocarbons (PAHs) by soil particles: influence on biodegradability and biotoxicity.*" Appl. Microbiol. Biotechnol., 36: 689-696.
- Wami, E. N. and Ogoni, H. A. (1997). "*Kinetic model for biodegradation of petroleum hydrocarbon mixture, Bonny light crude.*" J. of the Nigerian Soc. of Chemical Engineers, 16: 77-88.
- Weissenfels, W.D., Klewer, H.J. and Langhoff, J. (1992). "*Adsorption of Polycyclic Aromatic Hydrocarbons (PAHs) by Soil Particles- Influence on Biodegradability and Biotoxicity.*" Appl. Microbiol. Biotechnol., 36: 689-696.
- Wilson, S.C. and Jones, K.C. (1993). "*Bioremediation of soil contaminated with polynuclear aromatic hydrocarbons (PAHs): A*

- review." Environ. Pollut., 81: 229-249.
- Xu, R. and Obbard, J.P. (2003). "*Environmental health hazards of polycyclic aromatic hydrocarbons.*" Appl. Environ. Microbiol., 56: 1079-1086.
- Xu, R. and Obbard, J.P. (2004). "*Biodegradation of polycyclic aromatic hydrocarbons in oil-contaminated beach sediments treated with nutrients amendments.*" J. Environ. Qual., 33: 861-867.
- Zander, M. (1993) Physical and chemical properties of polycyclic aromatic hydrocarbons. Handbook of Polycyclic Aromatic Hydrocarbons. Marcel Dekker, Inc., New York, 1-26.
- Zhang, X., Peterson, C., Reece, D., Haws, R. and Moller, G. (1998). "*Biodegradability of biodiesel in aquatic environment.*" Trans. ASAE, 41: 1423-1430.
- Zhang, W., Bouwer, E.J. and Ball, W.P. (1998). "*Bioavailability of hydrophobic organic contaminants: effects and implications of sorption-related mass transfer on bioremediation.*" GWMR, 126-138.
- Zhu, L., Chen, B. and Tao, S. (2004). "*Sorption behaviour of polycyclic aromatic hydrocarbons in soil-water system containing non-ionic surfactant.*" Environ. Eng. Sci., 21: 263-272.
- Zobell, C.E. (1973). Microbial degradation of oil: present status, problems and perspectives in: Oil Spills in the Marine Environment, CJC Press (Nigerian) Limited, Yaba, Lagos, Nigeria.

APPENDIX A

Data from soil microcosm reactor for biodegradation studies. These values were obtained from the gas chromatogram readings of experimental samples.

Table A: Concentration of contaminant PAHs with time

Time (days)	Concentration (mg/l)		
	Naphthalene	Anthracene	Pyrene
0	100.00	100.00	100.00
7	99.7	28.0	44.18
14	66.49	23.5	35.54
21	4.44	18.48	23.60
28	1.62	9.33	17.02
35	1.30	4.13	16.12
42	0.82	1.64	2.26
49	0.00	0.57	0.00
56	0.00	0.00	0.00
63	0.00	0.00	0.00

To facilitate the determination of the biokinetic and kinetic constants, the concentration-time data obtained from the biodegradation experiment were fitted into the differential rate equation using the procedure described by Michaelis-Menten via the Lineweaver-Burk double reciprocal plot. The Lineweaver-Burk reciprocal plot is simply a linear transformation of the basic velocity of the Michaelis-Menten kinetic equation.

Thus,

$$-r_A = r_R = \frac{k[E_T][C]}{K_m + [C]} \quad \text{A.1}$$

But $k[E_T] = V_{\max} \quad \text{A.2}$

$$\text{Therefore, } -r_A = r_R = \frac{V_{\max} [C]}{K_m + [C]} \quad \text{A.3}$$

Inverting equation (A.3) yields:

$$\frac{V_{\max}}{-r_A} = \frac{K_m + [C]}{[C]} \quad \text{A.4}$$

Cross-multiplying:

$$\frac{1}{-r_A} = \frac{K_m + [C]}{V_{\max} [C]} \quad \text{A.5}$$

Therefore, separating terms, we would have

$$\frac{1}{-r_A} = \frac{K_m}{V_{\max}} + \frac{[C]}{V_{\max} [C]} \quad \text{A.6}$$

$$\text{Or} \quad \frac{1}{-r_A} = \frac{K_m}{V_{\max}} \frac{1}{[C]} + \frac{1}{V_{\max}} \quad \text{A.7}$$

Thus, if $\frac{1}{-r_A}$ is plotted against $\frac{1}{[C]}$, the slope = $\frac{K_m}{V_{\max}}$ and the intercept on the y-axis = $\frac{1}{V_{\max}}$. (See Figure A.1 below).

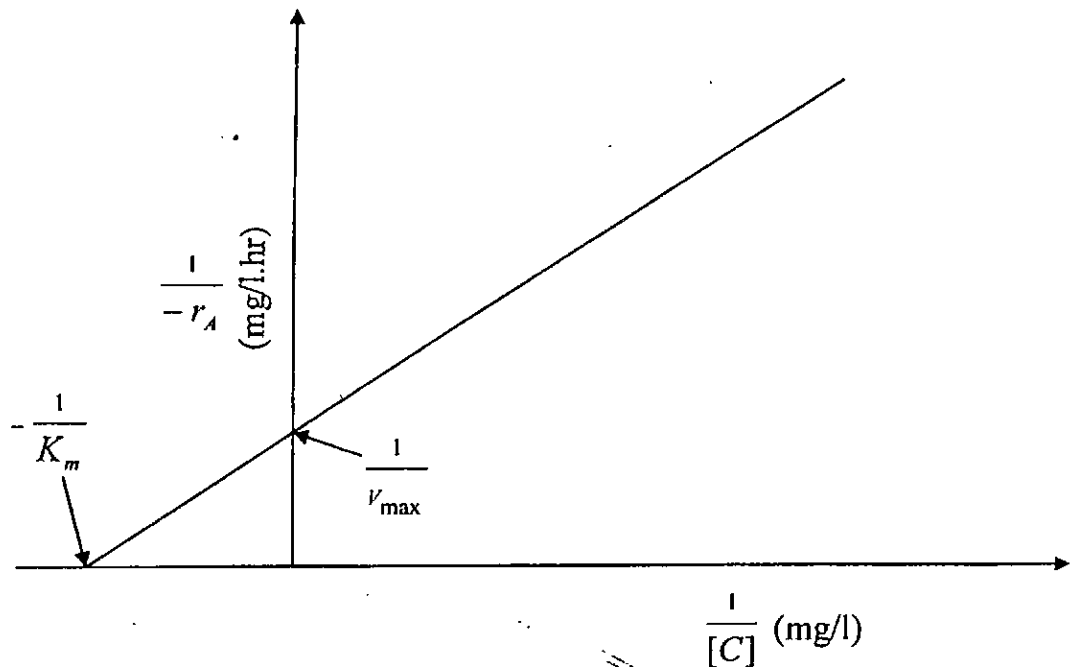


Figure A.1 Double reciprocal $1/r_A$ against $1/[C]$

V_{\max} and K_m are parameters whose numerical values provide a means of comparing enzyme activity from different microorganisms during biodegradation. V_{\max} is an indication of the maximal velocity that would be observed when all the enzyme is present as ES. K_m , the Michaelis constant is a dynamic pseudo-equilibrium constant expressing the relationship between the actual steady state concentration rather than the equilibrium concentrations.

APPENDIX B

Respirometric bioreactor data for oxygen uptake and carbon (iv) evolution kinetics.

Table B.1: Oxygen uptake data from Control Soil Microcosm Reactor (Spectronic 21D Spectrophotometer reading at 605 nm)

Time (days)	Absorbance (nm)	Amount consumed (mg/l)
0	0.00	0.0000
5	0.141	0.3052
10	.0246	0.5320
15	0.272	0.5887
20	0.281	0.6082
25	0.341	0.7380
30	0.344	0.7450
35	0.345	0.7500
40	0.443	0.9589
45	0.446	0.9654
50	0.468	1.0130
55	0.610	1.3200
60	0.655	1.3745
65	0.679	1.4697
70	0.679	1.4697

Table B.2: Oxygen uptake data from Experimental Soil Microcosm Reactor (Spectronic 21D Spectrophotometer reading at 605 nm)

Time (days)	Absorbance (nm)	Amount consumed (mg/l)
0	0.000	0.0000
5	0.2650	0.5740
10	0.2750	0.5950
15	0.3600	0.7790
20	0.3030	0.6558
25	0.5060	1.0952
30	0.5240	1.1340
35	0.5520	1.1950
40	0.6960	1.5060
45	0.8320	1.800
50	0.8660	1.8740
55	0.8820	1.9091
60	0.9720	2.1039
65	0.9930	2.1496
70	1.1270	2.4390

From the principle of Lambert-Beer which was described by Segel (1975), a standard curve was plotted using 1% alkaline pyrogallol and this was used to estimate the actual amount (concentration) of oxygen consumed in the soil microcosm reactor.

Table B.3: Standard curve determination for oxygen using pyrogallol

Concentration of pyrogallol (M)	Absorbance of pyrogallol at 650nm
0.1	0.015
0.2	0.024
0.3	0.030
0.4	0.036
0.5	0.039
0.6	0.043
0.7	0.051
0.8	0.055
0.9	0.072
1.0	0.076
2.0	0.102
3.0	0.122
4.0	0.133
5.0	0.143

Table B.4: Cumulative carbon (iv) oxide Evolution Data

Time (days)	Volume from experimental reactor (cm ³)	Volume from control reactor (cm ³)	Net Cumulative volume (cm ³)
0	0.00	0.00	0.00
10	15.20	12.00	3.20
20	24.00	19.20	4.80
30	30.00	22.80	7.20
40	24.00	13.00	11.00
50	22.00	9.00	13.00
60	22.00	8.00	14.00
70	22.00	8.00	14.00

Using the gas law relationship given as:

$$\frac{V_1}{T} = \frac{V_2}{T_2} \quad \text{B.1}$$

where V_1 = volume from orsat gas analyzer for control and experimental.

T_1 and T_2 are the ambient and reactor temperatures, 25°C and 27.7°C respectively. V_2 = volume evolved.

Substituting known values, we can estimate the corresponding volume at reactor temperature. These values are given in Table B.5 below.

**Table B.5: Net cumulative carbon (iv) oxide Evolution from the Soil
Microcosm Reactor**

Time (days)	Volume from (cm ³)
0	0.00
10	3.55
20	5.32
30	7.98
40	13.30
50	14.96
60	15.51
70	15.51

But at standard temperature and pressure (STP), a gas occupies 22.4dm³ (22400cm³)/mol. Thus the measured cumulative volumes in Table B.5 can be converted and expressed as the number of moles or the weight of carbon (iv) oxide evolved:

**Table B.6: Net cumulative carbon (iv) oxide Evolution from the Soil
Microcosm Reactor**

Time (days)	Amount x 10 ⁻⁴ (mols)
0	0.00
10	1.58
20	2.37
30	3.56
40	5.94
50	6.68
60	6.93
70	6.93

APPENDIX C

Result from the Adsorption/Desorption Experiments

In the adsorption/desorption experiments, assuming that the aqueous phase has a uniform concentration of contaminant PAHs, mass transfer from the fluid phase to the surface of the soil particle are presented in the tables below:

Table C.1: Adsorption kinetic data for naphthalene, anthracene and pyrene in a soil slurry reactor

Time (hours)	Concentration (mg/l)		
	Naphthalene	Anthracene	Pyrene
0	40.00	40.00	40.00
2	37.60	20.08	34.30
4	26.80	14.58	28.58
6	22.00	10.20	24.0
8	13.20	1.68	16.08
10	10.80	1.50	12.20
12	3.60	1.31	8.22
14	2.40	1.17	4.60
16	1.20	1.11	3.00
18	0.40	0.98	2.22
20	0.00	0.79	1.12
24	0.00	0.19	0.10
28	0.00	0.11	0.00
36	0.00	0.00	0.00

Table C.2: Desorption kinetic data for naphthalene, anthracene and pyrene in a soil slurry reactor

Time (hours)	Concentration (mg/l)		
	Naphthalene	Anthracene	Pyrene
0	25.59	30.57	31.68
4	30.13	32.57	33.17
8	34.21	33.98	34.04
16	38.81	35.12	35.67
24	38.87	36.63	36.93
48	38.94	37.10	37.59
72	38.99	37.47	37.64
96	38.99	37.51	37.70
120	39.08	37.62	38.13
144	0.00	37.93	38.18
168	0.00	38.45	38.22
192	0.00	38.58	38.22

Table C.3: Naphthalene Adsorption data for Freundlich and Langmuir isotherm plots

x/m (mg/g)	C _e (mg/l)	Log (x/m)	Log C _e	C _e /(x/m) (g/l)
0.084	8.4	-1.076	0.934	100.034
0.3933	39.33	-0.4053	1.594	100
0.3945	39.45	-0.4040	1.599	99.99
0.3967	39.67	-0.4015	1.599	100
0.3973	39.73	-0.4001	1.599	100
0.3991	39.91	-0.3989	1.601	100
0.4366	39.94	-0.3600	1.620	100

0.2546	39.97	-0.5942	1.373	100
0.1770	39.99	-0.7521	1.218	100
0.4688	40	-0.32904	1.602	100
0.4583	40	-0.3389	1.655	100
0.4829	40	-0.3161	1.710	100

Table C.4: Anthracene Adsorption data for Freundlich and Langmuir isotherm plots

x/m (mg/g)	C _e (mg/l)	Log (x/m)	Log C _e	C _e /(x/m) (g/l)
0.0996	19.925	-1.000	1.2840	200.050
0.1894	25.416	-0.873	1.4051	134.1922
0.1908	29.7988	-0.794	1.4742	156.178
0.1914	38.3195	-0.718	1.5834	200.2064
0.1920	38.499	-0.717	1.5855	200.516
0.1934	38.691	-0.714	1.58761	200.0569
0.1939	38.833	-0.712	1.5892	200.2728
0.1946	38.8955	-0.711	1.5899	199.8741
0.1951	39.0200	-0.710	1.5913	200.000
0.1957	39.810	-0.668	1.633	203.4236
0.1957	39.810	-0.591	1.707	203.4236

Table C.5: Pyrene Adsorption data for Freundlich and Langmuir isotherm plots

x/m (mg/g)	C_e (mg/l)	$\text{Log } (x/m)$	$\text{Log } C_e$	$C_e/(x/m)$ (g/l)
0.05704	5.704	-1.2438	0.7562	100
0.1142	11.420	-0.9423	1.0577	100.023
0.160	16.000	-0.7530	1.2041	99.912
0.2392	23.916	-0.6213	1.3787	100
0.2780	27.800	-0.4011	1.4440	100
0.3178	31.784	-0.4978	1.50221	100
0.3540	35.396	-0.4511	1.5489	100
0.370	370..	-0.3990	1.5682	100
0.3778	370780	-0.4227	1.5773	100
0.3888	38.876	-0.4103	1.5897	100
0.3989	38.896	-0.3991	1.601	100
0.4000	40	-0.3979	1.6021	100
0.400	40	-0.3979	1.6021	100

Table C.6: Naphthalene Desorption data for Freundlich and Langmuir isotherm plots

x/m (mg/g)	C_e (mg/l)	$\text{Log } (x/m)$	$\text{Log } C_e$	$C_e/(x/m)$ (g/l)
0.2011	25.586	-0.697	1.408	127.233
0.2395	30.130	-0.6207	1.479	125.8012
0.2630	34.213	-0.5800	1.5342	130.081
0.2978	38.872	-0.5262	1.562	130.552
0.2972	38.812	-0.5269	1.5754	130.584

0.3185	38.943	-0.54969	1.5904	122.279
0.30155	38.989	-0.51120	1.5909	127.618
0.3312	38.992	-0.4799	1.6038	117.74
0.3345	39.083	-0.4756	1.6162	116.829

**Table C.7: Anthracene Desorption data for Freundlich and
Langmuir isotherm plots**

x/m (mg/g)	C_e (mg/l)	$\text{Log } (x/m)$	$\text{Log } C_e$	$C_e/(x/m)$ (g/l)
0.0943	9.43	-1.0255	0.9745	100.034
0.0743	7.43	-1.129	0.8710	100
0.0602	6.02	-1.245	0.780	99.998
0.0488	4.88	-1.3116	0.688	100
0.0337	3.37	-1.4724	0.5276	100
0.0290	2.90	-1.473	0.4624	100
0.0253	2.53	-1.597	0.4031	100
0.0249	2.49	-1.6038	0.3962	100
0.0238	2.38	-1.634	0.3766	100
0.0207	2.07	-1.687	0.3160	100
0.0155	1.55	-1.8097	0.1903	100
0.0142	1.42	-1.8477	0.1523	100

Table C.8: Pyrene Desorption data for Freundlich and Langmuir isotherm plots

x/m (mg/g)	C_e (mg/l)	$\text{Log } (x/m)$	$\text{Log } C_e$	$C_e/(x/m)$ (g/l)
0.3168	31.68	-0.4992	1.5008	100
0.3317	33.17	-0.4793	1.5208	100
0.3404	34.04	-0.4680	1.5320	100
0.3567	35.67	-0.4568	1.5523	100
0.3693	36.93	-0.4326	1.5674	100
0.3759	37.59	-0.4249	1.5751	100
0.3764	37.64	-0.4246	1.5757	100
0.3770	37.70	-0.4213	1.5763	100
0.3813	38.13	-0.4187	1.5813	100
0.3818	38.18	-0.4182	1.5818	100
0.3822	38.22	-0.4177	1.5823	100
0.3822	38.22	-0.4177	1.5822	100

APPENDIX D

Cultural, Morphological and Biochemical Characterization of Microbial Colonies

Table D.1: Cultural characteristics

Bacteria isolates	Shape	Size	Elevation	Margin	Colour	Optical appearance
A	Circular	1-2mm	Raised	Smooth	Cream	Opaque
B	Circular	1-2mm	Raised	Smooth	Cream	Opaque
C	Irregular	2-2mm	Flat	Serrated	Yellow	Transparent
D	Circular	1-2mm	Flat	Smooth	White	Opaque

Table D.2: Morphological characteristics

Bacteria isolates	Cell shape	Cell arrangement	Gram reaction
A	Rods	Pairs	+ve
B	Rods	Pairs	+ve
C	Cocci	Group	+ve
D	Rods	Cluster	-ve

Table D.3: Biochemical characteristics

Bacteria isolates	Catalase	Oxidase	Spore stain	Glucose	Citrate	Urease
A	+ve	-ve	+ve	a and g	-ve	-ve
B	+ve	-ve	+ve	a	-ve	-ve
C	+ve	-ve	-ve	a	-ve	-ve
D	+ve	-ve	+ve	a and g	+ve	+ve

Key

a = Acid

g = gas

+ve = positive

-ve = negative

A = *Bacillus luteus*

B = *Bacillus sphaericus*

C = *Micrococcus luteus*

D = *Klebsiella pneumonia*

The presence of fungi colonies in the soil was also ascertained following the characterization tests listed in Table D.4 below:

Table D.4: Cultural, Morphological and Sugar Fermentation characterization

Fungi isolates	Cultural	Morphological	Sugar fermentation	
			Glucose	Lactose
E	Smooth and floxy white colonies	Hyphae is septated. Spores are also septated	Produces acid only	No acid or gas production
F	Velvety surface growth form. Colour is black	Hyphae is non septated. Spores are not septated	Produces acid and gas	Produces only acid

Key

E = *Fusarium* spp

F = *Aspergillus niger*

The ability of the indigenous microbes to degrade the polycyclic aromatic hydrocarbons was investigated using naphthalene. Cell concentration was measured as optical density at 436nm. Table D.5 show the experimental measurements used for the estimation of the growth parameters of the organisms.

Table D.5: Microbial Growth Study using Naphthalene as test contaminant at 436nm

Time (hours)	Bacillus luteus	Bacillus sphericus	Micrococcus luteus	Klebsiella pneumonia	Fusarium spp	Aspergillus niger
0	0.000	0.000	0.000	0.000	0.000	0.000
2	0.089	0.053	0.058	0.053	0.075	0.06
4	0.093	0.060	0.067	0.073	0.082	0.073
6	0.109	0.073	0.075	0.078	0.091	0.079
8	0.122	0.098	0.098	0.081	0.102	0.100
10	0.130	0.109	0.168	0.132	0.118	0.107
12	0.160	0.155	0.172	0.154	0.120	0.190
14	0.170	0.164	0.194	0.166	0.146	0.127
16	0.067	0.123	0.131	0.106	0.059	0.016
18	0.020	0.101	0.116	0.073	0.018	0.010
20	0.015	0.079	0.111	0.051	0.017	0.006

The rate of biodegradation is generally the focus of environmental studies. The microbial growth and substrate consumption rates are estimated from the experimental data on the growth and degradation studies. The estimation of the growth parameters: maximum specific growth rate, cell biomass yield and saturation constant using Monod kinetics is shown as follows:

From the plots, we have using:

Bacillus luteus:

$Y = 0.349$, slope = 1.1027, intercept = 12.063

$$1.1027 = \frac{M}{\mu_{\max}}$$

$$M = \mu_{\max} \times 1.1027$$

$$12.063 = \text{intercept} = \frac{1.1027\mu_{\max} + 1}{\mu_{\max}}$$

$$12.063\mu_{\max} - 1.1027\mu_{\max} = 1$$

$$\mu_{\max} = \frac{1}{10.9603} = 0.091 \text{ hr}^{-1}$$

$$M = 1.1027 \times 0.091 = 0.1006$$

$$k_s = M \left[C_o + \frac{1}{Y} X_o \right]$$

$$k_s = 0.1006 \left[0.024492 + \frac{1}{.349} \times 0.089 \right]$$

$$k_s = 0.028 \text{ kgm}^{-3}$$

Bacillus sphericus:

$Y = 0.272$, slope = 0.9482, intercept = 7.02

$$0.9482 = \frac{M}{\mu_{\max}}$$

$$M = \mu_{\max} \times 0.9482$$

$$7.02 = \text{intercept} = \frac{0.9482\mu_{\max} + 1}{\mu_{\max}}$$

$$7.02\mu_{\max} - 0.9482\mu_{\max} = 1$$

$$\mu_{\max} = \frac{1}{6.0718} = 0.165 \text{ hr}^{-1}$$

$$M = 0.9482 \times 0.165 = 0.156$$

$$k_s = 0.156 \left[0.024475 + \frac{1}{0.272} \times 0.053 \right]$$

$$k_s = 0.0343 \text{ kg m}^{-3}$$

Micrococcus luteus:

$Y = 0.222$, slope = 0.9156, intercept = 6.5772

$$0.9156 = \frac{M}{\mu_{\max}}$$

$$M = \mu_{\max} \times 0.9156$$

$$6.5772 = \text{intercept} = \frac{0.9156\mu_{\max} + 1}{\mu_{\max}}$$

$$6.5772\mu_{\max} - 0.9156\mu_{\max} = 1$$

$$\mu_{\max} = \frac{1}{5.6616} = 0.177 \text{ hr}^{-1}$$

$$M = 0.9156 \times 0.177 = 0.162$$

$$k_s = 0.162 \left[0.024476 + \frac{1}{0.222} \times 0.058 \right]$$

$$k_s = 0.046 \text{ kgm}^{-3}$$

Klebsiella pneumonia:

$$Y = 0.275, \text{ slope} = 0.1756, \text{ intercept} = 1.3097$$

$$0.1756 = \frac{M}{\mu_{\max}}$$

$$M = \mu_{\max} \times 0.1756$$

$$1.3097 = \text{intercept} = \frac{0.1756\mu_{\max} + 1}{\mu_{\max}}$$

$$1.3097 \mu_{\max} - 0.156 \mu_{\max} = 1$$

$$\mu_{\max} = \frac{1}{1.1341} = 0.88 \text{ hr}^{-1}$$

$$M = 0.1756 \times 0.88 = 0.1545$$

$$k_s = 0.1545 \left[0.024480 + \frac{1}{0.2705} \times 0.053 \right]$$

$$k_s = 0.034 \text{ kgm}^{-3}$$

Fusarium spp:

$$Y = 0.139, \text{ slope} = 1.4352, \text{ intercept} = 10.6732$$

$$1.4352 = \frac{M}{\mu_{\max}}$$

$$M = \mu_{\max} \times 1.4352$$

$$10.6732 = \text{intercept} = \frac{1.4352\mu_{\max} + 1}{\mu_{\max}}$$

$$10.6732\mu_{\max} - 1.4352\mu_{\max} = 1$$

$$\mu_{\max} = \frac{1}{9.238} = 0.108 \text{ hr}^{-1}$$

$$M = 1.4352 \times 0.108 = 0.155$$

$$k_s = 0.155 \left[0.024487 + \frac{1}{0.139} \times 0.098 \right]$$

$$k_s = 0.113 \text{ kg m}^{-3}$$

Aspergillus niger:

$$Y = 0.243, \text{ slope} = 1.776, \text{ intercept} = 9.7133$$

$$1.776 = \frac{M}{\mu_{\max}}$$

$$M = \mu_{\max} \times 1.776$$

$$9.7133 = \text{intercept} = \frac{1.776\mu_{\max} + 1}{\mu_{\max}}$$

$$10.6732\mu_{\max} - 1.776\mu_{\max} = 1$$

$$\mu_{\max} = \frac{1}{7.937} = 0.126 \text{ hr}^{-1}$$

$$M = 1.776 \times 0.126 = 0.224$$

$$k_s = 0.2238 \left[0.024485 + \frac{1}{0.1243} \times 0.060 \right]$$

$$k_s = 0.061 \text{ kg m}^{-3}$$

APPENDIX E

Interpretational rules generally adopted for tropical and subtropical soils.

1. Textured class

Sandy soils:

Coarse textured: Sands: S

Loamy sands LS

Moderately coarse textured:

Sandy loam: SL

Sandy clay loam: SCL

2. Soil Reaction

pH

Extremely acidic less than 4.5

Very strongly acidic 4.5-5.0

Strongly acidic 5.1-5.5

Moderately acidic 5.6-6.0

Slightly acidic 6.1-6.5

Neutral 6.6-7.5

3. Available phosphorus

(mg/kg)

Soil poor in phosphorus less than 5

Moderately supplied 5-8

Well supplied 8-10

Soil rich in phosphorus 10

4. Exchange Complex

		Very weak	Weak	Medium	Strong	Very strong
Exchangeable	Ca	1.0	1-2.3	2.3-3.5	3.5-7.0	> 7
	Mg	0.4	0.4-1.0	1.0-1.5	1.5-3.0	3.0
	K	0.1	0.1-0.2	0.2-0.4	0.4-0.8	> .8
	Na	0.1	0.1-0.3	0.3-0.7	0.7-2.0	> 2

7

Physical properties

Soil moisture % 3 – 5 Oven dried
 5 - 6.5 Air dried
 6.5 – 10 Field moist
 10 – 15 Wet

Bulk Density < 1 Rich in organic matter
 1 - 1.5 clayey soil
 1.5 – 2.0 Loamy soil
 2 – 2.5 Sand loam

APPENDIX F

Independent Estimation of the Transport parameters

The physical quantities contained in the mass transfer-limited numerical model for both macroporous and microporous systems i.e., the film mass transfer coefficient, pore and aqueous phase diffusivities of the contaminant PAHs were independently estimated for a reasonable solution of the model. For the film mass transfer coefficient, we have:

$$k_f = 0.32 \frac{D_m^{1/3}}{D_T} V^{1/3} \text{Re}_{dp}^{1/4} \left[\frac{D_i^{1/2} d_p^{-1/4}}{D_T^{1/2} H_L^{1/4}} \right] \quad (\text{F.1})$$

Therefore, substituting known values into equation F.1, we would have:

for naphthalene:

$$k_f = \frac{0.32(7.28 \times 10^{-5})^{1/3}}{0.11} \times (0.95 \times 10^{-3})^{1/3} \times 1254.31^{1/4} \frac{0.06^{1/2} \times 0.002^{-1/4}}{0.11^{1/2} \times 0.028^{1/4}}$$

$$k_f = 1.92 \times 10^{-3} \text{ m/day}$$

Similarly, for anthracene, $k_f = 1.72 \times 10^{-3} \text{ m/day}$

Pyrene, $k_f = 1.64 \times 10^{-3} \text{ m/day}$

The diffusivity of the fluid phase:

$$D_f = 7.4 \times 10^{-8} \frac{\sqrt{\psi_B M_B T}}{\mu V_A^{0.6}} \quad (\text{F.2})$$

Hence for naphthalene,

$$D_f = \frac{7.4 \times 10^{-8} (2.6 \times 18)^{1/2} (300)}{0.9 (147.6)^{0.6}}$$

$$= 8.429 \times 10^{-6} \text{ cm}^2/\text{s}$$

$$= 7.28 \times 10^{-5} \text{ m}^2/\text{day}.$$

Similarly,

$$\text{for anthracene } D_f = 6.10 \times 10^{-5} \text{ m}^2/\text{day}$$

$$\text{for pyrene } D_f = 6.08 \times 10^{-5} \text{ m}^2/\text{day}$$

and the pore diffusivities:

$$D_{pi} = \frac{E_p}{T} \left[\frac{3}{4\bar{r}} \left(\frac{mn}{2R\theta_s} \right)^{1/2} + \frac{1}{D_f} \right]^{-1} \quad (\text{F.3})$$

For naphthalene,

$$D_{pi} = \frac{0.481}{4} \left[\frac{3}{4(0.001)} \left(\frac{3.142 \times 128}{2 \times 8.314 \times 273} \right)^{1/2} + \frac{1}{7.28 \times 10^{-5}} \right]^{-1}$$

$$D_{pi} = 8.614 \times 10^{-6} \text{ m}^2/\text{day}$$

Similarly,

$$\text{for anthracene } D_{pi} = 8.59 \times 10^{-6} \text{ m}^2/\text{day}$$

$$\text{for pyrene } D_{pi} = 8.57 \times 10^{-6} \text{ m}^2/\text{day}$$

APPENDIX G

Simulation of the Concentration profiles for the Kinetic Models

Based on all measured quantities, the concentration of the single and multisubstrate catalysis using the kinetic models are as shown below:

(a) Rate Determining-step Model

(i) Single substrate catalyzed reaction:

$$C = \frac{1}{2} \left[\frac{C_o e^L}{e^L - 1} + C_o \right] - \left[\frac{C_o e^x}{2(e^L - 1)} \right] \quad (G.1)$$

on substituting known values we would have:

$$\begin{aligned} C &= \frac{1}{2} \left[\frac{100e^{15}}{e^{15} - 1} + 100 \right] - \left[\frac{100e^2}{2(e^{15} - 1)} \right] \\ &= \frac{1}{2} [100 + 100] - \left[\frac{738.9}{6.534 \times 10^6} \right] \\ &= 100 - 1.13084 \times 10^{-4} \\ &= 99.9998 \text{mg/l} \approx 100.00 \text{mg/l} \end{aligned}$$

(ii) Multi-substrate reaction,

$$C = \left[\frac{C_o e^L}{e^L - 1} + C_o \right] \left[\frac{C_o e^x}{2(e^L - 1)} \right] + \frac{n-1}{x} \quad (G.2)$$

Where n = number of contaminant PAHs we would have:

$$\begin{aligned} C &= \frac{1}{2} \left[\frac{300e^{15} + 300}{e^{15} - 1} \right] - \left[\frac{300e^2}{2(e^{15} - 1)} \right] + \frac{3-1}{2} - 1 \\ C &= 299.9997 \text{mg/l} \approx 300 \text{mg/l} \end{aligned}$$

A summary of the results for other specified time is shown in Table G.1.

Table G.1: Simulated concentration-time data for Rate-Determining Step Model

Time (days)	Concentration (mg/l)	
	Single substrate	Multisubstrate
0	99.9998 = 100	299.9997 = 300
7	14.286	42.857
14	7.143	21.429
21	4.762	14.286
28	3.571	10.714
35	2.857	8.571
42	2.310	7.143
49	2.041	6.122
56	1.786	5.357
63	1.587	4.762

b. For steady state approximation:

(i) Single substrate catalyzed reaction

$$C = \left(\frac{V_{\max} [C_o]}{K_m + [C_o]} \right) \frac{x}{D} \quad (\text{G.3})$$

$$C = \left(\frac{0.028 \times 100}{100.00314} \right) \left(\frac{2}{4.086 \times 10^{-5}} \right)$$

$$= 2.799 \times 10^{-3} \times 48,946.052$$

$$C = 137.26 \text{ mg/l}$$

(ii) Multi-substrate catalyzed reaction

$$C = \frac{V_{\max} \sum [C_o]}{K_m + \sum [C_o]} \frac{x}{D} \quad (\text{G.4})$$

$$C = \left(\frac{6.7 \times 10^{-3} \times 300}{300.0178} \right) \left(\frac{2}{7.3622 \times 10^{-5}} \right)$$

$$= 6.6996 \times 10^{-3} \times 27,165.801$$

$$C = 181.98 \text{ mg/l}$$

A summary of the results for other specified time is shown in Table G.2.

Table G.2: Simulated concentration-time data for Steady-State

Approximation Model

Time (days)	Concentration (mg/l)	
	Single substrate	Multisubstrate
0	137.26	182.00
7	19.57	26.00
14	9.79	13.00
21	6.52	8.67
28	4.89	6.50
35	3.91	5.20
42	3.26	4.33
49	2.80	3.71
56	2.45	3.25
63	2.19	2.89

APPENDIX H

**Concentration profiles at different time steps in both axial
and radial directions using the inverse matrix method.**

Naphthalene (Axial direction)

$j = 0$

$$\begin{bmatrix} C_{1,1} \\ C_{2,1} \\ C_{3,1} \\ C_{4,1} \\ C_{5,1} \\ C_{6,1} \\ C_{7,1} \\ C_{8,1} \\ C_{9,1} \end{bmatrix} = \begin{bmatrix} -2 & 1 & 0 & 0 & 0 & 0 & 0 & 0 & 0 \\ 1 & -2 & 1 & 0 & 0 & 0 & 0 & 0 & 0 \\ 0 & 1 & -2 & 1 & 0 & 0 & 0 & 0 & 0 \\ 0 & 0 & 1 & -2 & 1 & 0 & 0 & 0 & 0 \\ 0 & 0 & 0 & 1 & -2 & 1 & 0 & 0 & 0 \\ 0 & 0 & 0 & 0 & 1 & -2 & 1 & 0 & 0 \\ 0 & 0 & 0 & 0 & 0 & 1 & -2 & 1 & 0 \\ 0 & 0 & 0 & 0 & 0 & 0 & 1 & -2 & 1 \\ 0 & 0 & 0 & 0 & 0 & 0 & 0 & 1 & -2 \end{bmatrix}^{-1} \begin{bmatrix} -99.7 \\ 0 \\ 0 \\ 0 \\ 0 \\ 0 \\ 0 \\ 0 \\ 0 \end{bmatrix}$$

$$\begin{bmatrix} -0.9 & -0.8 & -0.7 & -0.6 & -0.5 & -0.4 & -0.3 & -0.2 & -0.1 \\ -0.8 & -1.6 & -1.4 & -1.2 & -1 & -0.8 & -0.6 & -0.4 & -0.2 \\ -0.7 & -1.4 & -2.1 & -1.8 & -1.5 & -1.2 & -0.9 & -0.6 & -0.3 \\ -0.6 & -1.2 & -1.8 & -2.4 & -2 & -1.6 & -1.2 & -0.8 & -0.4 \\ -0.5 & -1 & -1.5 & -2 & -2.5 & -2 & -1.5 & -1 & -0.5 \\ -0.4 & -0.8 & -1.2 & -1.6 & -2 & -2.4 & -1.8 & -1.2 & -0.6 \\ -0.3 & -0.6 & -0.9 & -1.2 & -1.5 & -1.8 & -2.1 & -1.4 & -0.7 \\ -0.2 & -0.4 & -0.6 & -0.8 & -1 & -1.2 & -1.4 & -1.6 & -0.8 \\ -0.1 & -0.2 & -0.3 & -0.4 & -0.5 & -0.6 & -0.7 & -0.8 & -0.9 \end{bmatrix}$$

$$\begin{bmatrix} 89.73 \\ 79.76 \\ 69.79 \\ 59.82 \\ 49.85 \\ 39.88 \\ 29.91 \\ 19.94 \\ 9.97 \end{bmatrix}$$

j=1

-2	1	0	0	0	0	0	0	0	-66.49
1	-2	1	0	0	0	0	0	0	-9.46E-02
0	1	-2	1	0	0	0	0	0	-8.46E-02
0	0	1	-2	1	0	0	0	0	-7.47E-02
0	0	0	1	-2	1	0	0	0	-6.47E-02
0	0	0	0	1	-2	1	0	0	-5.47E-02
0	0	0	0	0	1	-2	1	0	-4.48E-02
0	0	0	0	0	0	1	-2	1	-3.48E-02
0	0	0	0	0	0	0	1	-2	-2.48E-02

-0.9	-0.8	-0.7	-0.6	-0.5	-0.4	-0.3	-0.2	-0.1
-0.8	-1.6	-1.4	-1.2	-1	-0.8	-0.6	-0.4	-0.2
-0.7	-1.4	-2.1	-1.8	-1.5	-1.2	-0.9	-0.6	-0.3
-0.6	-1.2	-1.8	-2.4	-2	-1.6	-1.2	-0.8	-0.4
-0.5	-1	-1.5	-2	-2.5	-2	-1.5	-1	-0.5
-0.4	-0.8	-1.2	-1.6	-2	-2.4	-1.8	-1.2	-0.6
-0.3	-0.6	-0.9	-1.2	-1.5	-1.8	-2.1	-1.4	-0.7
-0.2	-0.4	-0.6	-0.8	-1	-1.2	-1.4	-1.6	-0.8
-0.1	-0.2	-0.3	-0.4	-0.5	-0.6	-0.7	-0.8	-0.9

60.0979
53.7057
47.219
40.6476
34.0015
27.2907
20.5252
13.715
6.86989

j = 2

$$\begin{bmatrix} -2 & 1 & 0 & 0 & 0 & 0 & 0 & 0 & 0 \\ 1 & -2 & 1 & 0 & 0 & 0 & 0 & 0 & 0 \\ 0 & 1 & -2 & 1 & 0 & 0 & 0 & 0 & 0 \\ 0 & 0 & 1 & -2 & 1 & 0 & 0 & 0 & 0 \\ 0 & 0 & 0 & 1 & -2 & 1 & 0 & 0 & 0 \\ 0 & 0 & 0 & 0 & 1 & -2 & 1 & 0 & 0 \\ 0 & 0 & 0 & 0 & 0 & 1 & -2 & 1 & 0 \\ 0 & 0 & 0 & 0 & 0 & 0 & 1 & -2 & 1 \\ 0 & 0 & 0 & 0 & 0 & 0 & 0 & 1 & -2 \end{bmatrix} \begin{bmatrix} -4.5096 \\ -6.27\text{E}-02 \\ -5.81\text{E}-02 \\ -5.06\text{E}-02 \\ -4.40\text{E}-02 \\ -3.74\text{E}-02 \\ -3.07\text{E}-02 \\ -2.39\text{E}-02 \\ -1.71\text{E}-02 \end{bmatrix}$$

$$\begin{bmatrix} -0.9 & -0.8 & -0.7 & -0.6 & -0.5 & -0.4 & -0.3 & -0.2 & -0.1 \\ -0.8 & -1.6 & -1.4 & -1.2 & -1 & -0.8 & -0.6 & -0.4 & -0.2 \\ -0.7 & -1.4 & -2.1 & -1.8 & -1.5 & -1.2 & -0.9 & -0.6 & -0.3 \\ -0.6 & -1.2 & -1.8 & -2.4 & -2 & -1.6 & -1.2 & -0.8 & -0.4 \\ -0.5 & -1 & -1.5 & -2 & -2.5 & -2 & -1.5 & -1 & -0.5 \\ -0.4 & -0.8 & -1.2 & -1.6 & -2 & -2.4 & -1.8 & -1.2 & -0.6 \\ -0.3 & -0.6 & -0.9 & -1.2 & -1.5 & -1.8 & -2.1 & -1.4 & -0.7 \\ -0.2 & -0.4 & -0.6 & -0.8 & -1 & -1.2 & -1.4 & -1.6 & -0.8 \\ -0.1 & -0.2 & -0.3 & -0.4 & -0.5 & -0.6 & -0.7 & -0.8 & -0.9 \end{bmatrix}$$

$$\begin{bmatrix} 4.23245 \\ 3.95531 \\ 3.61543 \\ 3.21747 \\ 2.76897 \\ 2.27646 \\ 1.74658 \\ 1.18603 \\ 0.60157 \end{bmatrix}$$

j = 3

$$\begin{bmatrix} -2 & 1 & 0 & 0 & 0 & 0 & 0 & 0 & 0 \\ 1 & -2 & 1 & 0 & 0 & 0 & 0 & 0 & 0 \\ 0 & 1 & -2 & 1 & 0 & 0 & 0 & 0 & 0 \\ 0 & 0 & 1 & -2 & 1 & 0 & 0 & 0 & 0 \\ 0 & 0 & 0 & 1 & -2 & 1 & 0 & 0 & 0 \\ 0 & 0 & 0 & 0 & 1 & -2 & 1 & 0 & 0 \\ 0 & 0 & 0 & 0 & 0 & 1 & -2 & 1 & 0 \\ 0 & 0 & 0 & 0 & 0 & 0 & 1 & -2 & 1 \\ 0 & 0 & 0 & 0 & 0 & 0 & 0 & 1 & -2 \end{bmatrix} \begin{bmatrix} -1.624 \\ -4.46E-03 \\ -4.21E-03 \\ -3.89E-03 \\ -3.50E-03 \\ -3.07E-03 \\ -2.58E-03 \\ -2.06E-03 \\ -1.50E-03 \end{bmatrix}$$

$$\begin{bmatrix} -0.9 & -0.8 & -0.7 & -0.6 & -0.5 & -0.4 & -0.3 & -0.2 & -0.1 \\ -0.8 & -1.6 & -1.4 & -1.2 & -1 & -0.8 & -0.6 & -0.4 & -0.2 \\ -0.7 & -1.4 & -2.1 & -1.8 & -1.5 & -1.2 & -0.9 & -0.6 & -0.3 \\ -0.6 & -1.2 & -1.8 & -2.4 & -2 & -1.6 & -1.2 & -0.8 & -0.4 \\ -0.5 & -1 & -1.5 & -2 & -2.5 & -2 & -1.5 & -1 & -0.5 \\ -0.4 & -0.8 & -1.2 & -1.6 & -2 & -2.4 & -1.8 & -1.2 & -0.6 \\ -0.3 & -0.6 & -0.9 & -1.2 & -1.5 & -1.8 & -2.1 & -1.4 & -0.7 \\ -0.2 & -0.4 & -0.6 & -0.8 & -1 & -1.2 & -1.4 & -1.6 & -0.8 \\ -0.1 & -0.2 & -0.3 & -0.4 & -0.5 & -0.6 & -0.7 & -0.8 & -0.9 \end{bmatrix}$$

$$\begin{bmatrix} 1.47476 \\ 1.32552 \\ 1.17181 \\ 1.0139 \\ 0.85211 \\ 0.68681 \\ 0.51844 \\ 0.3475 \\ 0.1745 \end{bmatrix}$$

j = 4

$$\begin{bmatrix} -2 & 1 & 0 & 0 & 0 & 0 & 0 & 0 & 0 \\ 1 & -2 & 1 & 0 & 0 & 0 & 0 & 0 & 0 \\ 0 & 1 & -2 & 1 & 0 & 0 & 0 & 0 & 0 \\ 0 & 0 & 1 & -2 & 1 & 0 & 0 & 0 & 0 \\ 0 & 0 & 0 & 1 & -2 & 1 & 0 & 0 & 0 \\ 0 & 0 & 0 & 0 & 1 & -2 & 1 & 0 & 0 \\ 0 & 0 & 0 & 0 & 0 & 1 & -2 & 1 & 0 \\ 0 & 0 & 0 & 0 & 0 & 0 & 1 & -2 & 1 \\ 0 & 0 & 0 & 0 & 0 & 0 & 0 & 1 & -2 \end{bmatrix} \begin{bmatrix} -1.301 \\ -1.56E-03 \\ -1.41E-03 \\ -1.25E-03 \\ -1.10E-03 \\ -9.37E-04 \\ -7.72E-04 \\ -6.05E-04 \\ -4.33E-04 \end{bmatrix}$$

$$\begin{bmatrix} -0.9 & -0.8 & -0.7 & -0.6 & -0.5 & -0.4 & -0.3 & -0.2 & -0.1 \\ -0.8 & -1.6 & -1.4 & -1.2 & -1 & -0.8 & -0.6 & -0.4 & -0.2 \\ -0.7 & -1.4 & -2.1 & -1.8 & -1.5 & -1.2 & -0.9 & -0.6 & -0.3 \\ -0.6 & -1.2 & -1.8 & -2.4 & -2 & -1.6 & -1.2 & -0.8 & -0.4 \\ -0.5 & -1 & -1.5 & -2 & -2.5 & -2 & -1.5 & -1 & -0.5 \\ -0.4 & -0.8 & -1.2 & -1.6 & -2 & -2.4 & -1.8 & -1.2 & -0.6 \\ -0.3 & -0.6 & -0.9 & -1.2 & -1.5 & -1.8 & -2.1 & -1.4 & -0.7 \\ -0.2 & -0.4 & -0.6 & -0.8 & -1 & -1.2 & -1.4 & -1.6 & -0.8 \\ -0.1 & -0.2 & -0.3 & -0.4 & -0.5 & -0.6 & -0.7 & -0.8 & -0.9 \end{bmatrix}$$

$$\begin{bmatrix} 1.1752 \\ 1.0494 \\ 0.92205 \\ 0.79328 \\ 0.66327 \\ 0.53216 \\ 0.40011 \\ 0.26729 \\ 0.13386 \end{bmatrix}$$

j=5

$$\begin{bmatrix} -2 & 1 & 0 & 0 & 0 & 0 & 0 & 0 & 0 \\ 1 & -2 & 1 & 0 & 0 & 0 & 0 & 0 & 0 \\ 0 & 1 & -2 & 1 & 0 & 0 & 0 & 0 & 0 \\ 0 & 0 & 1 & -2 & 1 & 0 & 0 & 0 & 0 \\ 0 & 0 & 0 & 1 & -2 & 1 & 0 & 0 & 0 \\ 0 & 0 & 0 & 0 & 1 & -2 & 1 & 0 & 0 \\ 0 & 0 & 0 & 0 & 0 & 1 & -2 & 1 & 0 \\ 0 & 0 & 0 & 0 & 0 & 0 & 1 & -2 & 1 \\ 0 & 0 & 0 & 0 & 0 & 0 & 0 & 1 & -2 \end{bmatrix} \begin{bmatrix} -0.821 \\ -1.24\text{E}-03 \\ -1.12\text{E}-03 \\ -9.86\text{E}-04 \\ -8.57\text{E}-04 \\ -7.29\text{E}-04 \\ -5.99\text{E}-04 \\ -4.65\text{E}-04 \\ -3.34\text{E}-04 \end{bmatrix}$$

$$\begin{bmatrix} -0.9 & -0.8 & -0.7 & -0.6 & -0.5 & -0.4 & -0.3 & -0.2 & -0.1 \\ -0.8 & -1.6 & -1.4 & -1.2 & -1 & -0.8 & -0.6 & -0.4 & -0.2 \\ -0.7 & -1.4 & -2.1 & -1.8 & -1.5 & -1.2 & -0.9 & -0.6 & -0.3 \\ -0.6 & -1.2 & -1.8 & -2.4 & -2 & -1.6 & -1.2 & -0.8 & -0.4 \\ -0.5 & -1 & -1.5 & -2 & -2.5 & -2 & -1.5 & -1 & -0.5 \\ -0.4 & -0.8 & -1.2 & -1.6 & -2 & -2.4 & -1.8 & -1.2 & -0.6 \\ -0.3 & -0.6 & -0.9 & -1.2 & -1.5 & -1.8 & -2.1 & -1.4 & -0.7 \\ -0.2 & -0.4 & -0.6 & -0.8 & -1 & -1.2 & -1.4 & -1.6 & -0.8 \\ -0.1 & -0.2 & -0.3 & -0.4 & -0.5 & -0.6 & -0.7 & -0.8 & -0.9 \end{bmatrix}$$

$$\begin{bmatrix} 0.74229 \\ 0.66358 \\ 0.58363 \\ 0.50257 \\ 0.42051 \\ 0.33761 \\ 0.25397 \\ 0.16974 \\ 0.08503 \end{bmatrix}$$

j = 6

-2	1	0	0	0	0	0	0	0	-8.60E-03
1	-2	1	0	0	0	0	0	0	-7.83E-04
0	1	-2	1	0	0	0	0	0	-7.04E-05
0	0	1	-2	1	0	0	0	0	-6.25E-05
0	0	0	1	-2	1	0	0	0	-5.45E-05
0	0	0	0	1	-2	1	0	0	-4.63E-05
0	0	0	0	0	1	-2	1	0	-3.80E-05
0	0	0	0	0	0	1	-2	1	-2.95E-05
0	0	0	0	0	0	0	1	-2	-2.12E-05

-0.9	-0.8	-0.7	-0.6	-0.5	-0.4	-0.3	-0.2	-0.1
-0.8	-1.6	-1.4	-1.2	-1	-0.8	-0.6	-0.4	-0.2
-0.7	-1.4	-2.1	-1.8	-1.5	-1.2	-0.9	-0.6	-0.3
-0.6	-1.2	-1.8	-2.4	-2	-1.6	-1.2	-0.8	-0.4
-0.5	-1	-1.5	-2	-2.5	-2	-1.5	-1	-0.5
-0.4	-0.8	-1.2	-1.6	-2	-2.4	-1.8	-1.2	-0.6
-0.3	-0.6	-0.9	-1.2	-1.5	-1.8	-2.1	-1.4	-0.7
-0.2	-0.4	-0.6	-0.8	-1	-1.2	-1.4	-1.6	-0.8
-0.1	-0.2	-0.3	-0.4	-0.5	-0.6	-0.7	-0.8	-0.9

0.00852
0.00844
0.00757
0.00664
0.00564
0.00459
0.00349
0.00235
0.00119

j=7

$$\begin{bmatrix} -2 & 1 & 0 & 0 & 0 & 0 & 0 & 0 & 0 \\ 1 & -2 & 1 & 0 & 0 & 0 & 0 & 0 & 0 \\ 0 & 1 & -2 & 1 & 0 & 0 & 0 & 0 & 0 \\ 0 & 0 & 1 & -2 & 1 & 0 & 0 & 0 & 0 \\ 0 & 0 & 0 & 1 & -2 & 1 & 0 & 0 & 0 \\ 0 & 0 & 0 & 0 & 1 & -2 & 1 & 0 & 0 \\ 0 & 0 & 0 & 0 & 0 & 1 & -2 & 1 & 0 \\ 0 & 0 & 0 & 0 & 0 & 0 & 1 & -2 & 1 \\ 0 & 0 & 0 & 0 & 0 & 0 & 0 & 1 & -2 \end{bmatrix} \begin{bmatrix} -8.62\text{E}-04 \\ -9.72\text{E}-06 \\ -8.96\text{E}-06 \\ -8.12\text{E}-06 \\ -7.20\text{E}-06 \\ -6.22\text{E}-06 \\ -5.16\text{E}-06 \\ -4.09\text{E}-06 \\ -2.94\text{E}-06 \end{bmatrix}$$

$$\begin{bmatrix} -0.9 & -0.8 & -0.7 & -0.6 & -0.5 & -0.4 & -0.3 & -0.2 & -0.1 \\ -0.8 & -1.6 & -1.4 & -1.2 & -1 & -0.8 & -0.6 & -0.4 & -0.2 \\ -0.7 & -1.4 & -2.1 & -1.8 & -1.5 & -1.2 & -0.9 & -0.6 & -0.3 \\ -0.6 & -1.2 & -1.8 & -2.4 & -2 & -1.6 & -1.2 & -0.8 & -0.4 \\ -0.5 & -1 & -1.5 & -2 & -2.5 & -2 & -1.5 & -1 & -0.5 \\ -0.4 & -0.8 & -1.2 & -1.6 & -2 & -2.4 & -1.8 & -1.2 & -0.6 \\ -0.3 & -0.6 & -0.9 & -1.2 & -1.5 & -1.8 & -2.1 & -1.4 & -0.7 \\ -0.2 & -0.4 & -0.6 & -0.8 & -1 & -1.2 & -1.4 & -1.6 & -0.8 \\ -0.1 & -0.2 & -0.3 & -0.4 & -0.5 & -0.6 & -0.7 & -0.8 & -0.9 \end{bmatrix}$$

$$\begin{bmatrix} 0.0008 \\ 0.00074 \\ 0.00068 \\ 0.0006 \\ 0.00051 \\ 0.00042 \\ 0.00032 \\ 0.00022 \\ 0.00011 \end{bmatrix}$$

j = 8

-2	1	0	0	0	0	0	0	0	-8.91E-05
1	-2	1	0	0	0	0	0	0	-8.47E-07
0	1	-2	1	0	0	0	0	0	-7.93E-07
0	0	1	-2	1	0	0	0	0	-7.26E-07
0	0	0	1	-2	1	0	0	0	-6.50E-07
0	0	0	0	1	-2	1	0	0	-5.69E-07
0	0	0	0	0	1	-2	1	0	-4.77E-07
0	0	0	0	0	0	1	-2	1	-3.78E-07
0	0	0	0	0	0	0	1	-2	-2.76E-07

-0.9	-0.8	-0.7	-0.6	-0.5	-0.4	-0.3	-0.2	-0.1
-0.8	-1.6	-1.4	-1.2	-1	-0.8	-0.6	-0.4	-0.2
-0.7	-1.4	-2.1	-1.8	-1.5	-1.2	-0.9	-0.6	-0.3
-0.6	-1.2	-1.8	-2.4	-2	-1.6	-1.2	-0.8	-0.4
-0.5	-1	-1.5	-2	-2.5	-2	-1.5	-1	-0.5
-0.4	-0.8	-1.2	-1.6	-2	-2.4	-1.8	-1.2	-0.6
-0.3	-0.6	-0.9	-1.2	-1.5	-1.8	-2.1	-1.4	-0.7
-0.2	-0.4	-0.6	-0.8	-1	-1.2	-1.4	-1.6	-0.8
-0.1	-0.2	-0.3	-0.4	-0.5	-0.6	-0.7	-0.8	-0.9

8.3E-05
7.6E-05
6.9E-05
6.1E-05
5.2E-05
4.3E-05
3.3E-05
2.2E-05
1.1E-05

Radial distribution

-3.4	1	0	0	0	0	0	0	0	-100.44
1	-3.4	1	0	0	0	0	0	0	-0.74
0	1	-3.4	1	0	0	0	0	0	-0.74
0	0	1	-3.4	1	0	0	0	0	-0.74
0	0	0	1	-3.4	1	0	0	0	-0.74
0	0	0	0	1	-3.4	1	0	0	-0.74
0	0	0	0	0	1	-3.4	1	0	-0.74
0	0	0	0	0	0	1	-3.4	1	-0.74
0	0	0	0	0	0	0	1	-3.4	-0.74

-0.034400193	-0.011187868	-0.003638557	-0.001183226	-0.00038441	-0.000123768	-3.64025E-0
-0.116960657	-0.03803875	-0.012371093	-0.004022967	-0.001306994	-0.000420812	-0.00012376
-0.363266041	-0.118143883	-0.03842316	-0.012494862	-0.004059369	-0.001306994	-0.00038441
-0.118143883	-0.363650451	-0.118267651	-0.038459563	-0.012494862	-0.004022967	-0.00118322
-0.03842316	-0.118267651	-0.363686854	-0.118267651	-0.03842316	-0.012371093	-0.00363855
-0.012494862	-0.038459563	-0.118267651	-0.363650451	-0.118143883	-0.03803875	-0.01118786
-0.004059369	-0.012494862	-0.03842316	-0.118143883	-0.363266041	-0.116960657	-0.03440019
-0.001306994	-0.004022967	-0.012371093	-0.03803875	-0.116960657	-0.359627484	-0.10577279
-0.00038441	-0.001183226	-0.003638557	-0.011187868	-0.034400193	-0.10577279	-0.32522729

32.78180725
11.01814465
3.939884552
1.63746283
0.88748907
0.640000007
0.548510955
0.484937239
0.360275659

j = 2

-3.4	1	0	0	0	0	0	0	0	-108.116
1	-3.4	1	0	0	0	0	0	0	-14.5392
0	1	-3.4	1	0	0	0	0	0	-5.667
0	0	1	-3.4	1	0	0	0	0	-2.845
0	0	0	1	-3.4	1	0	0	0	-1.915
0	0	0	0	1	-3.4	1	0	0	-1.6049
0	0	0	0	0	1	-3.4	1	0	-1.48418
0	0	0	0	0	0	1	-3.4	1	-1.3843
0	0	0	0	0	0	0	1	-3.4	-1.1651

-0.034400193	-0.011187868	-0.003638557	-0.001183226	-0.00038441	-0.000123768	-3.64025E-
-0.116960657	-0.03803875	-0.012371093	-0.004022967	-0.001306994	-0.000420812	-0.0001237
-0.363266041	-0.118143883	-0.03842316	-0.012494862	-0.004059369	-0.001306994	-0.000384
-0.118143883	-0.363650451	-0.118267651	-0.038459563	-0.012494862	-0.004022967	-0.0011832
-0.03842316	-0.118267651	-0.363686854	-0.118267651	-0.03842316	-0.012371093	-0.0036385
-0.012494862	-0.038459563	-0.118267651	-0.363650451	-0.118143883	-0.03803875	-0.0111878
-0.004059369	-0.012494862	-0.03842316	-0.118143883	-0.363266041	-0.116960657	-0.0344001
-0.001306994	-0.004022967	-0.012371093	-0.03803875	-0.116960657	-0.359627484	-0.105772
-0.00038441	-0.001183226	-0.003638557	-0.011187868	-0.034400193	-0.10577279	-0.3252272

36.93655199
17.46827677
7.916389024
3.780445911
2.092127074
1.417786141
1.123445805
0.917749596
0.612602822

$$j=3$$

-3.4	1	0	0	0	0	0	0	0	-52.259
1	-3.4	1	0	0	0	0	0	0	-22.93552
0	1	-3.4	1	0	0	0	0	0	-10.8374
0	0	1	-3.4	1	0	0	0	0	-5.619352
0	0	0	1	-3.4	1	0	0	0	-3.49227
0	0	0	0	1	-3.4	1	0	0	-2.63768
0	0	0	0	0	1	-3.4	1	0	-2.24922
0	0	0	0	0	0	1	-3.4	1	-1.9455
0	0	0	0	0	0	0	1	-3.4	-1.4629

-0.034400193	-0.011187868	-0.003638557	-0.001183226	-0.00038441	-0.000123768	-3.64025E-05
-0.116960657	-0.03803875	-0.012371093	-0.004022967	-0.001306994	-0.000420812	0.000123768
-0.363266041	-0.118143883	-0.03842316	-0.012494862	-0.004059369	-0.001306994	-0.00038441
-0.118143883	-0.363650451	-0.118267651	-0.038459563	-0.012494862	-0.004022967	0.001183226
-0.03842316	-0.118267651	-0.363686854	-0.118267651	-0.03842316	-0.012371093	0.003638557
-0.012494862	-0.038459563	-0.118267651	-0.363650451	-0.118143883	-0.03803875	0.011187868
-0.004059369	-0.012494862	-0.03842316	-0.118143883	-0.363266041	-0.116960657	0.034400193
-0.001306994	-0.004022967	-0.012371093	-0.03803875	-0.116960657	-0.359627484	-0.10577279
-0.00038441	-0.001183226	-0.003638557	-0.011187868	-0.034400193	-0.10577279	0.325227291

19.87467061
15.31488008
9.260401671
5.333085599
3.252737366
2.233951446
1.705017551
1.313888227
0.81670242

j = 4

-3.4	1	0	0	0	0	0	0	0	-28.8751
1	-3.4	1	0	0	0	0	0	0	-20.6636
0	1	-3.4	1	0	0	0	0	0	-12.7339
0	0	1	-3.4	1	0	0	0	0	-7.6836
0	0	0	1	-3.4	1	0	0	0	-5.0249
0	0	0	0	1	-3.4	1	0	0	-3.7171
0	0	0	0	0	1	-3.4	1	0	-3.0147
0	0	0	0	0	0	1	-3.4	1	-2.454
0	0	0	0	0	0	0	1	-3.4	-1.70371

-0.034400193	-0.011187868	-0.003638557	-0.001183226	-0.00038441	-0.000123768	-3.64025E-05
-0.116960657	-0.03803875	-0.012371093	-0.004022967	-0.001306994	-0.000420812	-0.000123768
-0.363266041	-0.118143883	-0.03842316	-0.012494862	-0.004059369	-0.001306994	-0.00038441
-0.118143883	-0.363650451	-0.118267651	-0.038459563	-0.012494862	-0.004022967	-0.001183226
-0.03842316	-0.118267651	-0.363686854	-0.118267651	-0.03842316	-0.012371093	-0.003638557
-0.012494862	-0.038459563	-0.118267651	-0.363650451	-0.118143883	-0.03803875	-0.011187868
-0.004059369	-0.012494862	-0.03842316	-0.118143883	-0.363266041	-0.116960657	-0.034400193
-0.001306994	-0.004022967	-0.012371093	-0.03803875	-0.116960657	-0.359627484	-0.10577279
-0.00038441	-0.001183226	-0.003638557	-0.011187868	-0.034400193	-0.10577279	-0.325227291

12.12483507
12.34933922
9.199318289
6.194442962
4.178187781
2.986495494
2.258796899
1.678713964
0.994830578

j = 5

-3.4	1	0	0	0	0	0	0	0	-18.8172
1	-3.4	1	0	0	0	0	0	0	-17.15208
0	1	-3.4	1	0	0	0	0	0	-12.83408
0	0	1	-3.4	1	0	0	0	0	-8.8851
0	0	0	1	-3.4	1	0	0	0	-6.2676
0	0	0	0	1	-3.4	1	0	0	-4.715824
0	0	0	0	0	1	-3.4	1	0	-3.74112
0	0	0	0	0	0	1	-3.4	1	-2.91985
0	0	0	0	0	0	0	1	-3.4	-1.9139

-0.034400193	-0.011187868	-0.003638557	-0.001183226	-0.00038441	-0.000123768	-3.64025E-05
-0.116960657	-0.03803875	-0.012371093	-0.004022967	-0.001306994	-0.000420812	-0.000123768
-0.363266041	-0.118143883	-0.03842316	-0.012494862	-0.004059369	-0.001306994	-0.00038441
-0.118143883	-0.363650451	-0.118267651	-0.038459563	-0.012494862	-0.004022967	-0.001183226
-0.03842316	-0.118267651	-0.363686854	-0.118267651	-0.03842316	-0.012371093	-0.003638557
-0.012494862	-0.038459563	-0.118267651	-0.363650451	-0.118143883	-0.03803875	-0.011187868
-0.004059369	-0.012494862	-0.03842316	-0.118143883	-0.363266041	-0.116960657	-0.034400193
-0.001306994	-0.004022967	-0.012371093	-0.03803875	-0.116960657	-0.359627484	-0.10577279
-0.00038441	-0.001183226	-0.003638557	-0.011187868	-0.034400193	-0.10577279	-0.325227291

8.505244566
10.10063152
8.684822614
6.593685364
4.848607623
3.623980554
2.75710226
2.009047129
1.153807979

j = 6

$$\begin{bmatrix} -3.4 & 1 & 0 & 0 & 0 & 0 & 0 & 0 & 0 \\ 1 & -3.4 & 1 & 0 & 0 & 0 & 0 & 0 & 0 \\ 0 & 1 & -3.4 & 1 & 0 & 0 & 0 & 0 & 0 \\ 0 & 0 & 1 & -3.4 & 1 & 0 & 0 & 0 & 0 \\ 0 & 0 & 0 & 1 & -3.4 & 1 & 0 & 0 & 0 \\ 0 & 0 & 0 & 0 & 1 & -3.4 & 1 & 0 & 0 \\ 0 & 0 & 0 & 0 & 0 & 1 & -3.4 & 1 & 0 \\ 0 & 0 & 0 & 0 & 0 & 0 & 1 & -3.4 & 1 \\ 0 & 0 & 0 & 0 & 0 & 0 & 0 & 1 & -3.4 \end{bmatrix} \begin{bmatrix} -13.61632 \\ -14.2245 \\ -12.25115 \\ -9.47E+00 \\ -7.18E+00 \\ -5.57E+00 \\ -4.39E+00 \\ -3.34E+00 \\ -2.10E+00 \end{bmatrix}$$

-0.325227291	-0.10577279	-0.034400193	-0.011187868	-0.003638557	-0.001183226	-0.00038441	-0.000123768	-3.64025E-05
-0.10577279	-0.359627484	-0.116960657	-0.03803875	-0.012371093	-0.004022967	-0.001306994	-0.000420812	-0.00012376
-0.034400193	-0.116960657	-0.363266041	-0.118143883	-0.03842316	-0.012494862	-0.004059369	-0.001306994	-0.00038441
-0.011187868	-0.03803875	-0.118143883	-0.363650451	-0.118267651	-0.038459563	-0.012494862	-0.004022967	-0.001183226
-0.003638557	-0.012371093	-0.03842316	-0.118267651	-0.363688854	-0.118267651	-0.03842316	-0.012371093	-0.00363855
-0.001183226	-0.004022967	-0.012494862	-0.038459563	-0.118267651	-0.363650451	-0.118143883	-0.03803875	-0.01118786
-0.00038441	-0.001306994	-0.004059369	-0.012494862	-0.03842316	-0.118143883	-0.363266041	-0.116960657	-0.03440019
-0.000123768	-0.000420812	-0.001306994	-0.004022967	-0.012371093	-0.03803875	-0.116960657	-0.359627484	-0.10577279
-3.64025E-05	-0.000123768	-0.00038441	-0.001183226	-0.003638557	-0.011187868	-0.034400193	-0.10577279	-0.32522729

6.495269994
8.467597979
8.070063134
6.719466677
5.303963568
4.133709453
3.184846574
2.300198897
1.294599676

j = 7

-3.4	1	0	0	0	0	0	0	0	-9.88E+00
1	-3.4	1	0	0	0	0	0	0	-12.27645
0	1	-3.4	1	0	0	0	0	0	-11.58402
0	0	1	-3.4	1	0	0	0	0	-9.72E+00
0	0	0	1	-3.4	1	0	0	0	-7.82E+00
0	0	0	0	1	-3.4	1	0	0	-6.25E+00
0	0	0	0	0	1	-3.4	1	0	-4.96E+00
0	0	0	0	0	0	1	-3.4	1	-3.71E+00
0	0	0	0	0	0	0	1	-3.4	-2.27E+00

-0.325227291	-0.10577279	-0.034400193	-0.011187868	-0.003638557	-0.001183226	-0.00038441	-0.000123768	-3.64025E-05
-0.10577279	-0.359627484	-0.116960657	-0.03803875	-0.012371093	-0.004022967	-0.001306994	-0.000420812	-0.000123768
-0.034400193	-0.116960657	-0.363266041	-0.118143883	-0.03842316	-0.012494862	-0.004059369	-0.001306994	-0.00038441
-0.011187868	-0.03803875	-0.118143883	-0.363650451	-0.118267651	-0.038459563	-0.012494862	-0.004022967	-0.001183226
-0.003638557	-0.012371093	-0.03842316	-0.118267651	-0.363688854	-0.118267651	-0.03842316	-0.012371093	-0.003638557
-0.001183226	-0.004022967	-0.012494862	-0.038459563	-0.118267651	-0.363650451	-0.118143883	-0.03803875	-0.011187868
-0.00038441	-0.001306994	-0.004059369	-0.012494862	-0.03842316	-0.118143883	-0.363266041	-0.116960657	-0.034400193
-0.000123768	-0.000420812	-0.001306994	-0.004022967	-0.012371093	-0.03803875	-0.116960657	-0.359627484	-0.10577279
-3.64025E-05	-0.000123768	-0.00038441	-0.001183226	-0.003638557	-0.011187868	-0.034400193	-0.10577279	-0.32522729

5.058892776
7.315455439
7.537205717
6.727023998
5.612244876
4.53157458
3.541136696
2.550380186
1.417055937

j = 7

-3.4	1	0	0	0	0	0	0	0	-8.17E+00
1	-3.4	1	0	0	0	0	0	0	-10.87968
0	1	-3.4	1	0	0	0	0	0	-10.97931
0	0	1	-3.4	1	0	0	0	0	-9.80E+00
0	0	0	1	-3.4	1	0	0	0	-8.27E+00
0	0	0	0	1	-3.4	1	0	0	-6.80E+00
0	0	0	0	0	1	-3.4	1	0	-5.43E+00
0	0	0	0	0	0	1	-3.4	1	-4.03E+00
0	0	0	0	0	0	0	1	-3.4	-2.41E+00

-0.325227291	-0.10577279	-0.034400193	-0.011187888	-0.003838557	-0.001183226	-0.00038441	-0.000123768	-3.64025E-
-0.10577279	-0.359827484	-0.116960657	-0.03803875	-0.012371093	-0.004022967	-0.001306994	-0.000420812	-0.0001237
-0.034400193	-0.116960657	-0.363266041	-0.118143883	-0.03842318	-0.012494862	-0.004059369	-0.001306994	-0.000384
-0.011187888	-0.03803875	-0.118143883	-0.363650451	-0.118267651	-0.038459583	-0.012494862	-0.004022967	-0.0011832
-0.003838557	-0.012371093	-0.03842318	-0.118267651	-0.363686854	-0.118267651	-0.03842318	-0.012371093	-0.0036385
-0.001183226	-0.004022967	-0.012494862	-0.038459583	-0.118267651	-0.363650451	-0.118143883	-0.03803875	-0.0111878
-0.00038441	-0.001306994	-0.004059369	-0.012494862	-0.03842318	-0.118143883	-0.363266041	-0.116960657	-0.0344001
-0.000123768	-0.000420812	-0.001306994	-0.004022967	-0.012371093	-0.03803875	-0.116960657	-0.359827484	-0.105772
-3.64025E-05	-0.000123768	-0.00038441	-0.001183226	-0.003838557	-0.011187888	-0.034400193	-0.10577279	-0.3252272

4.33685769
6.572731146
7.130748207
6.692502758
5.823431169
4.838403218
3.831639773
2.76055201
1.521377062

j = 8

-3.4	1	0	0	0	0	0	0	0	-7.17203
1	-3.4	1	0	0	0	0	0	0	-9.92197
0	1	-3.4	1	0	0	0	0	0	-10.4928
0	0	1	-3.4	1	0	0	0	0	-9.80184
0	0	0	1	-3.4	1	0	0	0	-8.57933
0	0	0	0	1	-3.4	1	0	0	-7.21564
0	0	0	0	0	1	-3.4	1	0	-5.81345
0	0	0	0	0	0	1	-3.4	1	-4.30173
0	0	0	0	0	0	0	1	-3.4	-2.53523

-0.325227291	-0.10577279	-0.034400193	-0.011187868	-0.003638557	-0.001183226	-0.00038441	-0.000123768	-3.64025E-05
-0.10577279	-0.359627484	-0.116960657	-0.03803875	-0.012371093	-0.004022967	-0.001306994	-0.000420812	-0.000123768
-0.034400193	-0.116960657	-0.363266041	-0.118143883	-0.03842316	-0.012494862	-0.004059369	-0.001306994	-0.00038441
-0.011187868	-0.03803875	-0.118143883	-0.303650451	-0.118267651	-0.038459563	-0.012494862	-0.004022967	-0.001183226
-0.003638557	-0.012371093	-0.03842316	-0.118267651	-0.363888854	-0.118267651	-0.03842316	-0.012371093	-0.003638557
-0.001183226	-0.004022967	-0.012494862	-0.038459563	-0.118267651	-0.363650451	-0.118143883	-0.03803875	-0.011187868
-0.00038441	-0.001306994	-0.004059369	-0.012494862	-0.03842316	-0.118143883	-0.363266041	-0.116960657	-0.034400193
-0.000123768	-0.000420812	-0.001308994	-0.004022967	-0.012371093	-0.03803875	-0.116960657	-0.359627484	-0.10577279
-3.64025E-05	-0.000123768	-0.00038441	-0.001183226	-0.003638557	-0.011187868	-0.034400193	-0.10577279	-0.325227291

3.895243933
6.071799374
6.826903938
6.646874014
5.97062771
5.0739302
4.06509497
2.933942699
1.608580206

The procedure above is applicable to both pyrene and anthracene.

APPENDIX I

Non-Steady State Model

Results of the numerical solution to the non-steady state model are shown in the Microsoft Excel template in Tables I.1 to I.6. The table is subdivided into j^{th} and i^{th} columns indicating the depth and radius of the soil depending on the direction of solute transport. At the point of interception of j and i , the solute concentration was computed using the finite difference scheme. For each PAH, the changes in concentration with time, depth and radius were calculated.

Table I.1: Results obtained from the Finite difference solution to the non-steady state macro porous system
Naphthalene

	i	0	1	2	3	4	5	6	7	8	9
J	$Z(m)$ $t(days)$	0	0.015	0.03	0.045	0.06	0.075	0.09	0.105	0.12	0.135
0	0	100	0	0	0	0	0	0	0	0	0
1	7	99.7	89.73	79.76	69.76	59.82	49.85	39.88	29.91	19.94	9.97
2	14	66.49	60.09787	53.70574	47.64759	40.64759	34.00152	27.29075	20.52524	13.71496	6.869891
3	21	4.44	4.232454	3.955309	3.61543	3.217474	2.768967	2.27646	1.746583	1.186033	0.60157
4	28	1.62	1.4747	1.3255	1.1718	1.0139	0.8521	0.686808	0.51844	0.3475	0.1744
5	35	1.3	1.1752	1.0494	0.922	0.7932	0.6632	0.5321	0.4001	0.2672	0.13386
6	42	0.82	0.7422	0.6635	0.5836	0.5025	0.4205	0.3376	0.2539	0.1697	0.085
7	49	0	0.00851	0.00843	0.00757	0.00663	0.00563	0.00458	0.00348	0.00235	0.00118
8	56	0	0.000804	0.000745	0.000677	0.00599	0.005141	0.000422	0.000322	0.000218	0.0001109
9	63	0	8.27E-05	7.62E-05	6.89E-05	6.08E-05	5.20E-05	4.26E-05	3.25E-05	2.70E-05	1.12E-05

Table I.2: Results obtained from the Finite difference solution to the non-steady state macro porous system

Pyrene

	<i>i</i>	0	1	2	3	4	5	6	7	8	9
<i>j</i>	$\frac{Z(m)}{t(days)}$	0	0.015	0.03	0.045	0.06	0.075	0.09	0.105	0.12	0.135
0	0	100	0	0	0	0	0	0	0	0	0
1	7	44.18	39.762	35.344	30.926	26.508	22.09	17.672	13.254	8.836	4.418
2	14	35.21	32.14152	28.7165	25.20966	21.68572	18.12838	14.54237	10.93211	7.302018	3.6565
3	21	23.6	21.3662	19.1116	16.7903	14.4549	12.0925	9.70665	7.30089	4.87878	2.4439
4	28	17.02	15.402	13.7702	12.094	10.4084	8.7049	6.9857	5.2532	3.5098	1.7579
5	35	16.12	14.5685	13.00708	11.4136	9.8135	8.20035	6.5759	4.94202	3.300216	1.6523
6	42	2.26	2.0912	1.9129	1.7044	1.4895	1.2624	1.02471	0.7779	0.52387	0.26399
7	49	0	0.2184	0.2026	0.1815	0.156	0.1366	0.11156	0.0852	0.0576	0.029139
8	56	0	0.02244	0.020813	0.018695	0.016487	0.014095	0.011536	0.008814	0.005967	0.00302
9	63	0	0.002306	0.00214	0.001922	0.001696	0.00145	0.001186	0.000906	0.000314	0.0003106

Table I. 3: Results obtained from the Finite difference solution to the non-steady state macro porous system

Anthracene

	i	0	1	2	3	4	5	6	7	8	9
j	$Z(m)$	0	0.015	0.03	0.045	0.06	0.075	0.09	0.105	0.12	0.135
	$T(days)$										
0	0	100	0	0	0	0	0	0	0	0	0
	7	28	25.2	22.4	19.6	16.8	14	11.2	8.4	5.6	2.8
2	14	23.5	21.248	18.967	16.66	14.329	11.976	9.6066	7.221	4.822	2.414
3	21	18.48	16.71572	14.92644	13.11476	11.2829	9.433	7.5683	5.69005	3.8009	1.90349
4	28	9.33	8.4627	7.57606	6.67169	5.75149	4.8172	3.87076	2.9139	1.94863	0.97668
5	35	4.123	3.7485	3.3592	2.961	2.5548	2.1415	1.7218	1.29696	0.867719	0.435076
6	42	1.64	1.49077	1.3372	1.1797	1.0186	0.85439	0.68738	0.518015	0.34671	0.17387
7	49	0.57	0.518872	0.466034	0.411624	0.355794	0.298701	0.240505	0.181369	0.12146	0.060946
8	56	0	0.05533	0.05084	0.04582	0.040316	0.034368	0.028034	0.021373	0.01444	0.007296
9	63	0	0.005742	0.005289	0.004778	0.004212	0.003598	0.00294	0.002244	0.001516	0.000767

Table I.4: Results obtained from the Finite difference solution to the non-steady state micro porous system

Naphthalene

	l	0	1	2	3	4	5	6	7	8	9
	$r(m)$	0	0.001	0.002	0.003	0.004	0.005	0.006	0.007	0.008	0.009
j	$t(days)$										
0	0	100	0	0	0	0	0	0	0	0	0
1	7	99.7	32.78181	11.01814	3.939885	1.637463	0.887489	0.64	0.548511	0.484937	0.360276
2	14	66.49	36.93655	17.46828	7.916389	3.780446	2.092127	1.417786	1.123446	0.91775	0.612603
3	21	4.44	19.87467	15.314488	9.260402	5.333086	3.252737	2.233951	1.705018	1.313888	0.787859
4	28	1.62	12.12484	12.34934	9.199318	6.194443	4.178188	2.986495	2.258797	1.6787714	0.943646
5	35	1.3	8.505245	10.10063	8.684823	6.593685	4.848608	3.623981	2.2757102	2.009047	1.07901
6	42	0.82	6.49529	8.467598	8.070063	6.719467	5.303964	4.133709	3.184847	2.300199	1.19864
7	49	0	5.058893	7.315455	7.537206	6.727024	5.612245	4.531575	3.541137	2.55038	1.304435
8	56	0	4.336858	6.572731	7.130748	6.692503	5.823431	4.838403	3.83164	2.760552	1.397346
9	63	0	3.895244	6.071799	6.826904	6.646874	5.970628	5.07393	4.0651	2.933943	1.478164

Table I.5: Results obtained from the Finite difference solution to the non-steady state micro porous system

Anthracene

	<i>i</i>	0	1	2	3	4	5	6	7	8	9
<i>j</i>	<i>r</i> (m) <i>t</i> (days)	0	0.001	0.002	0.003	0.004	0.005	0.006	0.007	0.008	0.009
0	0	100	0	0	0	0	0	0	0	0	0
1	7	28	9.46301	3.43424	1.47339	0.835293	0.62661	0.555163	0.520949	0.476063	0.357666
2	14	23.5	12.394393	6.05458	3.104099	1.853696	1.34747	1.137263	1.019927	0.880589	0.600776
3	21	18.48	12.51398	7.49123	4.450976	2.868487	2.10498	1.730928	1.494225	1.2298804	0.816702
4	28	9.33	9.957993	7.522378	5.233291	3.704962	2.817769	2.305384	1.939186	1.538698	0.994831
5	35	4.128	7.37155	6.940362	5.56248	4.31506	3.43336	2.832229	2.348042	1.815133	1.153808
6	42	1.64	5.49732	6.2244	5.6235	4.72876	3.93578	3.294799	2.714896	2.06213	1.2946
7	49	0.57	4.310748	5.614822	5.570147	5.002197	4.33526	3.688593	3.036849	2.280683	1.417056
8	56	0	3.560213	5.155073	5.48752	5.189242	4.64661	4.017948	3.314505	2.471747	1.521377
9	63	0	3.186559	4.8622	5.42443	5.327276	4.995677	4.291436	3.51125	2.636888	1.60858

Table I.6: Results obtained from the Finite difference solution to the non-steady state microporous system

Pyrene

	<i>i</i>	0	1	2	3	4	5	6	7	8	9
	<i>r</i> (m)	0	0.001	0.002	0.003	0.004	0.005	0.006	0.007	0.008	0.009
<i>j</i>	<i>t</i> (days)										
0	0	100	0	0	0	0	0	0	0	0	0
1	7	44.18	14.48452	5.067368	2.00453	1.008033	0.68784	0.573432	0.526884	0.477974	0.358228
2	14	35.21	18.47886	8.772926	4.228688	2.297654	1.517296	1.200751	1.043231	0.888913	0.603419
3	21	23.21	16.98305	10.23272	5.870371	3.537159	2.4012771	1.856625	1.545715	1.25001	0.794719
4	28	17.02	14.80693	10.49702	6.893599	4.56674	3.23923	2.50181	2.026934	1.575829	0.95694
5	35	16.12	13.82358	10.55858	7.570403	5.392991	3.989164	3.10714	2.478873	1.873704	1.100854
6	42	2.26	9.014189	9.224703	7.636596	5.988051	4.82125	3.71719	2.91456	2.152499	1.232796
7	49	0	6.200641	7.852181	7.37827	6.27515	5.18653	4.18656	3.33859	2.55496	1.3969
8	56	0	4.87701	6.8889	7.0523	6.3874	5.4828	4.45567	3.6622	2.7042	1.4978
9	63	0	4.14845	6.232	6.761	6.4162	5.6805	4.7967	3.8981	2.8546	1.5771